The COSMOS Airborne Campaigns in Support of the SMOS Mission

N. Skou, S. S. Søbjærg, J. Balling, and S. S. Kristensen

DTU Space

Technical University of Denmark

ns@space.dtu.dk

L-band Radiometer System

- EMIRAD-2 is a fully polarimetric radiometer operating in the 1400 - 1427 MHz protected band
- EMIRAD-2 consists of:
  - 2 antennas, one pointing 40 deg aft, one pointing nadir. The antennas are Potter horns with no sidelobes
  - radiometer unit with dual inputs
  - EGI (INU + GPS) for attitude and navigation
  - industrial PC for fast data recording
  - laptop for instrument control and normal data recording
- Installed on 2 small aircraft

40 deg Potter Horn

40 deg Horn Pattern

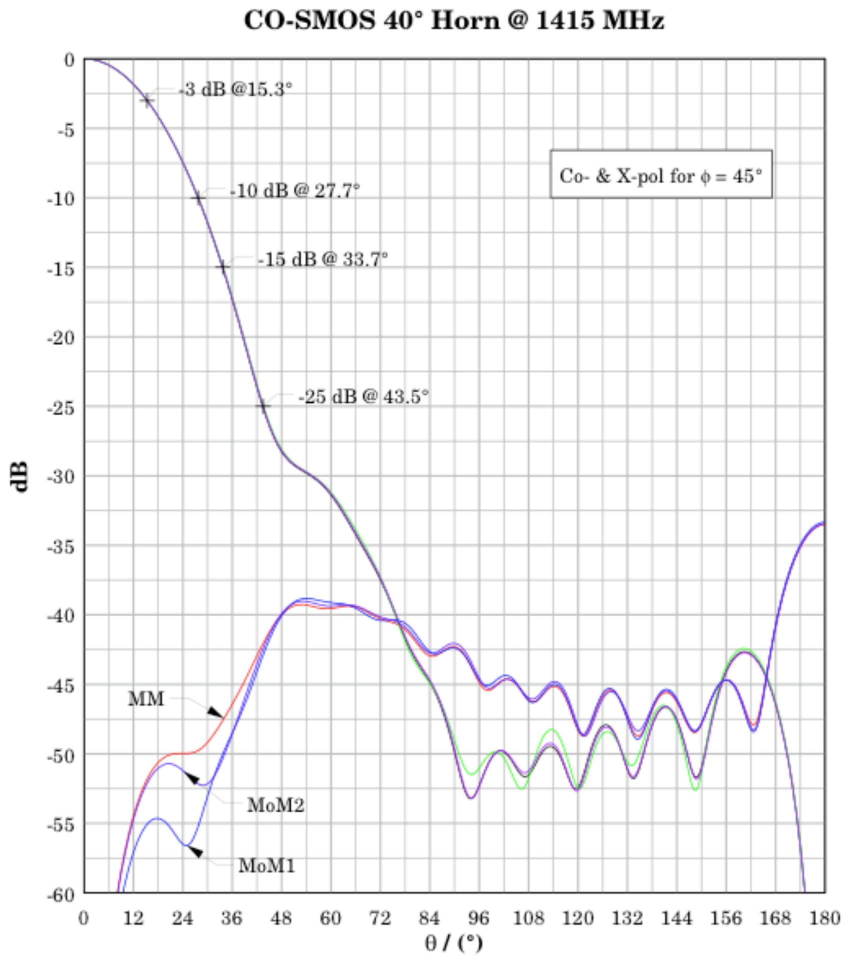

HPBW=30.6°
i.e.:
FPL = 932 m
FPX = 714 m
from 1000 m
altitude

Nadir Potter Horn

Nadir Horn Pattern

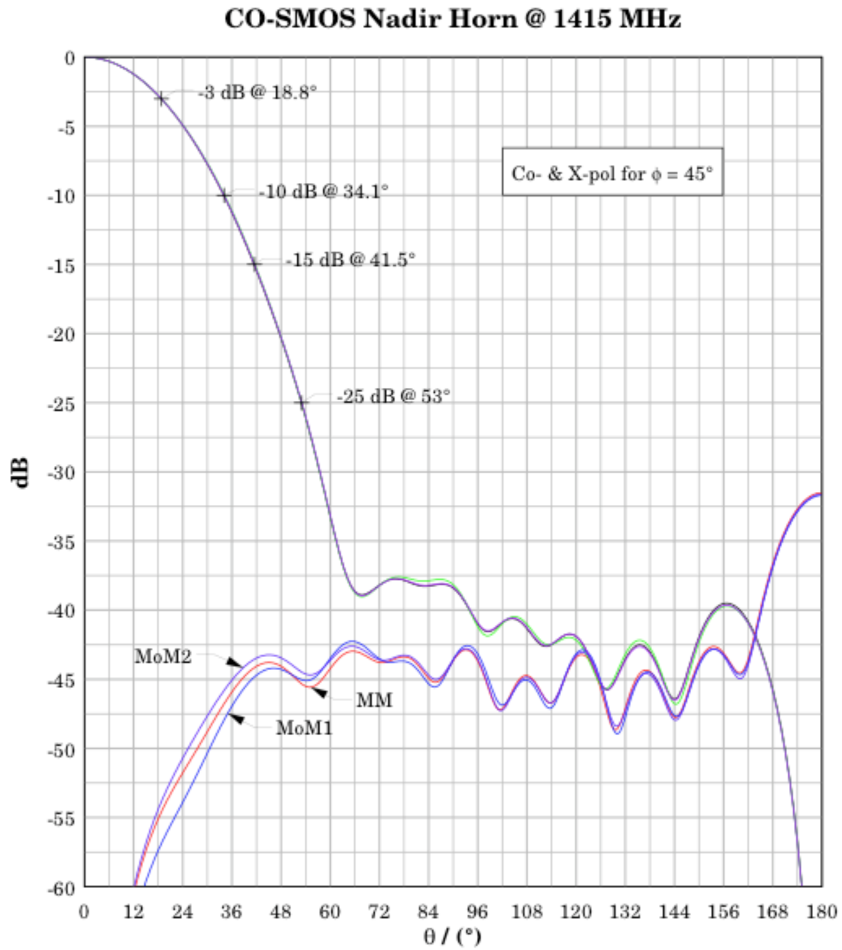

HPBW=37.6°
i.e.:
FP = 680 m
from 1000 m
altitude

OMT

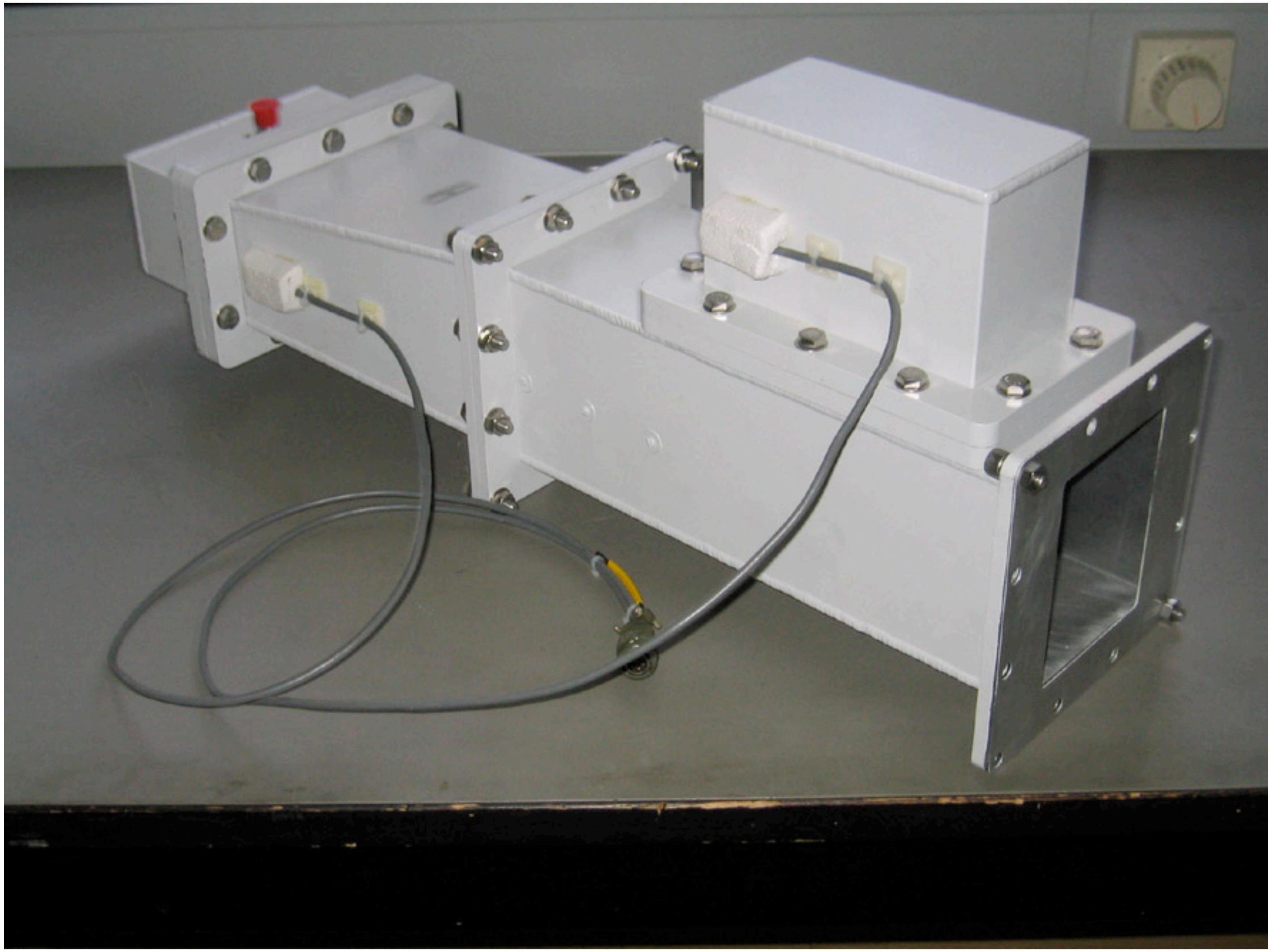

Radiometer Description

- Digital radiometer with subharmonic sampling. A to D converters directly sample the L-band signals with a clock frequency of 139.4 MHz.
- The data from the converters are fed into an FPGA where correlation, calculation of second and fourth order moments of the PDF, and integration is performed digitally
- Data integrated to 1 msec (8 msec before the Rehearsal Campaign). is stored on the laptop computer also controlling the system. These data will be available in near real time.
- A second data stream - fast data - is implemented for test and development, done off-line for optimum performance. In the normal mode of operation, data only pre-integrated to 14.4 μsec (1.8 μsec before the Rehearsal Campaign) is recorded on a fast HD in an industrial PC.
- The fast data channel can also be operated in a special mode where raw data from the converters are stored. 2 x 32 K samples are stored with a 25% duty cycle.

Data Output

- "Slow data", 1 msec integration:
  - $<x^2>$ for H-pol
  - $<x^2>$ for V-pol
  - $<x^4>$ for H-pol
  - $<x^4>$ for V-pol
  - $<xy>$ 0° for 3'rd Stokes
  - $<xy>$ 90° for 4'th Stokes
- "Fast data" 14.7 μsec integration:
  - as above.
- "Raw" A to D converter samples may be recorded for special investigations.

EMIRAD-2 Specifications

- Digital correlation radiometer with direct sampling at 139.4 MHz
- Fully polarimetric (i.e. 4 Stokes)
- Frequency: 1400.5 - 1426.5 MHz (-3 dB BW)
  1392 - 1433 MHz (-60 dB BW)
- Additional digital filter bank: 4 sub-bands
- Data integrated to 1 msec recorded on laptop.
- "Fast data" integrated to 14.4 μsec is recorded on industrial PC
- RFI flagging by kurtosis
- Sensitivity: 0.1 K for 1 sec. integration time
- Stability: better than 0.1 K over 15 min.
- Calibration: internal load and noise diode
- 2 antennas - one nadir pointing, one pointing 40 deg. aft
- Antennas are Potter horns (no sidelobes) with 37.6° and 30.6° HPBW and very low cross pol: better than -40 dB
- Antennas are multiplexed through receiver, minimum cycle: 2 sec.
- Minimum operating AGL is 250 m at 110 knots

Block Diagram

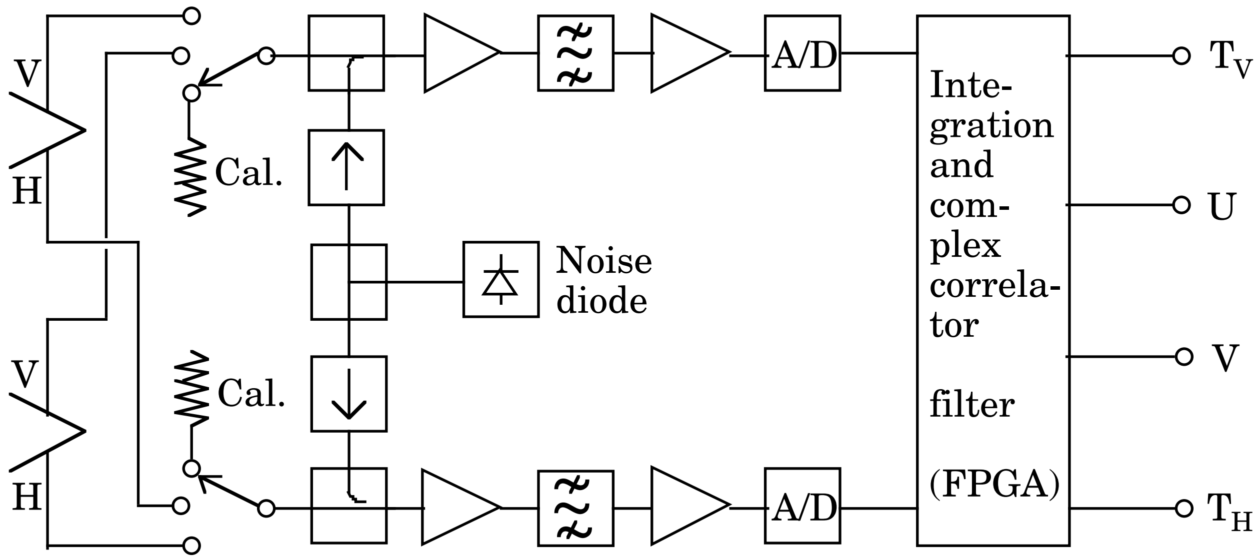

Block Diagram

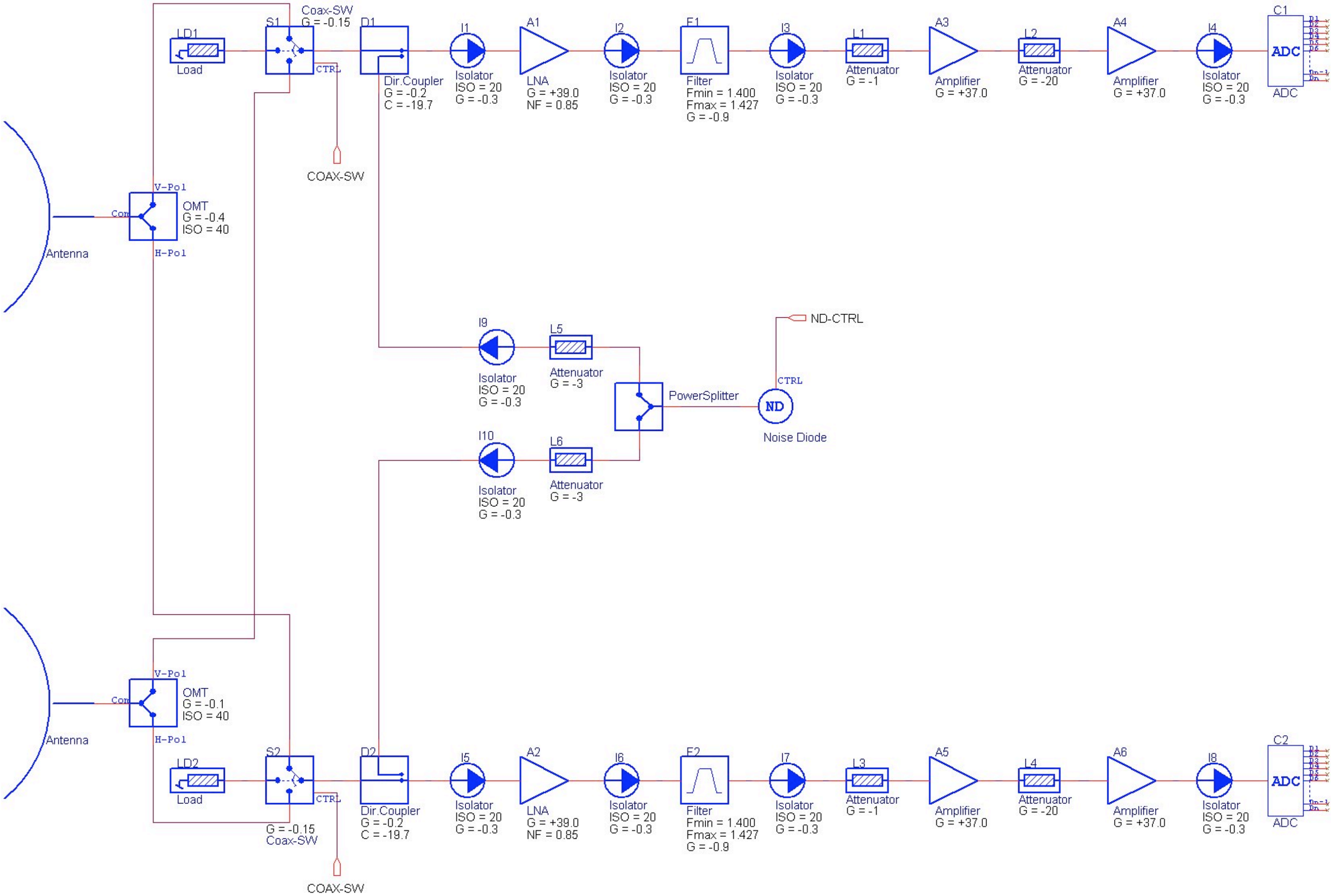

Temperature stabilized enclosure

- 2 digital PI-regulators
- stability of microwave section better than 0.02 °C for 15 °C change in ambient temperature
- DFE stability better than 0.1 °C for same change

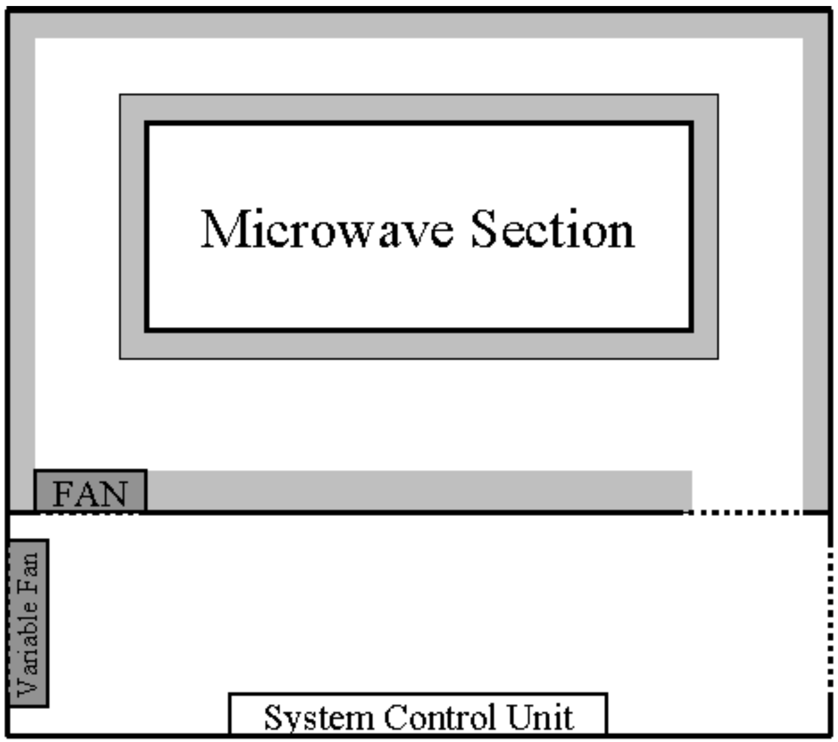

AFE-1

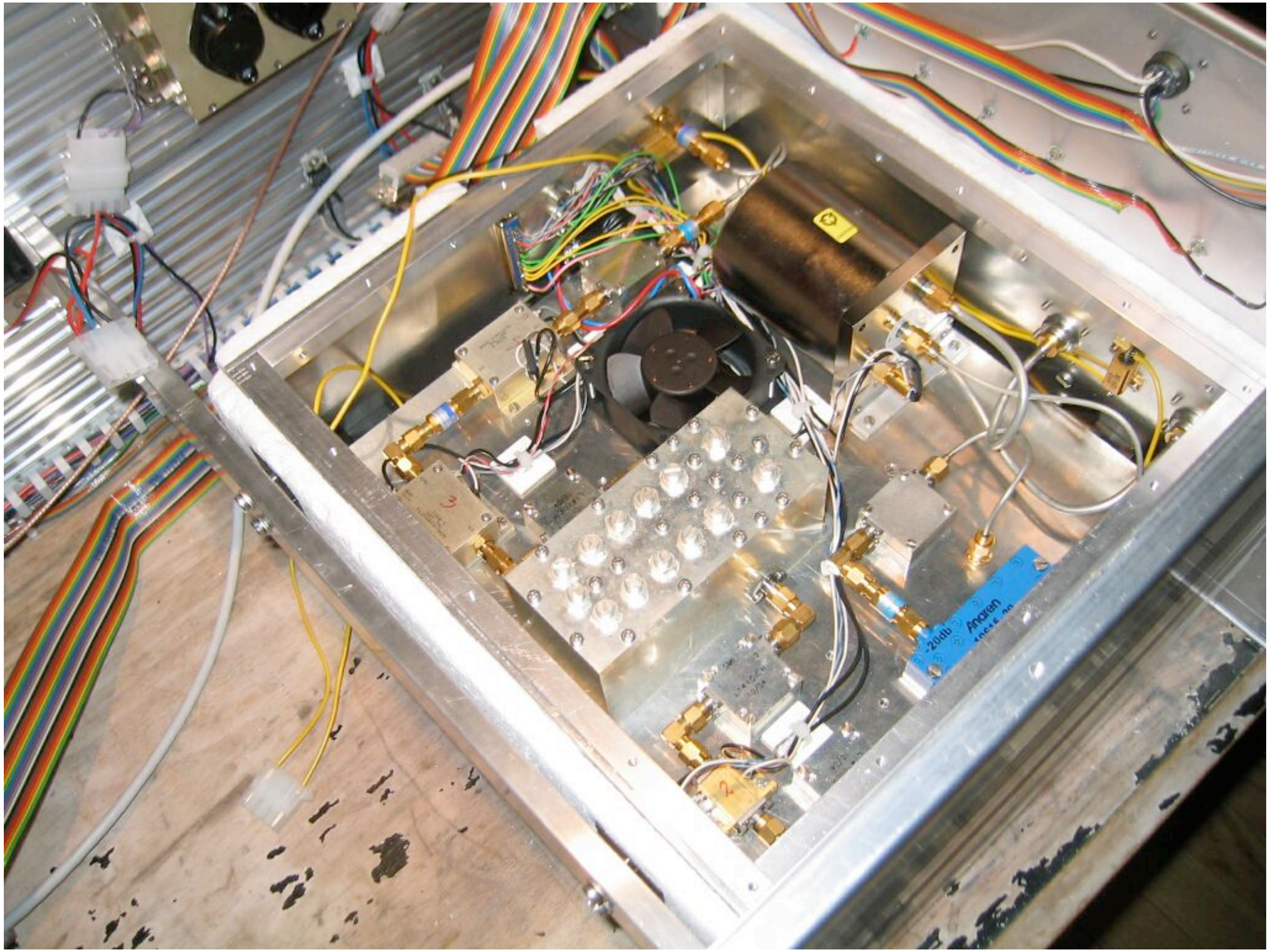

DFE

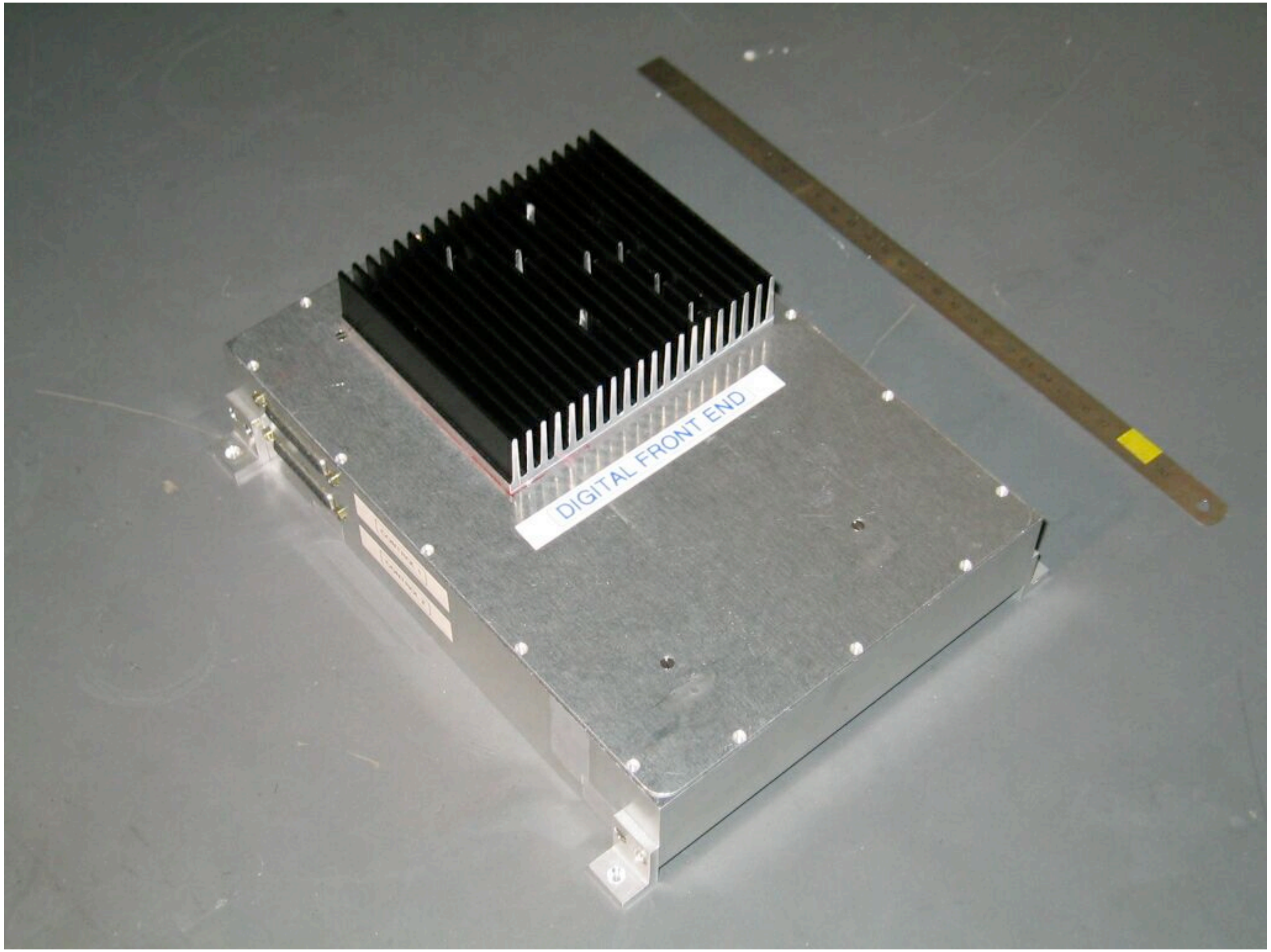

Radiometer Control - screen dump

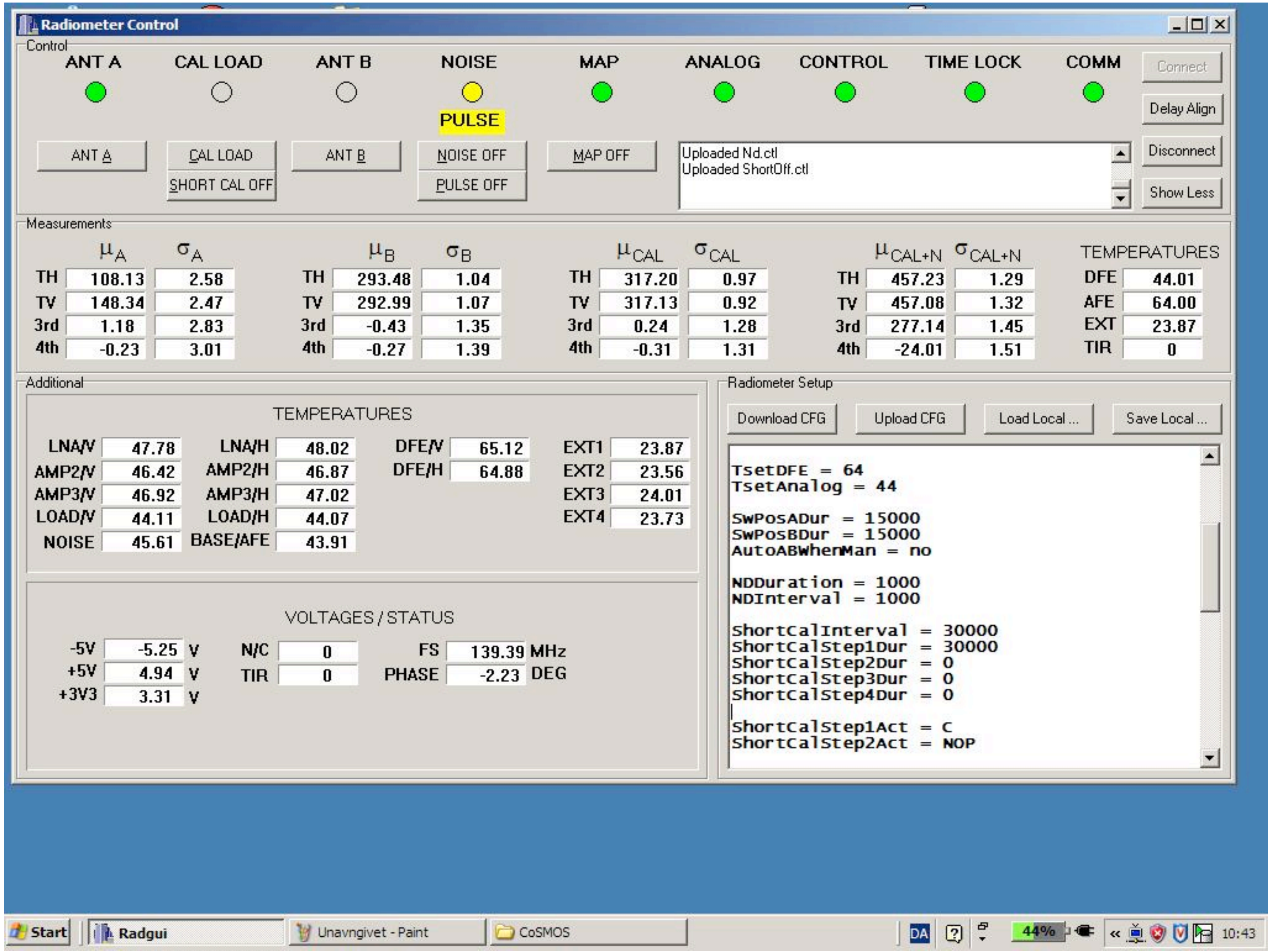

Measured Radiometer Performance

- Sensitivities for 8 msec integration:
  - $\Delta T_H = 0.9$ K
  - $\Delta T_V = 0.9$ K
  - $\Delta U = 1.2$ K
  - $\Delta V = 1.2$ K
- Receiver noise temperature: $T_N = 115$ K
- Internal noise diode injects 130 K correlated signal in channels
- Channel phase imbalance below 10° (compensated in digital section)
- Offsets in U and V are around 0.5 K (compensated in data processing)
- Microwave section (AFE) stabilized to better than 0.02 °C for 15 °C ambient change
- Digital front end (DFE) stabilized to better than 0.1 °C for 15 °C ambient change

Large Antenna on C-130 (LOSAC Flights)

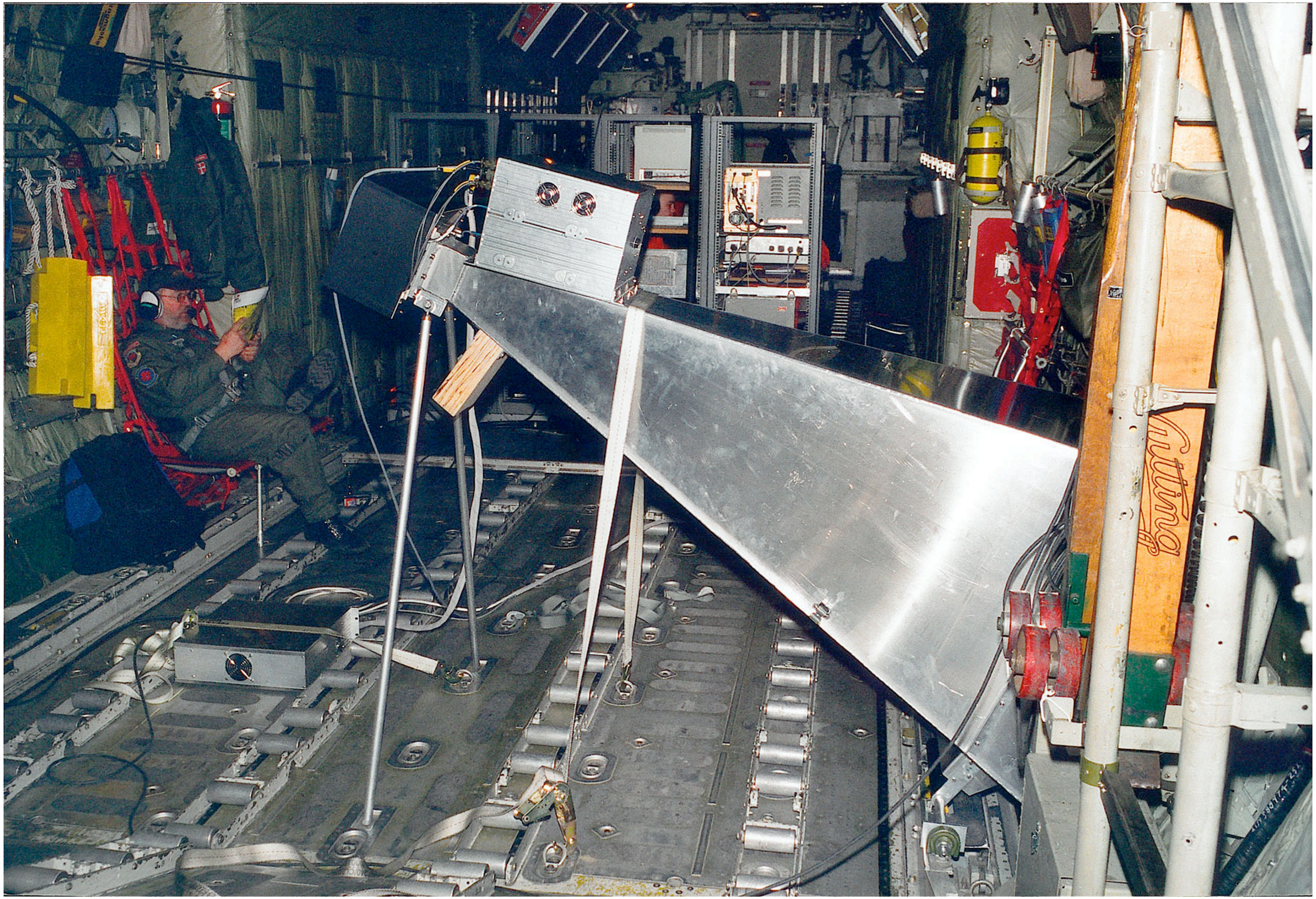

Aero Commander

EMIRAD-2 on Aero Commander

EMIRAD-2 on Aero Commander

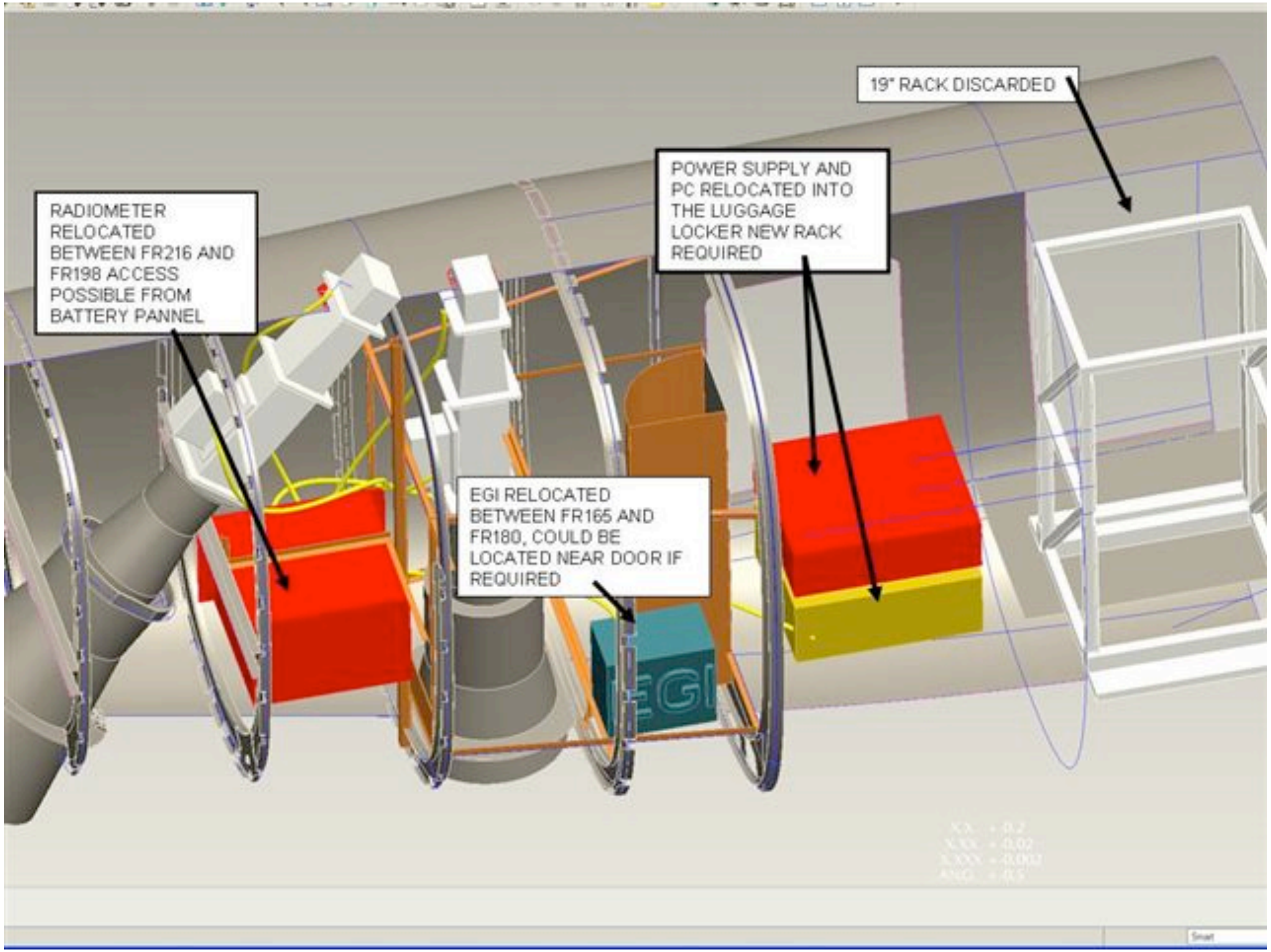

EMIRAD-2 on Aero Commander

CoSMOS “Down Under” Campaign

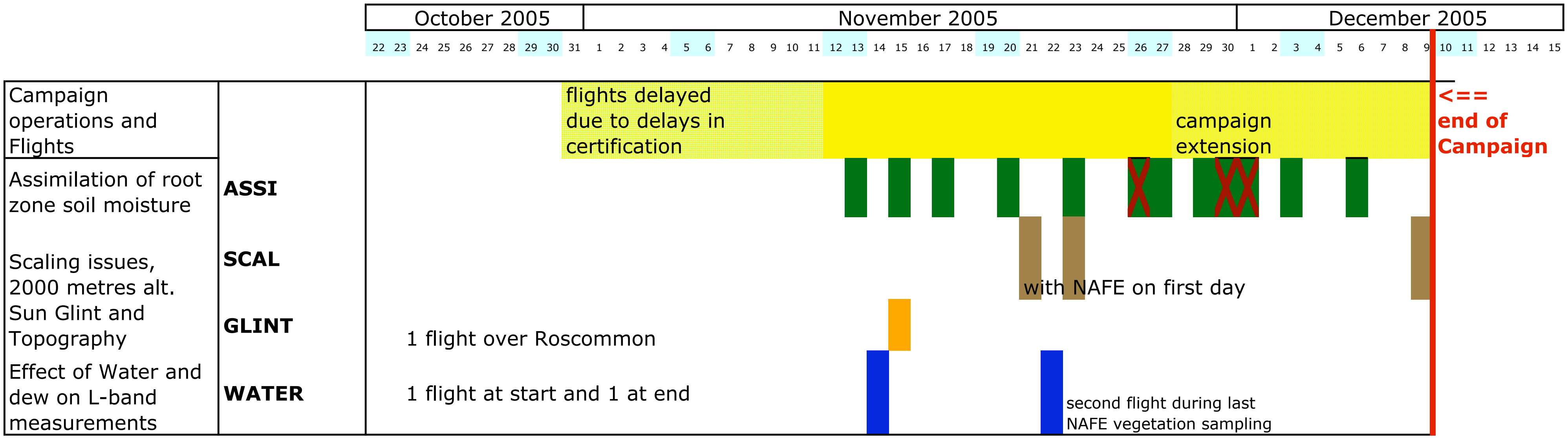

SMOS

Skyvan

EMIRAD Horns in Skyvan

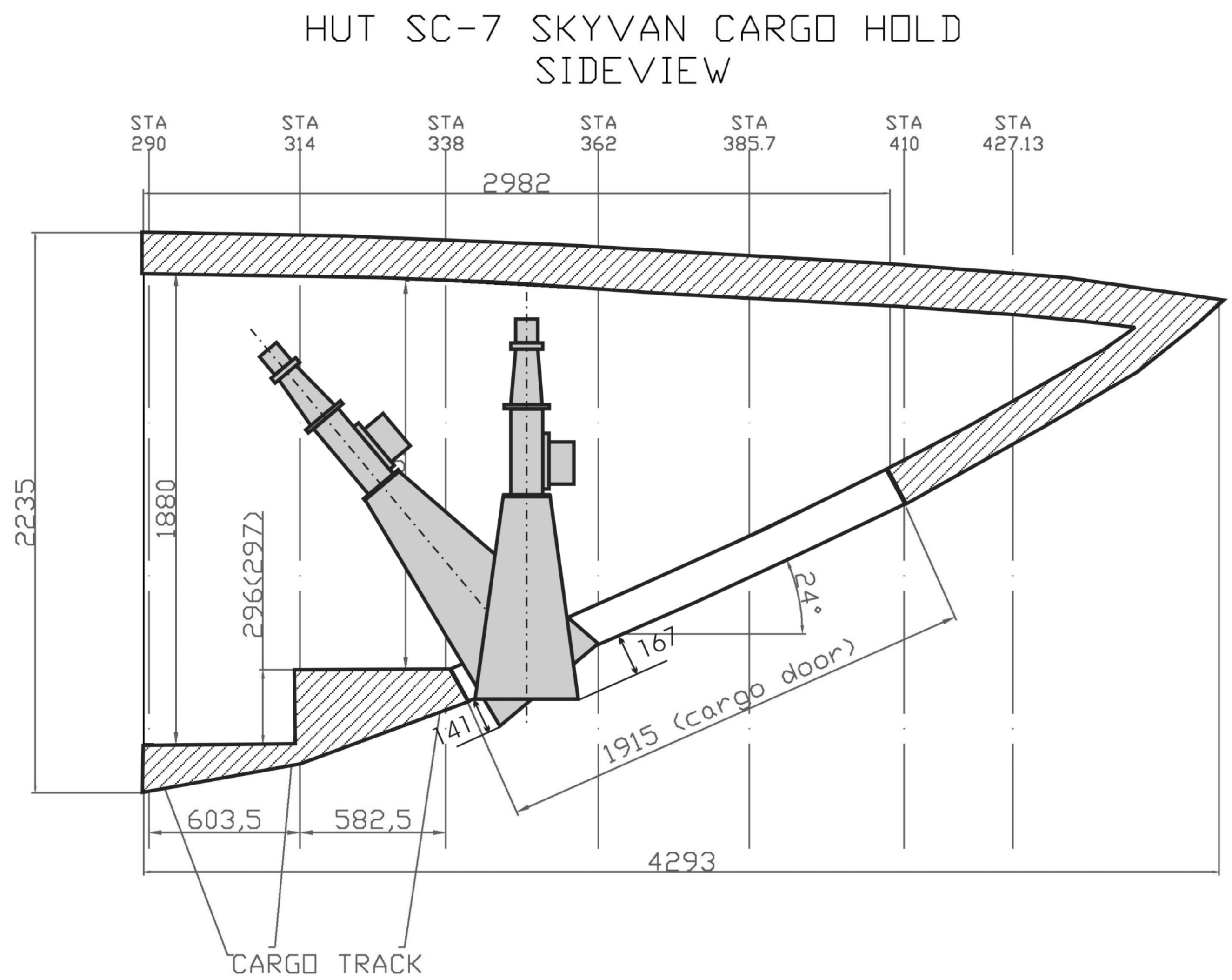

EMIRAD Horns in Skyvan

Installation Inside Skyvan

Two Flight Patterns off Norway

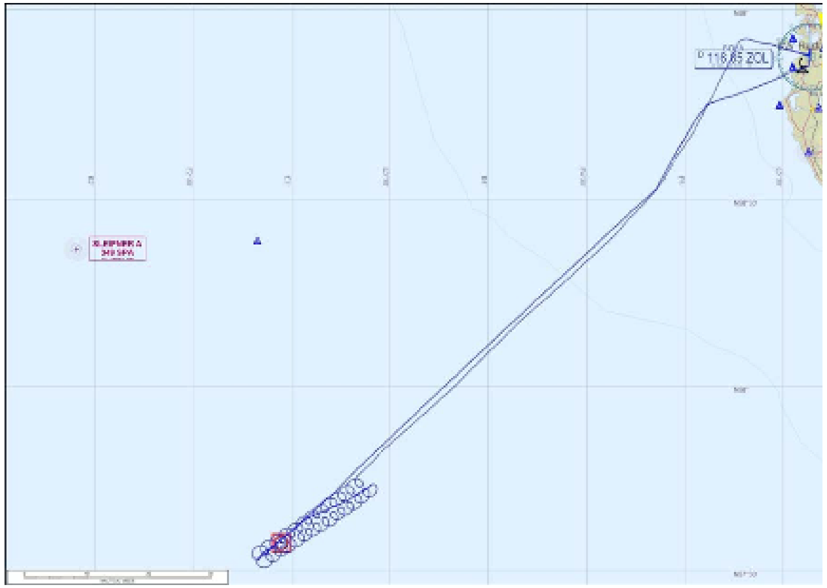

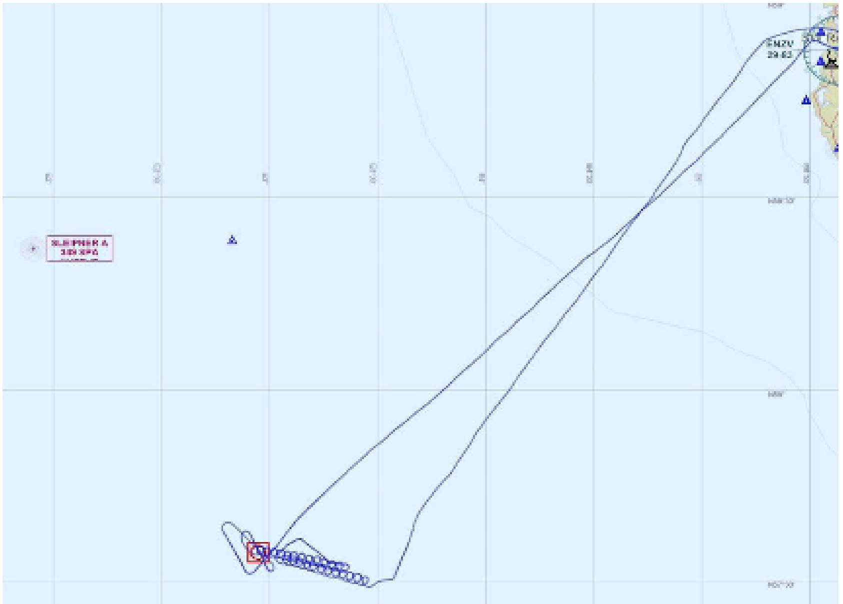

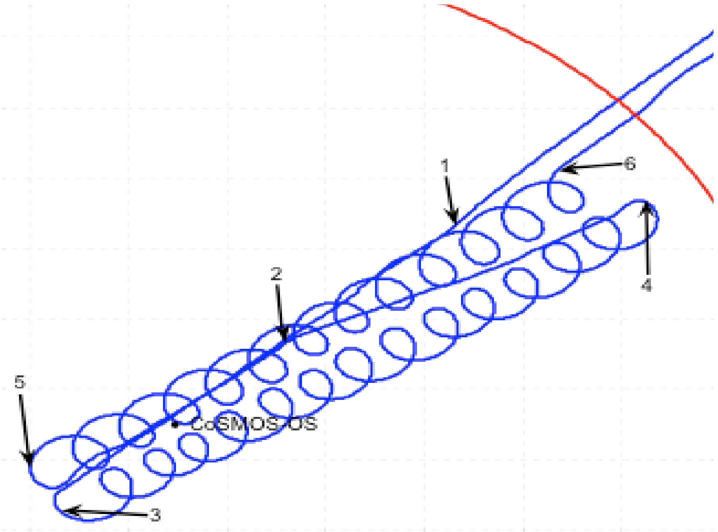

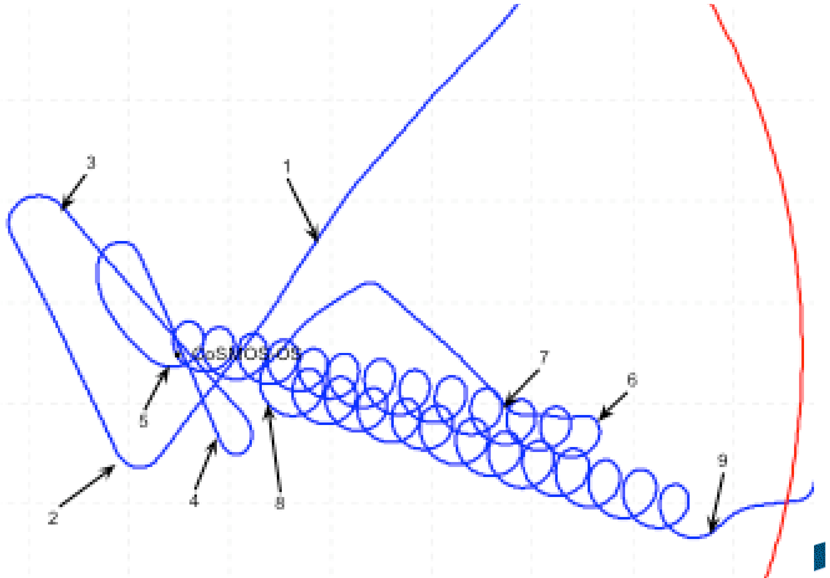

CoSMOS-OS Campaign

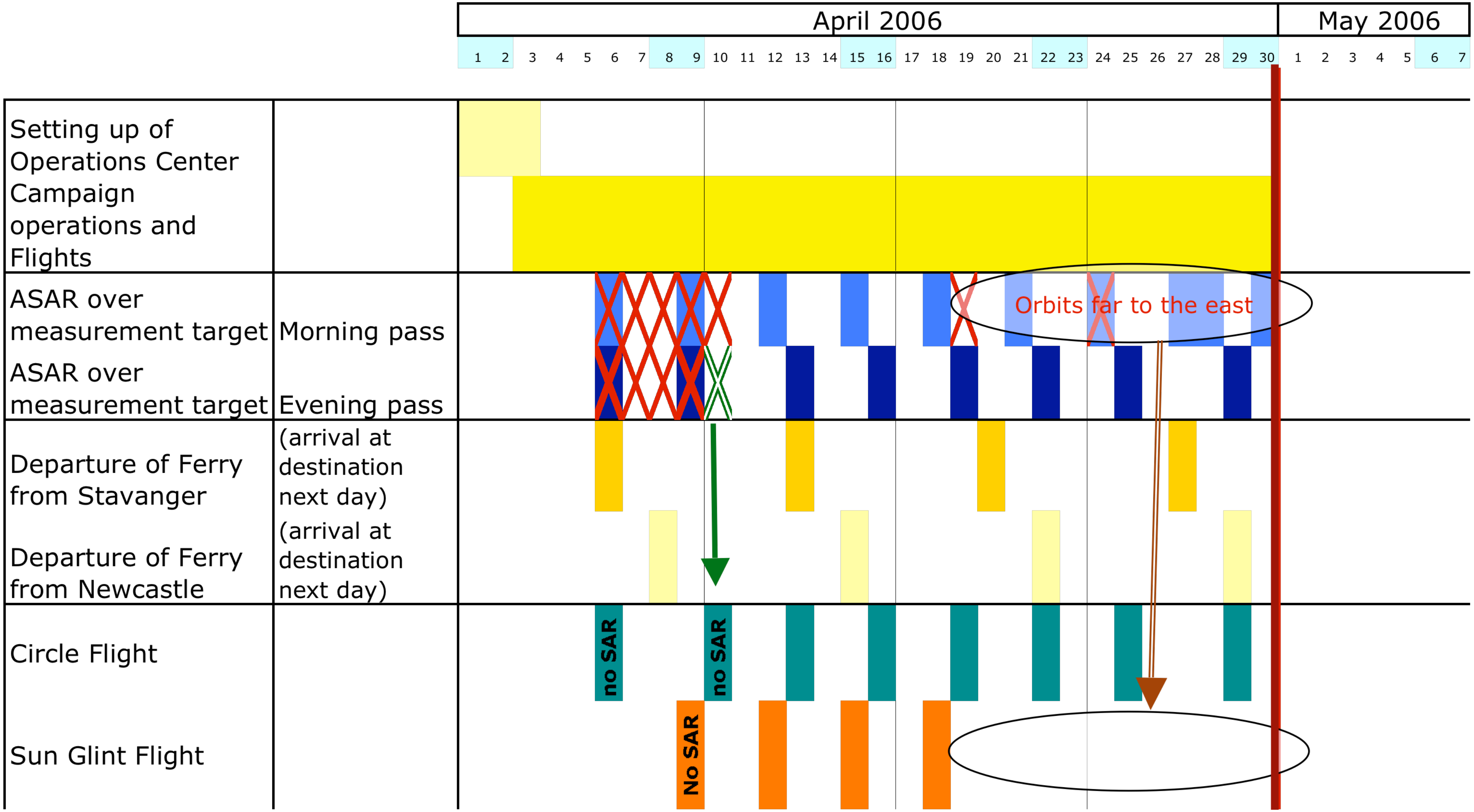

Pol-Ice Campaign, 2007

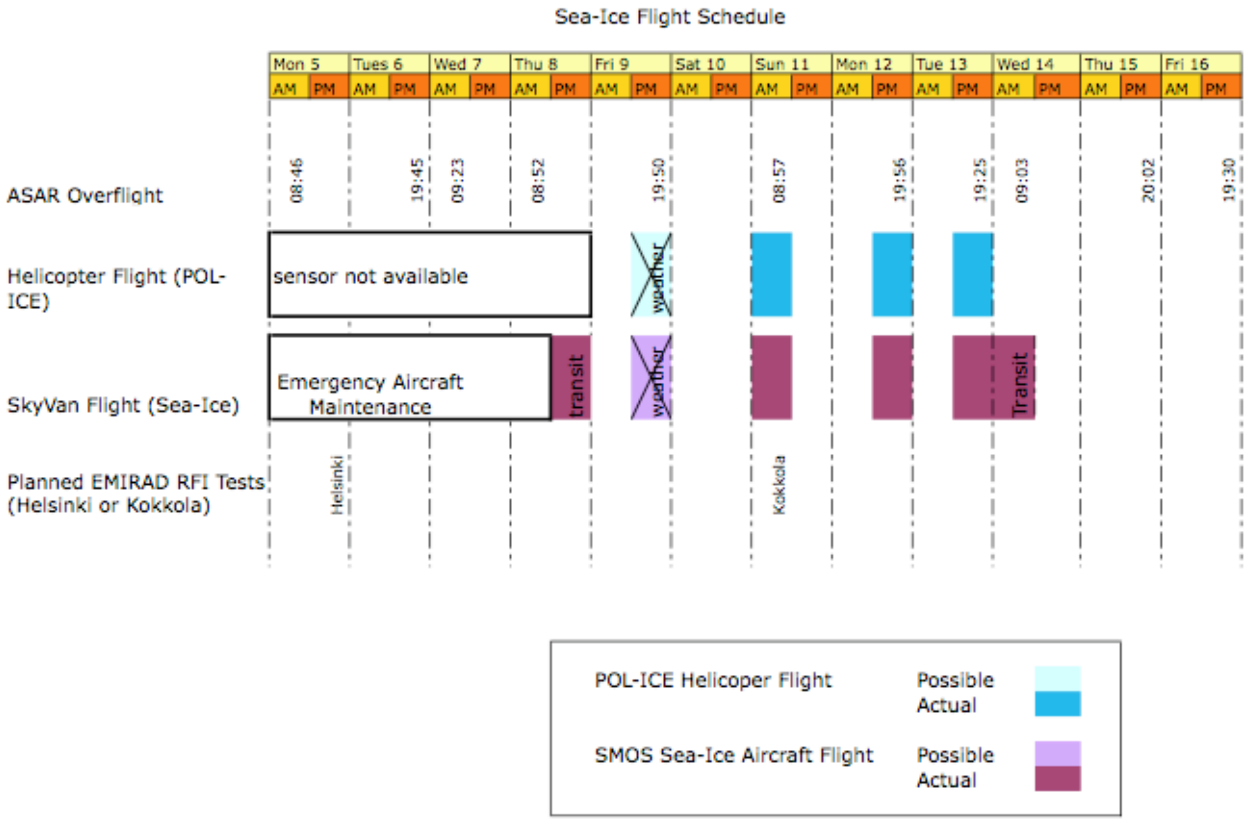

Demo Flight, 2007

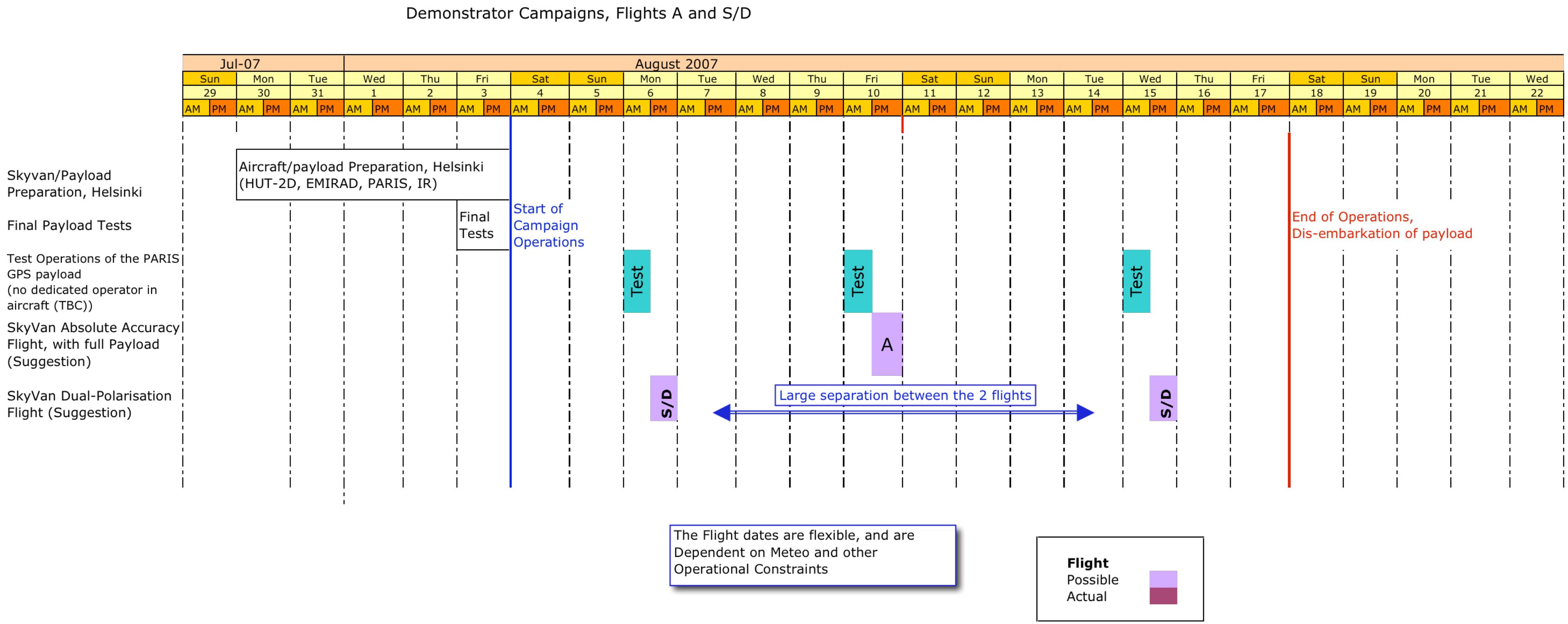

Rehearsal Campaign, 2008

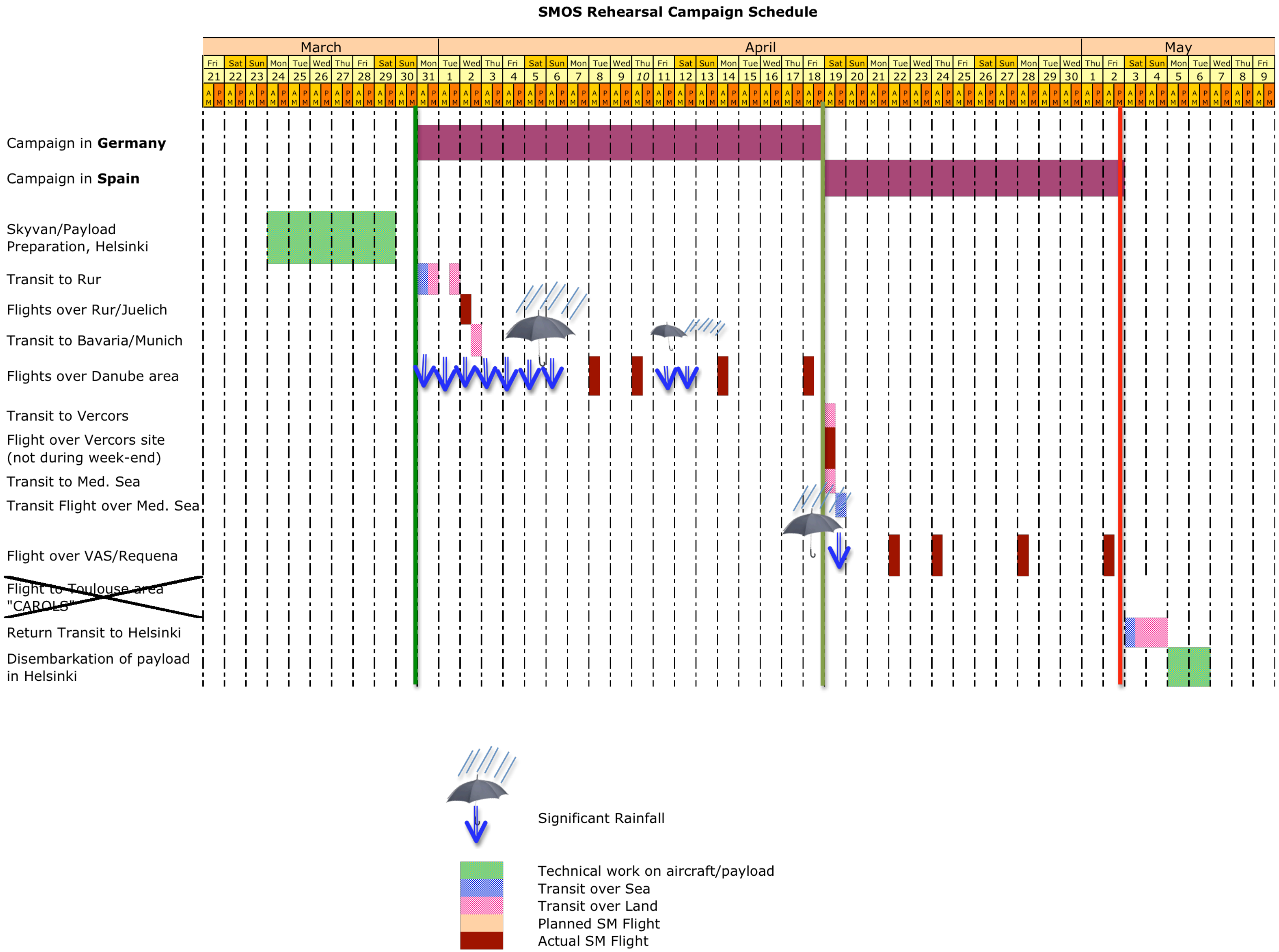

Cal / Val Campaign

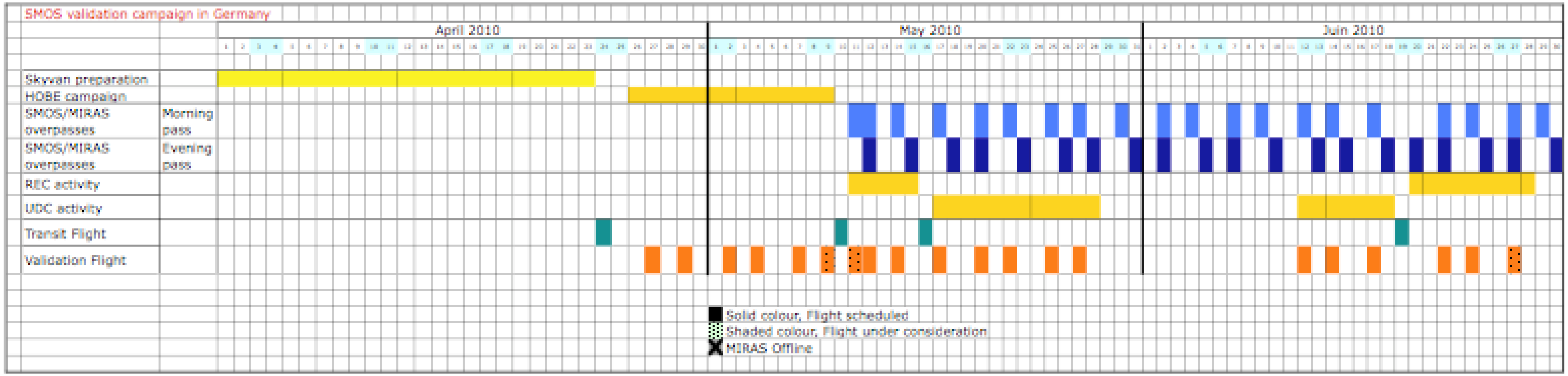

Conclusions

- EMIRAD-2 has worked very satisfactorily as:
  - supplier of well calibrated TB data
  - fully polarimetric instrument
  - built-in RFI detection by kurtosis
- EMIRAD-2 was installed on 2 small aircraft:
  - Aero Commander for Australian campaign
  - Skyvan for: - ocean campaign off Norway
  - - sea ice campaign in northern Finland
  - - salinity front campaign near Helsinki
  - - rehearsal campaign near München and Valencia
  - - Cal/Val campaign in Germany
  - - (cal/val campaign in Denmark)
- Consistently successful missions with good data quality and no loss of data!
- The RFI situation became a major issue!

AIRBORNE L-BAND RADIOMETER OBSERVATIONS OF SEA SURFACE SALINITY GRADIENTS AND AZIMUTH SIGNATURES.

Sten Schmidl Søbjærg and Niels Skou
DTU Space
Technical University of Denmark
sss@space.dtu.dk

Motivation

- ESA/SMOS mission, Launch fall 2009
- For Ocean, ΔTB / Δ SSS ≈ 1 K / psu <u>at best</u> (for warm water / high SSS)
- To find SSS to 0.1 psu level requires ΔT = 0.1 K and perfect knowledge/correction of other effects
- Worse sensitivity for low temperatures and low salinities
- TB depends also on SST and WS
- Azimuthal variations??
- Wiggles???

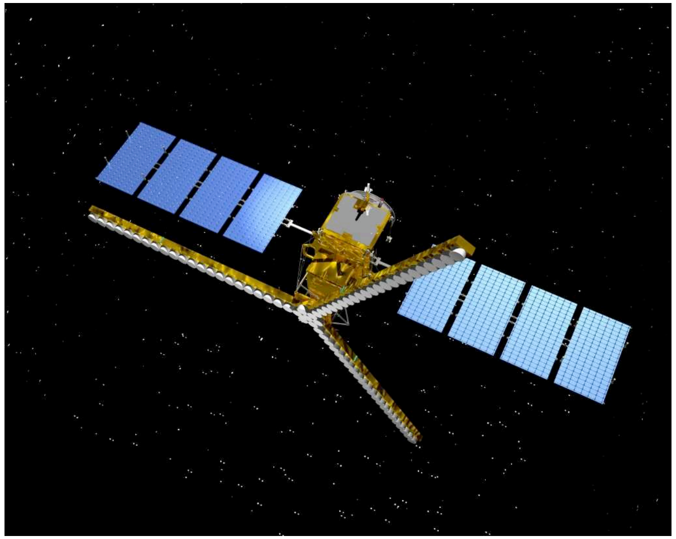

- **QUESTION ?**

  Is it realistic to detect small changes in SSS to any useful level, when so many corrections must be applied?

Campaign Activities
- Flight Tracks

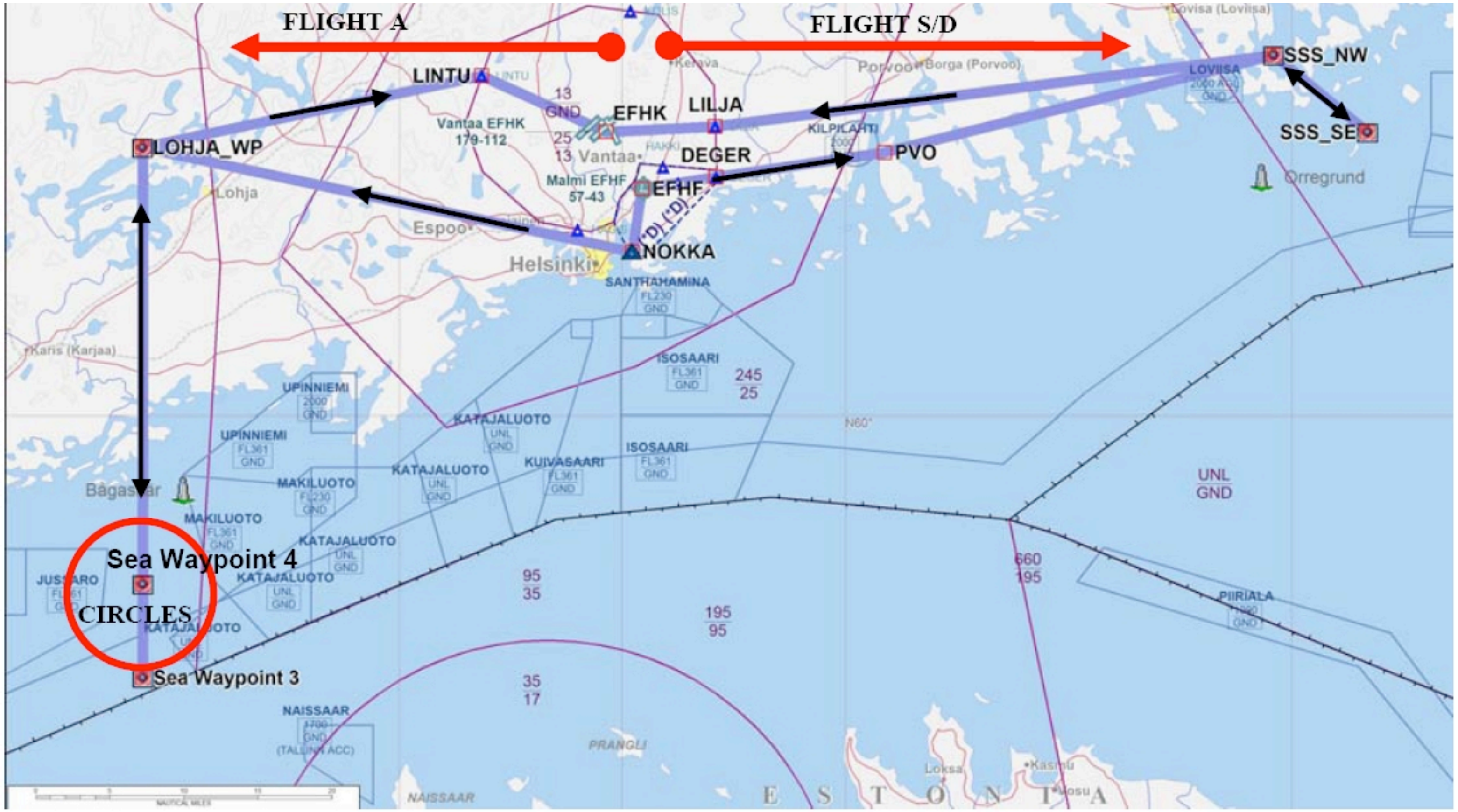

All airborne operations performed at night time!

Attitude Corrections
- Nose Wags (Raw Data)

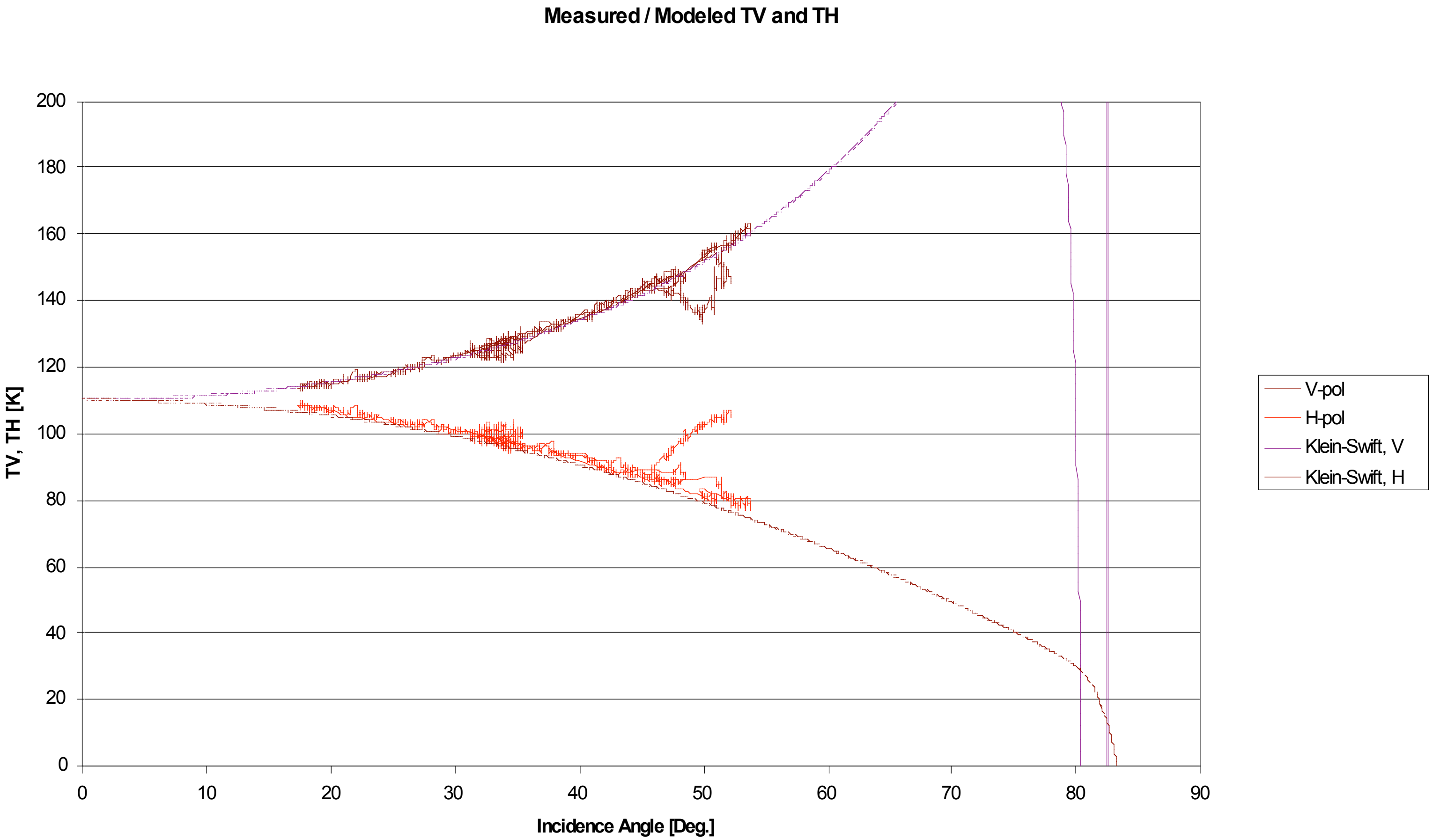

Attitude Corrections
- Polarization Rotation

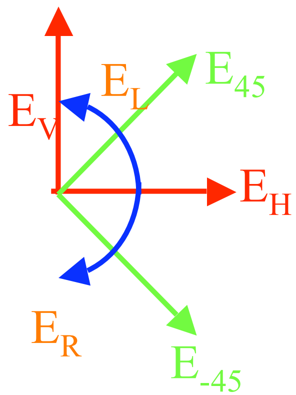

The Stokes vector in the ideal situation

$$\overline{T_B} = \begin{pmatrix} I \\ Q \\ U \\ V \end{pmatrix} = \begin{pmatrix} T_V + T_H \\ T_V - T_H \\ T_{45^o} - T_{-45^o} \\ T_l - T_r \end{pmatrix} = \frac{\lambda^2}{k \cdot z} \begin{pmatrix} \langle E_V^2 \rangle + \langle E_H^2 \rangle \\ \langle E_V^2 \rangle - \langle E_H^2 \rangle \\ 2\,\mathrm{Re}\langle E_V E_H^* \rangle \\ 2\,\mathrm{Im}\langle E_V E_H^* \rangle \end{pmatrix}$$

Antenna rotation => Polarization mixing

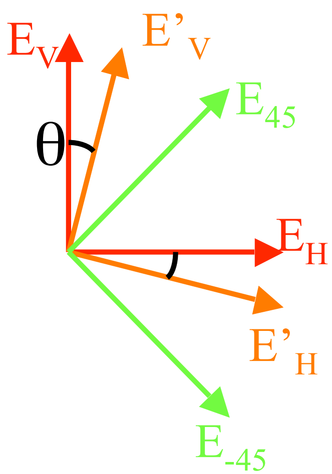

$$\overline{T_B}' = \begin{pmatrix} I' \\ Q' \\ U' \\ V' \end{pmatrix} = \begin{pmatrix} I \\ Q * \cos(2\theta) + U \sin(2\theta) \\ -Q * \sin(2\theta) + U \cos(2\theta) \\ V \end{pmatrix}$$

Measured Stokes vector with antenna rotation θ.
Q=70 K and 0.05° error will cause an uncompensated error of 120 mK to U

Data Validation

- Incidence angle variations corrected for roll

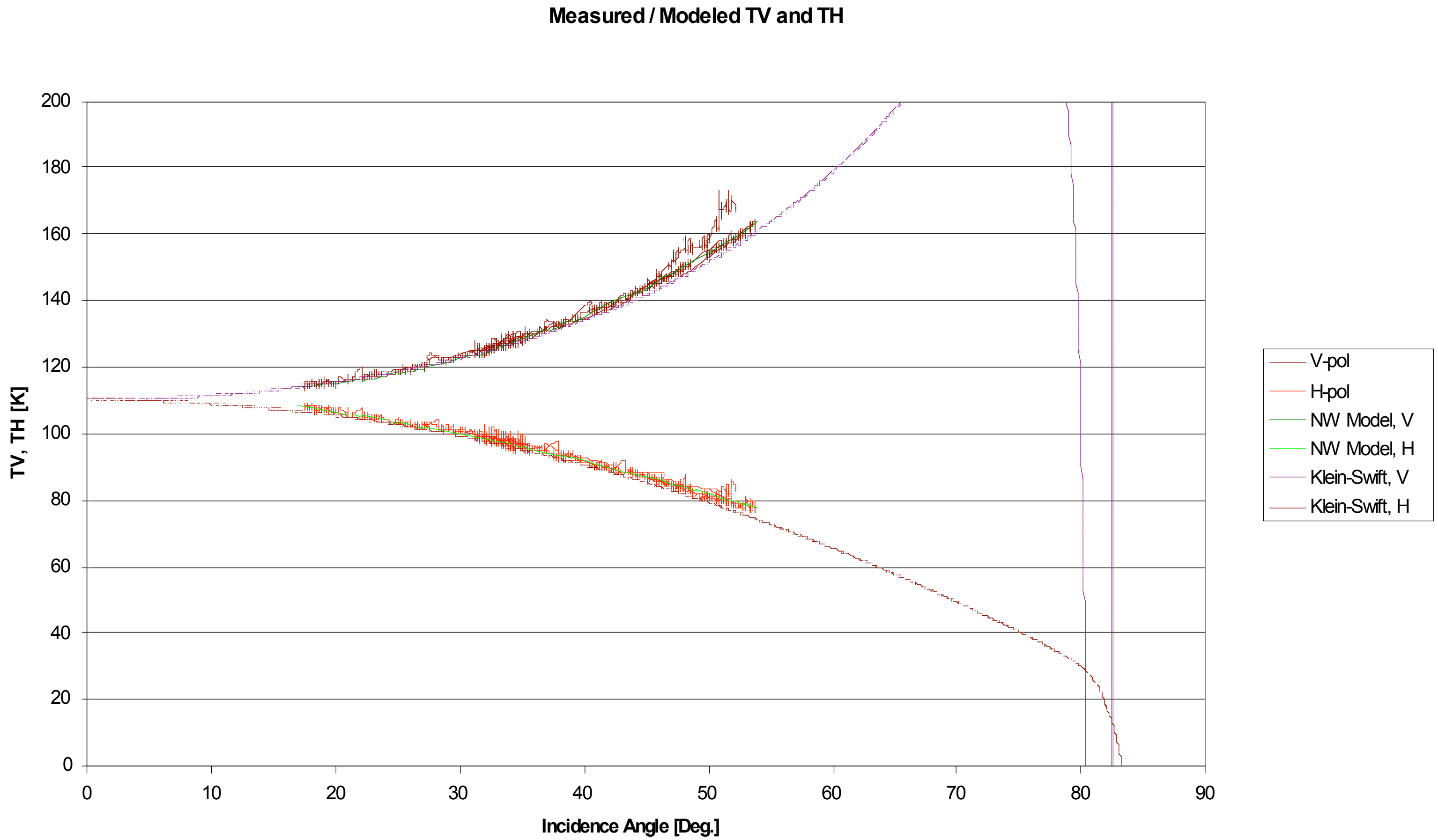

Data Validation
- Nose Wags (Normalized to 43º Incidence)

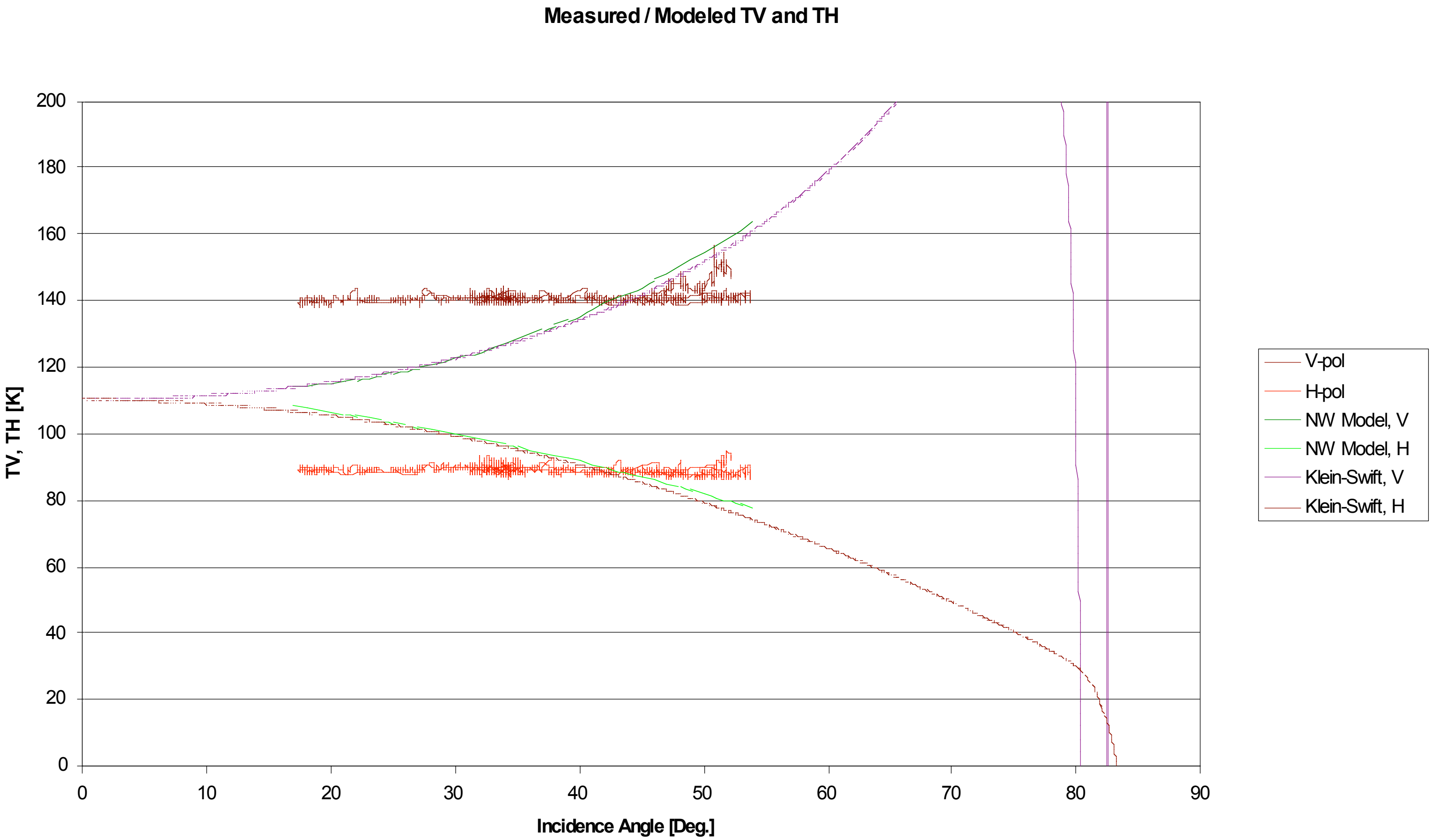

Campaign Activities
- Salinity Gradient Site

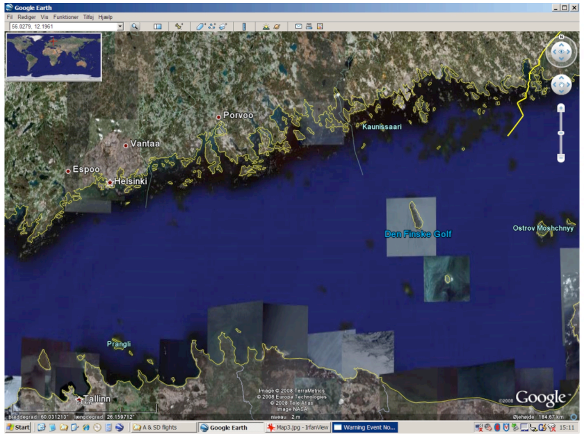

- Close to Aircraft Base in Helsinki
- Access to boat from HUT for ground truth
- River Outlet behind narrow strait
  => Salinity Gradient
- Almost no wind for several days!
- VERY low salinity in the Gulf of Finland
- Temperature gradient along flight track

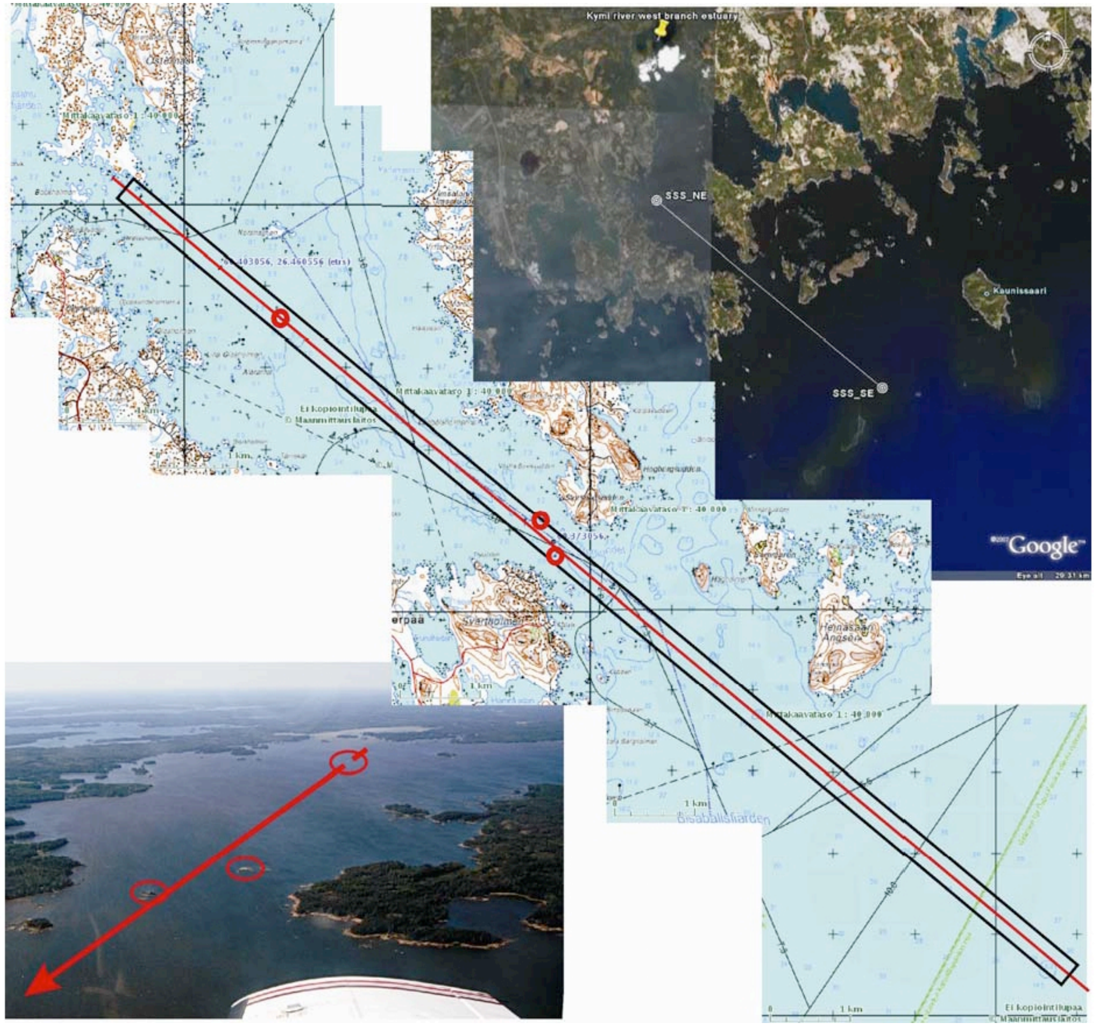

Salinity Measurement
- Sensitivities to Sea Surface Salinity

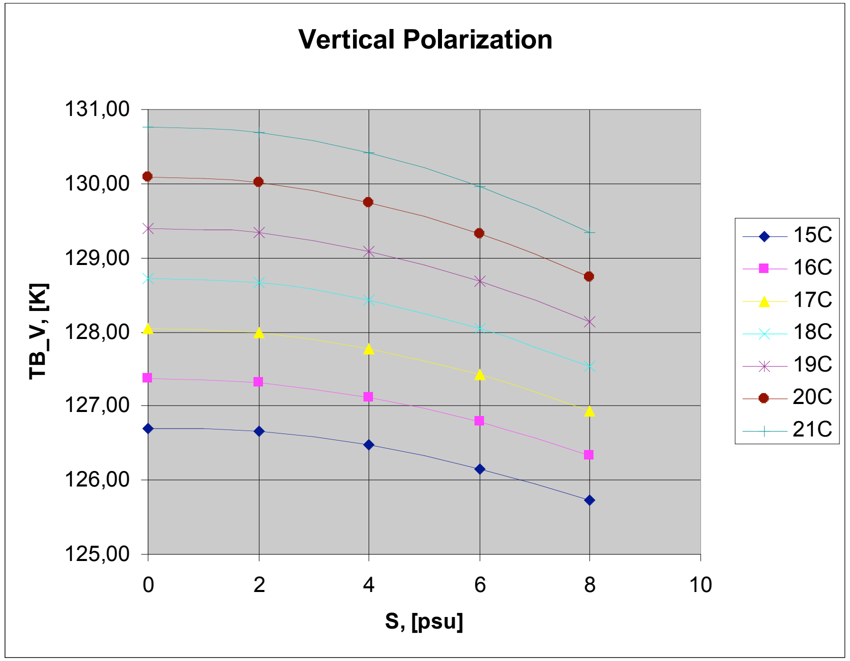

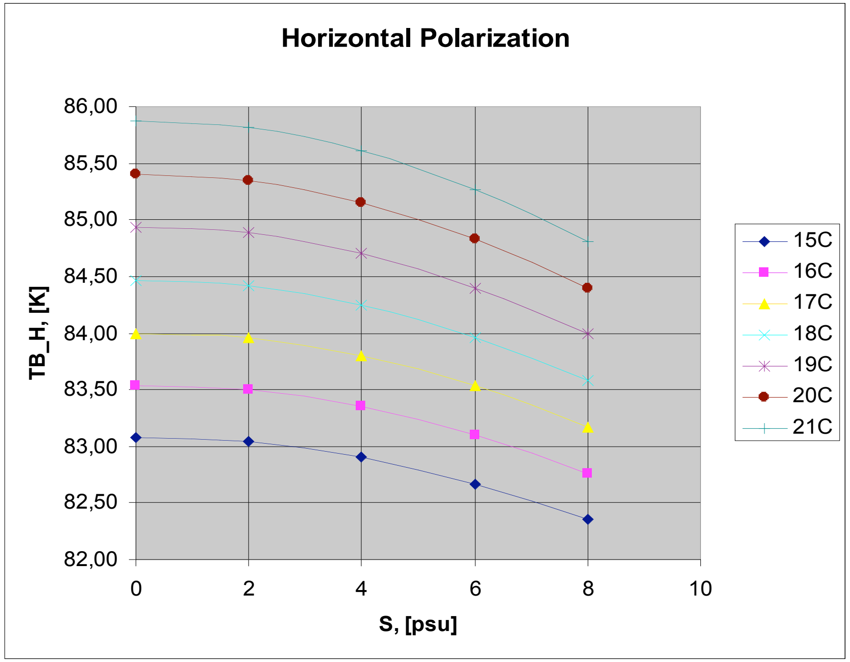

- Very small sensitivity at low salinities
- $\Delta TB/\Delta S \approx 0.10$ K/psu @ V-pol
- $\Delta TB/\Delta S \approx 0.05$ K/psu @ H-pol

Salinity Measurement
- Sensitivities to Sea Surface Temperature

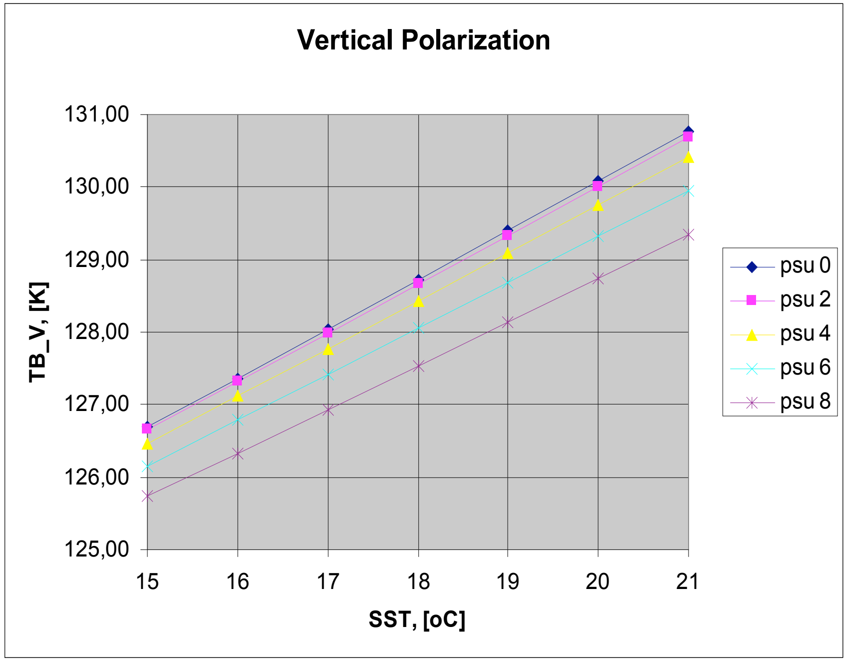

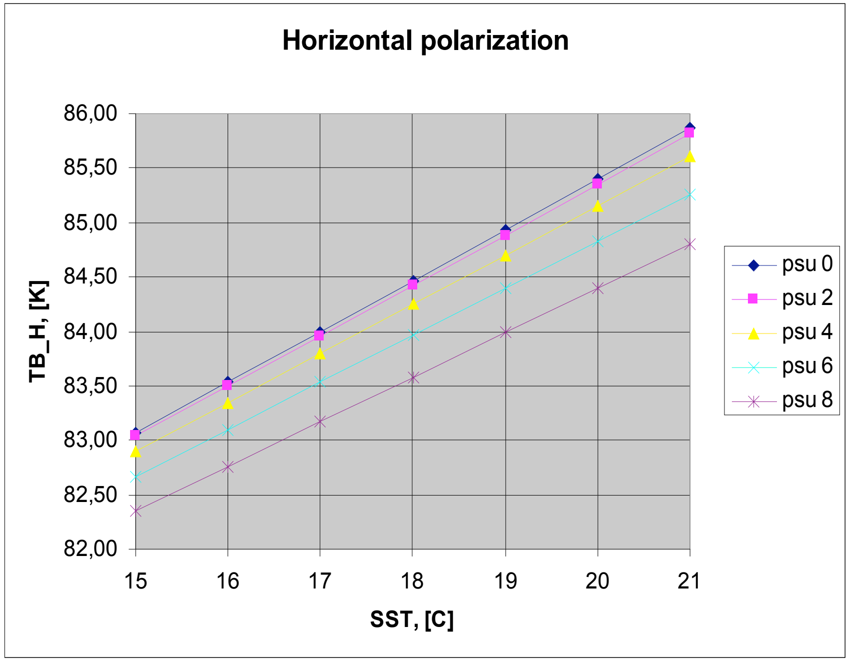

- Influence from SST
- ΔTB/ΔT ≈ 0.6 K/°C @ V-pol
- ΔTB/ΔT ≈ 0.5 K/°C @ H-pol
- Sensitivities almost independent from SSS

Influence from the Galactic Background

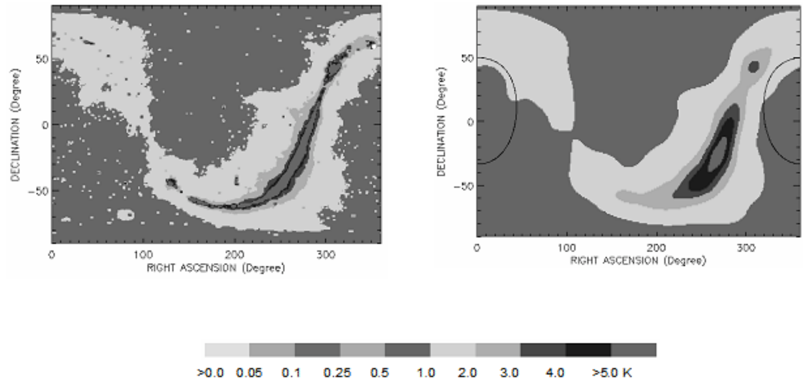

4.5 passes are shown in the figure.

A clear two-step shape is identified.

Correction must be applied to remove the galactic background change!

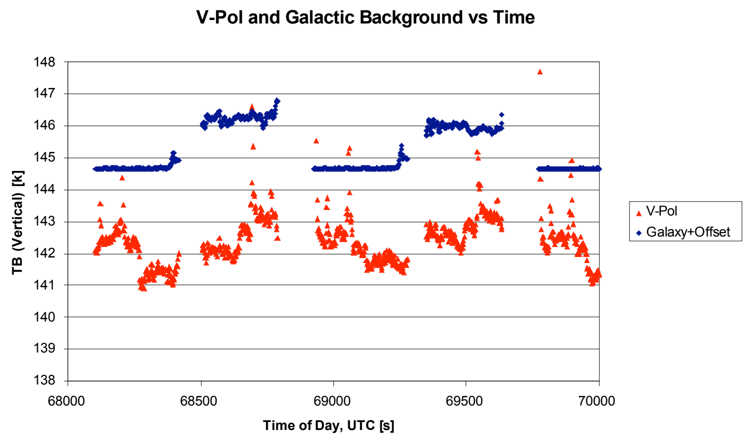

Test Area
- Salinity Profile and Expected Response

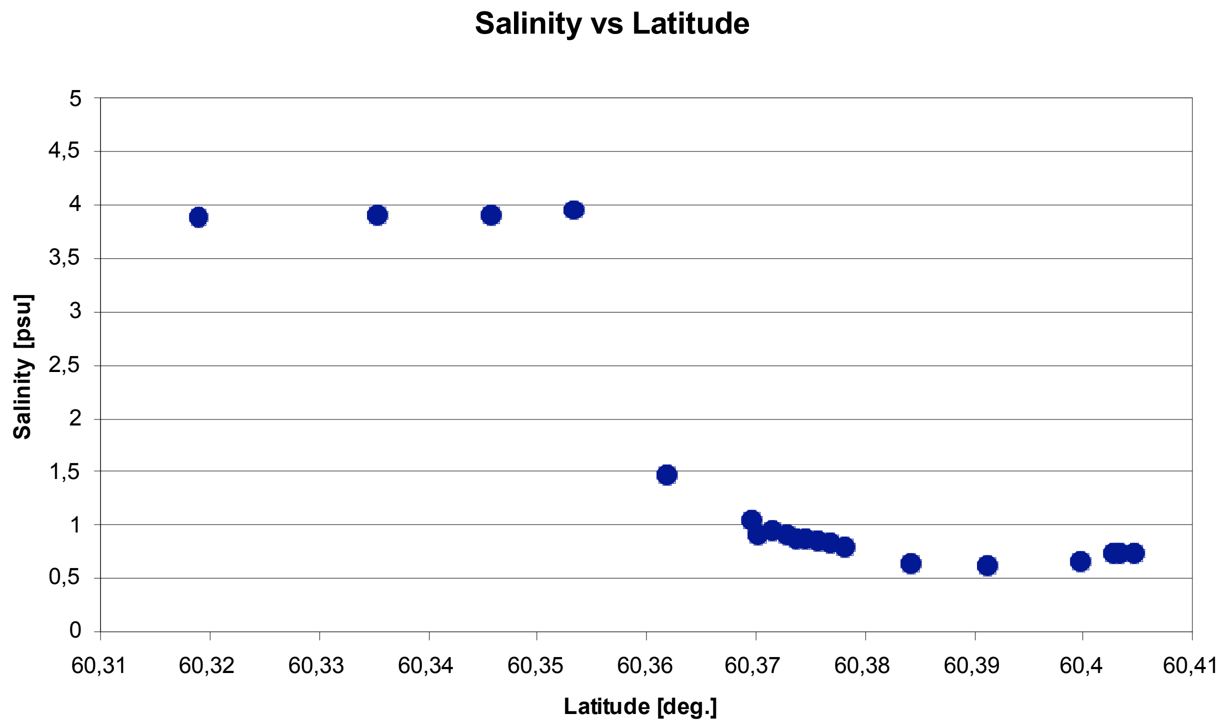

	Aft Horn	Nadir Horn
V-Pol	+0.32 K	+0.28 K
H-Pol	+0.23 K	+0.28 K

Test Area
- Temperature Profile and Expected Response

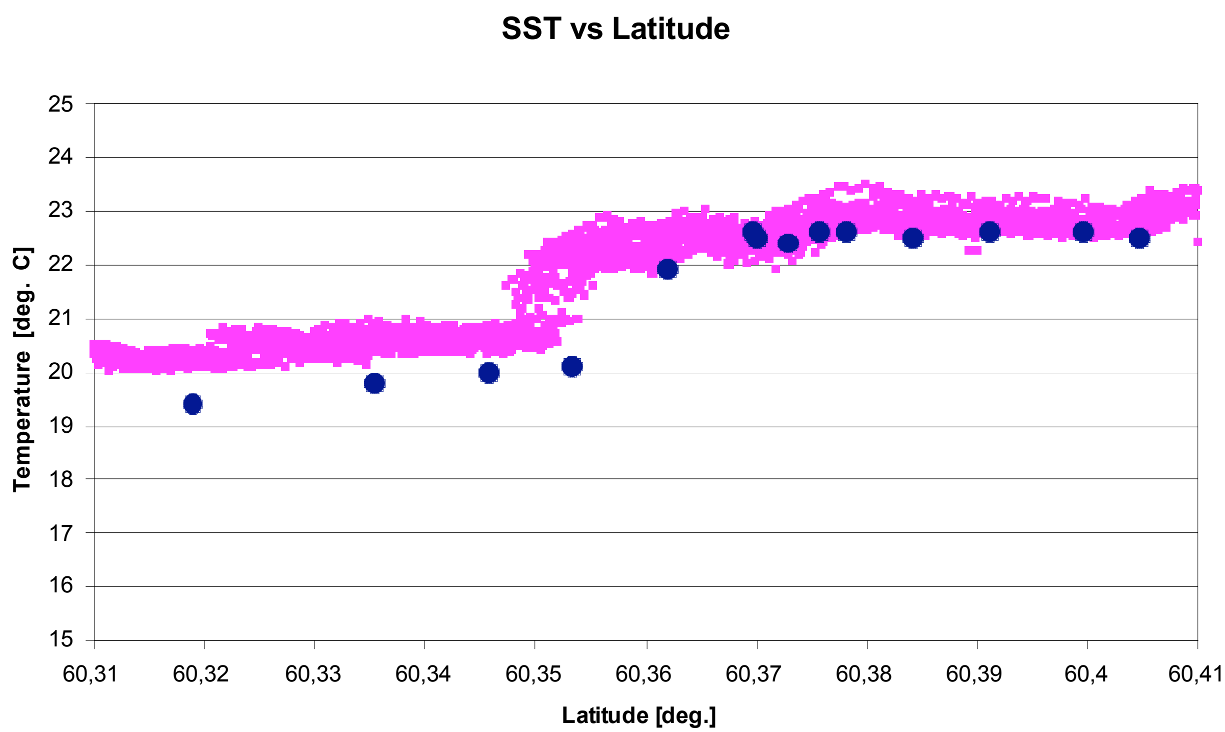

Purple:

Internal TIR

Blue:

In-Situ

	Aft Horn	Nadir Horn
V-Pol	+1.39 K	+1.13 K
H-Pol	+0.89 K	+1.13 K

Measured Data (40 deg. Incidence Angle) - Data for 20 Overpasses (V-pol and H-pol)

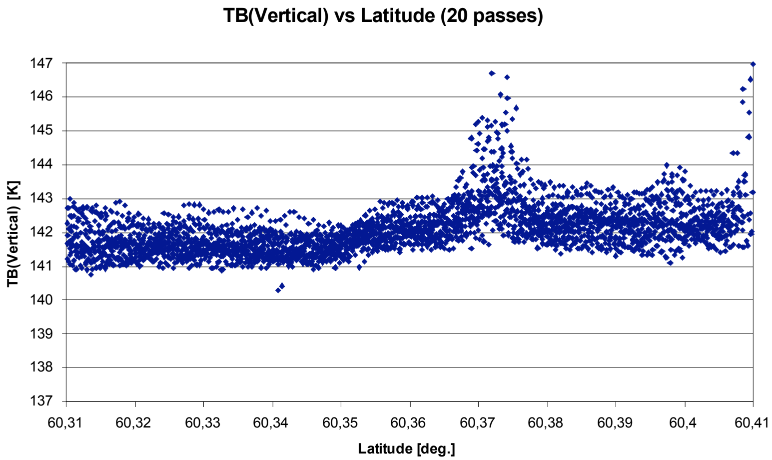

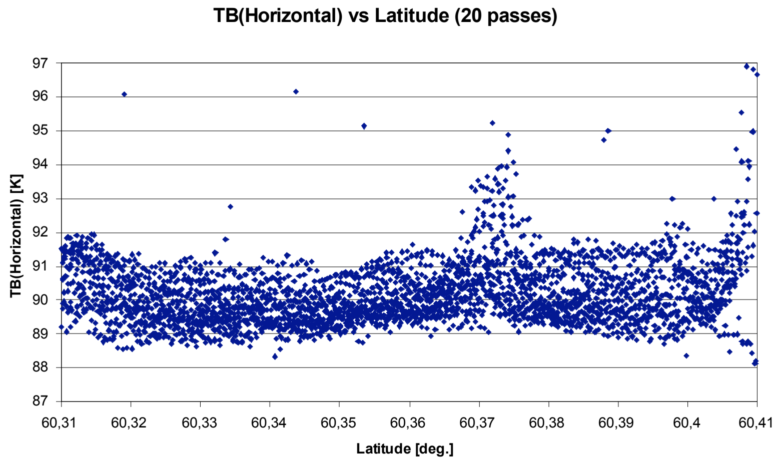

- SST change removal based on Klein-Swift Model
- Expected deviation from Normalization Temperature is subtracted

Measured Data (40 deg. Incidence Angle) - All Overpasses Averaged

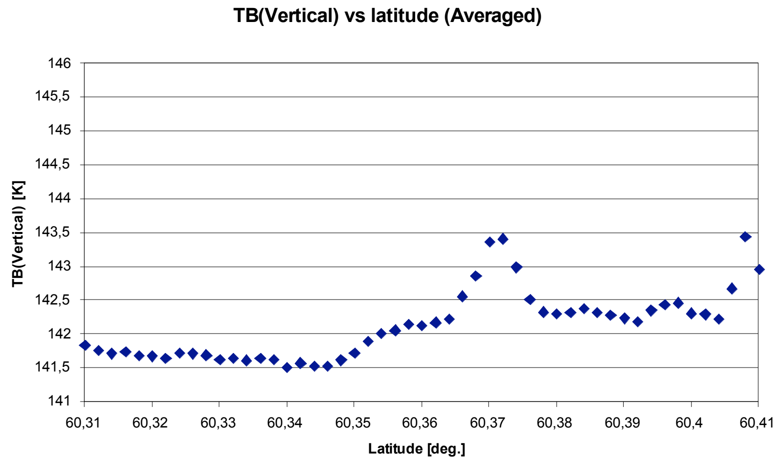

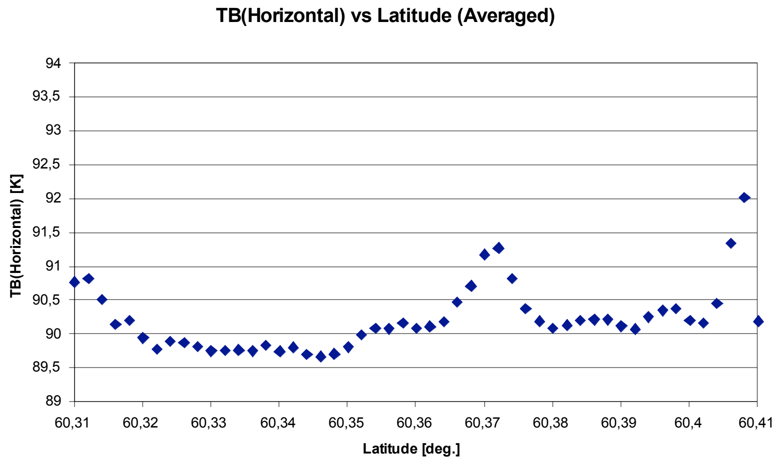

- All data points for each latitude bin are averaged
- We find ≈ 0.5 K for V (0.32 expected)
- We find ≈ 0.4 K for H (0.23 expected)

Measured Data (0 deg. Incidence Angle) - All Overpasses Averaged

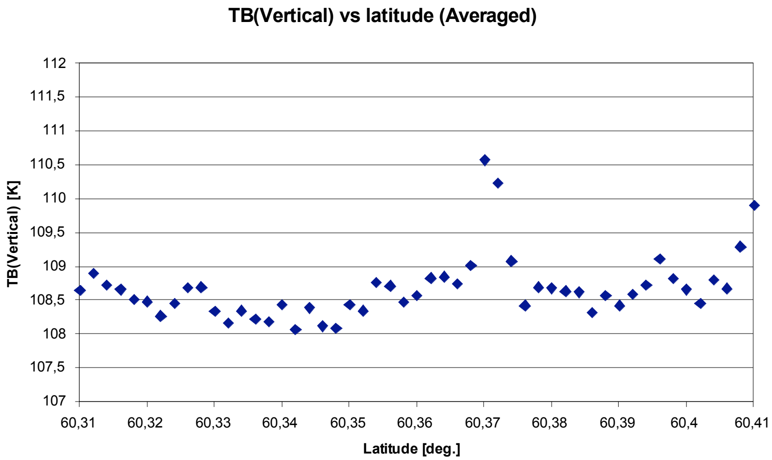

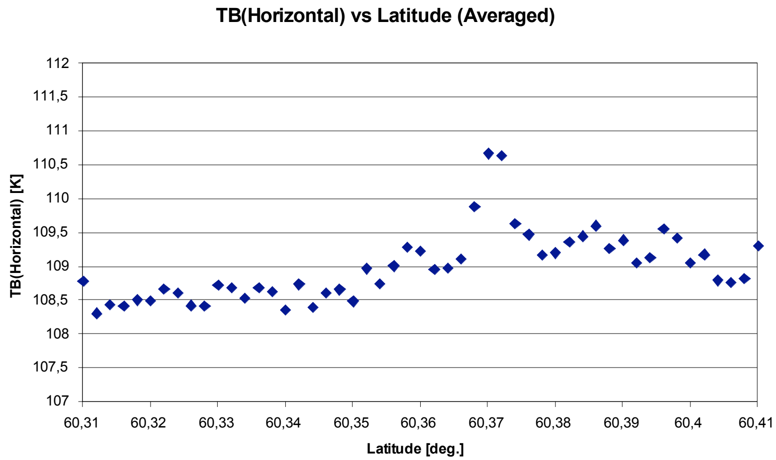

- All data points for each latitude bin are averaged
- We find ≈ 0.4 K for V (0.28 expected)
- We find ≈ 0.6 K for H (0.28 expected)

Azimuth Signatures- Raw Data (V-Pol)
3 + 5 circles with 15° roll

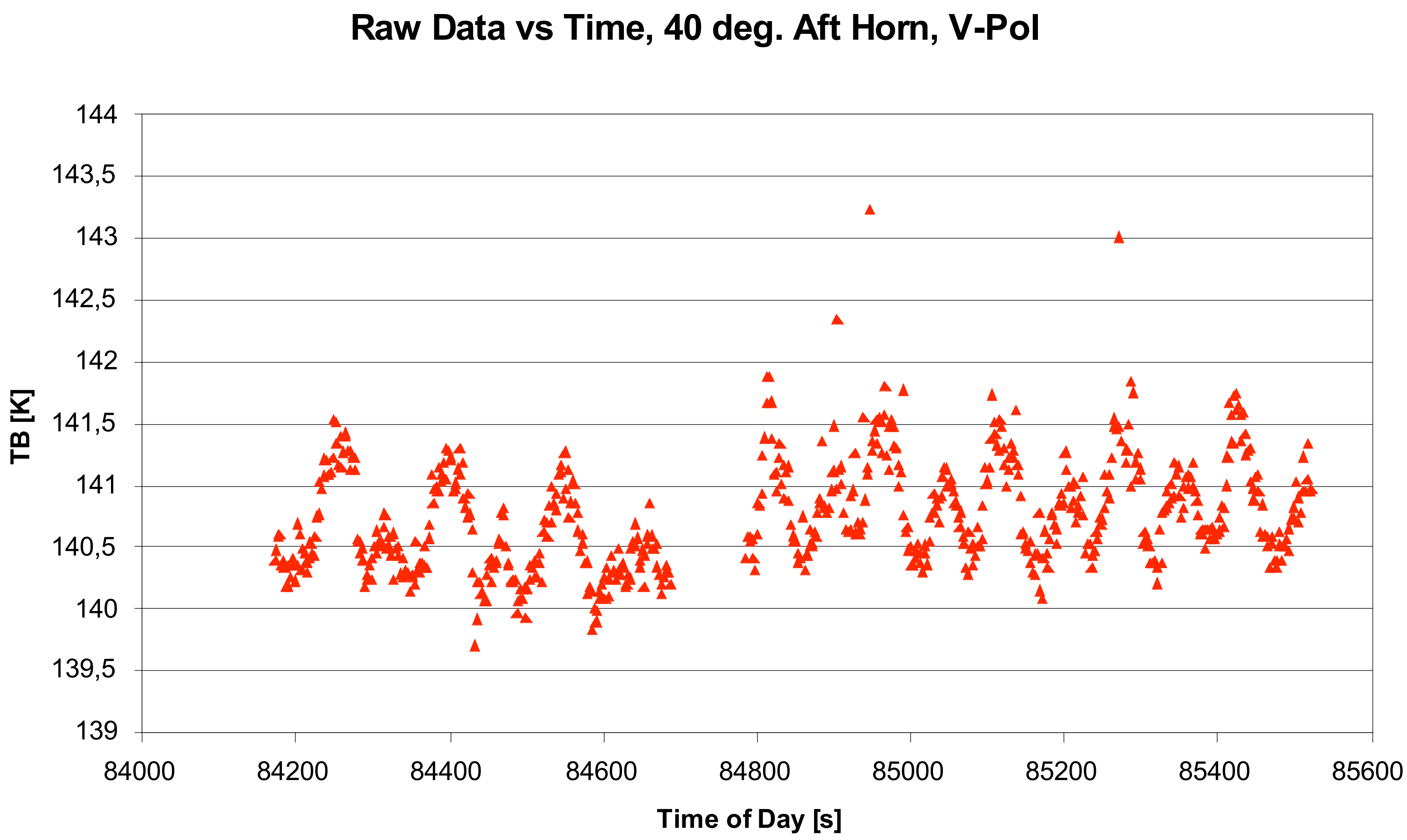

Azimuth Signatures - Attitude corrected Data vs. Azimuth Angle (0 = North)

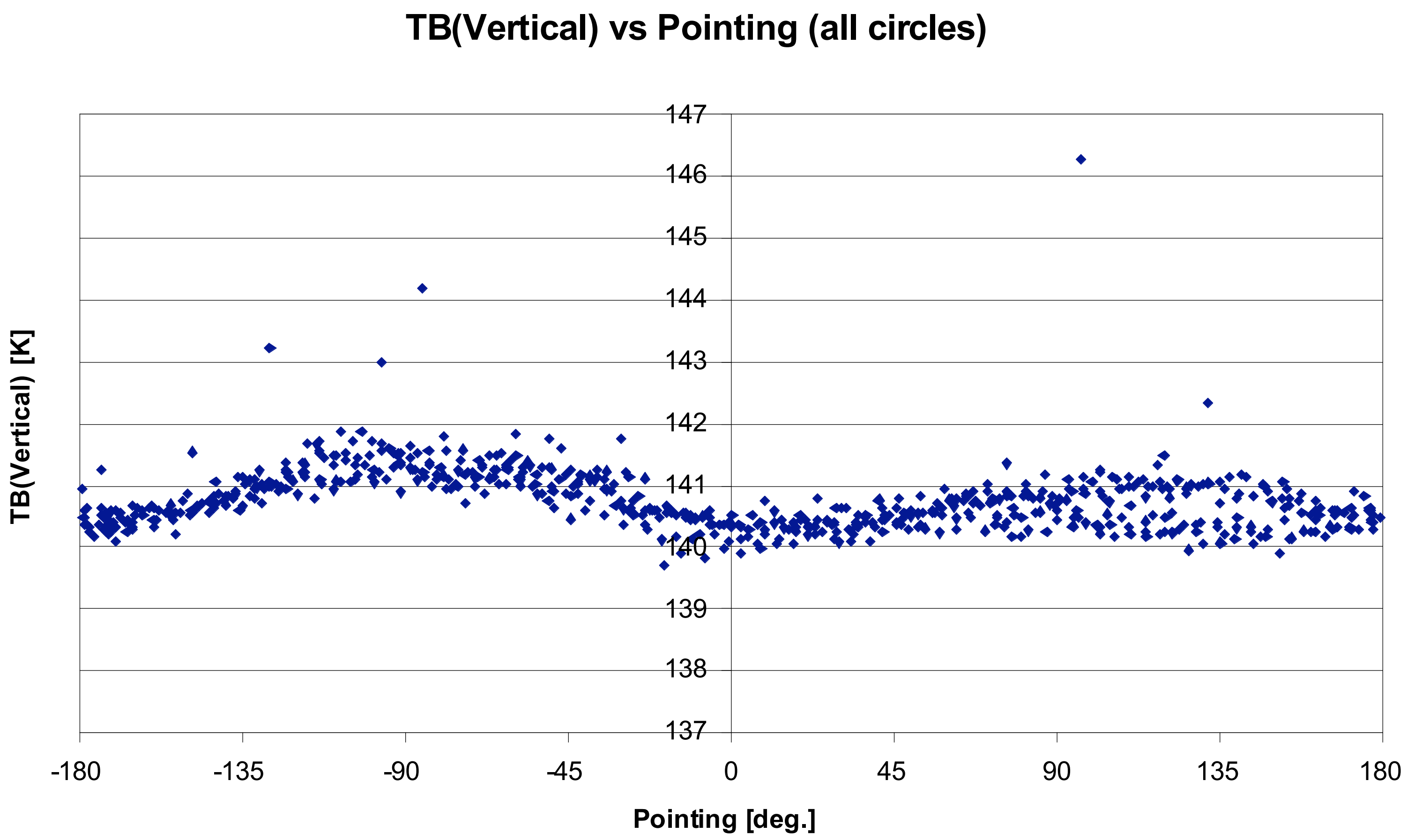

Azimuth Signatures
- Galactic Background Signature

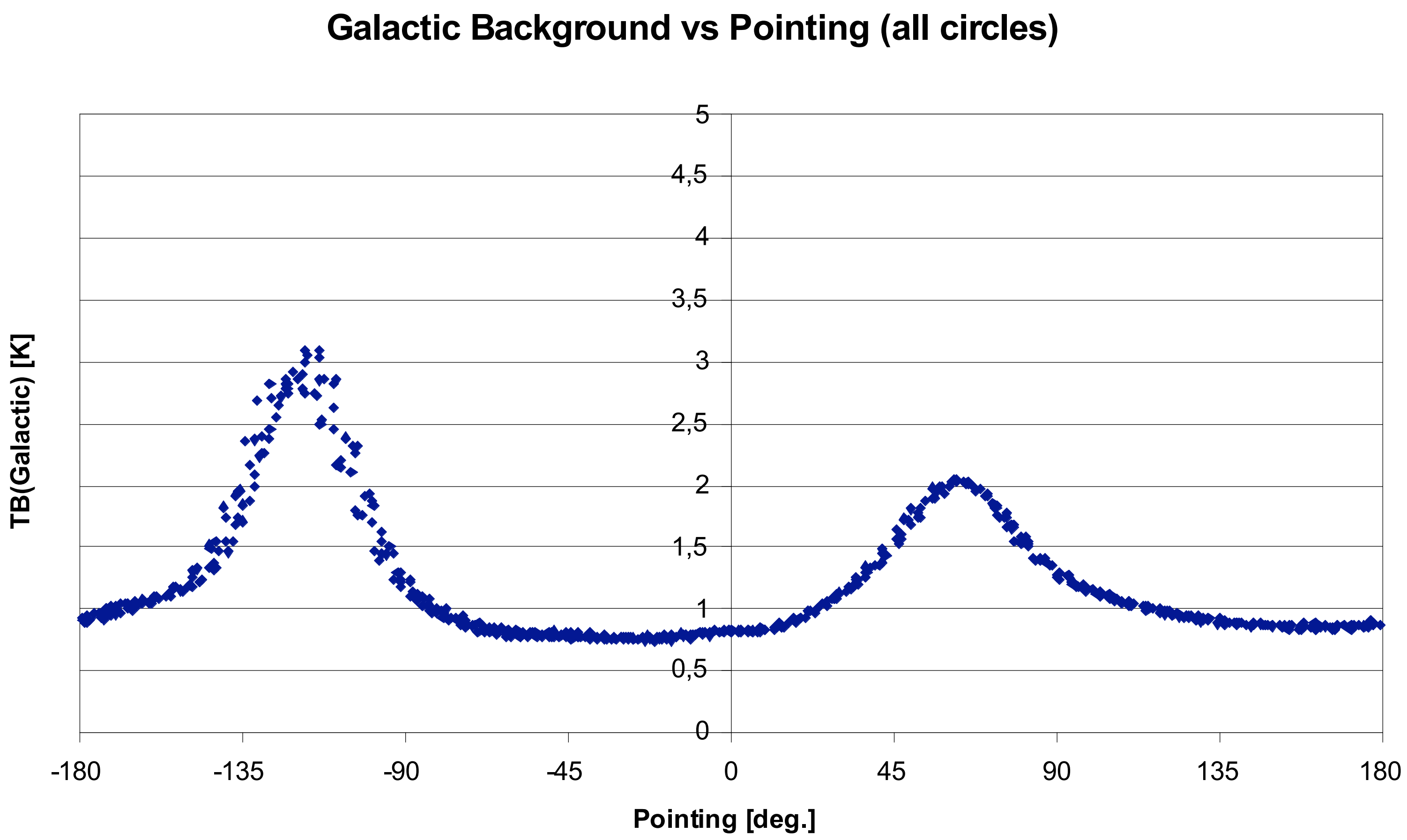

Averaged Azimuth Signatures (40 deg.) - Without Galactic Background (V and H)

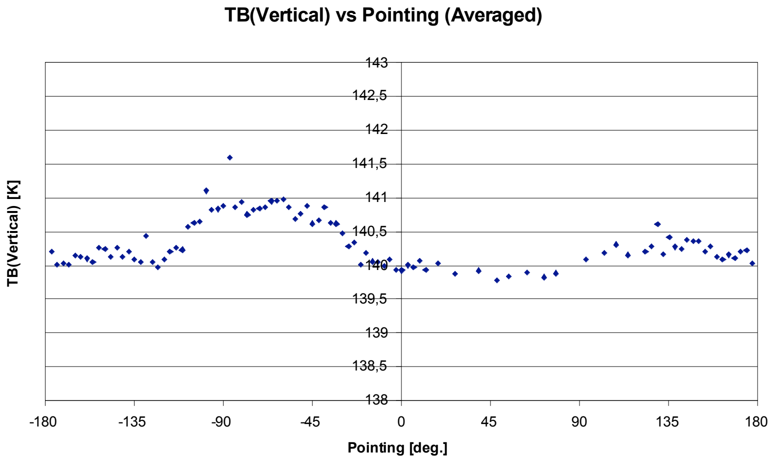

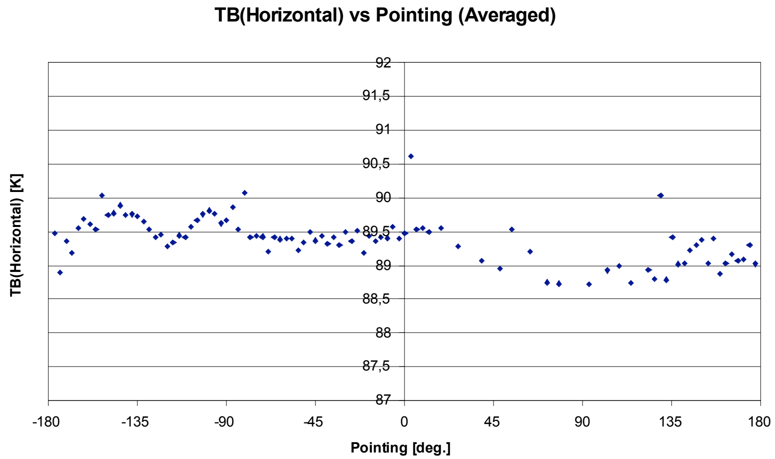

Azimuth Signatures (Aft Horn) - Full Stokes Vector Response

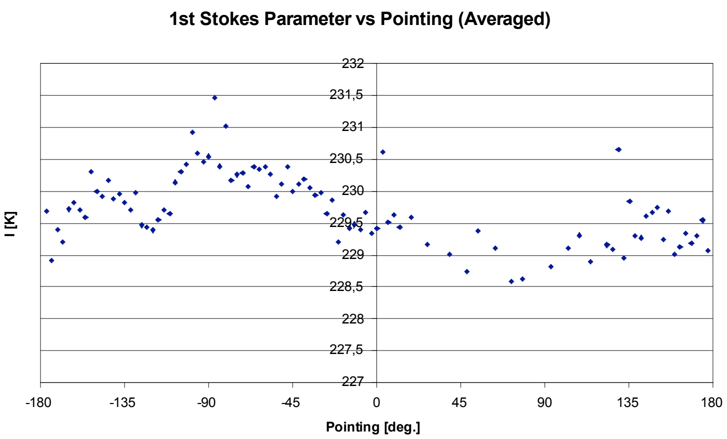

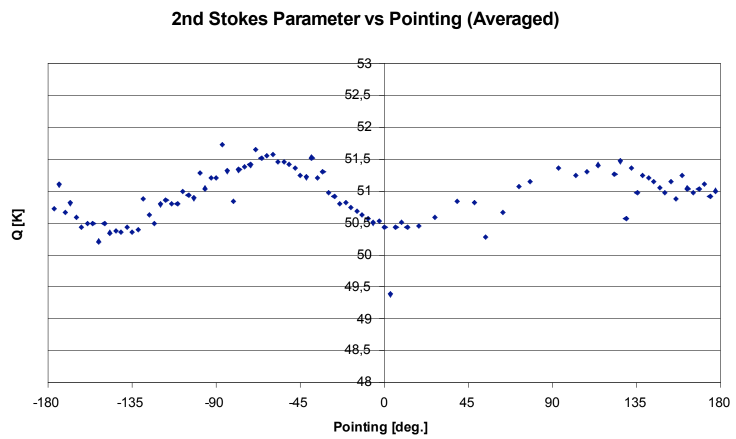

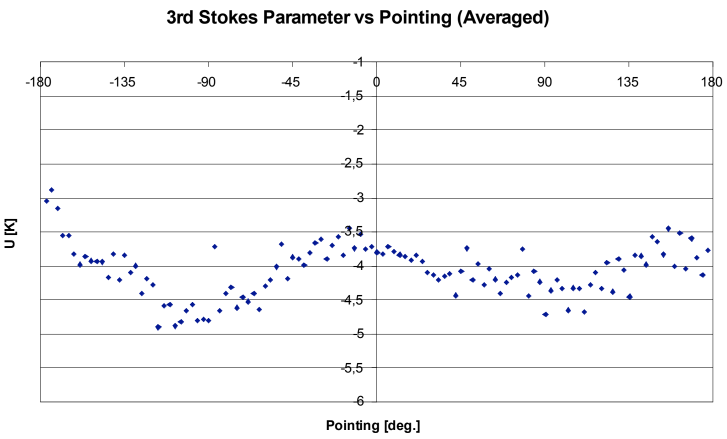

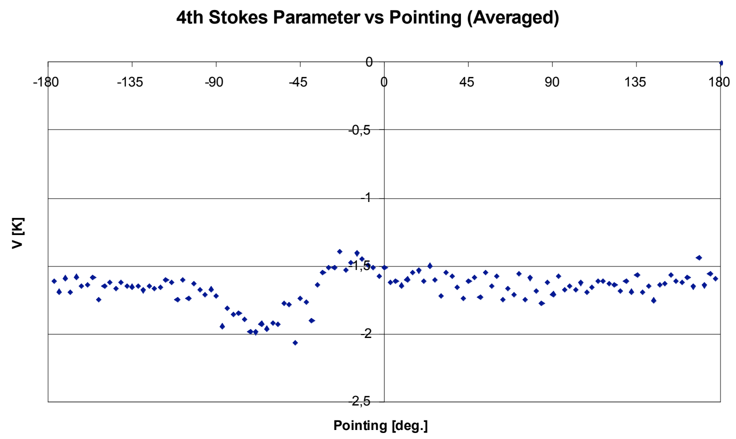

Typical Model Function (much higher freq.)

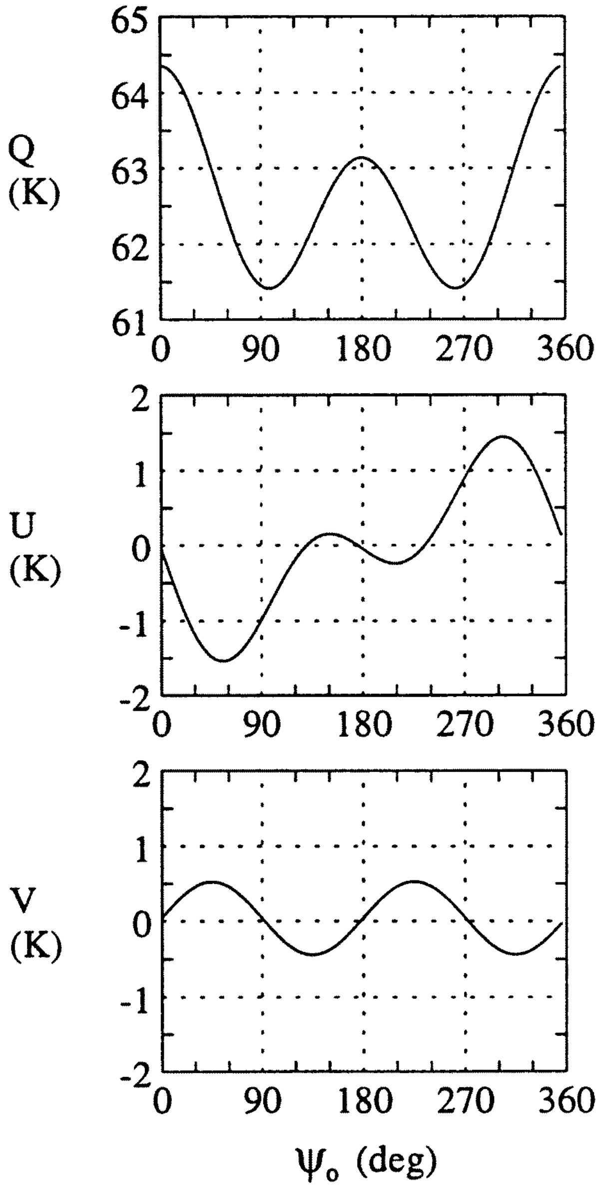

Azimuth Signatures (Nadir Horn @ 15 deg.) - Full Stokes Vector Response

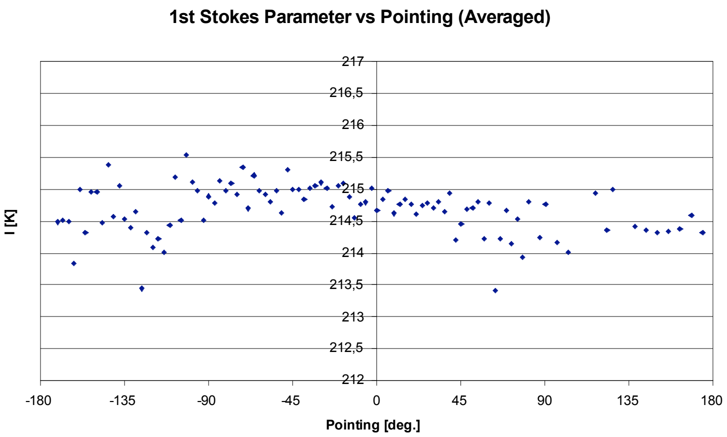

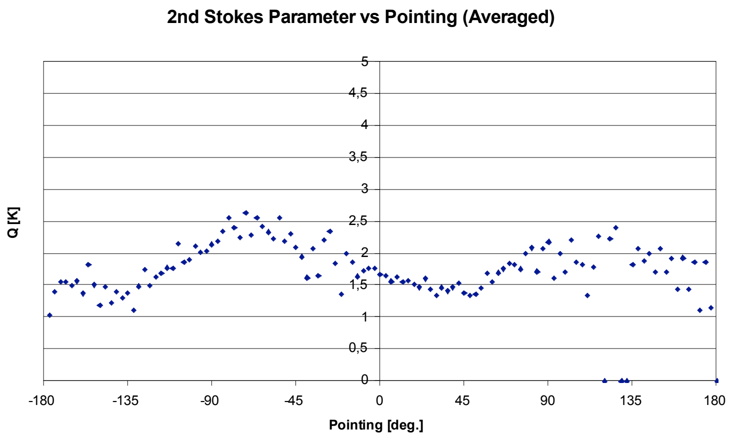

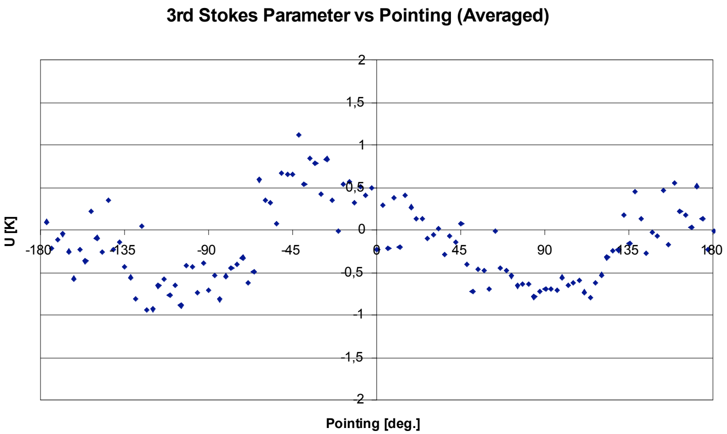

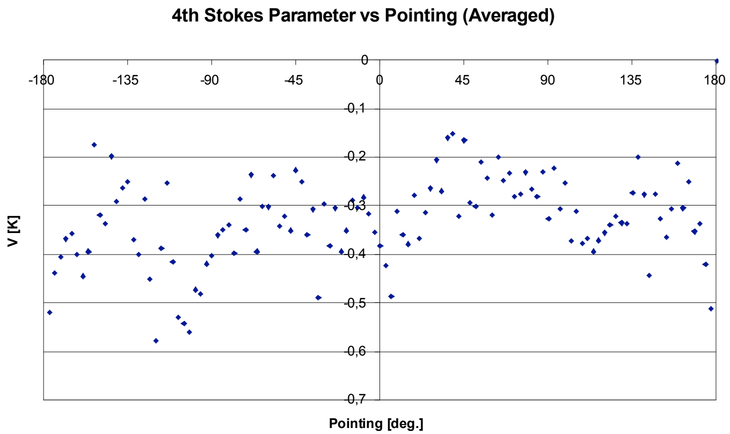

Discussion and Conclusions

- Very difficult salinity front selected: low salinity => low TB signal
- But realistic signal considering what we want SMOS to see!
- 20 passes (back and forth) over salinity front - wiggles disappear
- Corrected for temperature
- Corrected for Galactic radiation
- Good consistency back and forth
- Salinity front detected! (slightly over-estimated)

- Circle flights over relatively shallow water
- Corrected for aircraft attitude
- Corrected for Galactic radiation
- Wiggles averages away
- Clear azimuthal signature - the polarimetric channels show the features known for other frequencies
- Hard to see what could cause this if not a genuine ocean signal
- Small signal in line with what was seen in LOSAC

CoSMOS: Instruments and Airplanes

Niels Skou, Sten Søbjærg, and Steen Kristensen
DTU Space
Technical University of Denmark
ns@space.dtu.dk

Mission requirements

- **Land**
  - time series of flights (typically simple tracks) to monitor changes
  - series of flight lines to image area
  - moderate altitude
  - many different sites in different countries
  - many flight hours foreseen
- **Sea**
  - moderate to high altitude / large footprint flights to study wiggles and how they reduce with integration (altitude & area).
  - cloverleaf (more azimuth signatures) - could be high altitude
  - circle flights (more azimuth signatures) - moderate altitude
  - Fly over 1 psu front

Radiometer requirements

- **L-band (protected 1400 - 1427 MHz)**
- **Fully polarimetric**
- **Good stability & accuracy**
- **RFI resistant**
- **2 beams: nadir and 30 - 40 deg. incidence angle. Aft looking preferred.**
- **In principle narrow beams to avoid integration over large range of incidence angles, but this is in conflict with realistic antenna sizes. Around 30 deg. seems acceptable.**

Scatterometer requirements

- Frequency near protected band (PALS uses 1.26 GHz)
- Require radiometer antennas be used as receiving antennas!
- Use a small dedicated transmitter antenna for flood illumination so that footprint is the same for scatterometer and radiometer

Auxiliary instruments requirements

- INU / GPS for attitude sensing (better than 0.1 deg.)
- GPS for positioning
- Thermal infrared radiometer
- GPS reflectometry receiver
- Recording equipment
- RTP (Real Time Processor) for on-board validation
- Fast data delivery to users

Aircraft requirements

- Large apertures like photo holes / doors / ramps for antennas. Cost of making dedicated holes prohibitive.
- Apertures should preferably enable antenna installation without radome in order to minimize unpredictable losses.
- High altitude and large range preferred for some ocean flights
- Agility preferred for some land scenes and some sea scenes
- Availability must be certain for complicated campaigns. Military planes are ruled out.
- Operational cost is an issue.

3 month baseline campaign

- Main base: Toulouse
- Period: spring 2005 (generally wet to dry) or fall 2005 (dry to wet)
- One dawn flight every 3 days around Toulouse, i.e. 30 flights each 1.5 h
- Flights to Valencia (two periods of dryouts each 1-2 weeks): 2 x 5 flights each 4 h transit + 2 h on target i.e. 6 h
- 5 flights to Bay of Biscay each 5 h
- 2 flights to the Atlantic off the coast of Norway (Trondheim), each 14 h transit + 5 h on target.
- 2 transits: aircraft home base – Toulouse each ?? h

• Flight hours:	30 x 1.5 h	=	45 h
•	2 x 5 x 6 h	=	60 h
•	5 x 5 h	=	25 h
•	2 x 19 h	=	38 h
•	In total:		<u>168 h</u> (+ transit)

Aircraft options & performances

	max altitude	range	endurance	speed
M 55	20000 m	1800 NM	5 h	360 KTAS
DLR DO228	7600 m	1600 NM	9 h	190 KTAS
CASA-212	8000 m	950 NM	4 h	170 KTAS
HUT Skyvan	6800 m	530 NM	4 h	160 KTAS
ATR 42	8000 m	1400 NM	6 h	230 KTAS
Convair 580	7000 m	1400 NM	6 h	220 KTAS

ATR 42 presentation

- Relatively big cargo plane
- Long range
- 2 photo holes around 65 x 44 cm already installed
- The aft hole is just before the rear doors, and a pressurized installation of the nadir looking horn seems possible here
- A trap door around 63 x 50 cm is present in the tail (unpressurized), and a horn with 35 deg. incidence seems a possibility here
- Windows (radomes) are a requirement for aerodynamic reasons!

ATR 42

ATR 42 rear section

EMIRAD on ATR

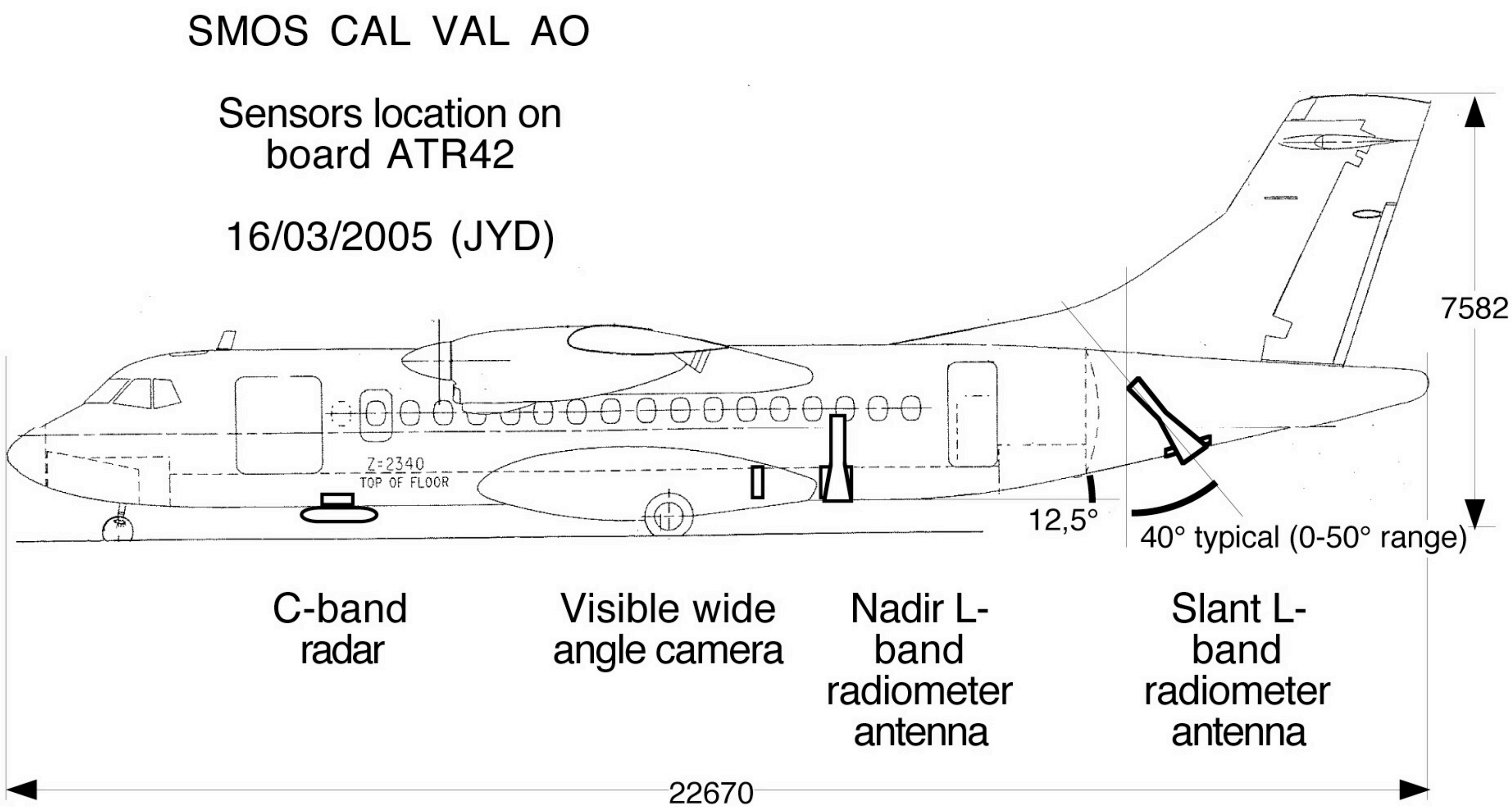

ATR 42 discussion

- Suitable aircraft for most of the tasks - especially remote targets
- A nadir and an aft (TBC) looking horn can be installed
- The horns are on the small side but acceptable
- Aerodynamic windows (radomes) are a serious drawback
- The distance between the 2 horns is too large for multiplex into one radiometer i.e. significant instrument cost increase
- Relatively large and expensive aircraft
- Scheduling problems in 2005

M 55 presentation

- Airplane with unique altitude capability!
- Fast and long range
- Aircraft designed for high altitude (very high wing area to weight ratio) so it is very sensitive to turbulence at low altitude and not agile
- Bay II offers space for a nadir looking antenna + an sideways looking antenna both with short sub-optimal OMT
- Severe environment for equipment: unpressurized + high altitude, temperature, vibration
- Strong and sturdy radome cannot be avoided
- Rigorous and tough tests required (recommend building of engineering model in order not to damage flight model unduly!)

M 55 overview

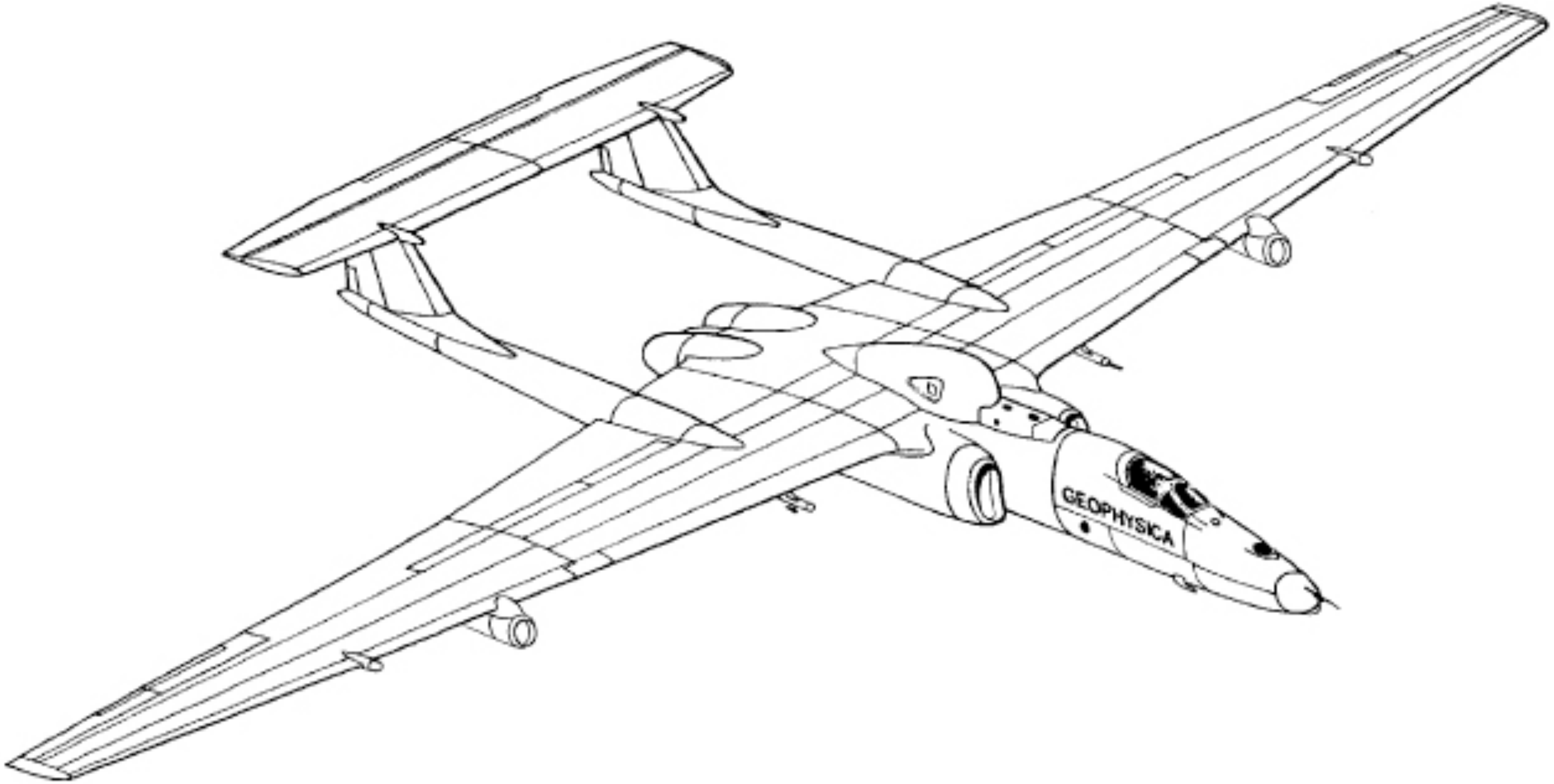

M 55 front bays

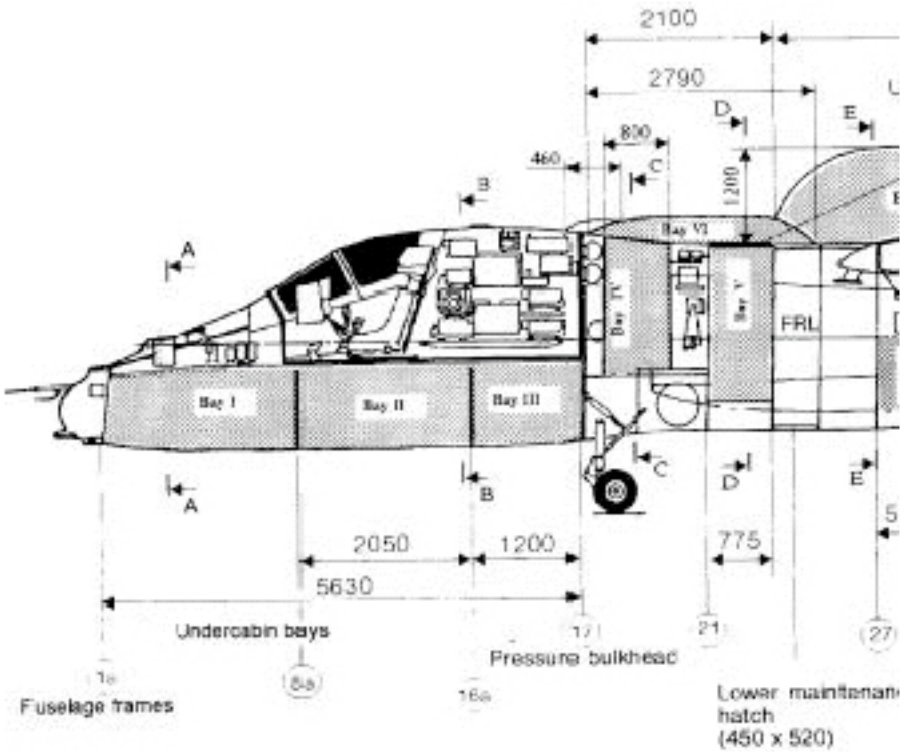

M 55 discussion

- The aircraft option that can really do the wiggle thing in an optimal way!
- Not well suited for complicated flights over land targets
- Radome cannot be avoided and short OMT has larger loss, so calibration cannot be ensured.
- In short: can only be used for high flying wiggle campaign where absolute accuracy can be relaxed.
- Very expensive installation and expensive to fly.
- Dramatic increase of instrument design and development costs compared with other aircraft options

DLR DO228 presentation

- Moderately sized plane with good performance
- Long range (5 - 6 h open ocean incl. equipment and emergency gear)
- Very large hole 200 x 50 cm for good installation possibilities
- One nadir and one 40 deg aft looking antenna easily accommodated
- No windows required

DO228

DO228

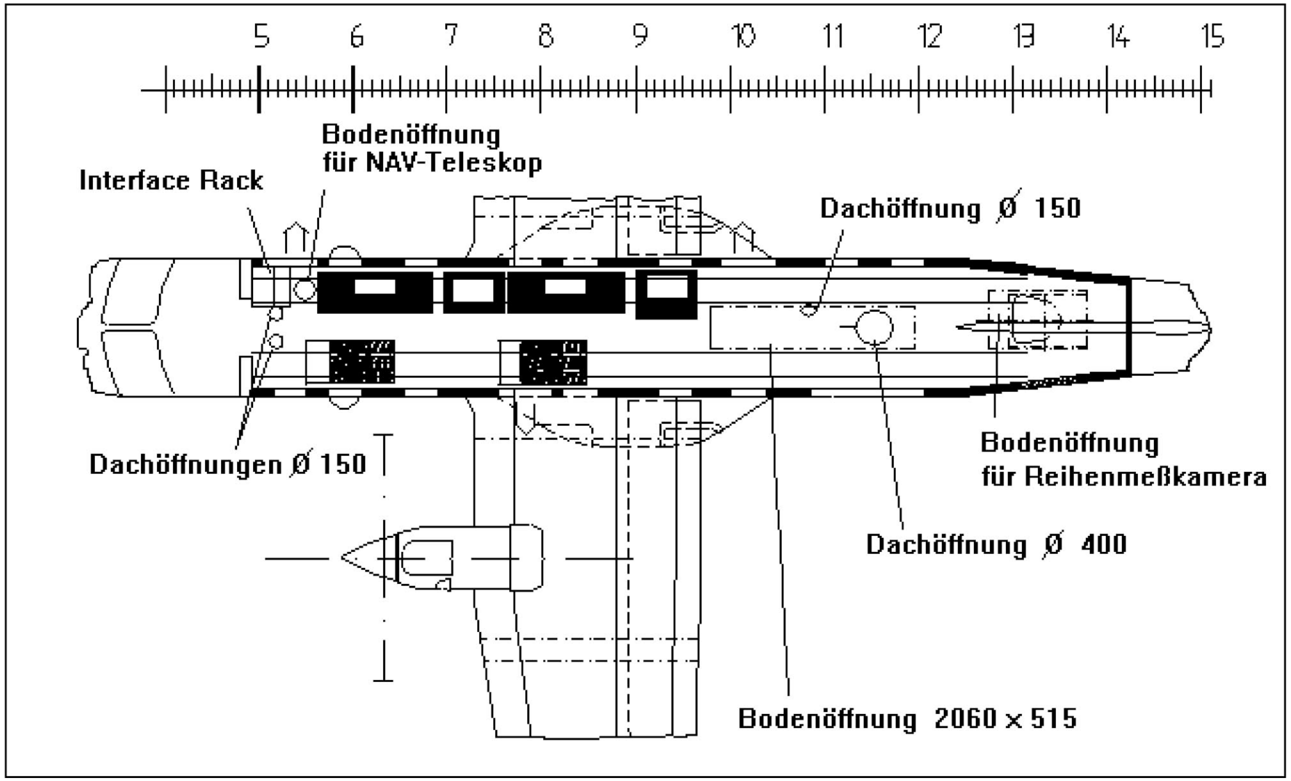

5
6
7
8
9
10
11
12
13
14
15
Bodenöffnung
für NAV-Teleskop
Interface Rack
Dachöffnung Ø 150
Dachöffnungen Ø 150
Bodenöffnung
für Reihenmeßkamera
Dachöffnung Ø 400
Bodenöffnung 2060 x 515

DO228

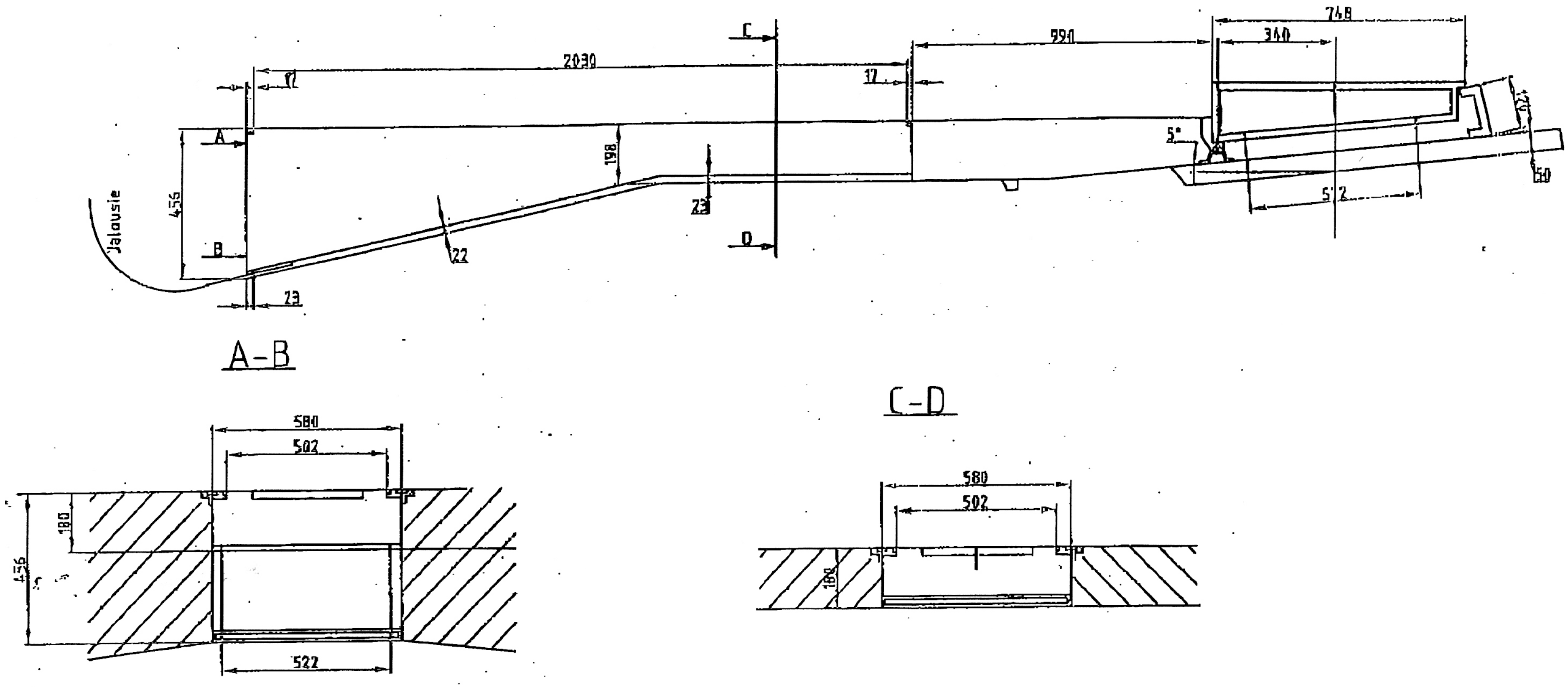

748
340
990
2030
17
17
C
D
A
B
198
456
23
22
23
5°
512
50
Jalousie
A-B
C-D
580
502
180
456
522
580
502
180

2 antennas & radiometer on DO228

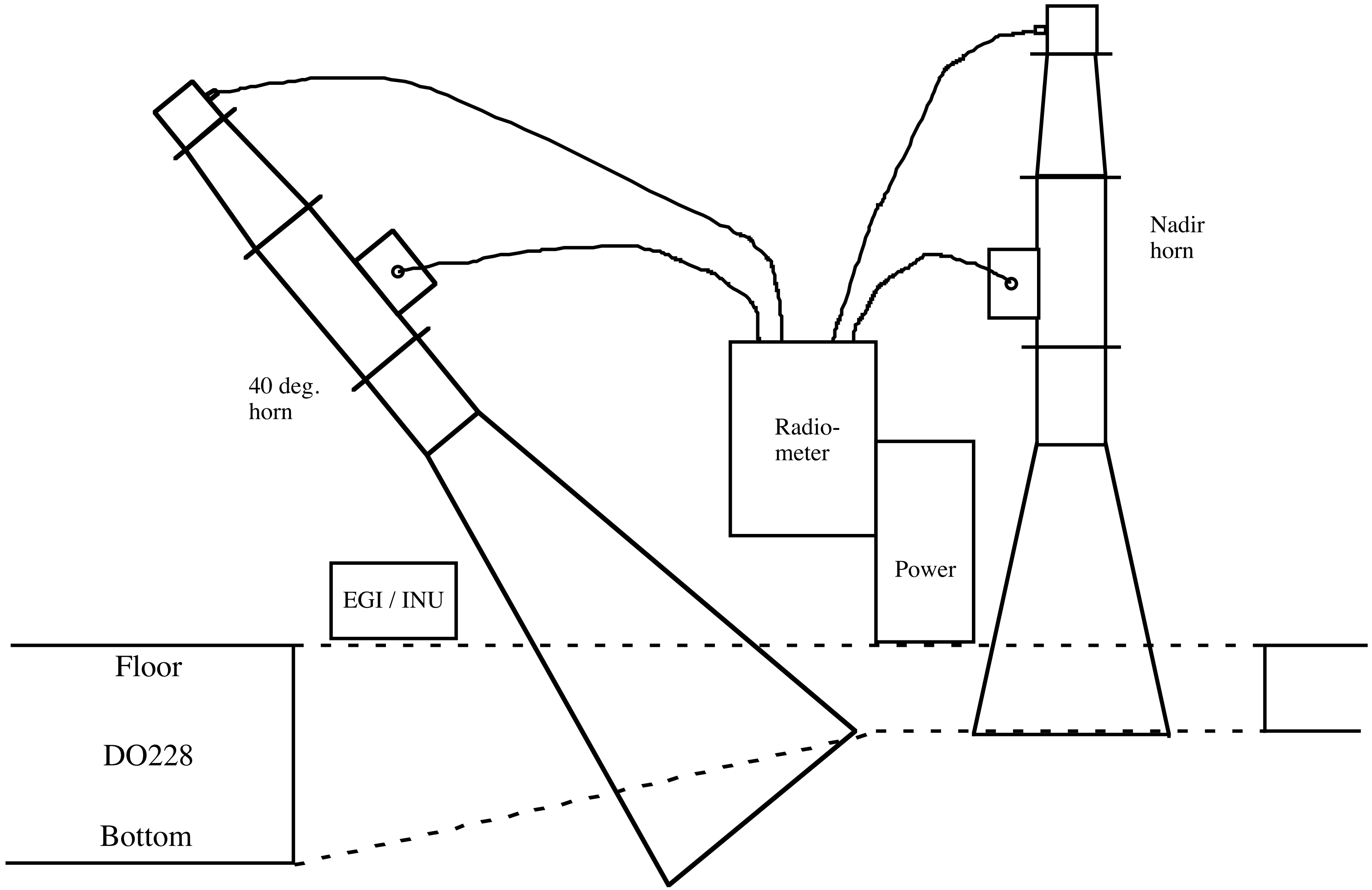

DO228 discussion

- Suitable aircraft for most tasks - including remote targets
- A very satisfactory installation of a nadir and an aft looking horn can be implemented without need for radome
- Only one radiometer needed - not only cost issue but also inter-calibration issue!
- Relatively small and agile aircraft
- The operator is well acquainted with scientific campaigns and has in-house installation capability.
- Relatively cheap operation
- Available fall 2005 - but not spring 2005

INTA CASA-212 presentation

- **micro C-130 with ramp and door**
- **Moderately sized plane with good performance (altitude and performance with open ramp must be checked)**
- **Moderate but acceptable range**
- **One nadir and one aft looking antenna can be installed on the open ramp much like DTU did in the past on C-130**
- **No radomes**

CASA-212

CASA-212 discussion

- Suitable aircraft for most tasks - including remote targets
- A very satisfactory installation of a nadir and an aft looking horn can be implemented
- A relatively sturdy sliding arrangement must be made to push the radiometer system out to the edge when the ramp has been lowered.
- Only one radiometer needed
- Flying many hours with open ramp may be less convenient
- Max altitude with open ramp not known
- Relatively small and agile aircraft
- Range may be a problem
- Relatively expensive aircraft

HUT Skyvan presentation and discussion

- nano C-130 with open rear end (door removed)
- Small plane with short range
- Very satisfactory installation of nadir and aft looking horn.
- Small and agile aircraft
- Excellent availability
- Cheap installation and operation
- The operator is well acquainted with scientific campaigns and installation of this kind of instruments
- Simultaneous operation of HUT 2D is feasible!
- Range is limited - no large scale ocean missions

Skyvan

Convair 580 presentation

- Relatively big airplane
- Long range
- 2 photo holes about 41 x 41 cm and 55 x 55 cm side by side
- Additional 80 x 80 cm hole ("antenna platform tunnel") right behind
- Easy installation of one nadir and one 40 deg aft looking antenna. If parts of them sticks out beneath the skin, it is easy to make a wind deflector
- No windows required
- Good availability - BUT

CV 580

CV 580 discussion

- Suitable aircraft for all tasks - including remote targets
- A very satisfactory installation of a nadir and an aft looking horn can be implemented without need for radome
- Only one radiometer needed - not only cost issue but also inter-calibration issue!
- Moderately sized aircraft, yet feasible also over complicated targets
- The operator is well acquainted with scientific campaigns and has in-house installation capability.
- Relatively cheap operation - quite comparable to DO228
- Relatively cumbersome installation far away from home (DTU)
- Availability is so good that it might be a problem. If coSMOS is delayed to spring 2006 the aircraft may be out of service due to lack of business!

Conclusions and recommendations

- Make radiometer installation in DO228 or CV580 with preference for DO228 due to easier logistics during installation phase.
- CASA-212 is a backup solution (only for a short while!)
- M55, ATR 42, and HUT Skyvan not further considered
- No active channel
- Fall 2005 campaign

- BUT MANY THINGS WENT DIFFERENTLY!

Detection and mitigation of RFI within the context of EMIRAD

J.E. Balling, N. Skou, S.S. Søbjærg, and S.S. Kristensen
National Space Institute
Technical University of Denmark
jeb@space.dtu.dk

CoSMOS final meeting, ESTEC, May 26th, 2011

Background

The EMIRAD-2 radiometer has been employed in the following CoSMOS campaigns:

Campaign:	Where:	When:	What:
CoSMOS - Aus	Australia	(European) Fall 05	Land
CoSMOS - OS	Norway	Spring 06	Ocean
POL-ICE	Finland	Winter 07	Ice
Demonstrator	Finland	Summer 07	Ocean
Rehearsal	Germany - Spain	Spring 08	Land
Cal / Val	Germany	Spring 10	Land

Data acquired during the campaigns have all been affected by Radio Frequency Interference (RFI) to varying extents.

RFI detection methods

The ideal RFI detection method:

- Detects all contaminated samples
- Leaves all clean samples alone

However, we will most probably have to settle for less…

RFI detection methods – visual inspection

Method: Throw away all samples with a TB larger than e.g. 350 K

Pros:

- Easy to implement and automate
- Detects large deviations of TB due to RFI

However:

This method is by no means able to detect the most "dangerous" kind of RFI contamination, i.e. the kind of contamination resulting in a contribution to TB of a few K

How do we find the ”concealed” RFI samples?

- Radiometric signals (coming from natural sources) have a Gaussian probability density function (PDF)
- Man-made RFI is generally assumed to have non-Gaussian PDFs

Thus, the PDF of the received signal indicates its amount of RFI contamination.

The ratio $$k = \frac{< x^4(t) >}{< x^2(t) >^2}$$ (kurtosis)

equals 3 for a Gaussian PDF, i.e.

Natural targets have a kurtosis of 3, whereas man-made signals (RFI) exhibit kurtosis values above and below 3, depending on the PDF of the signal.

Threshold: kurtosis mean ± 4 times kurtosis std. dev.

Kurtosis properties and "blind spot"

Kurtosis is:

- = 3 for Gaussian
- > 3 for pulse
- = 1.5 for CW
- = 3 for 50% duty cycle

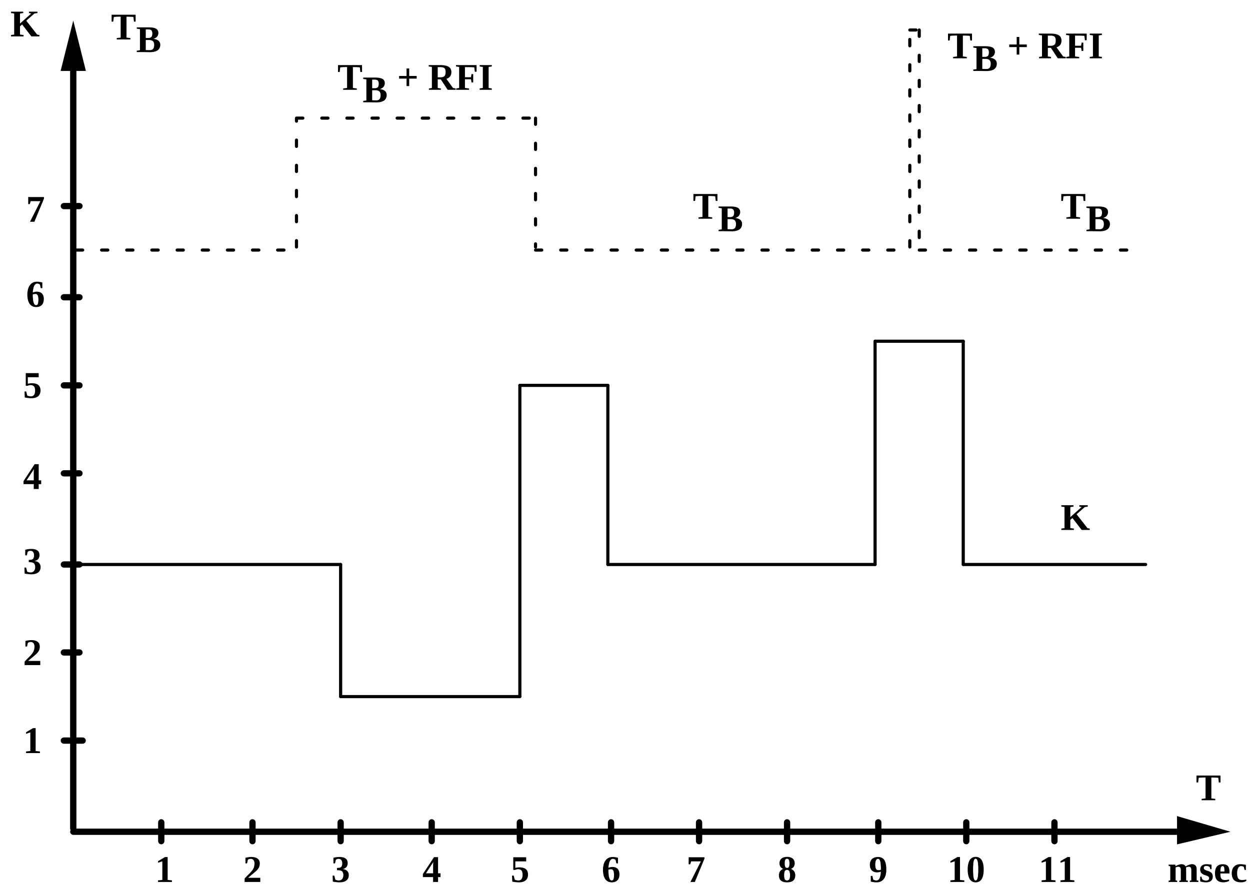

RFI contribution to TB constant = 100 K

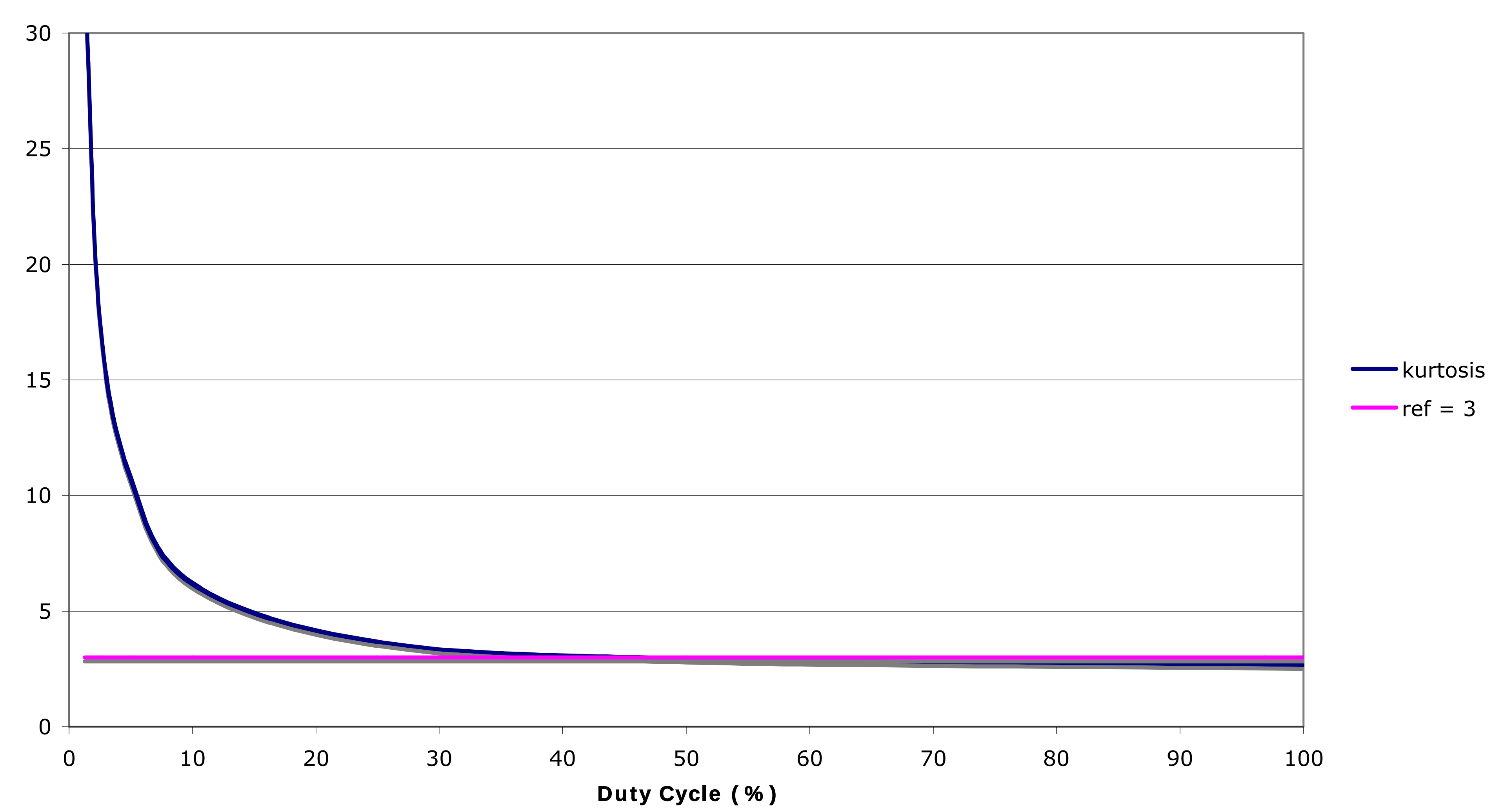

RFI amplitude constant, contribution = 1000 K for 100% duty cycle

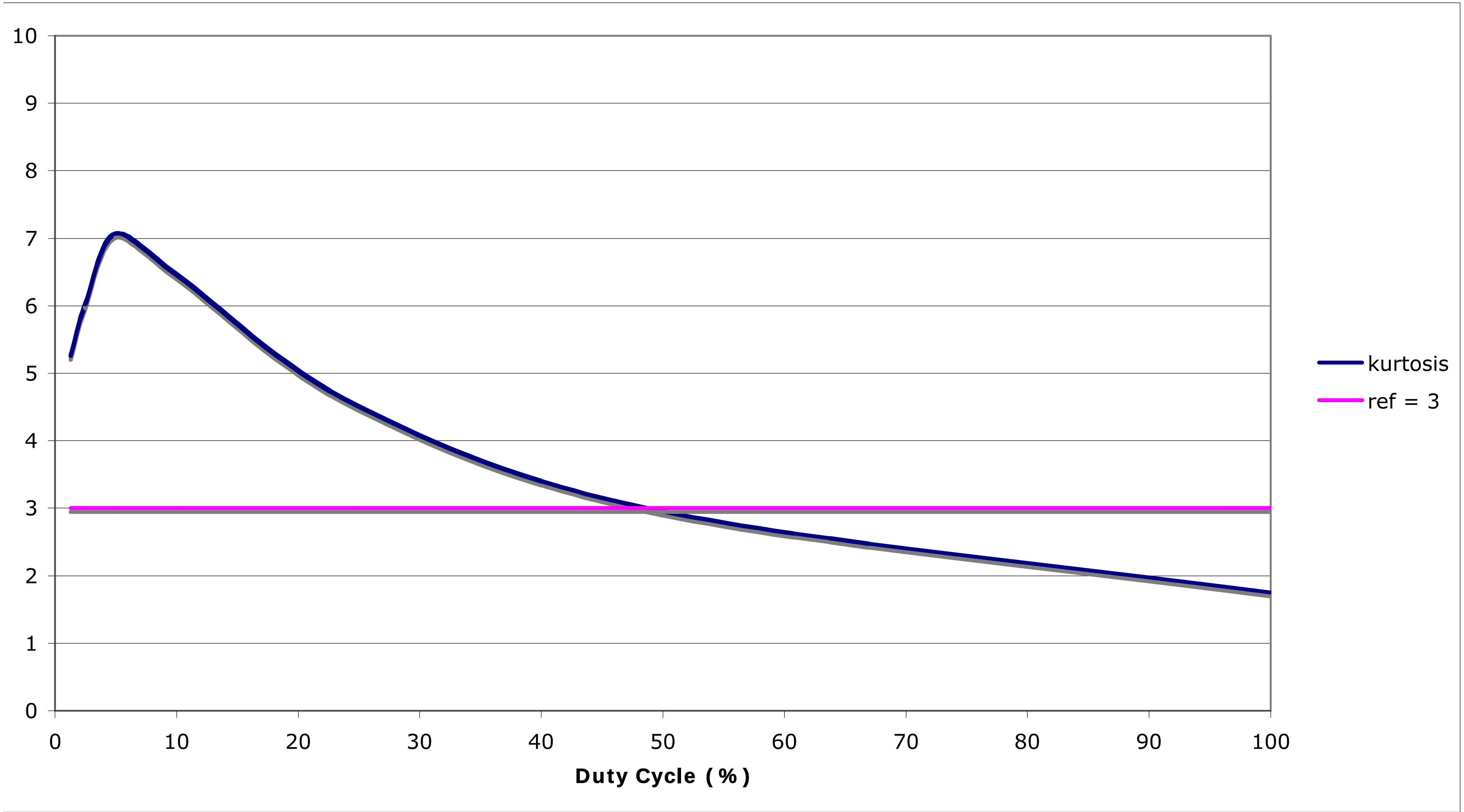

Kurtosis properties and “blind spot”

- “Duty cycle” corresponds to the percentage of each EMIRAD integration window (1 ms) which is affected by RFI.
- Kurtosis sensitivity depends heavily on duty cycle as well as RFI-to-TB ratio
- RFI detection by means of kurtosis inspection is:

Well suited for large, short, radar-like pulses.

Less suited for RFI with high duty cycles.

Taking kurtosis as the truth – a look at the RFI situation from 2005 to 2010

RFI percentages from the CoSMOS-Aus campaign, december 2005

Date	Aft H	Aft V	Nadir H	Nadir V
15/11 - 05	2.99%	0.83%	15.0%	2.58%
27/11 – 05	2.26%	0.55%	17.4%	2.69%
29/11 - 05	2.94%	0.78%	16.0%	1.22%
3/12 - 05	5.44%	5.70%	30.0%	5.34%
6/12 - 05	4.03%	2.10%	21.8%	4.97%

Taking kurtosis as the truth – a look at the RFI situation from 2005 to 2010

RFI percentages from the CoSMOS-OS campaign

Date	Aft H	Aft V	Nadir H	Nadir V
6/4 - 06	0.44%	0.53%	0.31%	0.49%
9/4 - 06	0.06%	0.37%	0.06%	0.44%
10/4 - 06	0.03%	0.36%	0.05%	0.43%
12/4 - 06	0.04%	0.31%	0.04%	0.36%
13/4 - 06	0.57%	1.02%	0.87%	1.16%
15/4 - 06	0.05%	0.61%	0.06%	0.72%
16/4 - 06	1.97%	2.44%	3.37%	1.52%
18/4 - 06	0.13%	0.46%	0.06%	0.56%
19/4 - 06	0.70%	1.45%	2.34%	0.90%
22/4 - 06	35.9%	41.6%	43.9%	18.0%
25/4 - 06	0.05%	0.27%	0.06%	0.29%
29/4 - 06	31.2%	35.4%	53.3%	18.7%
30/4 - 06	0.99%	0.28%	0.44%	0.60%

Taking kurtosis as the truth – a look at the RFI situation from 2005 to 2010

RFI percentages from the PolIce and Demonstrator campaigns

Date	Aft H	Aft V	Nadir H	Nadir V
8/3 - 07	0.86%	1.6%	0.59%	0.81%
11/3 - 07	0.07%	0.16%	0.12%	0.10%
12/3 - 07	10.8%	21.5%	8.6%	20.8%
13/3 - 07	0.17%	0.22%	0.12%	0.09%
13/8 - 07	0.08%	0.50%	0.07%	0.56%
13/8 - 07	0.23%	3.8%	0.61%	0.46%
15/8 - 07	0.22%	0.42%	0.11%	0.38%

RFI percentages during the SMOS validation rehearsal campaign (2008)

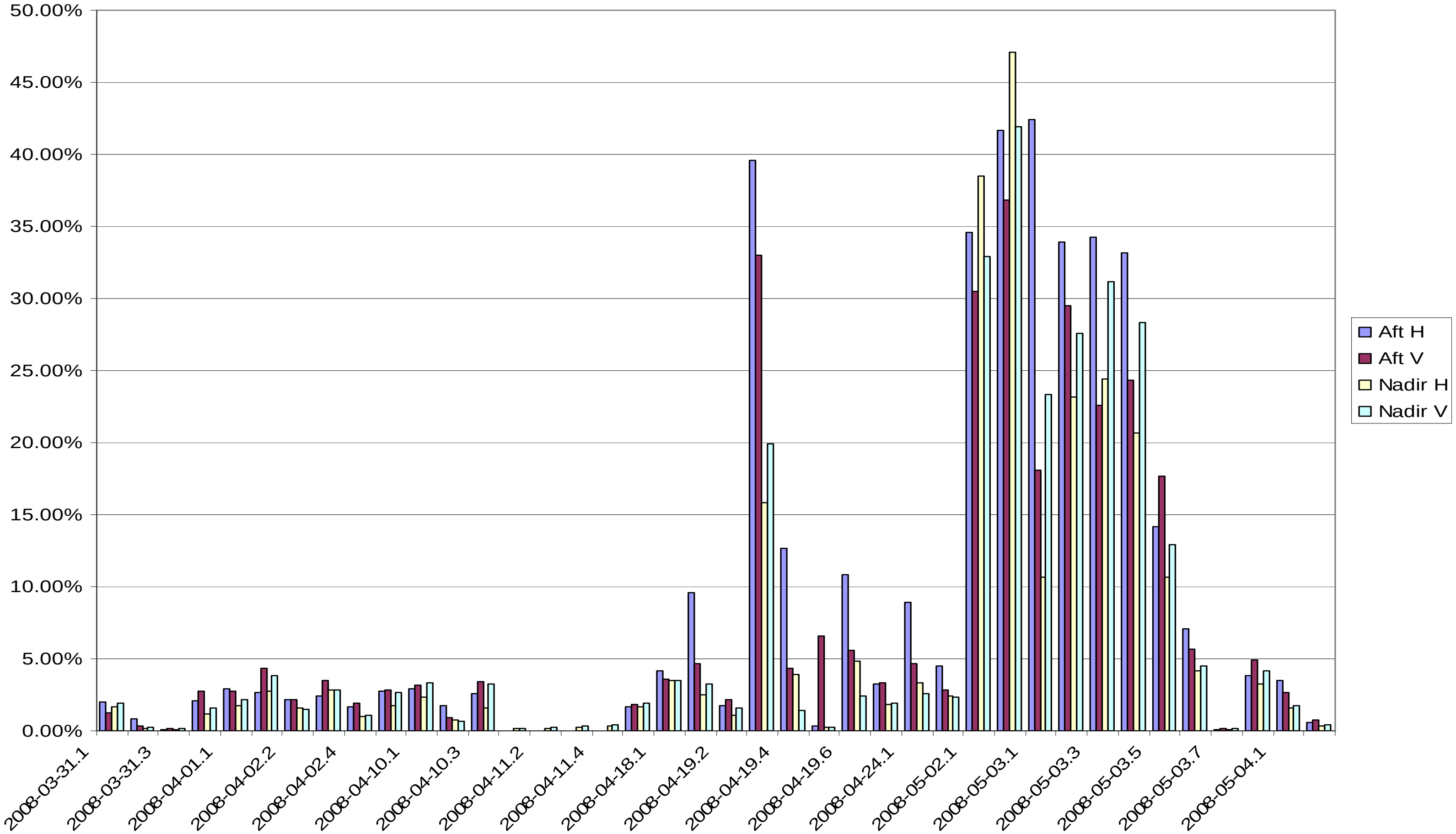

RFI percentages during the SMOS validation rehearsal campaign (2008)

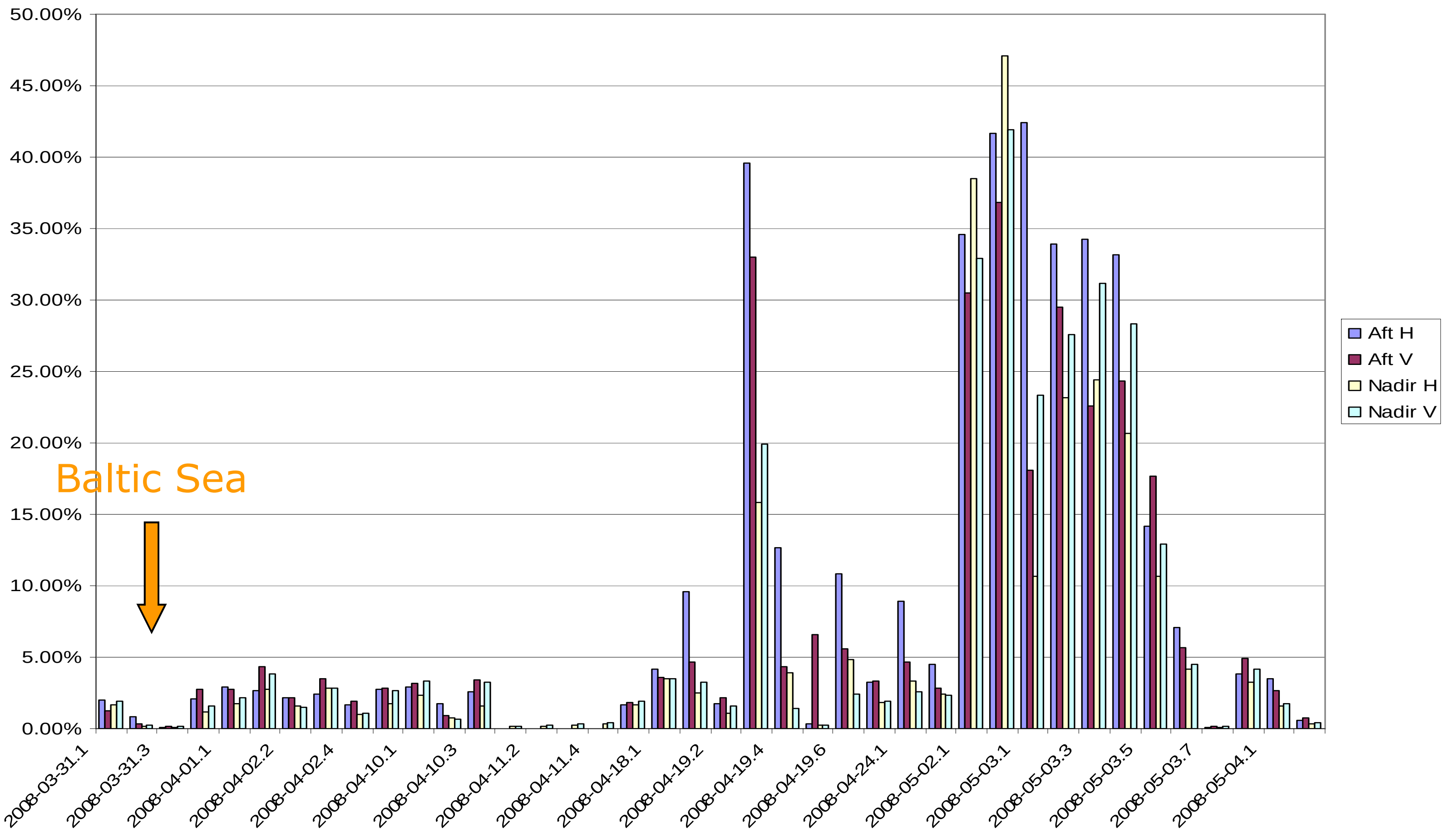

RFI percentages during the SMOS validation rehearsal campaign (2008)

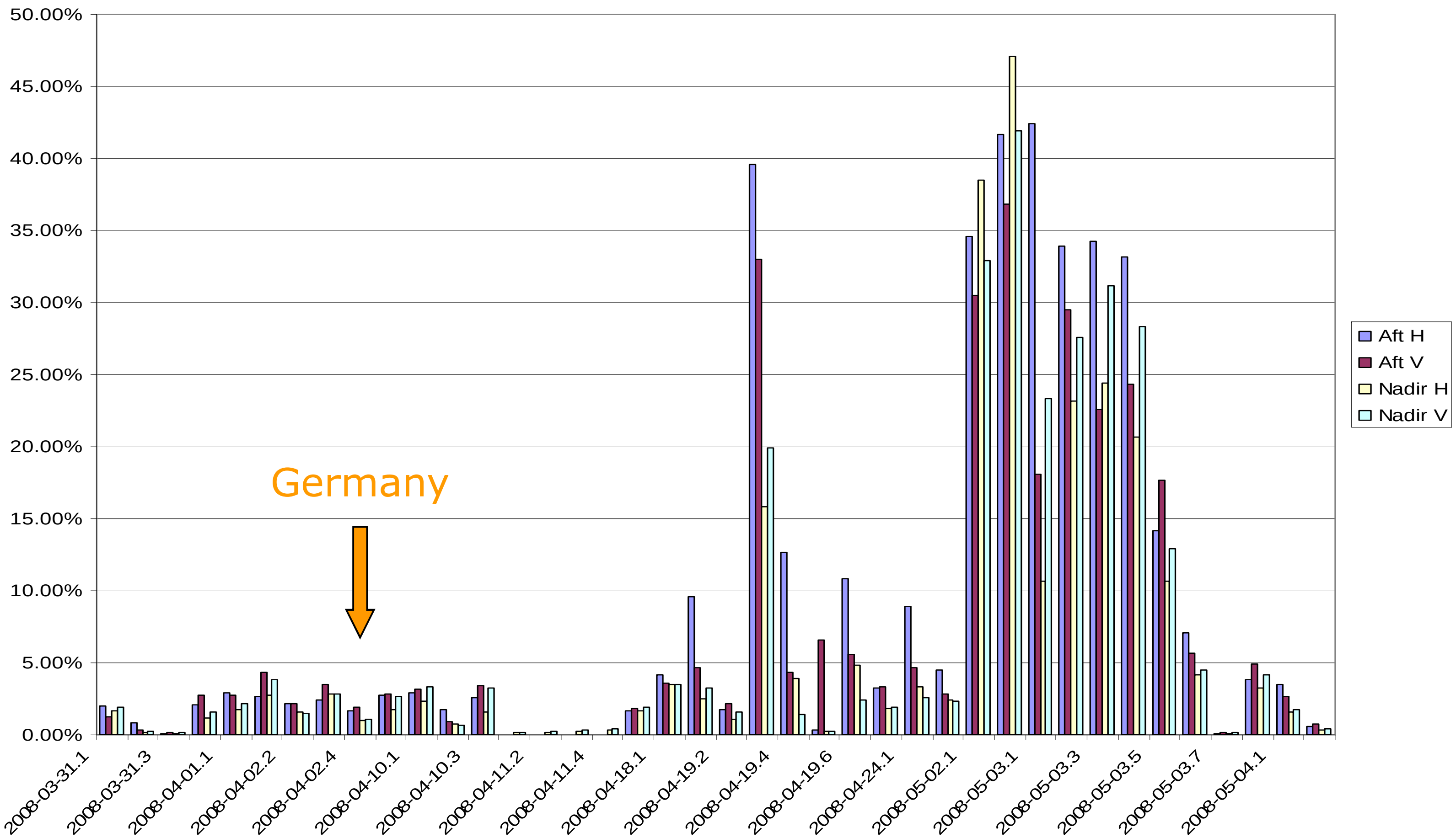

RFI percentages during the SMOS validation rehearsal campaign (2008)

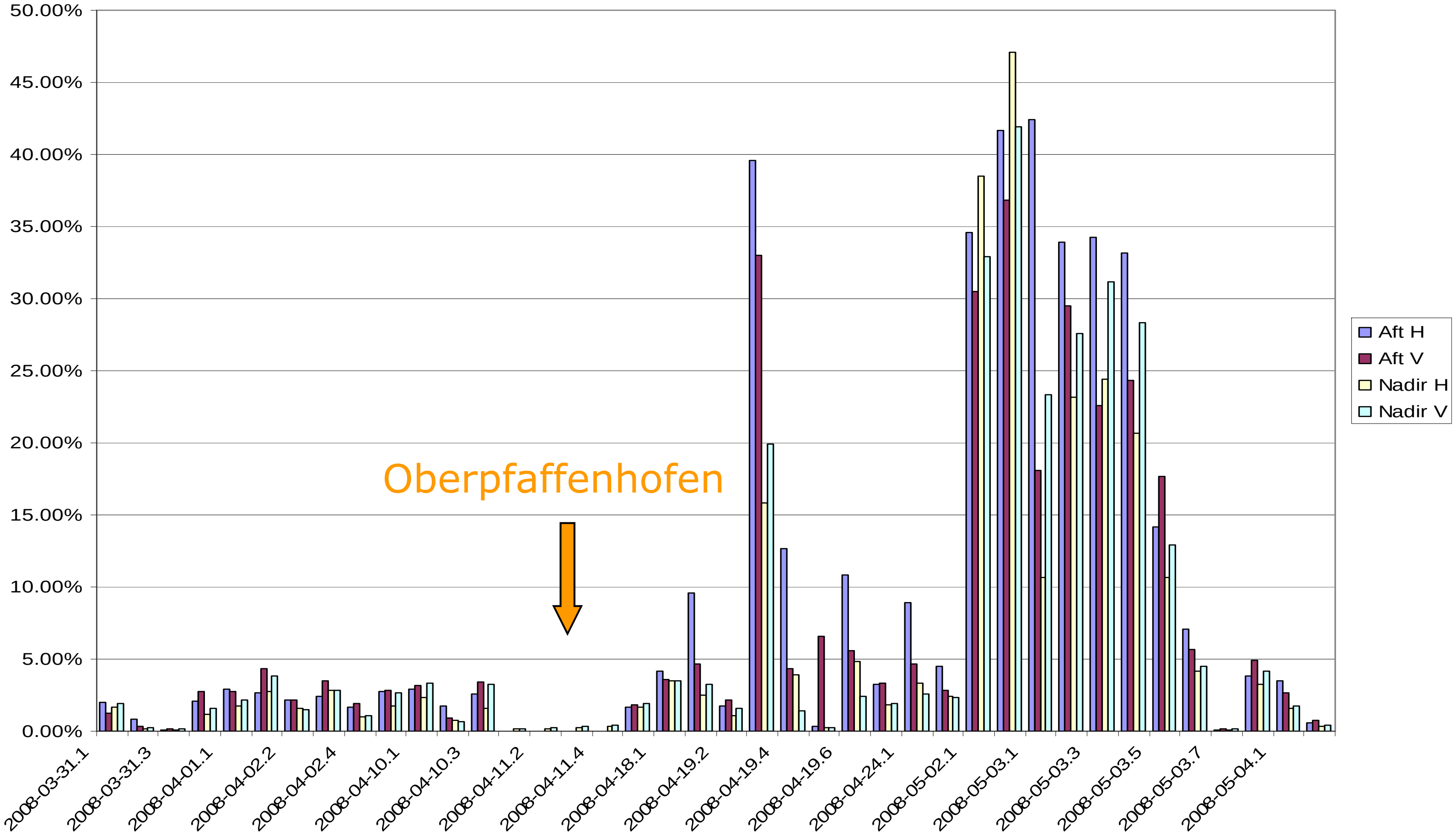

RFI percentages during the SMOS validation rehearsal campaign (2008)

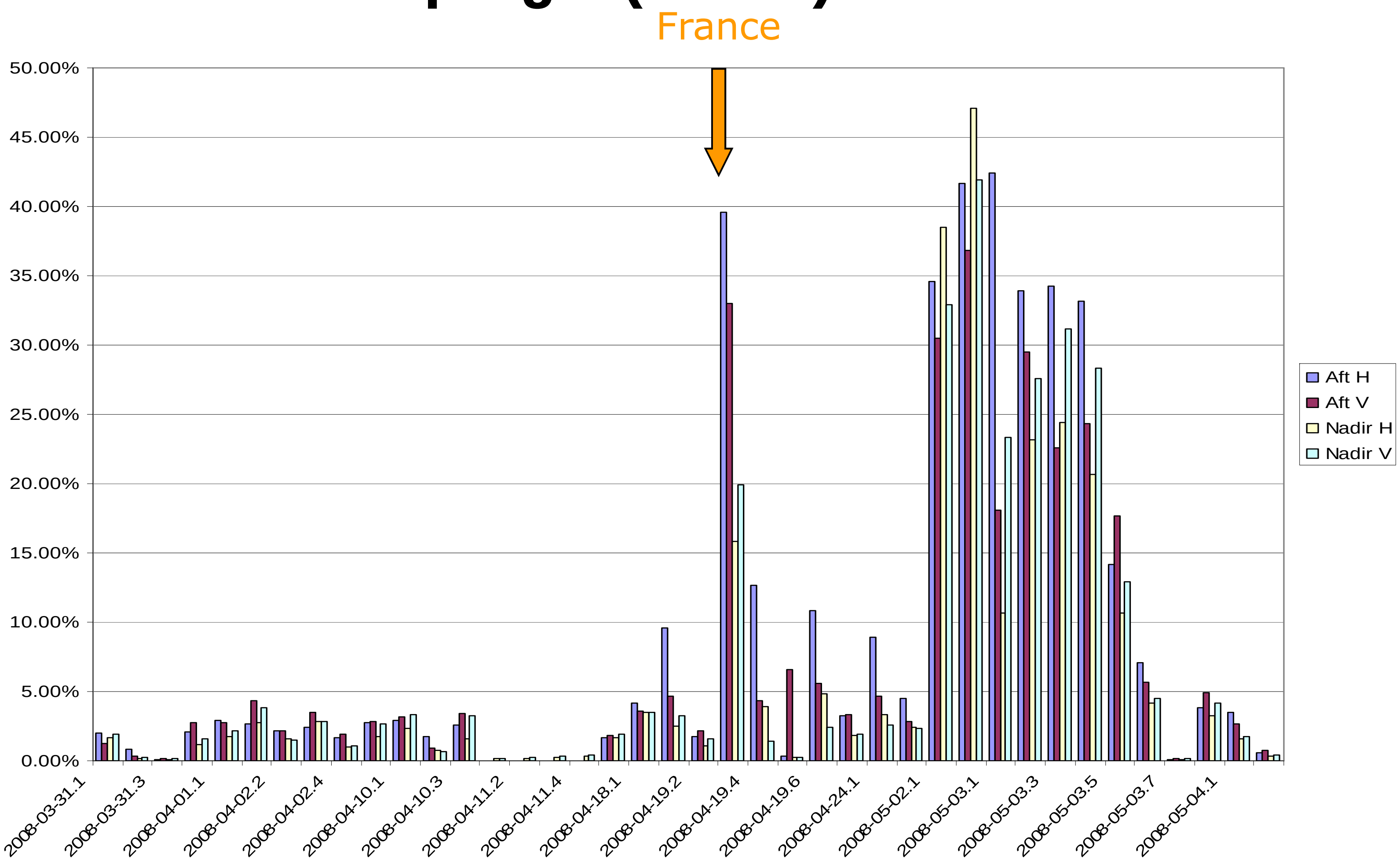

RFI percentages during the SMOS validation rehearsal campaign (2008)

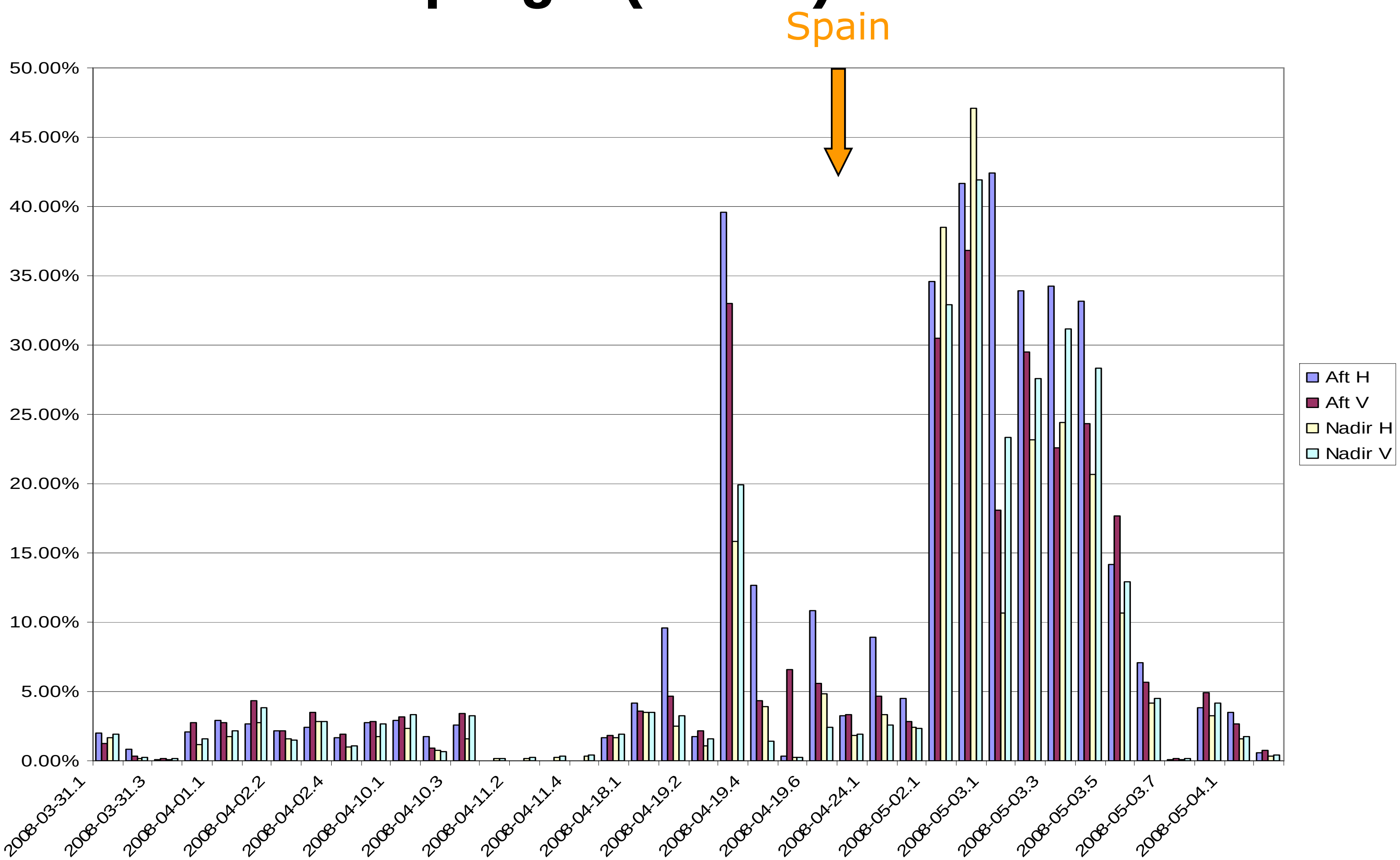

RFI percentages during the SMOS validation rehearsal campaign (2008)

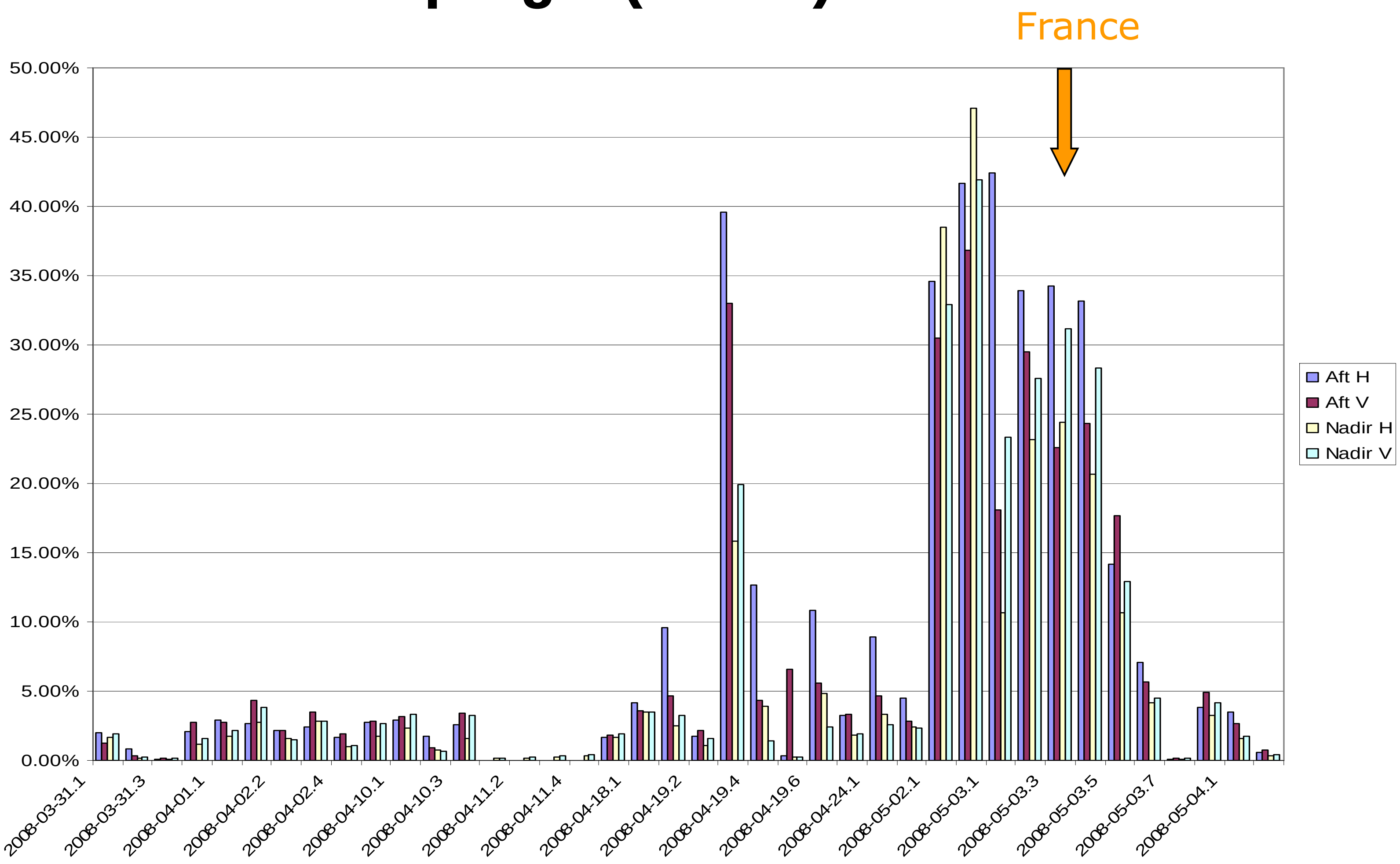

RFI percentages during the SMOS validation rehearsal campaign (2008)

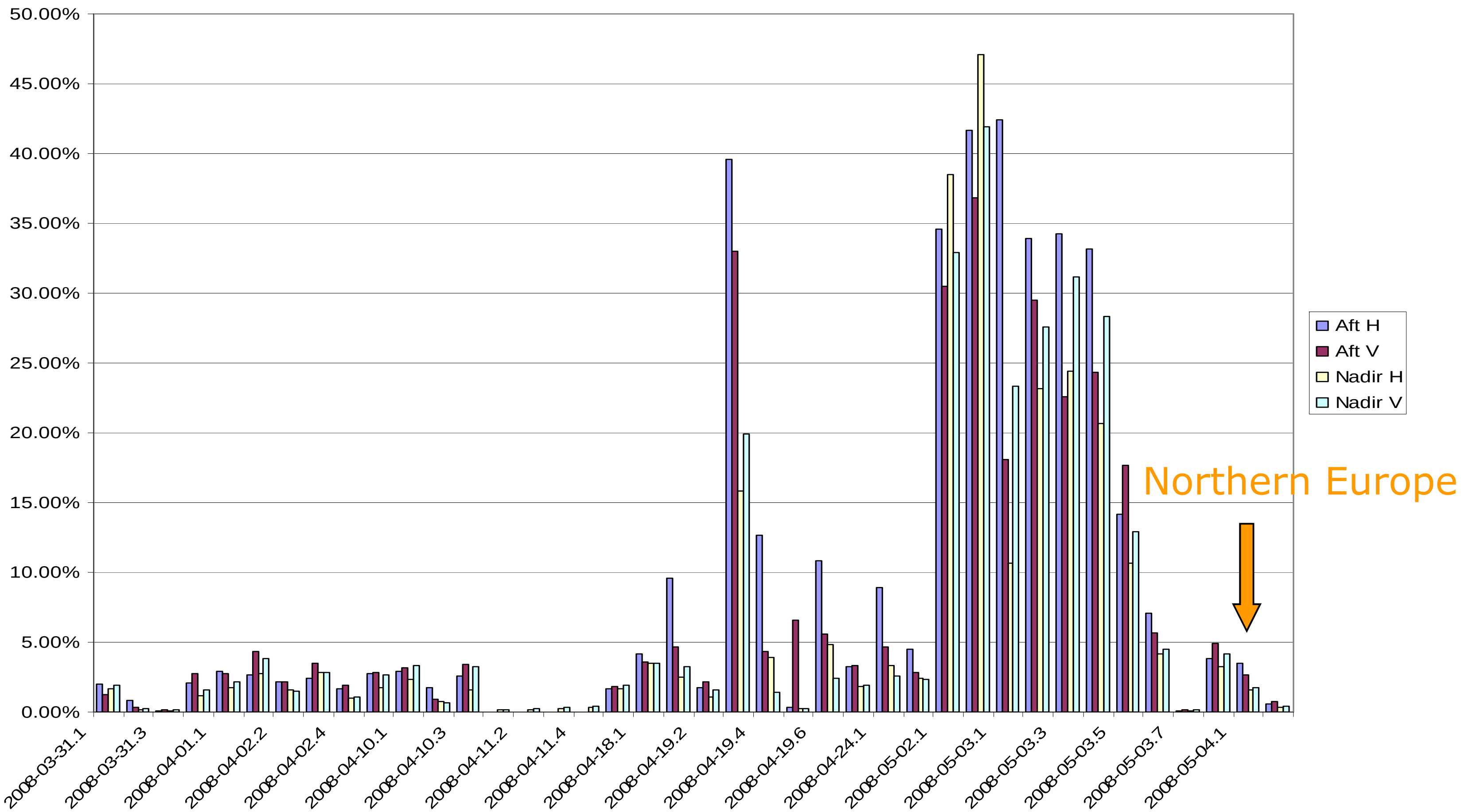

RFI percentages during the HOBE (DK) and SMOS cal/val (D) campaigns (2010)

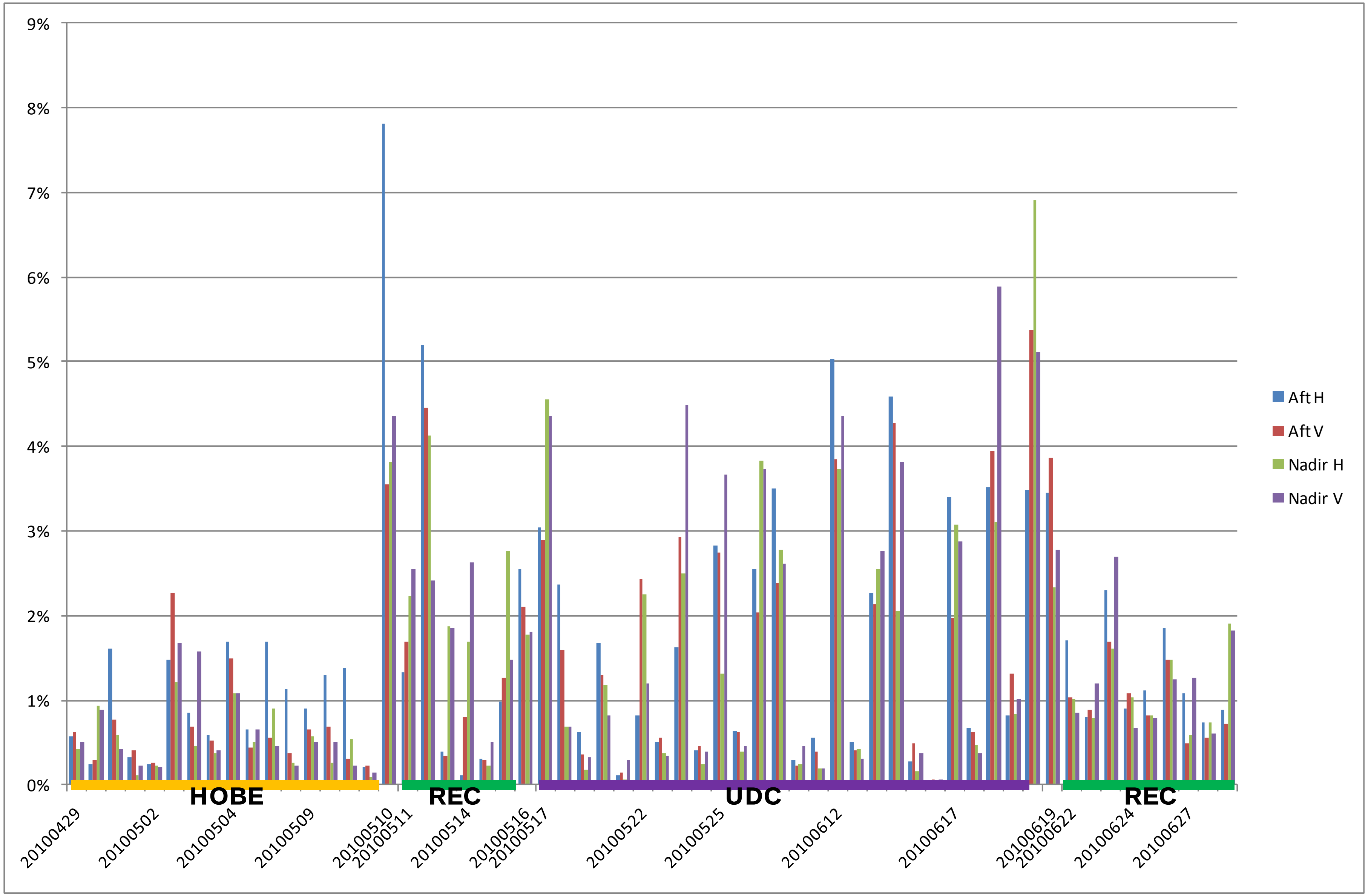

Three cases of RFI contamination

Case no.	Date	Place	RFI pct. Aft H	RFI pct. Aft V	RFI pct. Nadir H	RFI pct. Nadir V
1	2008-04-14	Danube catchment	1.66 %	1.82 %	1.70 %	1.89%
2	2008-04-28	Valencia	4.50 %	2.87 %	2.39 %	2.31 %
3	2008-05-02 Part 1	Valencia	34.59 %	30.47 %	38.48 %	32.93 %
	2008-05-02 Part 2		41.70 %	36.83 %	47.07 %	41.88 %

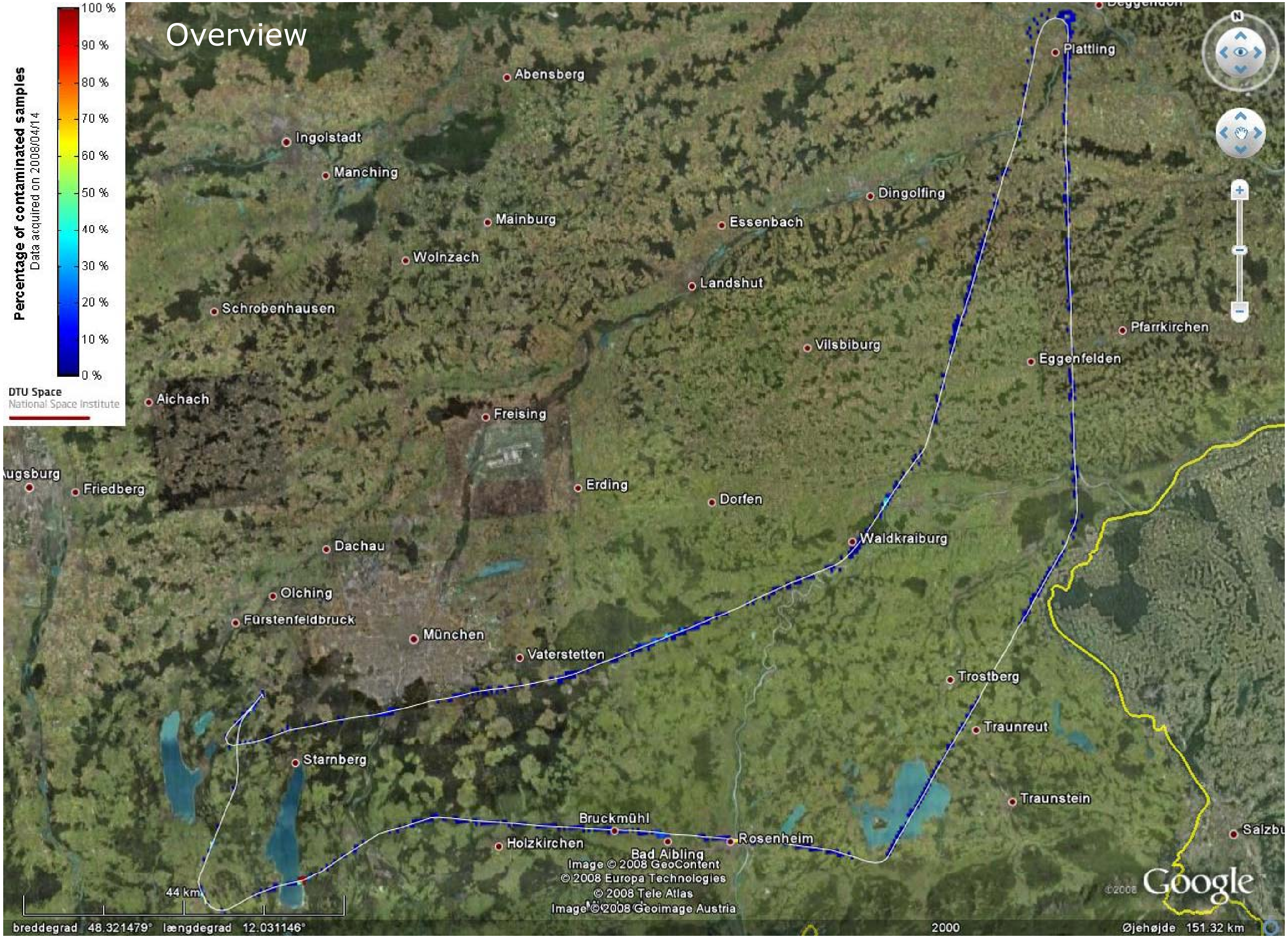
Overview
Percentage of contaminated samples
Data acquired on 2008/04/14
100 %
90 %
80 %
70 %
60 %
50 %
40 %
30 %
20 %
10 %
0 %
DTU Space
National Space Institute
Abensberg
Ingolstadt
Manching
Mainburg
Wolnzach
Essenbach
Dingolfing
Plattling
Landshut
Schrobenhausen
Vilsbiburg
Pfarrkirchen
Eggenfelden
Aichach
Freising
Augsburg
Friedberg
Erding
Dorfen
Dachau
Waldkraiburg
Olching
Fürstenfeldbruck
München
Vaterstetten
Trostberg
Traunreut
Starnberg
Traunstein
Bruckmühl
Holzkirchen
Rosenheim
Bad Aibling
Image © 2008 GeoContent
© 2008 Europa Technologies
© 2008 Tele Atlas
Image © 2008 Geoimage Austria
44 km
breddegrad 48.321479° længdegrad 12.031146°
2000
Øjehøjde 151.32 km
Google


Starnberger See
Percentage of contaminated samples
Data acquired on 2008/04/14
100 %
90 %
80 %
70 %
60 %
50 %
40 %
30 %
20 %
10 %
0 %
DTU Space
National Space Institute
Fürstenried
Gauting
München, gemeindefrei
Seefeld
Starnberg
Schäftlarn
Herrsching am Ammersee
Berg
Icking
Egling
Wolfratshausen
Tutzing
Münsing
Geretsried
Eurasburg
Weilheim in Oberbayern
11.7 km
Image © 2008 GeoContent
© 2008 Europa Technologies
© 2008 Tele Atlas
Image © 2008 AeroWest
©2008 Google
breddegrad 47.954466° længdegrad 11.341747°
2000
Øjehøjde 40.19 km

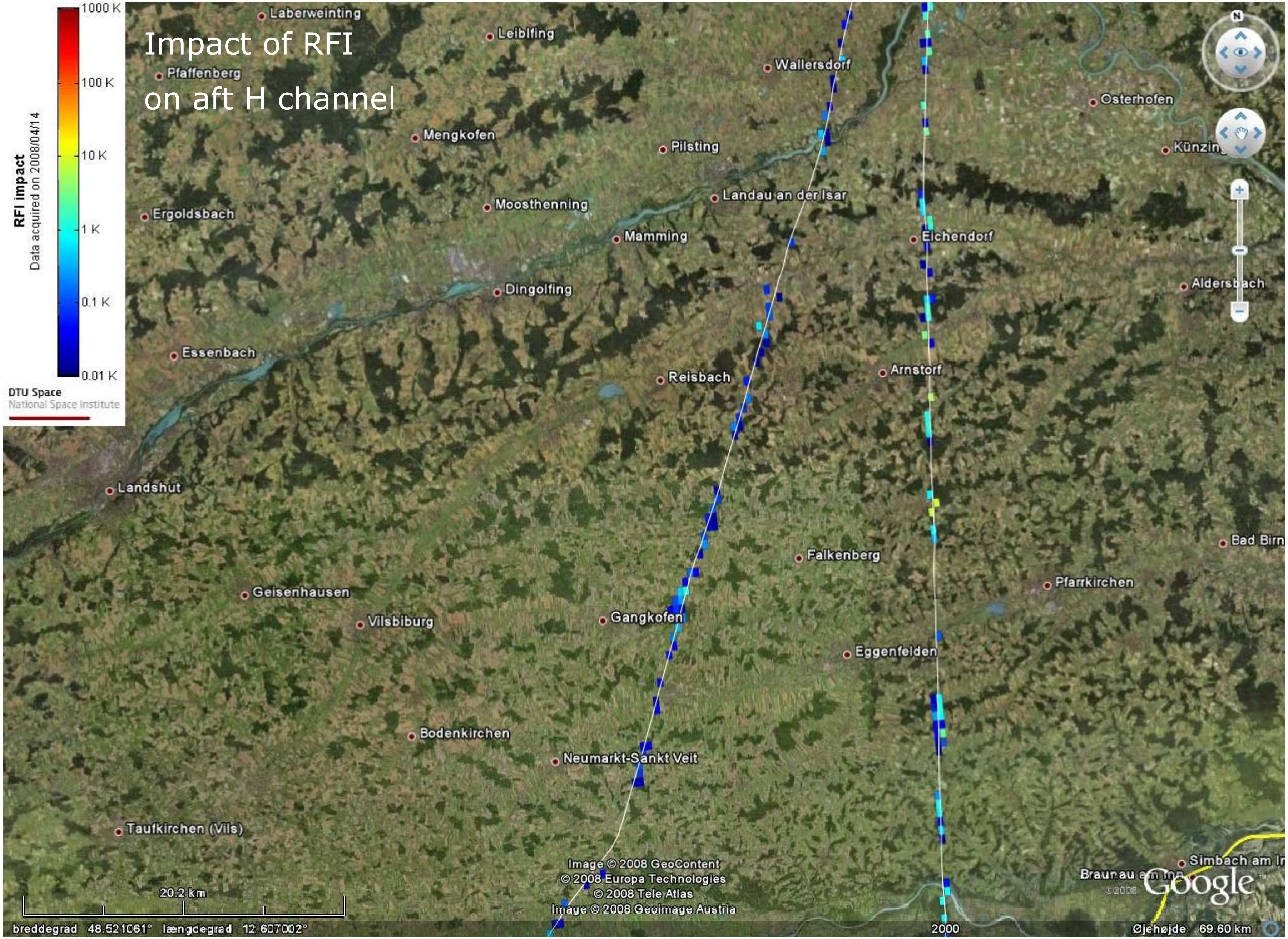
Impact of RFI
on aft H channel
RFI impact
Data acquired on 2008/04/14
1000 K
100 K
10 K
1 K
0.1 K
0.01 K
DTU Space
National Space Institute
Laberweinting
Leiblfing
Pfaffenberg
Wallersdorf
Osterhofen
Mengkofen
Pilsting
Künzing
Landau an der Isar
Ergoldsbach
Moosthenning
Mamming
Eichendorf
Dingolfing
Aldersbach
Essenbach
Reisbach
Arnstorf
Landshut
Falkenberg
Bad Birn
Pfarrkirchen
Geisenhausen
Vilsbiburg
Gangkofen
Eggenfelden
Bodenkirchen
Neumarkt-Sankt Veit
Taufkirchen (Vils)
Simbach am In
Braunau am Inn
Image © 2008 GeoContent
© 2008 Europa Technologies
© 2008 Tele Atlas
Image © 2008 Geoimage Austria
20.2 km
breddegrad 48.521061° længdegrad 12.607002°
2000
Øjehøjde 69.60 km
Google

RFI impact
Munich 2008-04-14
aft H channel

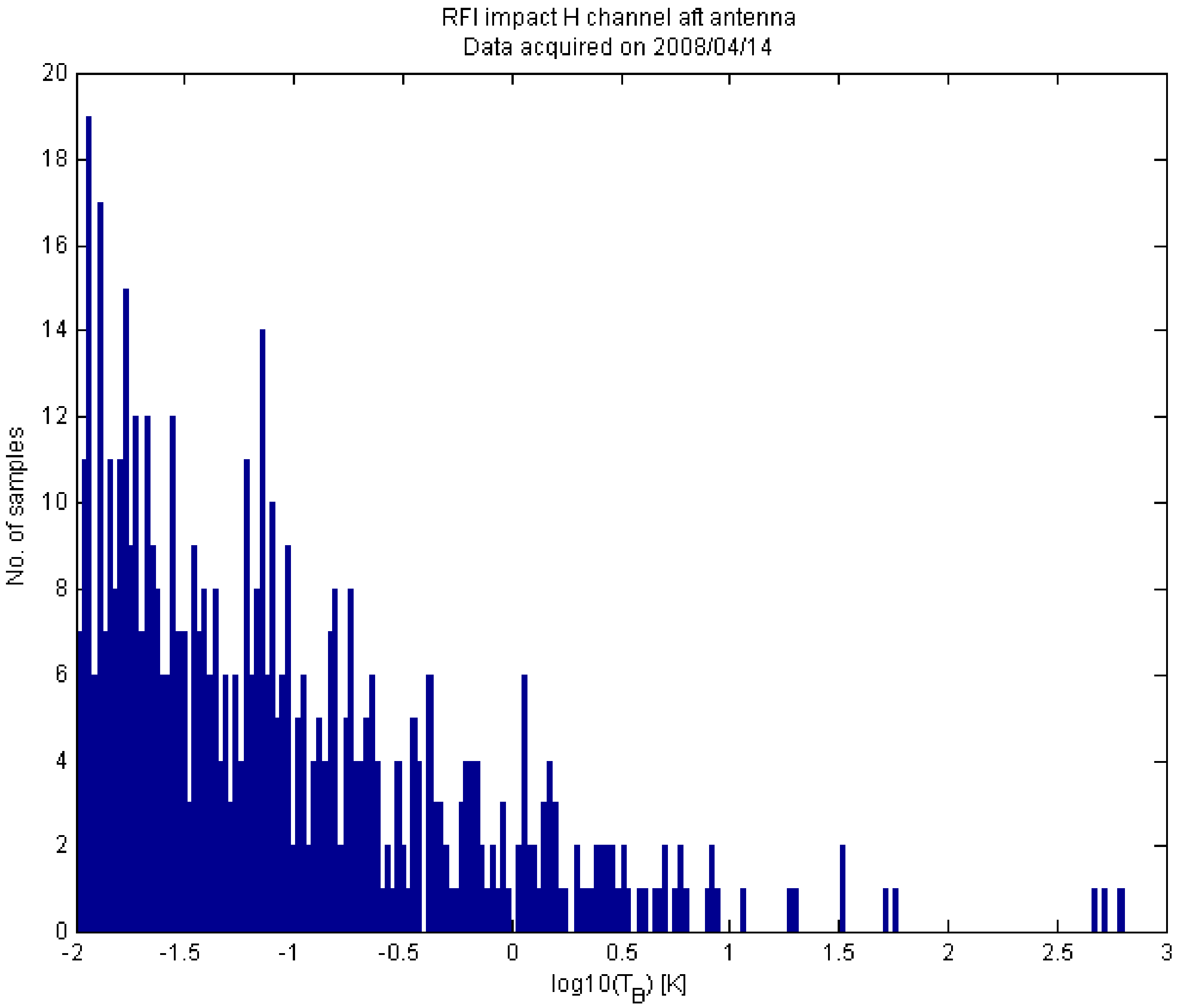

RFI impact
Munich 2008-04-14
aft V channel

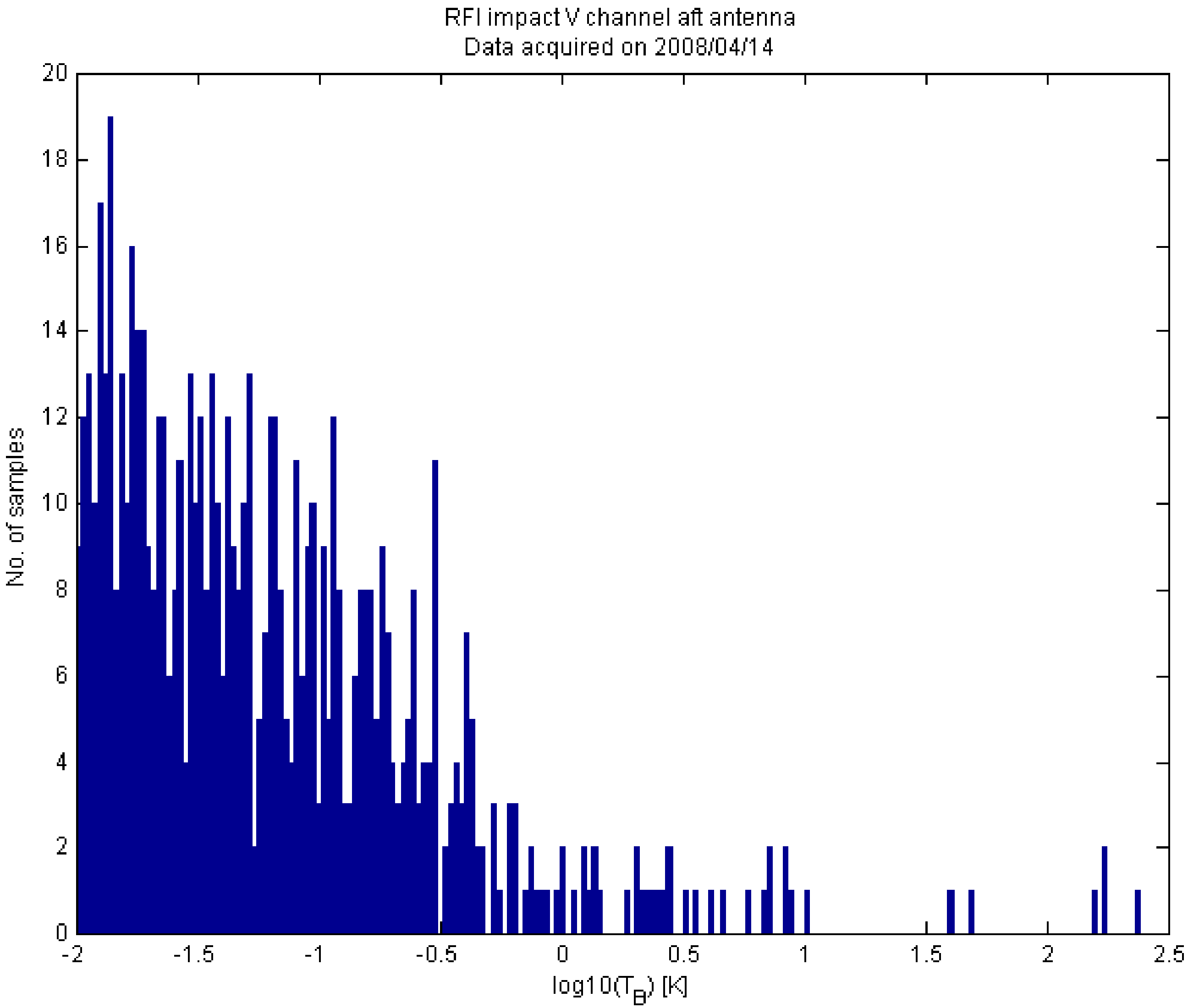

RFI impact
Munich 2008-04-14
nadir H channel

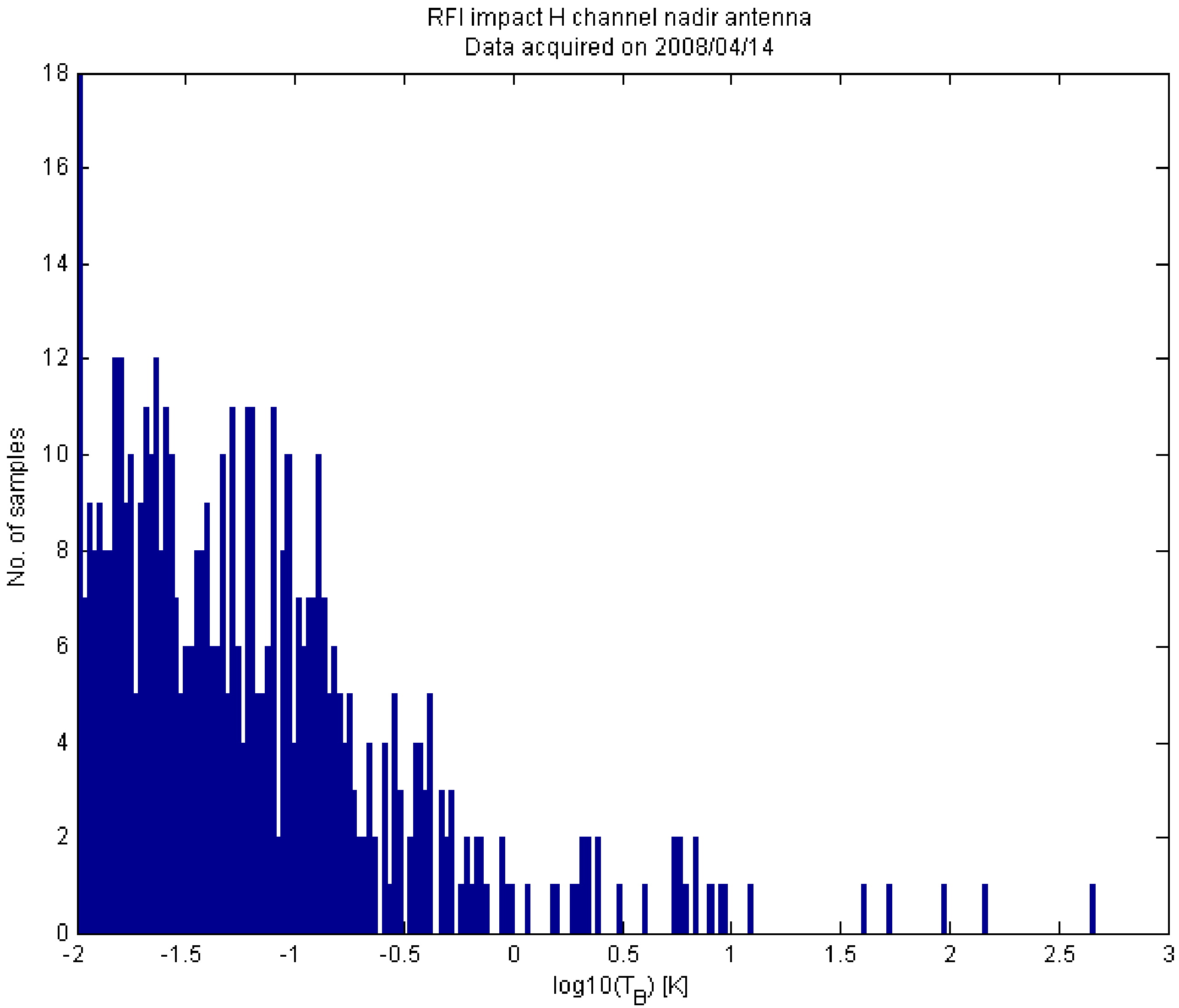

RFI impact
Munich 2008-04-14
nadir V channel

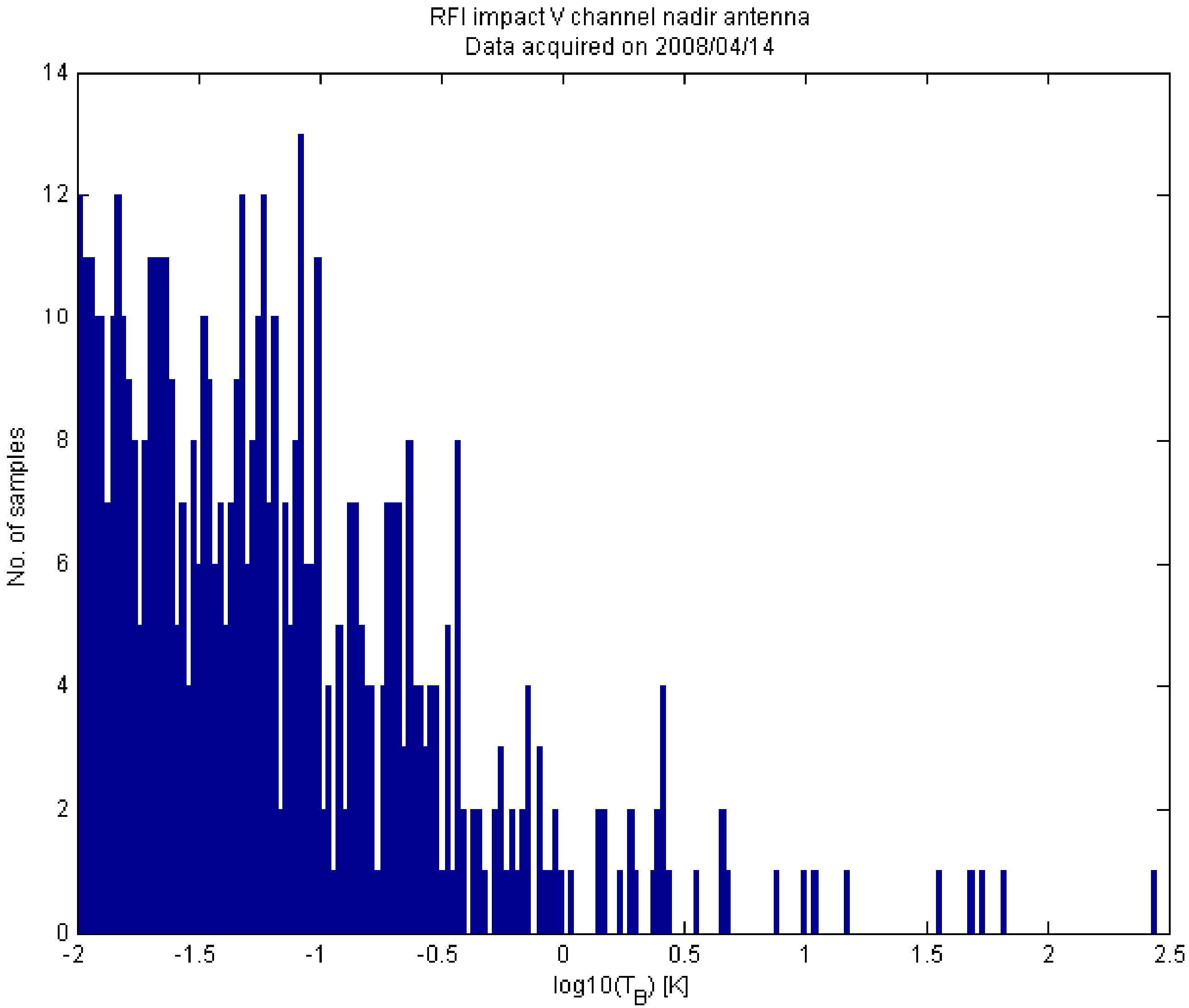

Overview

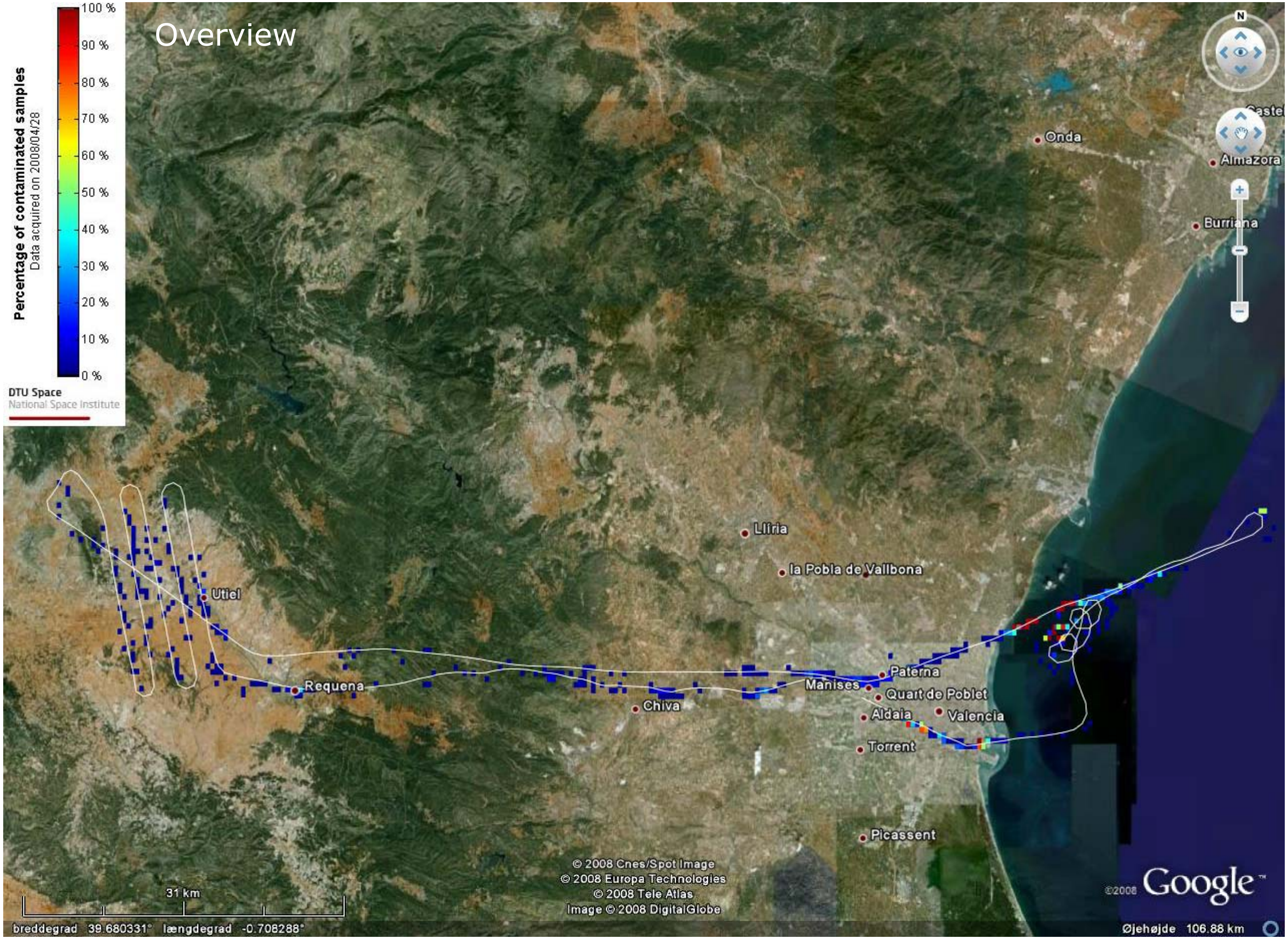
100 %
90 %
80 %
70 %
60 %
50 %
40 %
30 %
20 %
10 %
0 %
Percentage of contaminated samples
Data acquired on 2008/04/28
DTU Space
National Space Institute
Onda
Almazora
Burriana
Llíria
la Pobla de Vallbona
Utiel
Requena
Chiva
Manises
Paterna
Quart de Poblet
Aldaia
Valencia
Torrent
Picassent
© 2008 Cnes/Spot Image
© 2008 Europa Technologies
© 2008 Tele Atlas
Image © 2008 DigitalGlobe
31 km
breddegrad 39.680331° længdegrad -0.708288°
©2008 Google
Øjehøjde 106.88 km

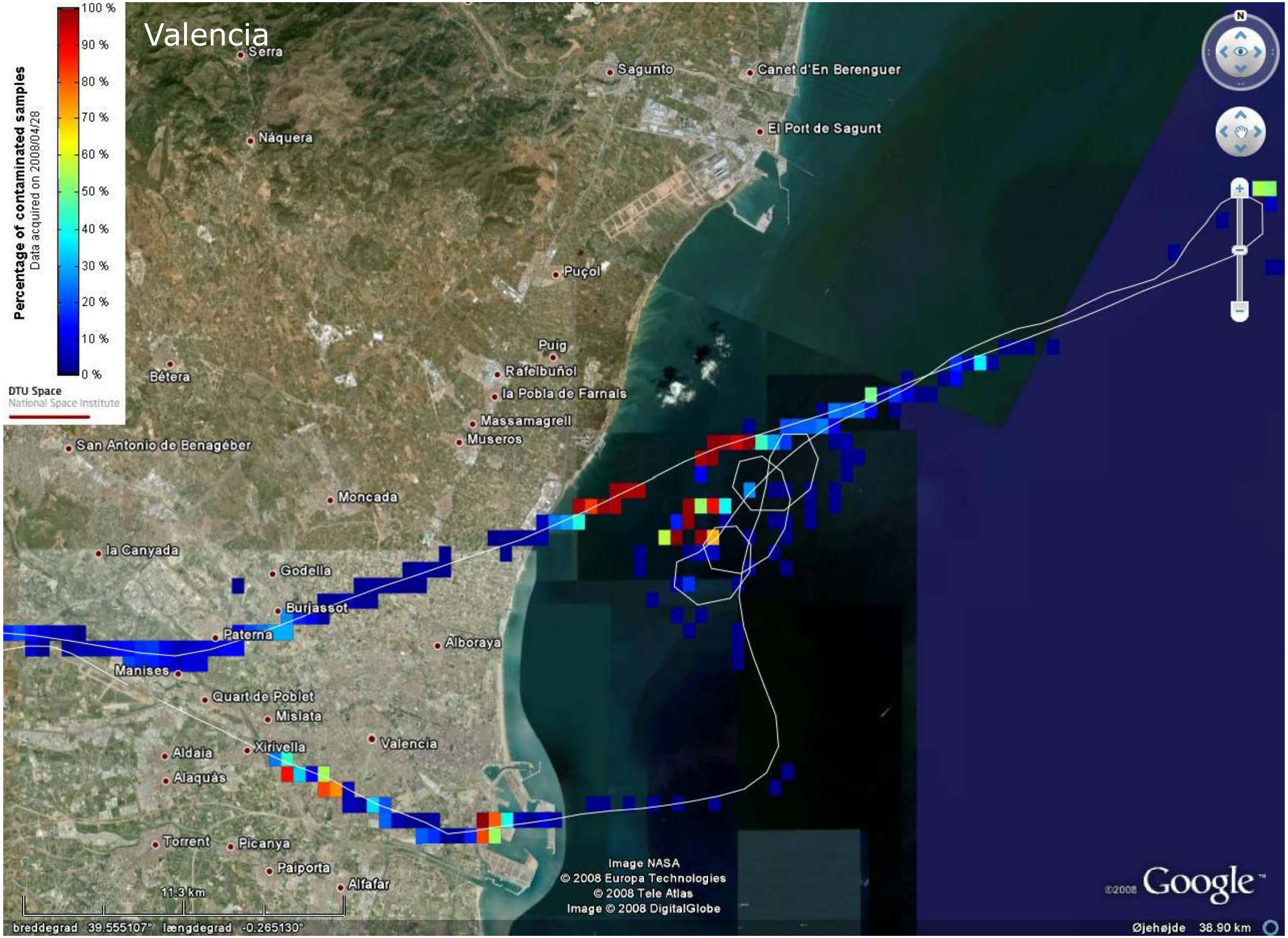
Valencia
100 %
90 %
80 %
70 %
60 %
50 %
40 %
30 %
20 %
10 %
0 %
Percentage of contaminated samples
Data acquired on 2008/04/28
DTU Space
National Space Institute
Serra
Sagunto
Canet d'En Berenguer
El Port de Sagunt
Náquera
Puçol
Puig
Bétera
Rafelbuñol
la Pobla de Farnals
Massamagrell
Museros
San Antonio de Benagéber
Moncada
la Canyada
Godella
Burjassot
Paterna
Alboraya
Manises
Quart de Poblet
Mislata
Valencia
Xirivella
Aldaia
Alaquàs
Torrent
Picanya
Paiporta
Alfafar
11.3 km
Image NASA
© 2008 Europa Technologies
© 2008 Tele Atlas
Image © 2008 DigitalGlobe
©2008 Google
breddegrad 39.555107° længdegrad -0.265130°
Øjehøjde 38.90 km

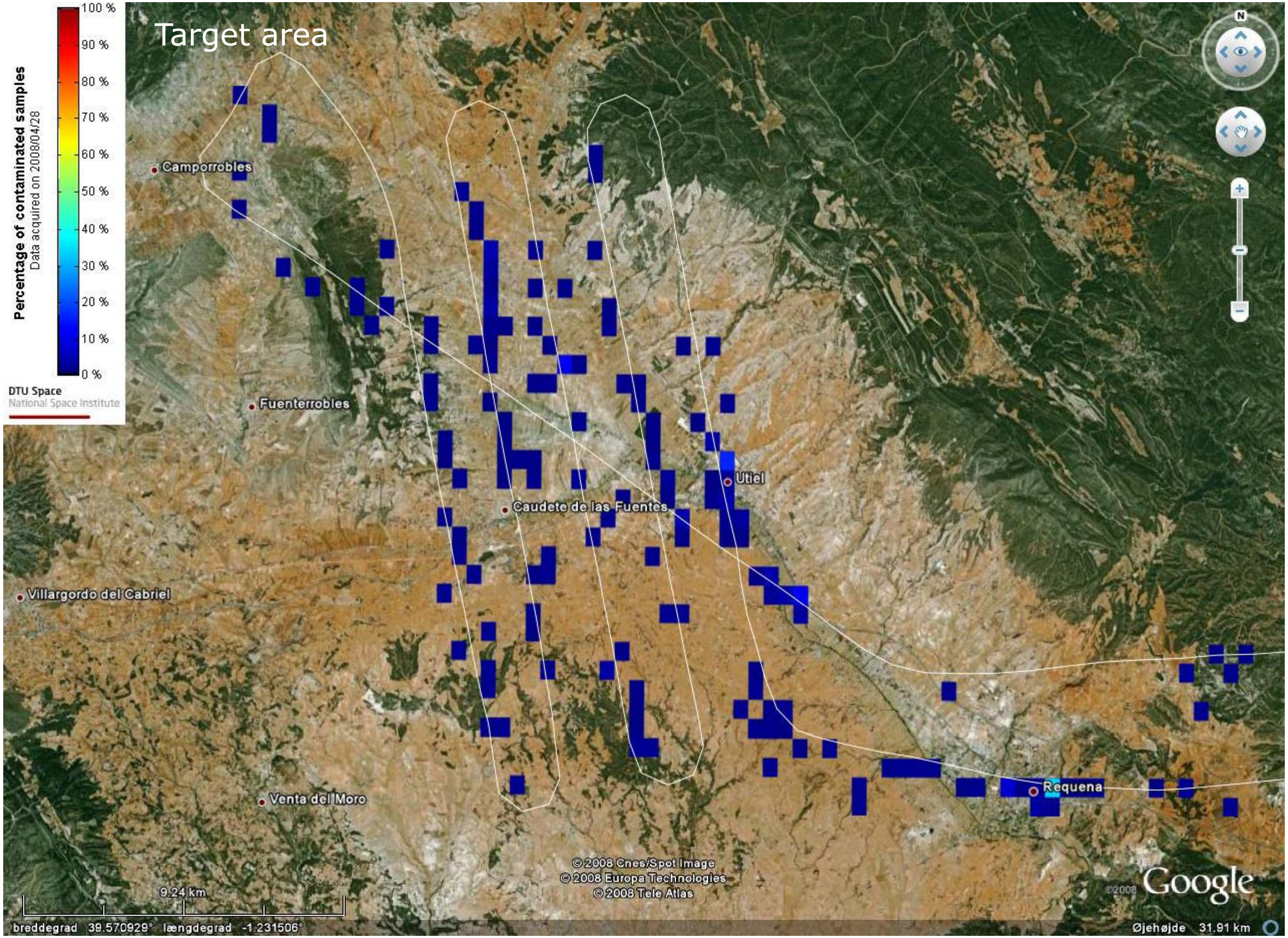
Target area
100 %
90 %
80 %
70 %
60 %
50 %
40 %
30 %
20 %
10 %
0 %
Percentage of contaminated samples
Data acquired on 2008/04/28
DTU Space
National Space Institute
Camporrobles
Fuenterrobles
Utiel
Caudete de las Fuentes
Villargordo del Cabriel
Requena
Venta del Moro
© 2008 Cnes/Spot Image
© 2008 Europa Technologies
© 2008 Tele Atlas
9.24 km
breddegrad 39.570929° længdegrad -1.231506°
Øjehøjde 31.91 km
Google

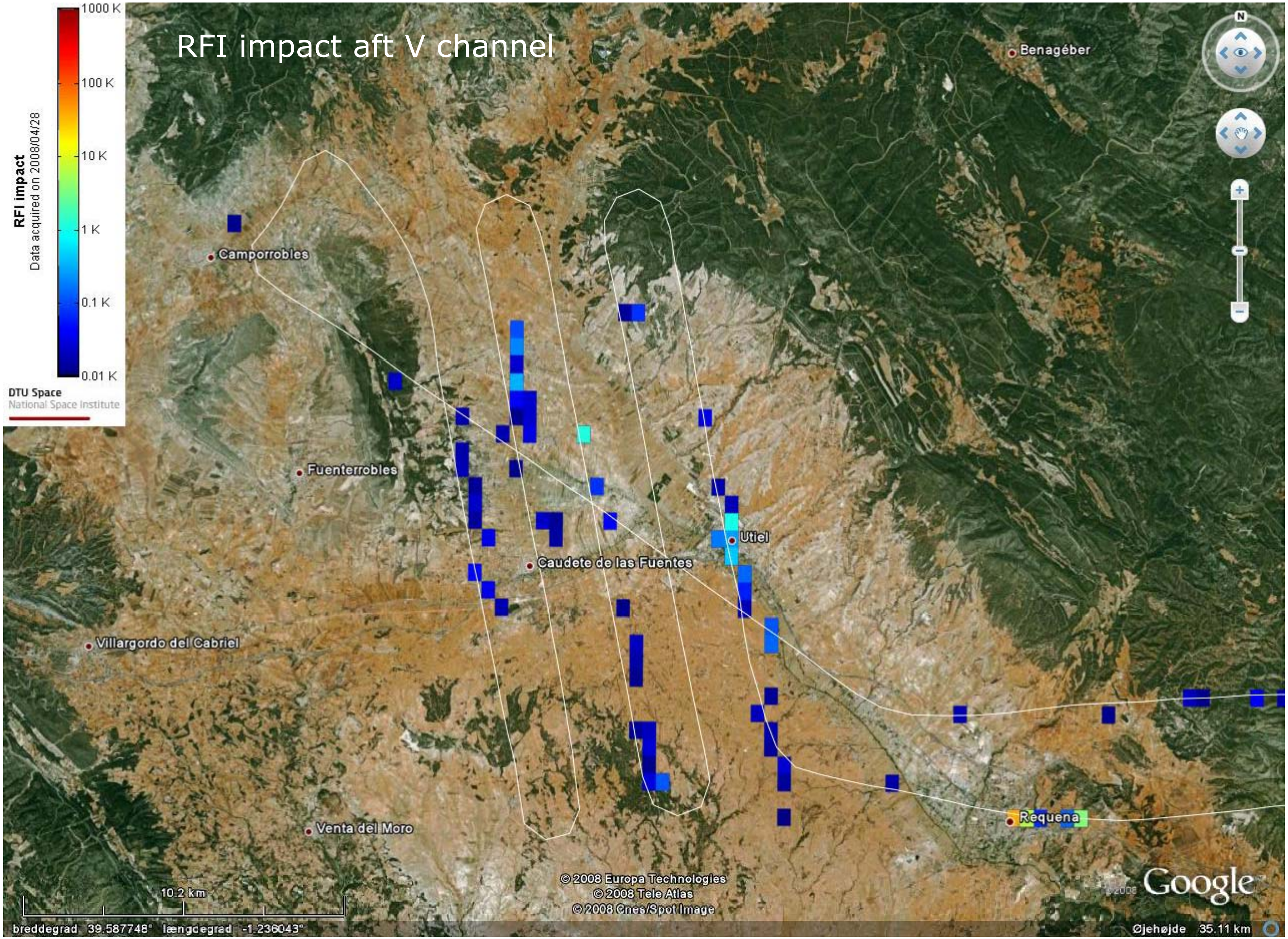

RFI impact aft V channel
RFI impact
Data acquired on 2008/04/28
1000 K
100 K
10 K
1 K
0.1 K
0.01 K
DTU Space
National Space Institute
Benagéber
Camporrobles
Fuenterrobles
Utiel
Caudete de las Fuentes
Villargordo del Cabriel
Requena
Venta del Moro
10.2 km
© 2008 Europa Technologies
© 2008 Tele Atlas
© 2008 Cnes/Spot Image
Google
breddegrad 39.587748° længdegrad -1.236043°
Øjehøjde 35.11 km

RFI impact
Valencia 2008-04-28
aft H channel

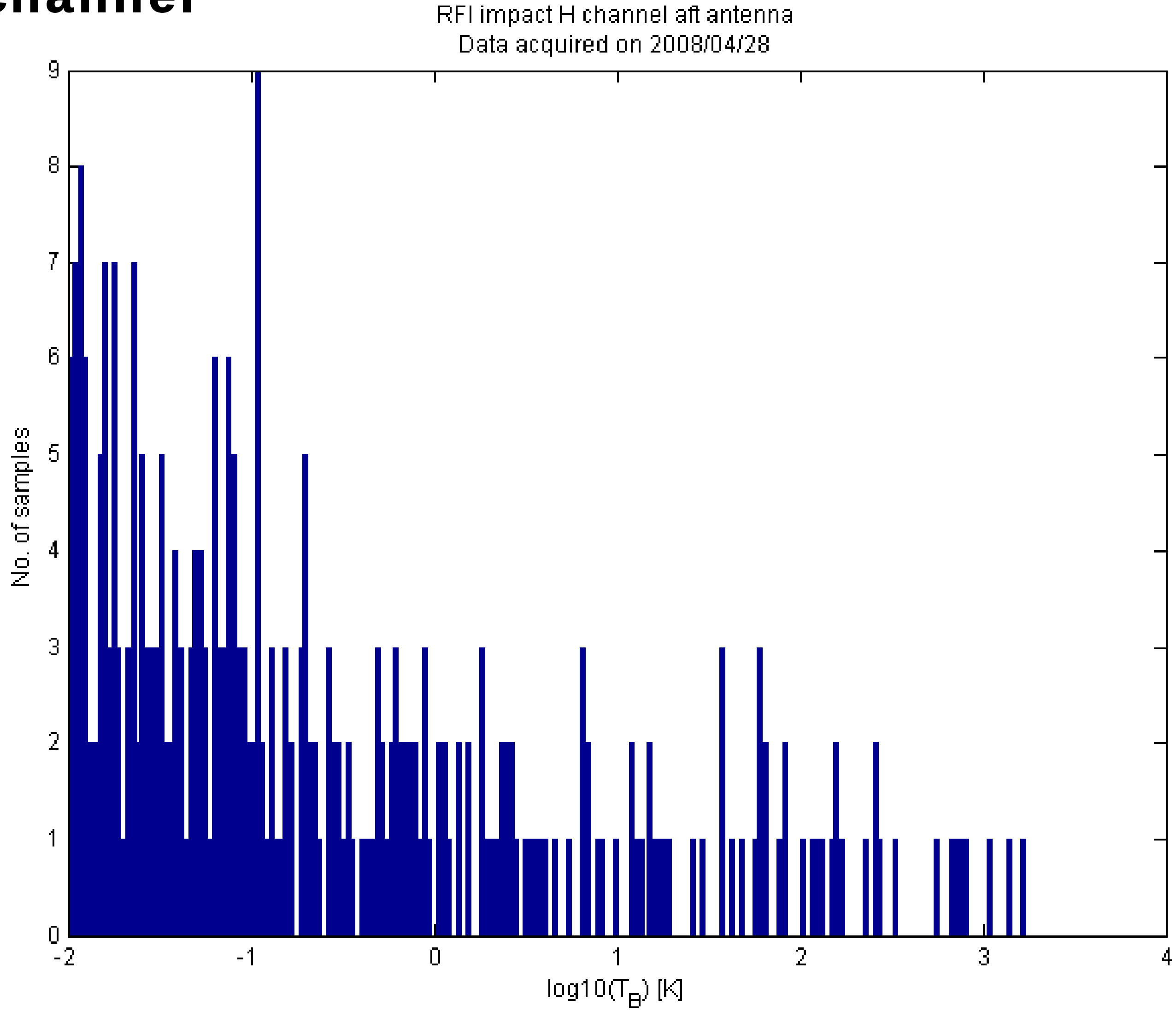

RFI impact
Valencia 2008-04-28
aft V channel

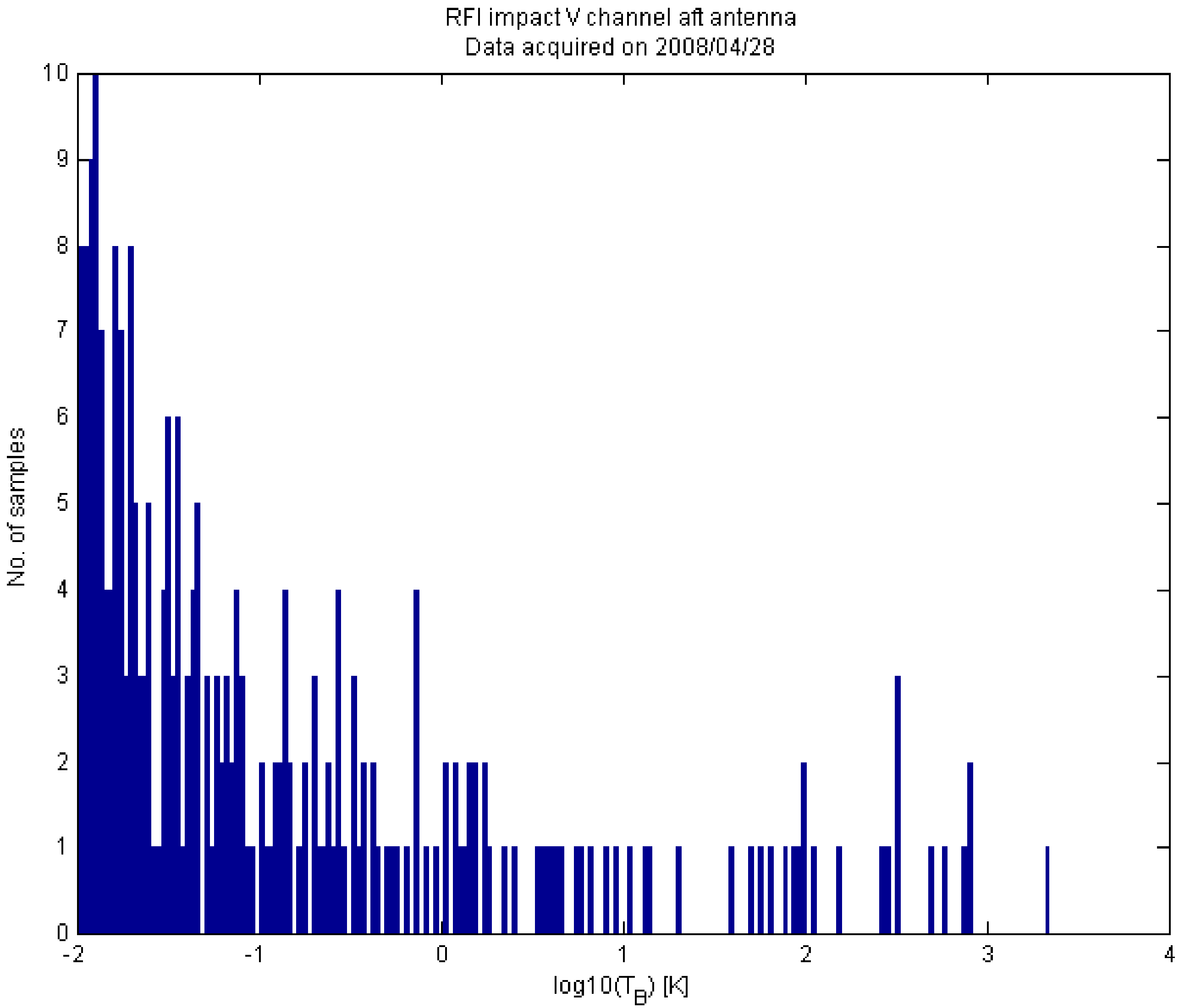

RFI impact
Valencia 2008-04-28
nadir H channel

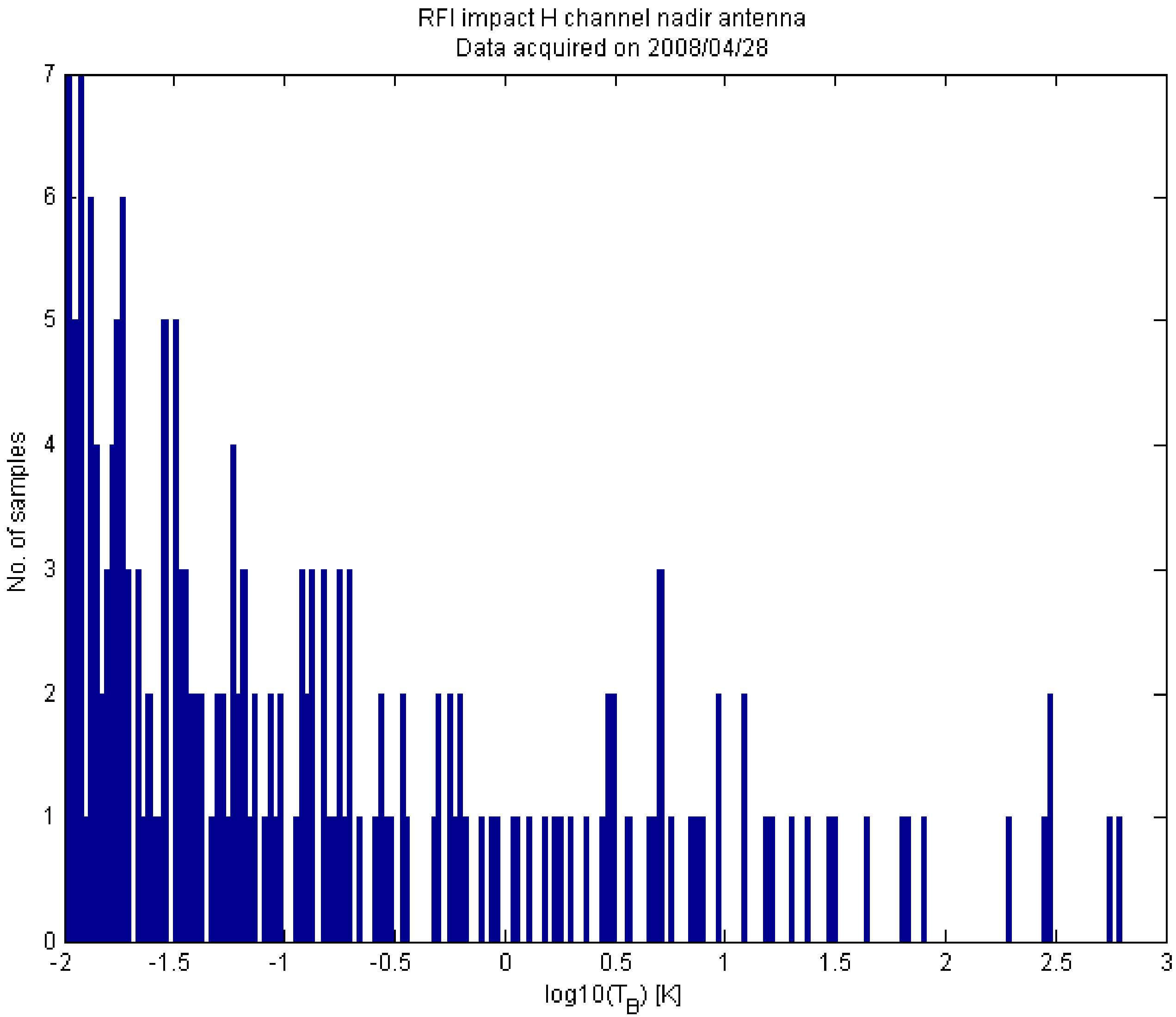

RFI impact
Valencia 2008-04-28
nadir V channel

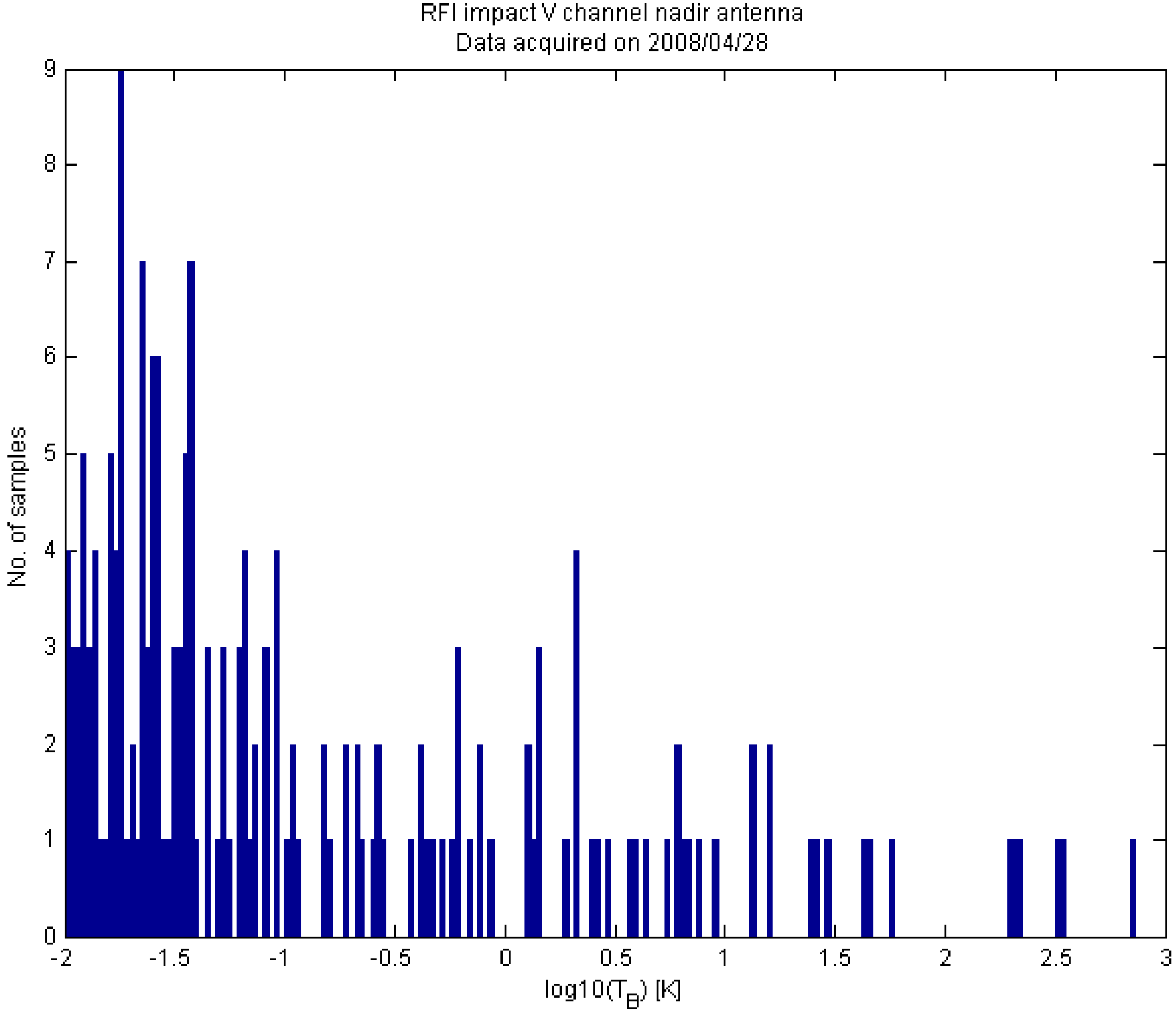

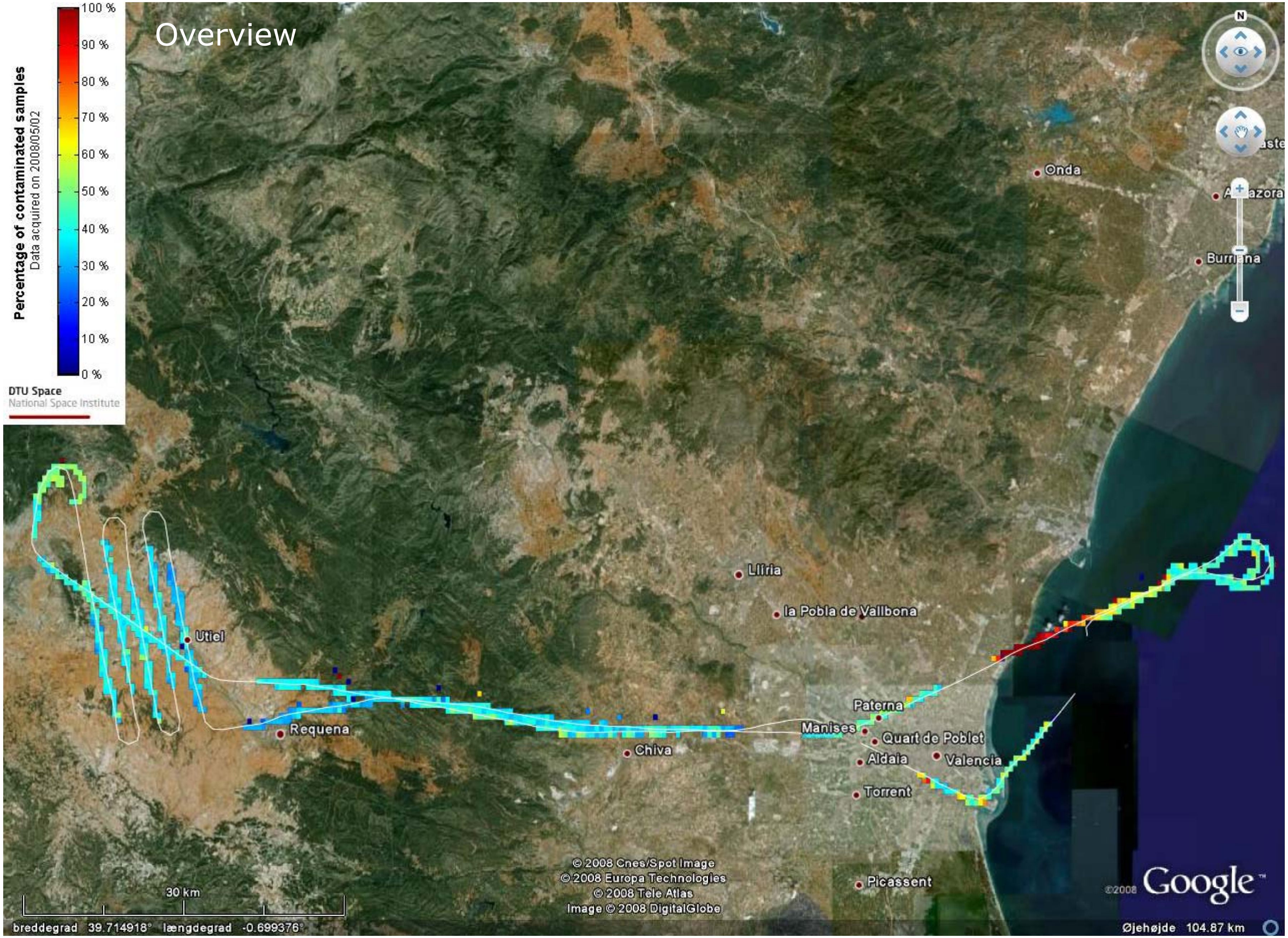
Overview
Percentage of contaminated samples
Data acquired on 2008/05/02
100 %
90 %
80 %
70 %
60 %
50 %
40 %
30 %
20 %
10 %
0 %
DTU Space
National Space Institute
Onda
Burriana
Llíria
la Pobla de Vallbona
Utiel
Requena
Chiva
Paterna
Manises
Quart de Poblet
Aldaia
Valencia
Torrent
Picassent
30 km
© 2008 Cnes/Spot Image
© 2008 Europa Technologies
© 2008 Tele Atlas
Image © 2008 DigitalGlobe
Google
breddegrad 39.714918° længdegrad -0.699376°
Øjehøjde 104.87 km

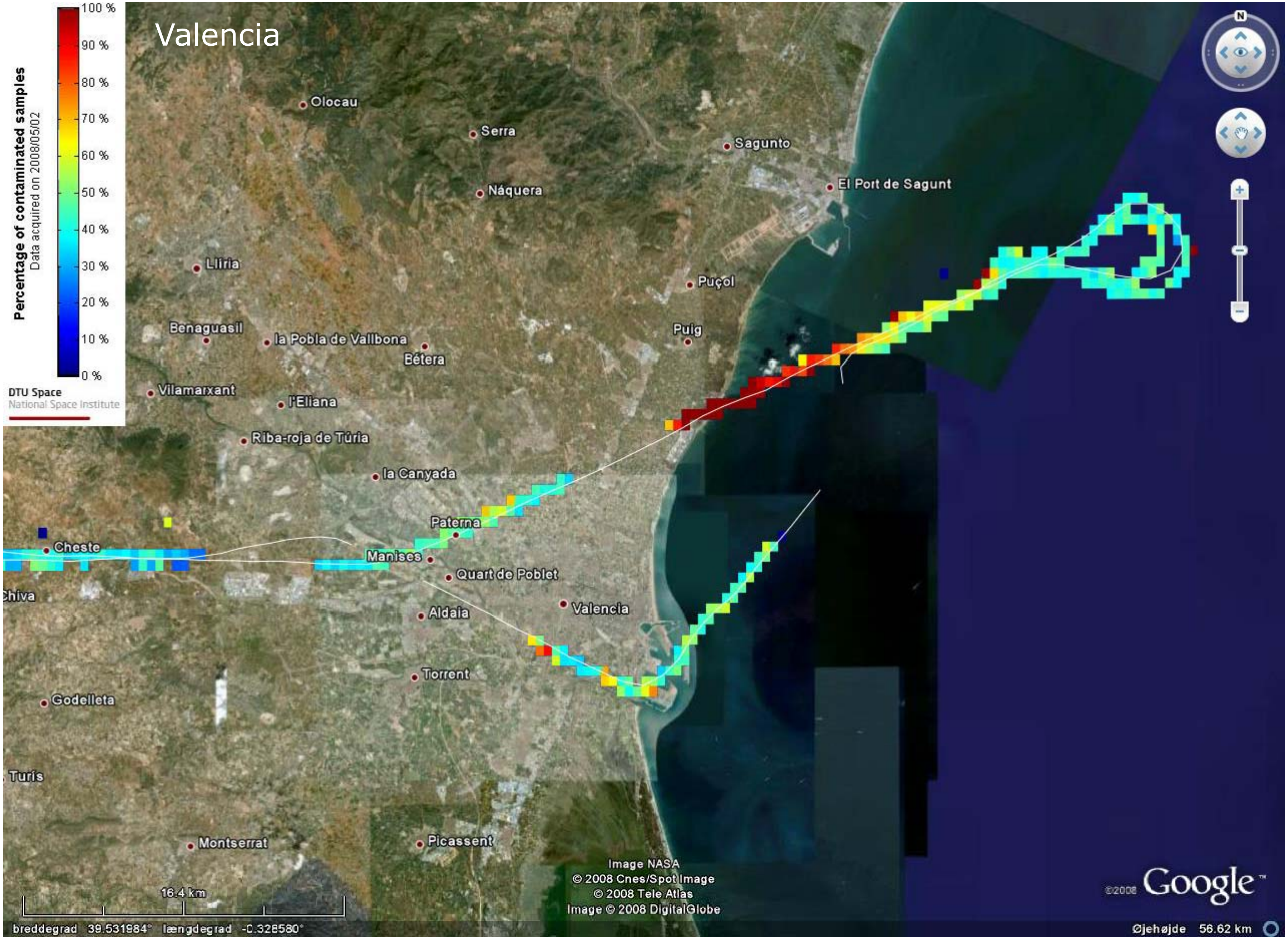
Valencia
Percentage of contaminated samples
Data acquired on 2008/05/02
100 %
90 %
80 %
70 %
60 %
50 %
40 %
30 %
20 %
10 %
0 %
DTU Space
National Space Institute
Olocau
Serra
Sagunto
El Port de Sagunt
Náquera
Llíria
Puçol
Puig
Benaguasil
la Pobla de Vallbona
Bétera
Vilamarxant
l'Eliana
Riba-roja de Túria
la Canyada
Paterna
Cheste
Manises
Quart de Poblet
Chiva
Valencia
Aldaia
Torrent
Godelleta
Turís
Montserrat
Picassent
Image NASA
© 2008 Cnes/Spot Image
© 2008 Tele Atlas
Image © 2008 DigitalGlobe
16.4 km
breddegrad 39.531984° længdegrad -0.328580°
©2008 Google
Øjehøjde 56.62 km

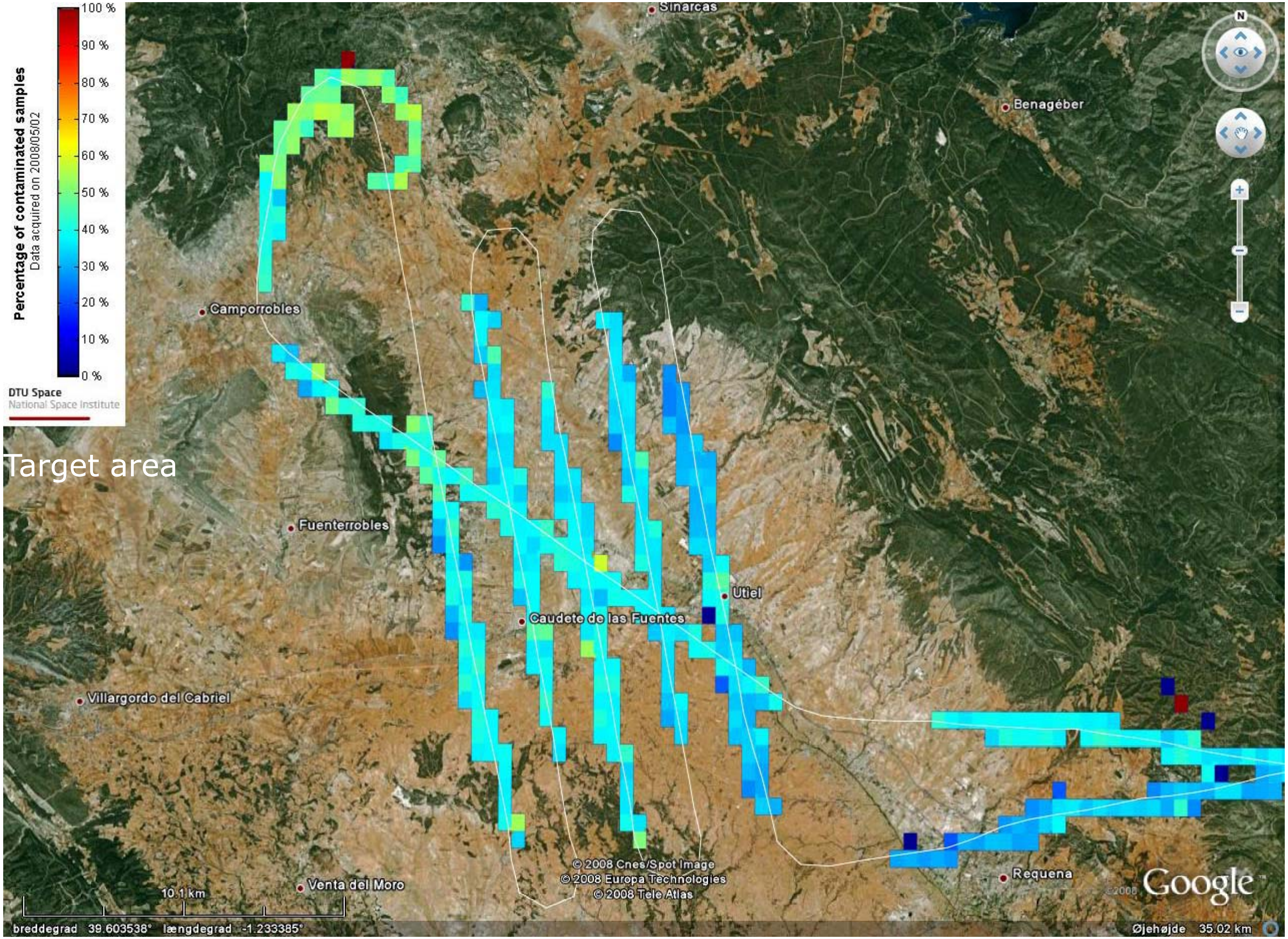
Percentage of contaminated samples
Data acquired on 2008/05/02
100 %
90 %
80 %
70 %
60 %
50 %
40 %
30 %
20 %
10 %
0 %
DTU Space
National Space Institute
Target area
Sinarcas
Benagéber
Camporrobles
Fuenterrobles
Utiel
Caudete de las Fuentes
Villargordo del Cabriel
Requena
Venta del Moro
10.1 km
© 2008 Cnes/Spot Image
© 2008 Europa Technologies
© 2008 Tele Atlas
Google
breddegrad 39.603538° længdegrad -1.233385°
Øjehøjde 35.02 km

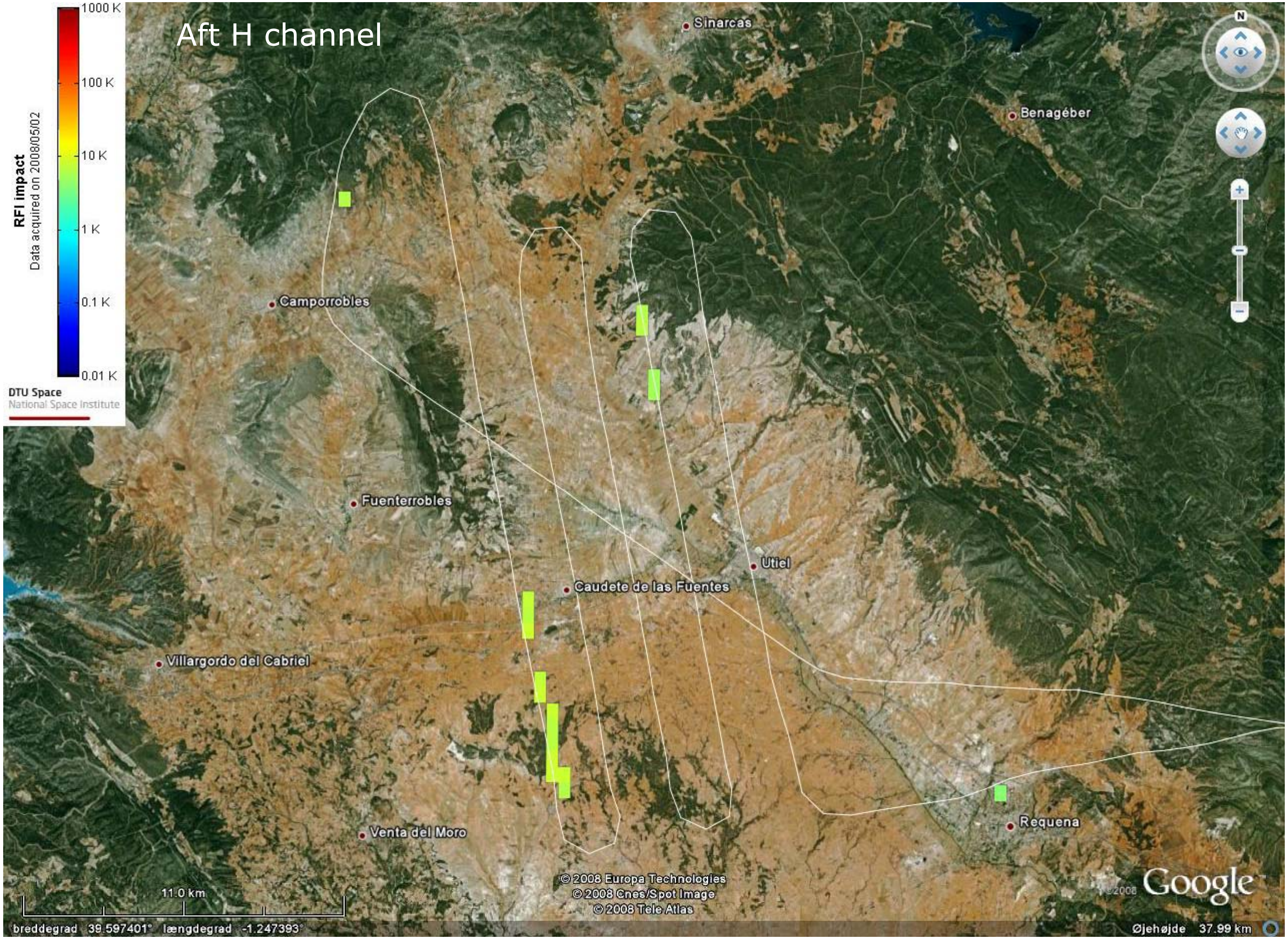
Aft H channel
RFI impact
Data acquired on 2008/05/02
1000 K
100 K
10 K
1 K
0.1 K
0.01 K
DTU Space
National Space Institute
Sinarcas
Benagéber
Camporrobles
Fuenterrobles
Utiel
Caudete de las Fuentes
Villargordo del Cabriel
Venta del Moro
Requena
© 2008 Europa Technologies
© 2008 Cnes/Spot Image
© 2008 Tele Atlas
Google
11.0 km
breddegrad 39.597401° længdegrad -1.247393°
Øjehøjde 37.99 km

RFI impact
Valencia 2008-05-02
aft H channel

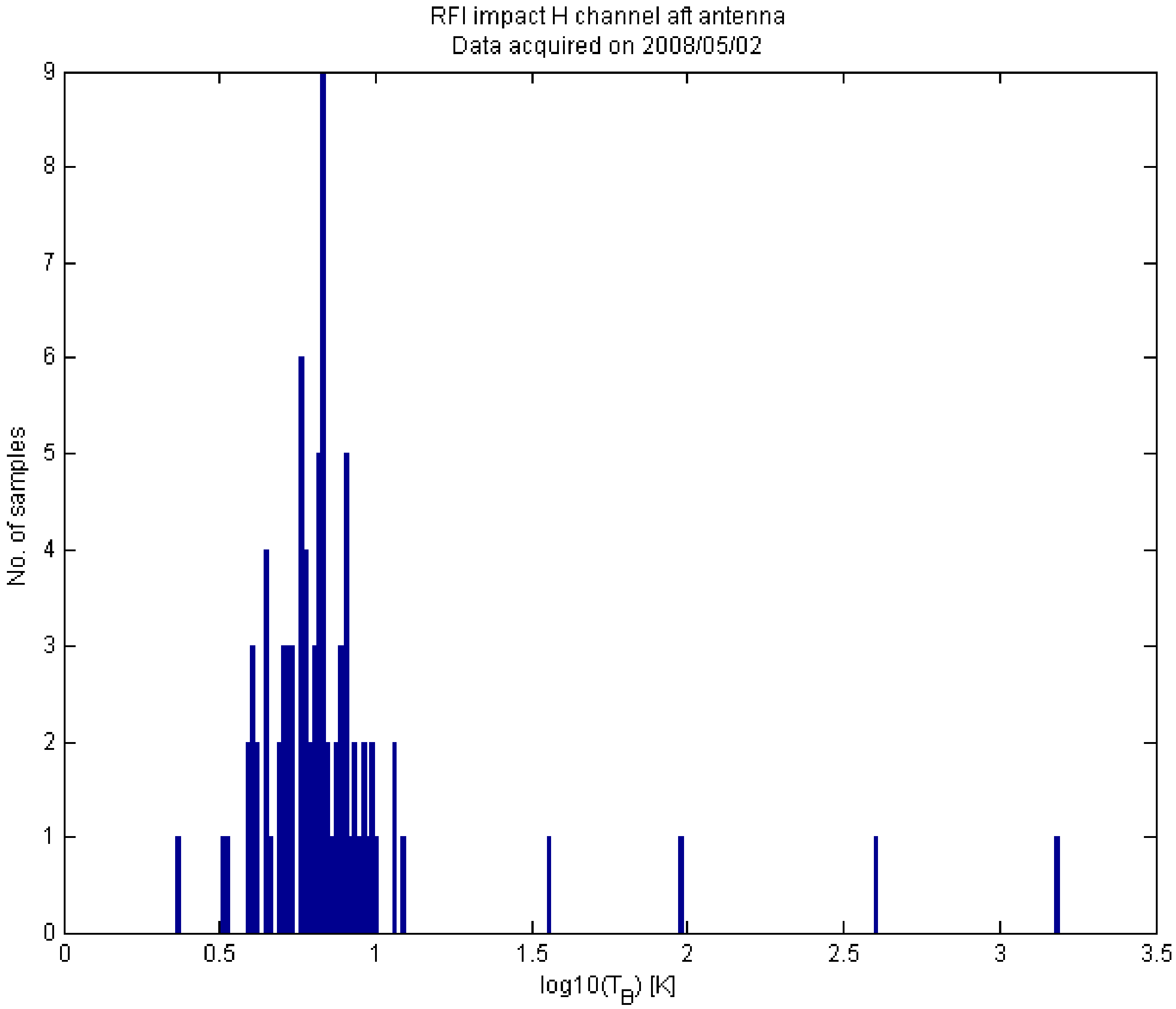

RFI impact
Valencia 2008-05-02
aft V channel

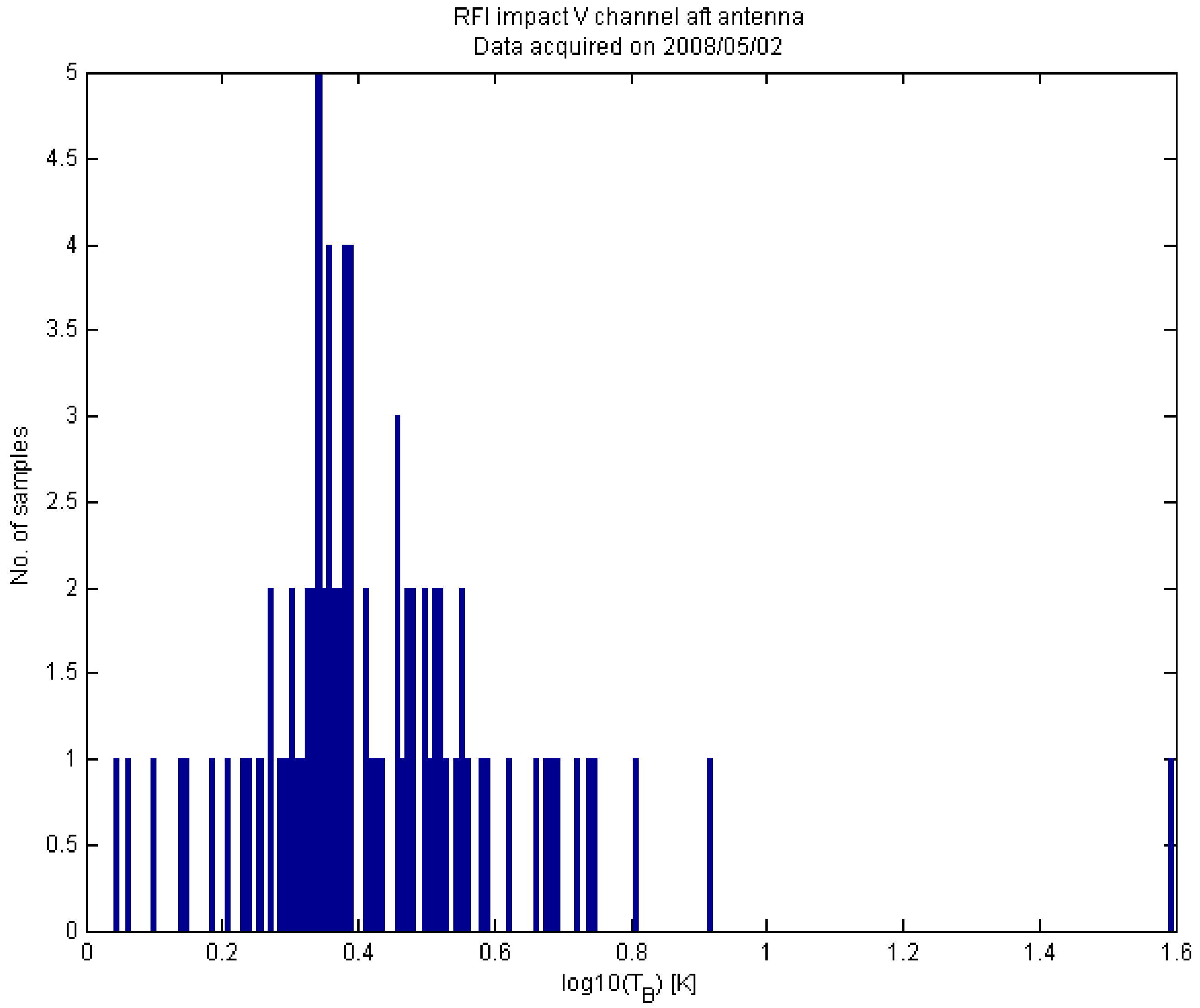

RFI impact
Valencia 2008-05-02
nadir H channel

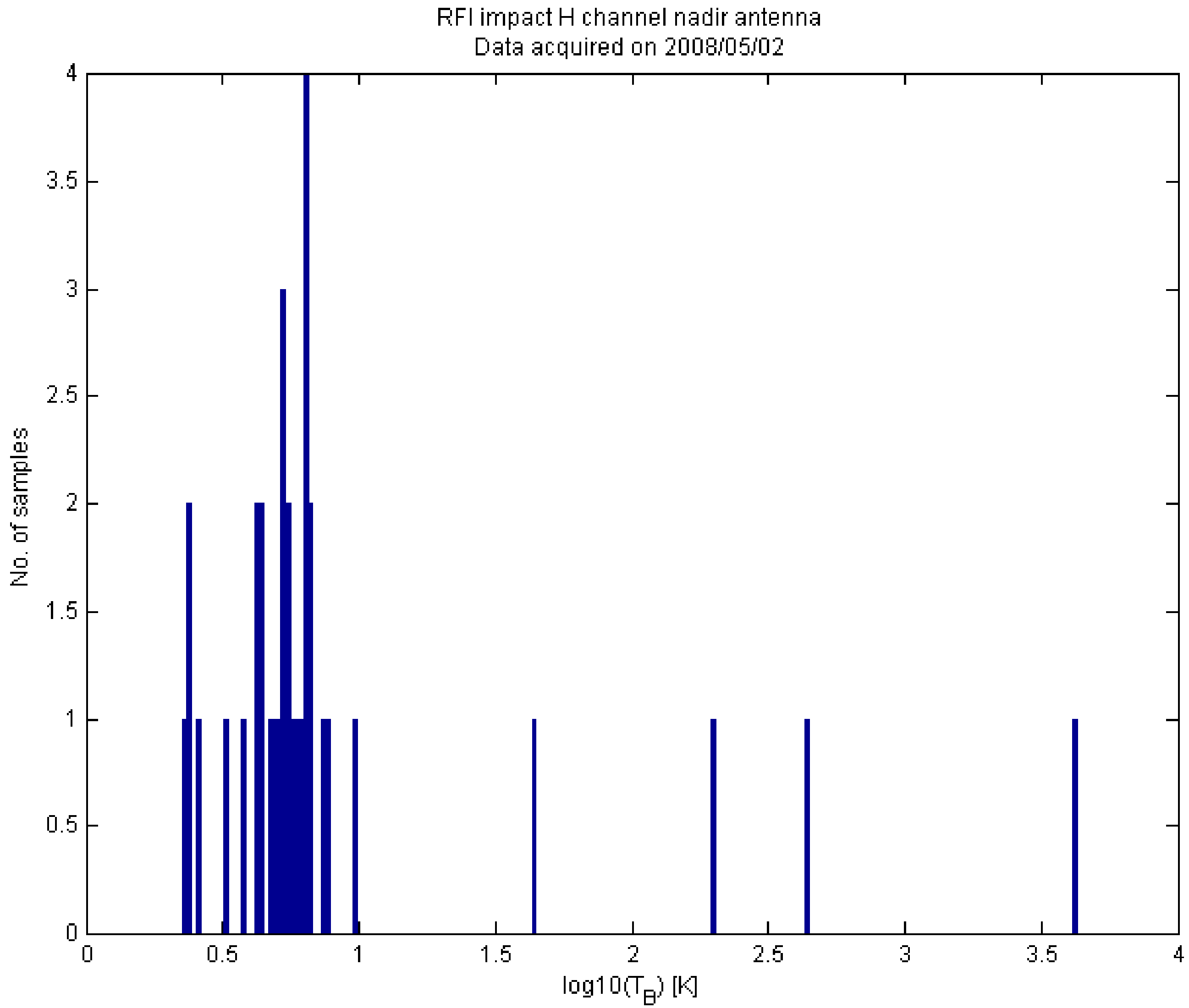

RFI impact
Valencia 2008-05-02
nadir V channel

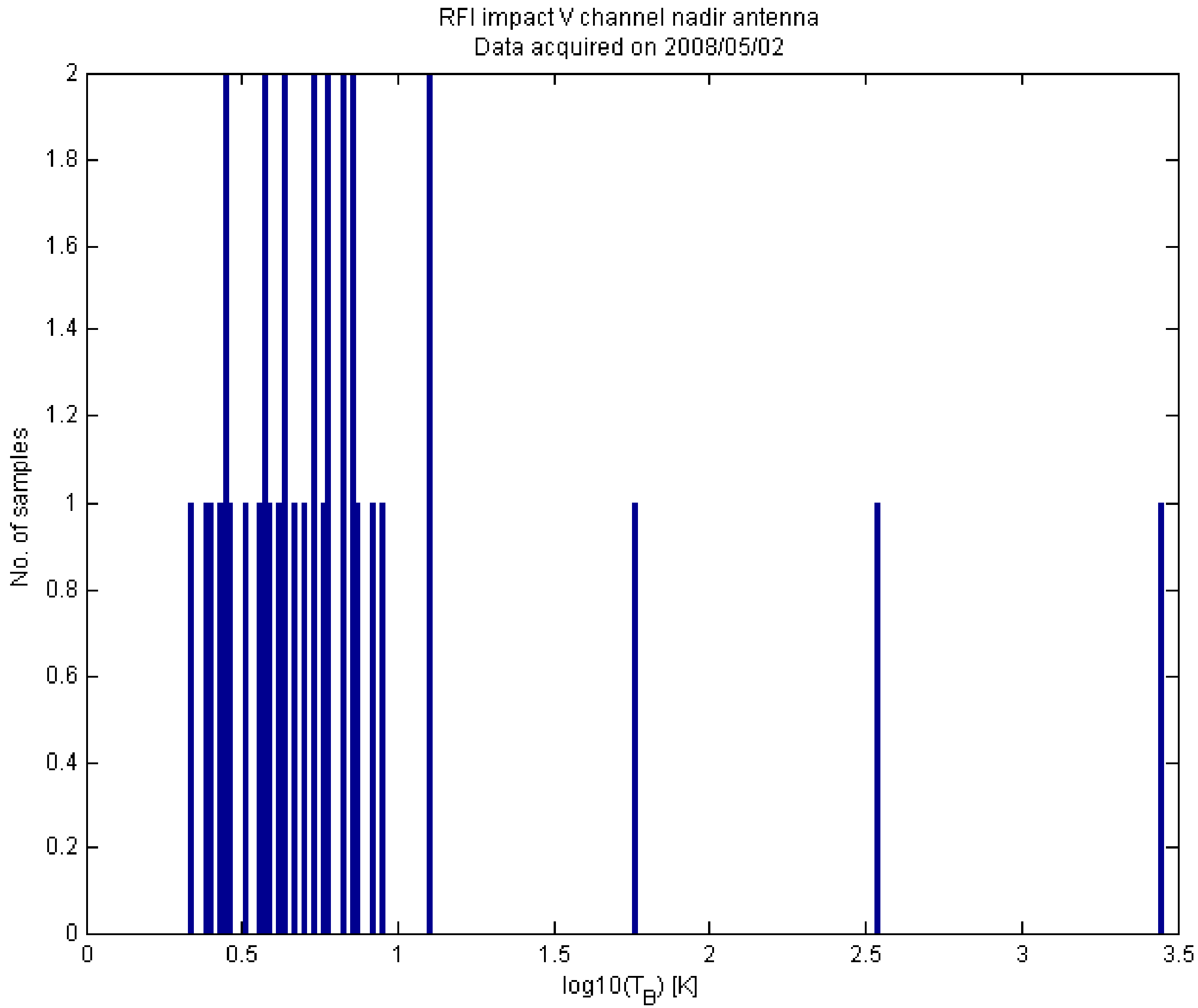

Amount of RFI encountered during campaigns - conclusion

- The amount of RFI is generally low in northern Europe – especially in Finland and over the North Sea – Australia does not stand out in this manner, either.
- In Australia, Germany, and Spain, RFI is generally seen around urban centers, airports etc.
- Much of the kurtosis-detected RFI has an impact on the data below 1K
- Southern France is a special case – very high levels of RFI were encountered in this area. This is due to the French National railways operating communications links close to the protected L-band frequencies. In response, EMIRAD (and CAROLS) filters have been re-tuned.

How reliable is the kurtosis-based detection method really?

Evaluating the kurtosis method

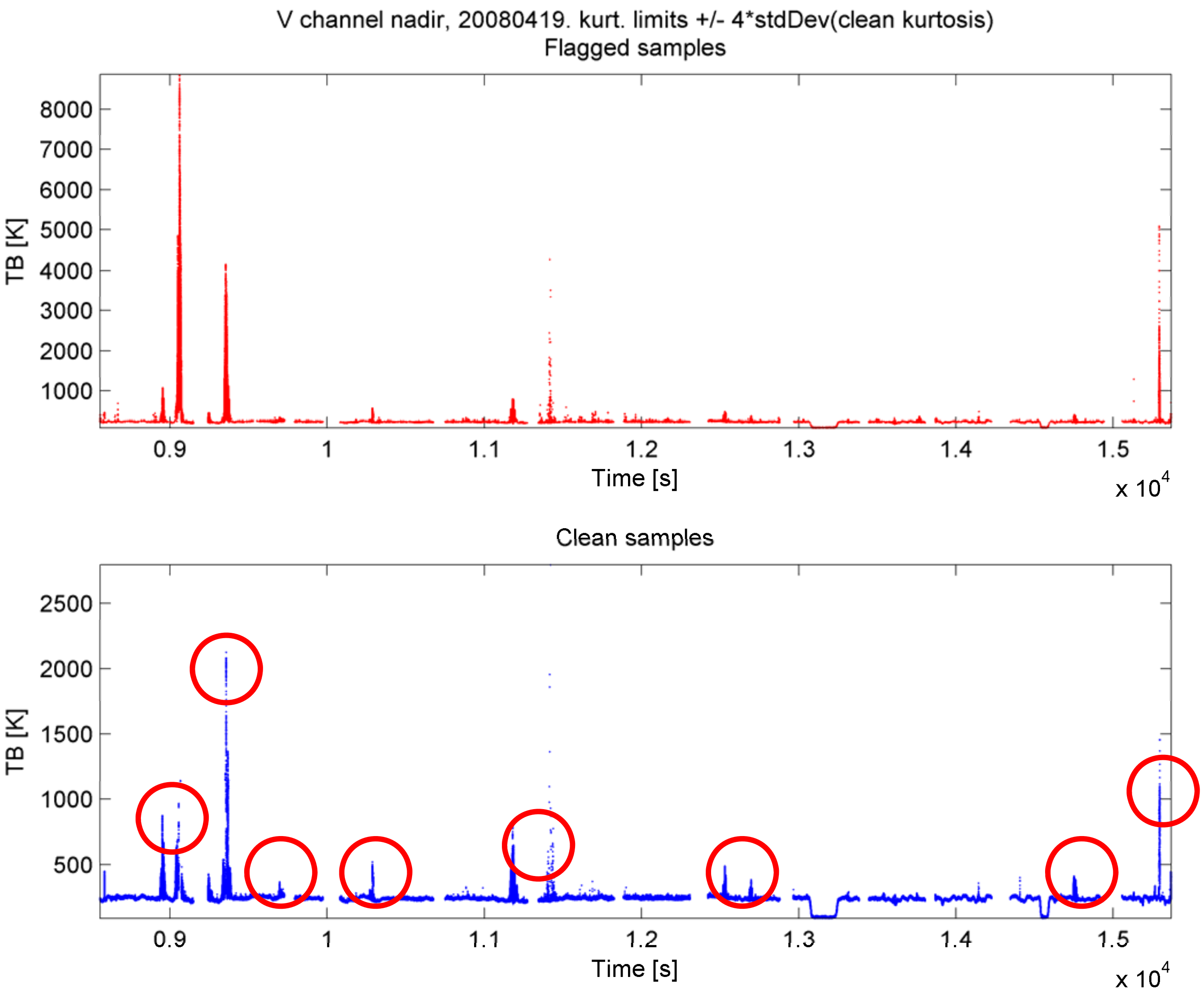

Evaluating the kurtosis method

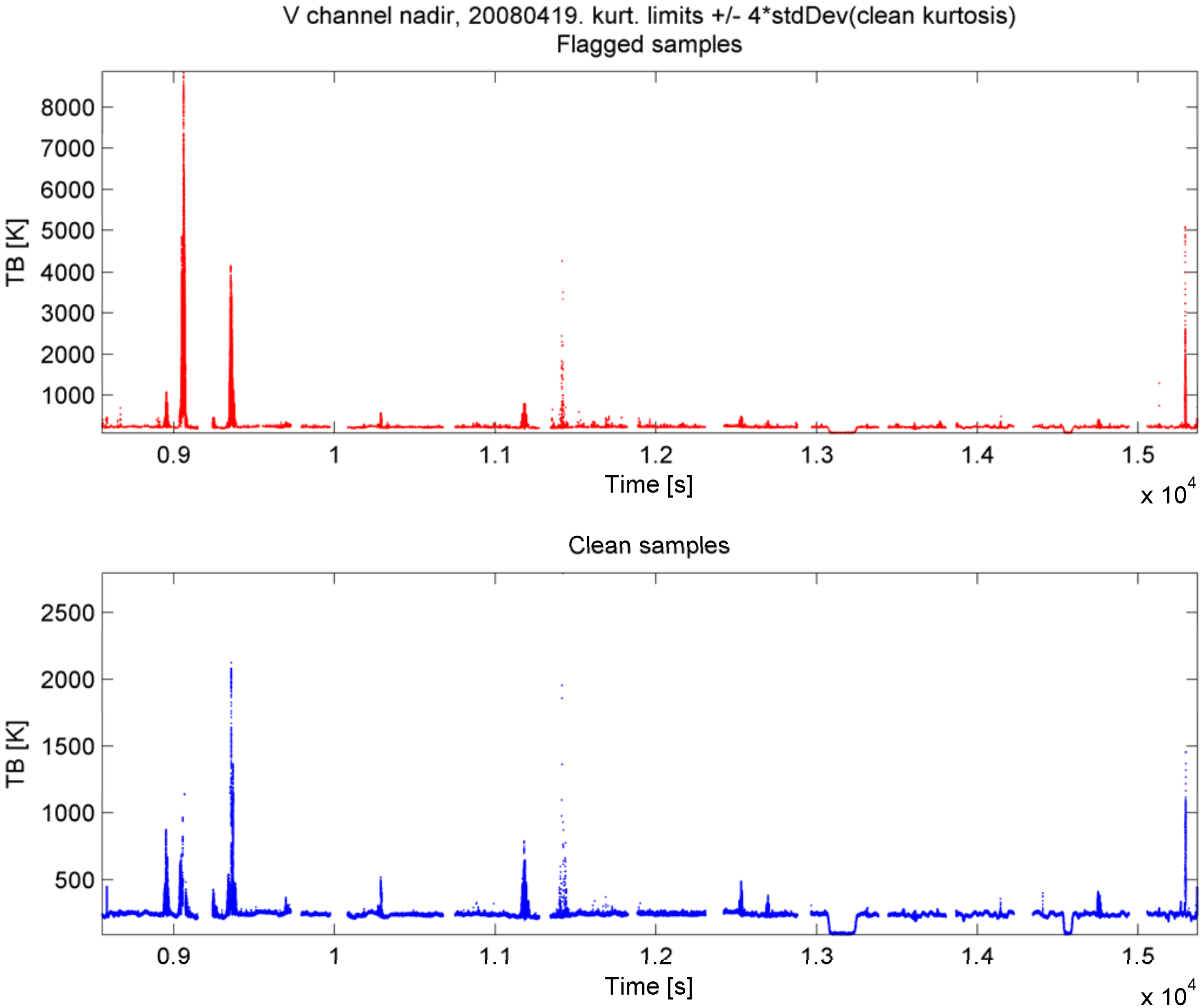

3.5% flagged

1.27% > 300K

Evaluating the kurtosis method

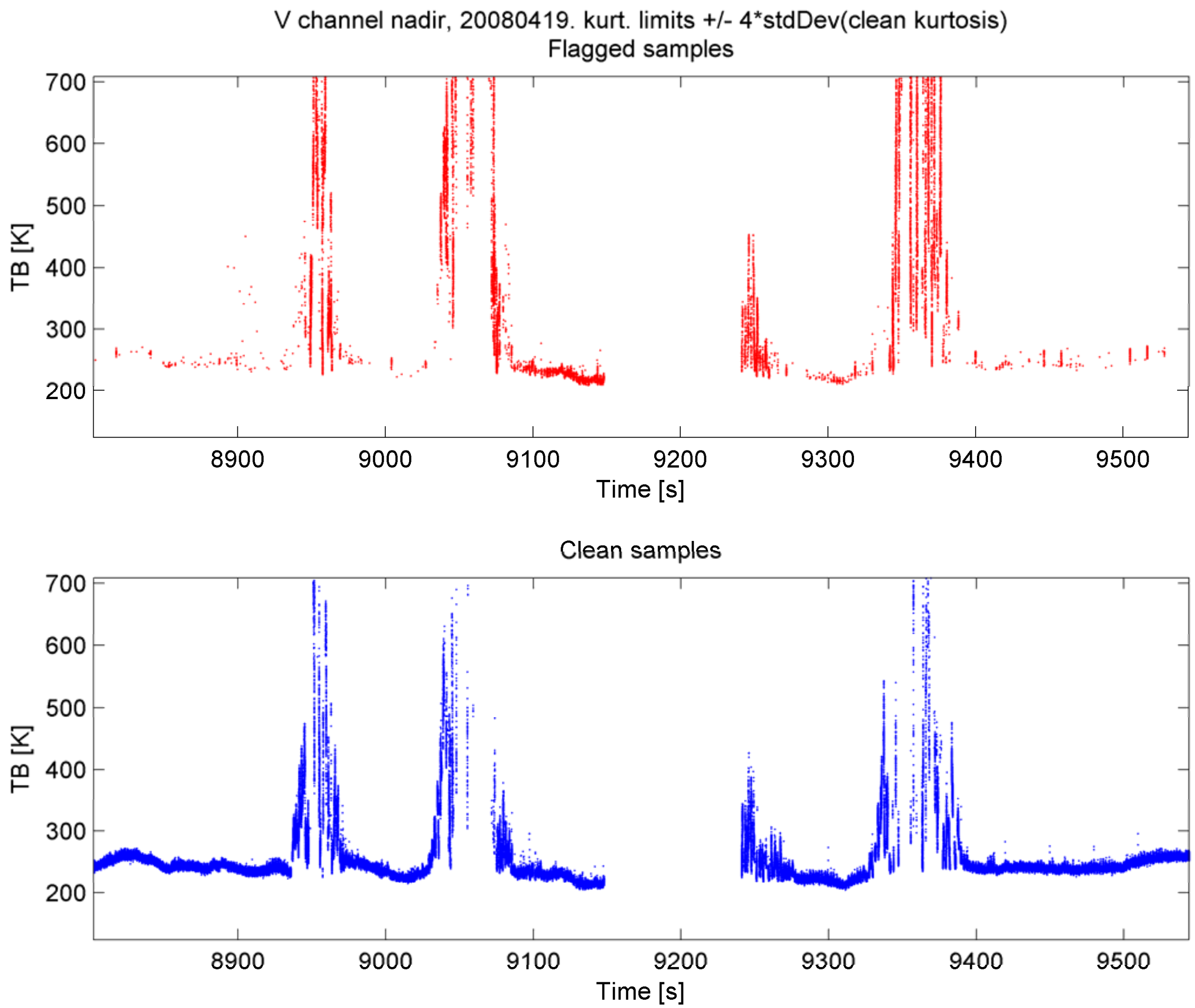

Evaluating the kurtosis method

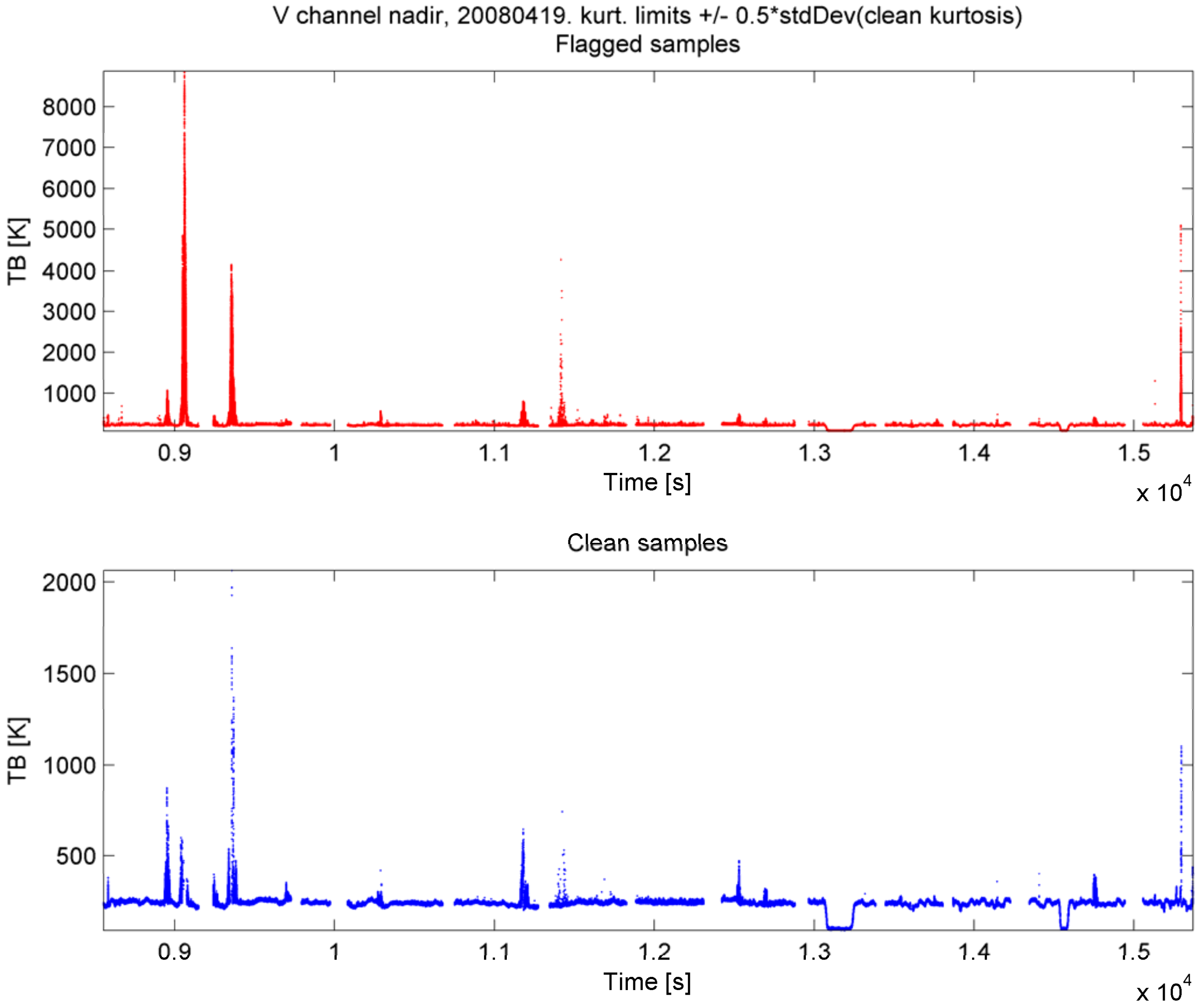

65% flagged

0.73% > 300 K

Evaluating the kurtosis method

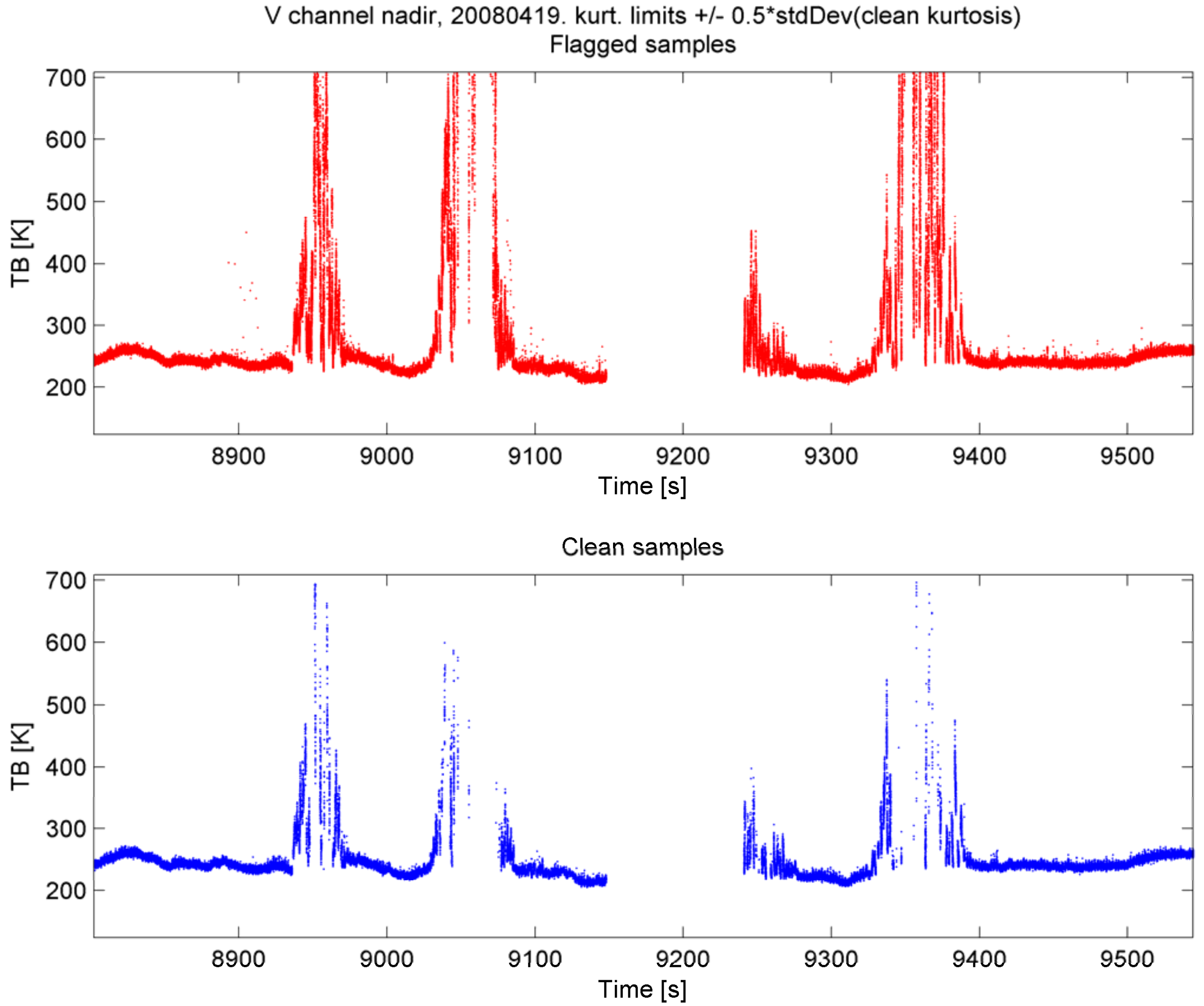

Evaluating the kurtosis method

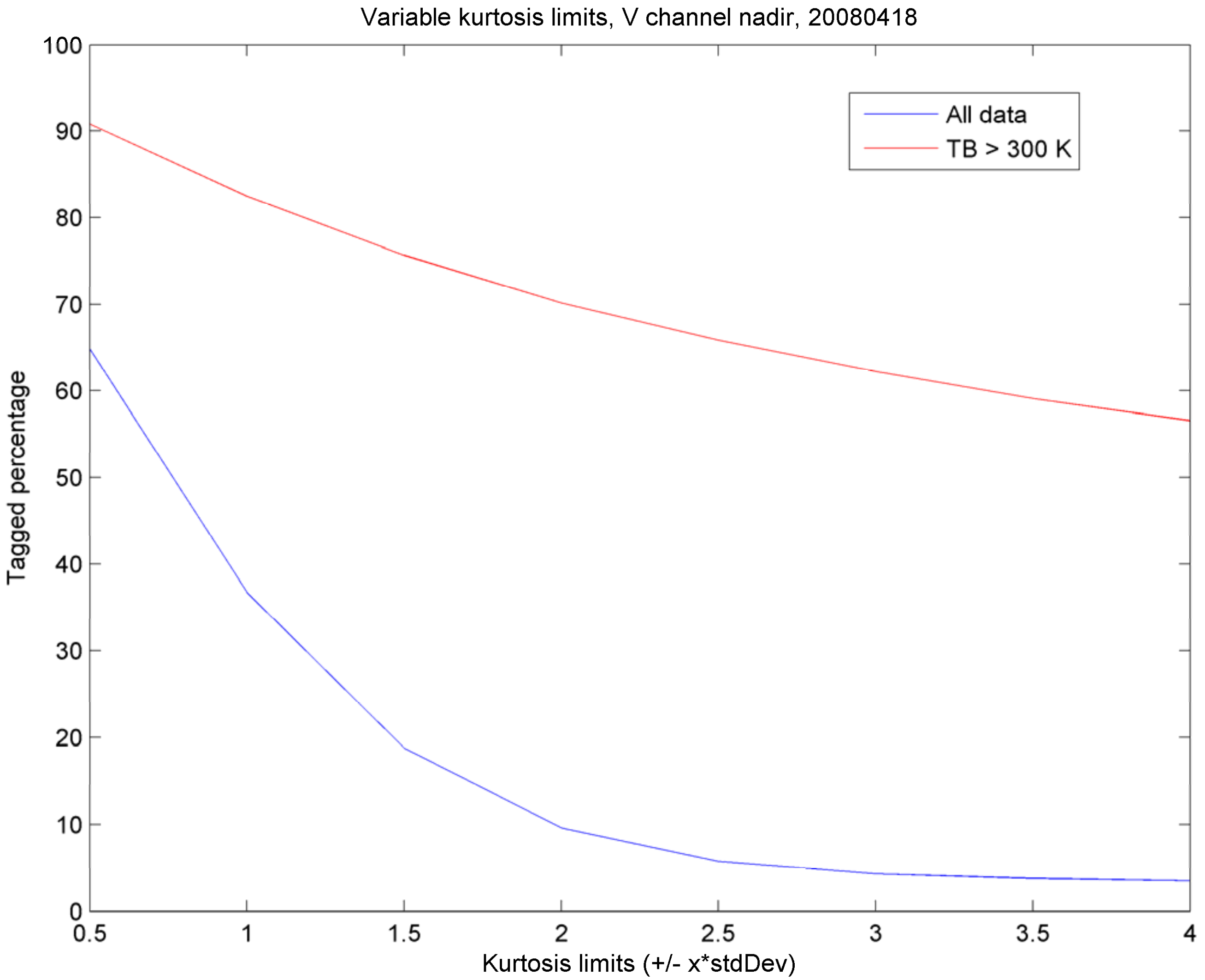

Evaluating the kurtosis method

- Inspection of kurtosis the way it has been done until now does NOT provide the full truth about RFI contamination, although a fair amount of RFI can be detected in this way

- Being more “conservative”, i.e. lowering the threshold for kurtosis values being accepted as clean does not remove some persistant spikes, instead the overall percentage of tagged samples rises rapidly.

Proposals for improved RFI detection

In some cases, RFI contamination has been seen to affect neighbouring samples, which are otherwise flagged as clean by means of kurtosis inspection.

For each sample tagged as contaminated by the conventional kurtosis method, a number of neighbouring samples should be tagged as well.

Proposals for improved RFI detection – tagging neighbours

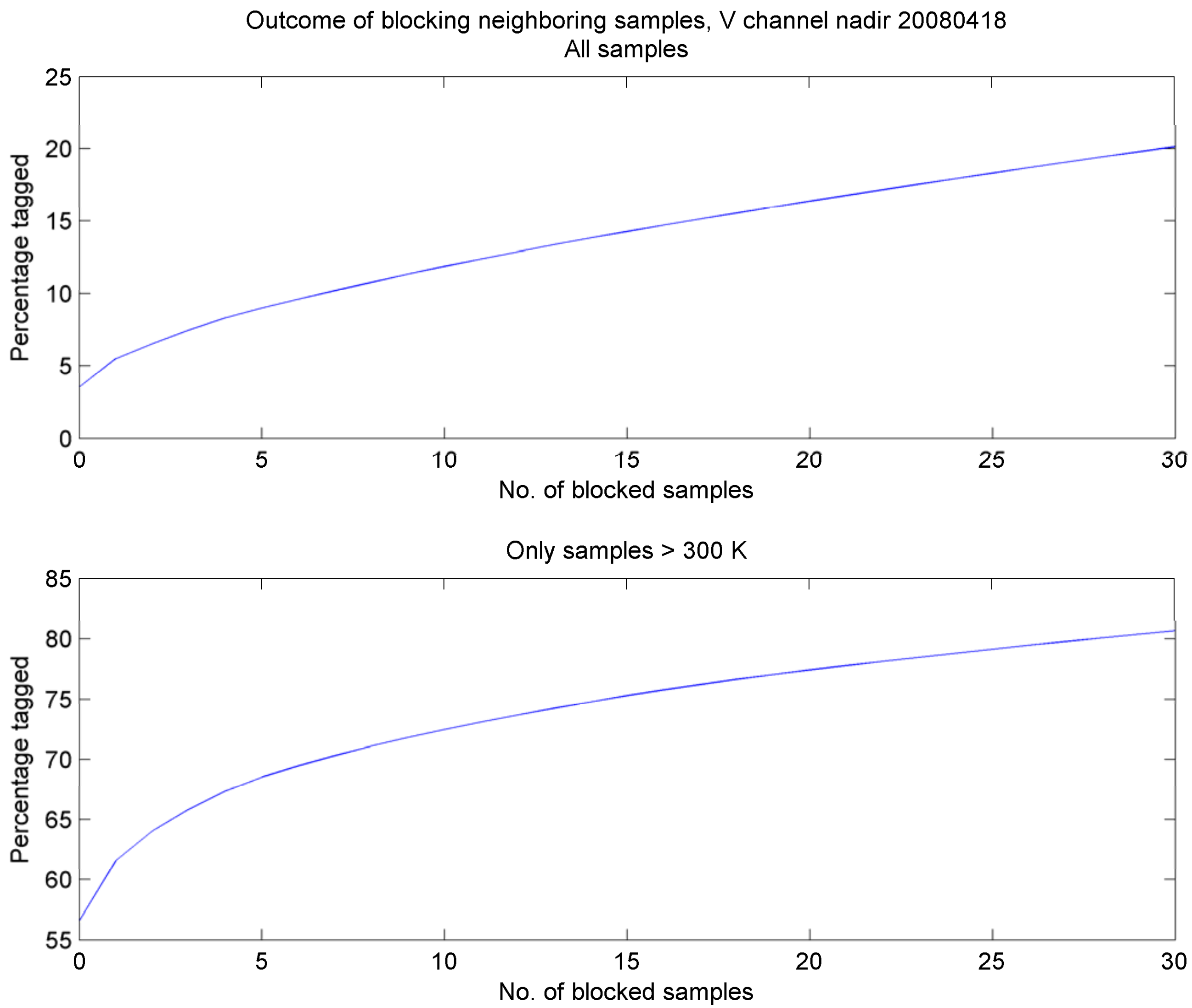

Proposals for improved RFI detection – tagging neighbours

- Tagging 30 samples on each side of every contaminated one result in:
  - 20.51 % of all samples being tagged
  - 80 % of all samples with TB > 300 K being tagged
  - 0.67 % of all “clean” samples exhibiting TB > 300 K

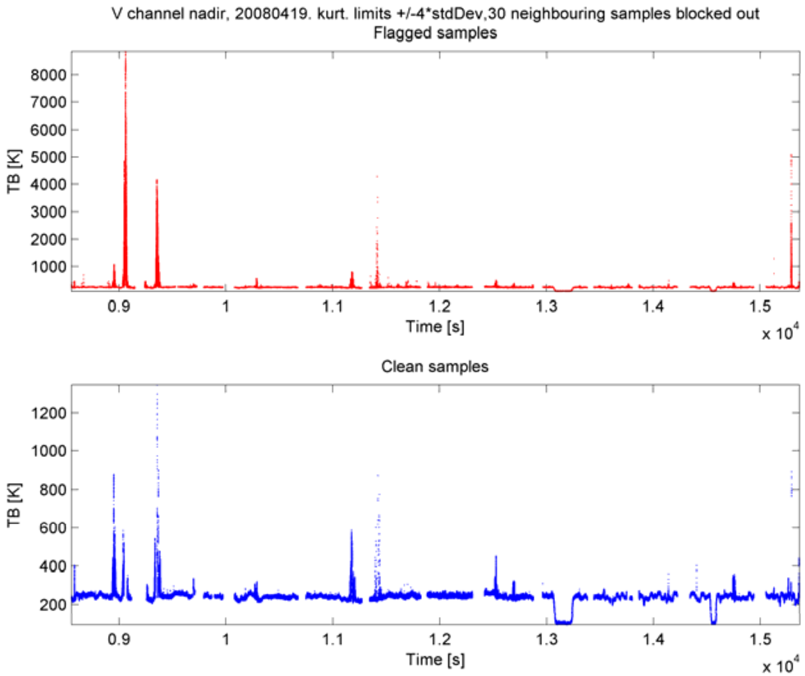

Peaks due to RFI are still clearly visible

Proposals for improved RFI detection – tagging neighbours

- In order to get anywhere near removing visible RFI contamination, many (>> 100) neighbouring samples have to be tagged as well
  - Tagging 950 neighbouring samples gets rid of all TB > 300 K, but throws away 95 % of the entire data set!!

- As a consequence, a large number of uncontaminated samples are falsely thrown away

- The method may be a supplement to other RFI detection methods, however,

  Tagging neighbouring samples is not a viable method when it comes to detect RFI contamination left undetected by kurtosis inspection

Proposals for improved RFI detection – A closer look at kurtosis

- Ideally, the kurtosis for a gaussian signal equals 3.00000…. and deviations from this indicate a non-gaussian PDF of the signal
  - In this ideal world, any deviations would be very easy to detect!

- In practise, things are not so simple:
  - Kurtosis is not calculated for an infinitely long signal, but merely for 1 ms at a time
  - Performing A to D conversion of the signal also gives rise to limitations

- As a consequence, the kurtosis data exhibit some sort of distribution characterized by a mean ≠ 3.0000… as well as a standard deviation. We could call it a noisy signal

What could be done about this noisy signal?

A closer look at kurtosis

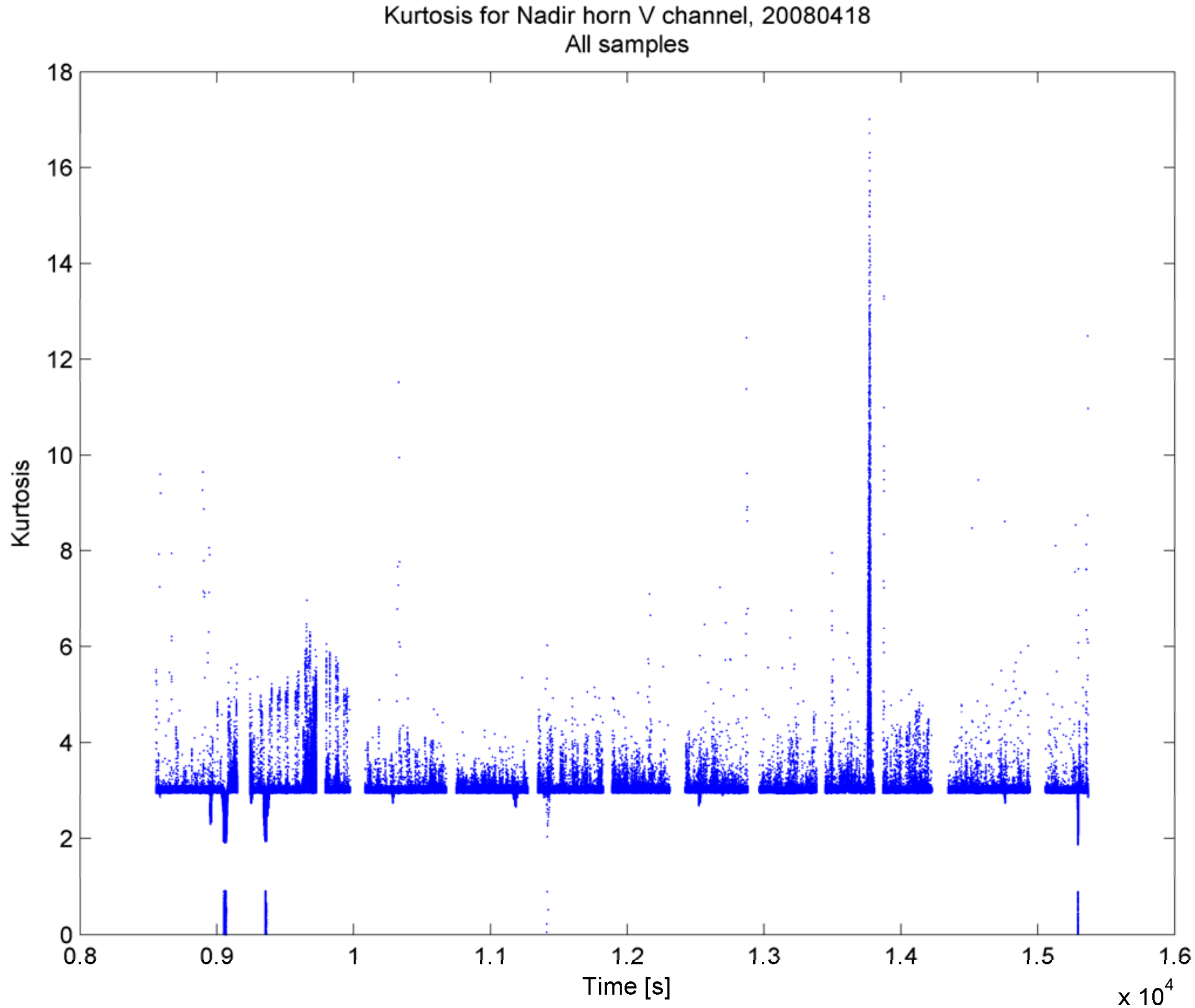

A closer look at kurtosis

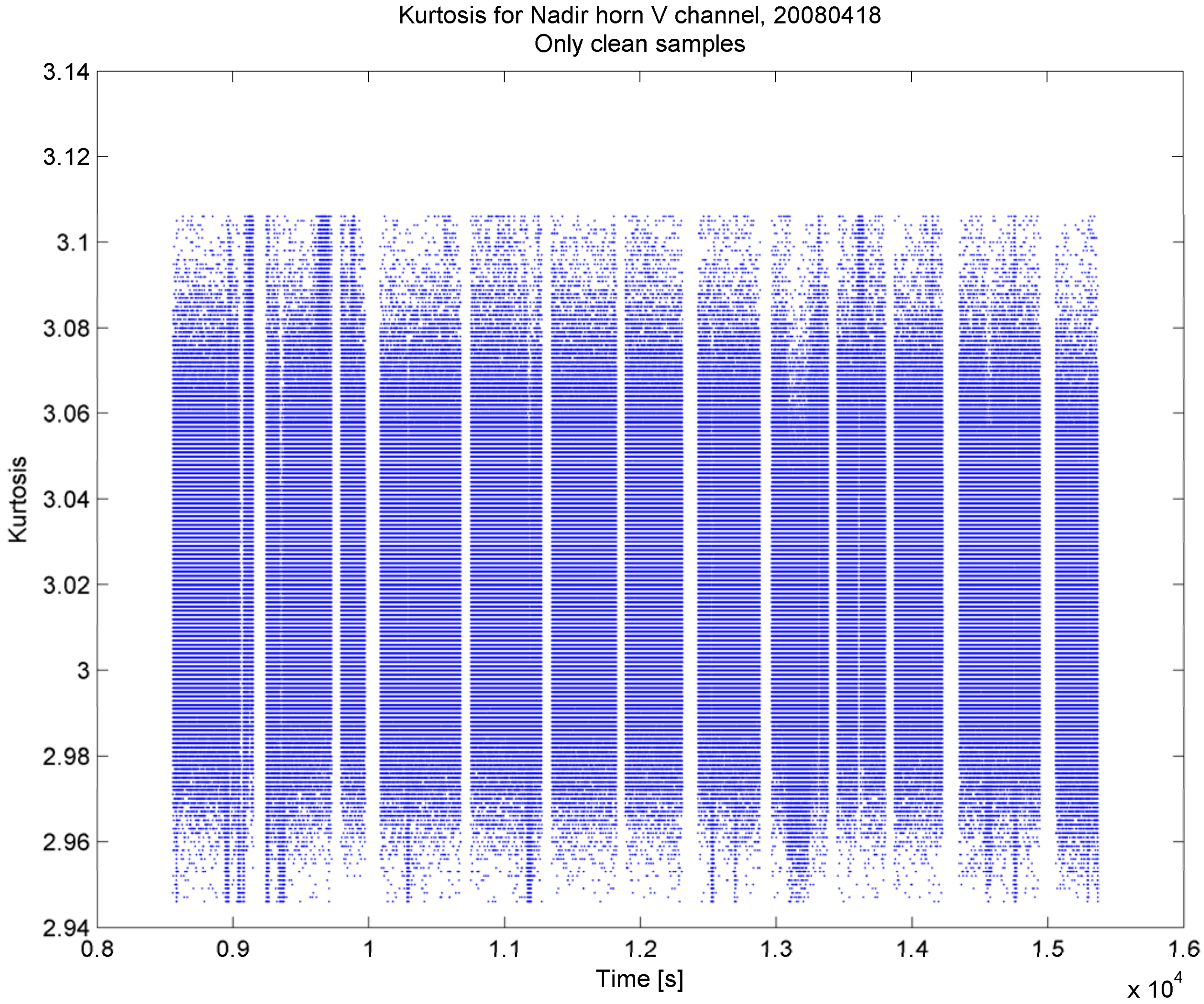

A closer look at kurtosis

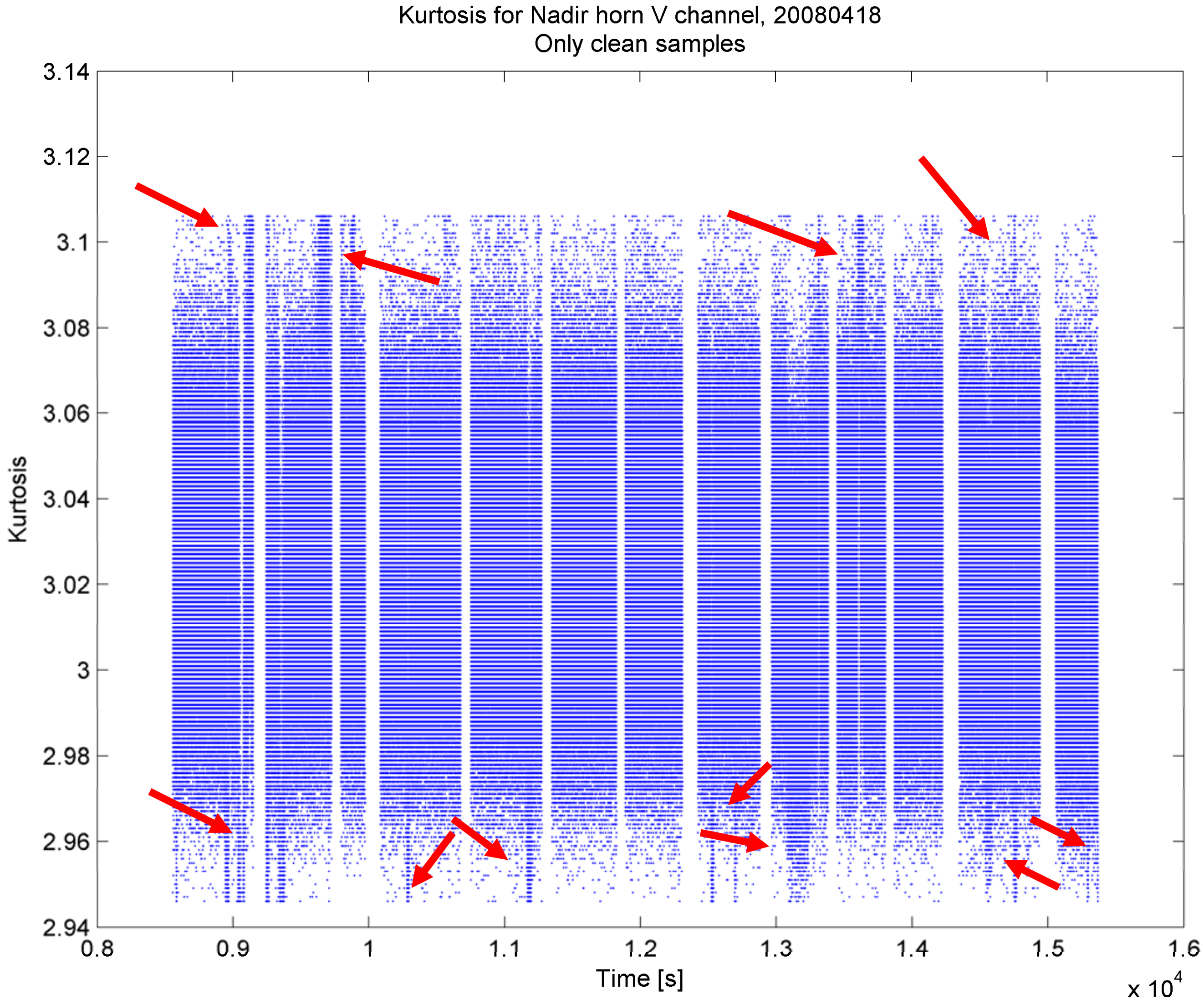

Proposals for improved RFI detection – a closer look at kurtosis

Chapter 15- Moving Average Filters 279

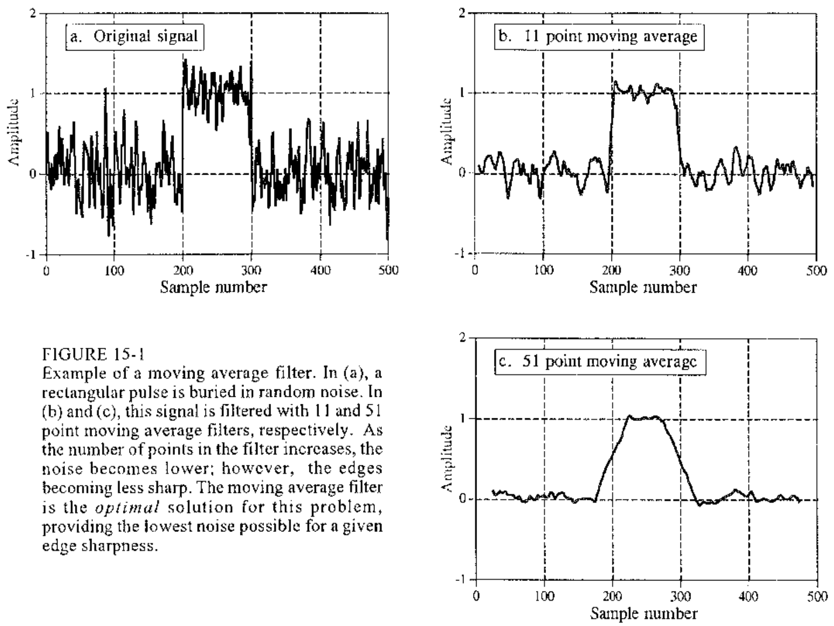

FIGURE 15-1
Example of a moving average filter. In (a), a rectangular pulse is buried in random noise. In (b) and (c), this signal is filtered with 11 and 51 point moving average filters, respectively. As the number of points in the filter increases, the noise becomes lower; however, the edges becoming less sharp. The moving average filter is the *optimal* solution for this problem, providing the lowest noise possible for a given edge sharpness.

The moving average filter provides

"the lowest noise possible for a given edge sharpness"

A closer look at kurtosis

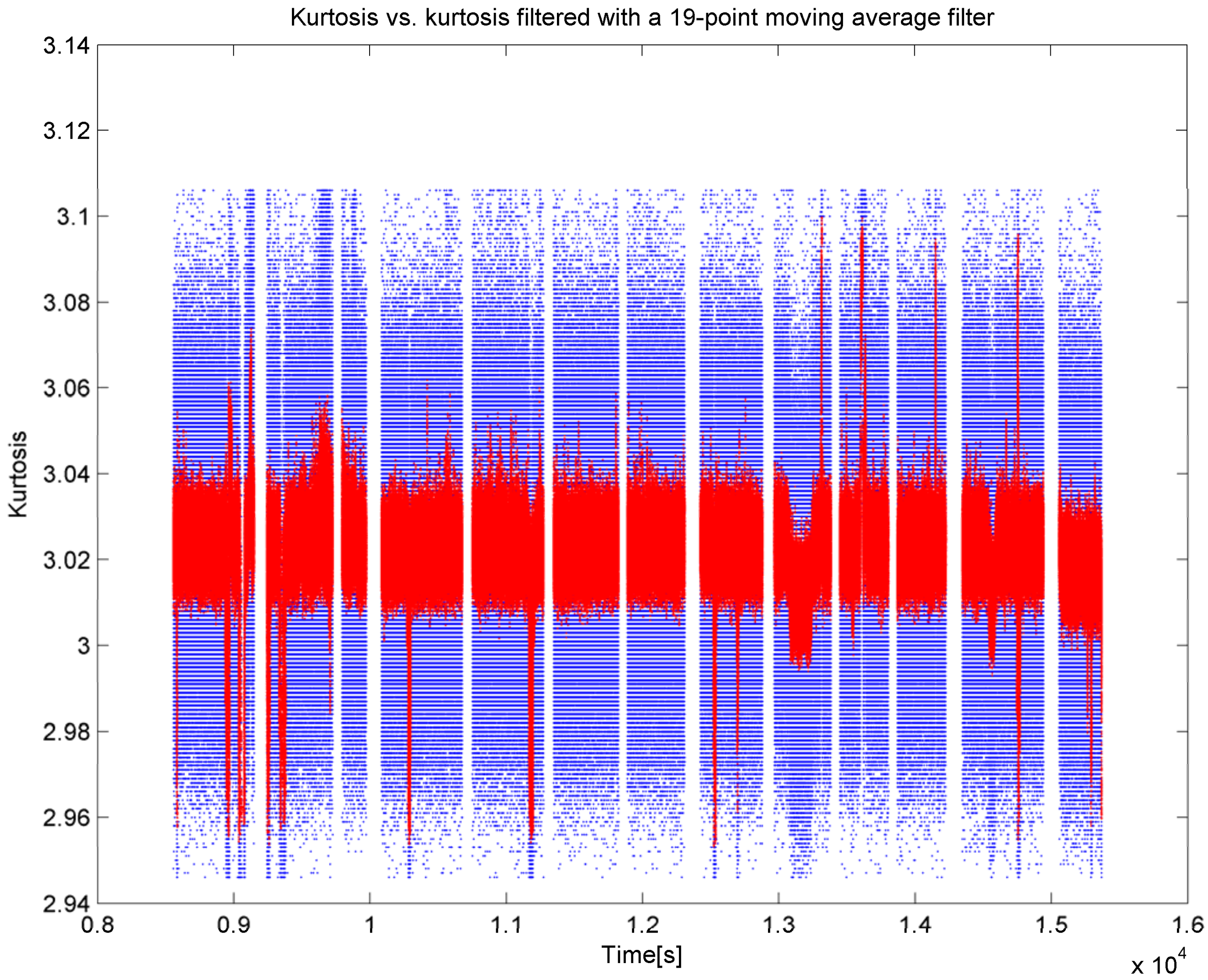

A closer look at kurtosis

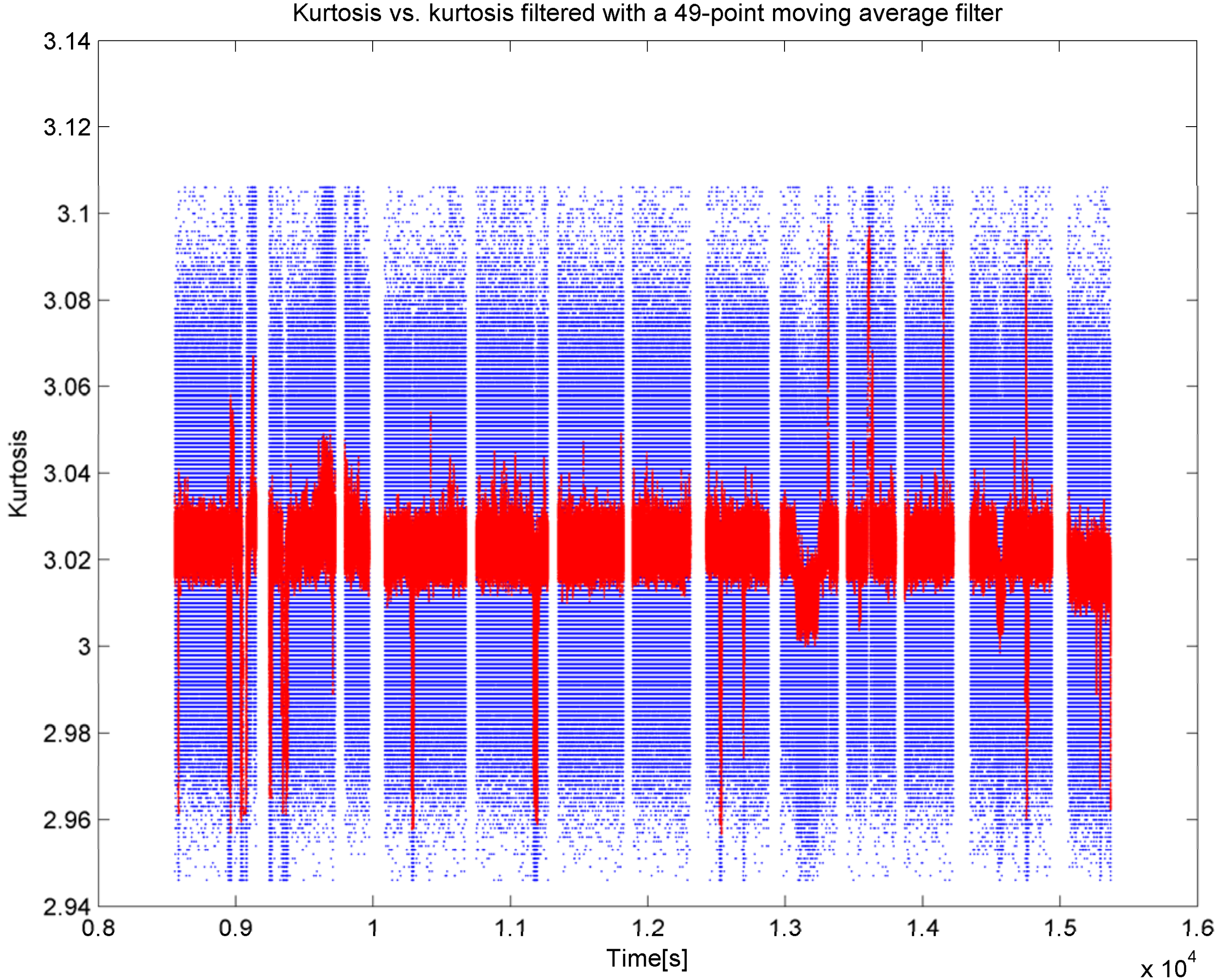

A closer look at kurtosis

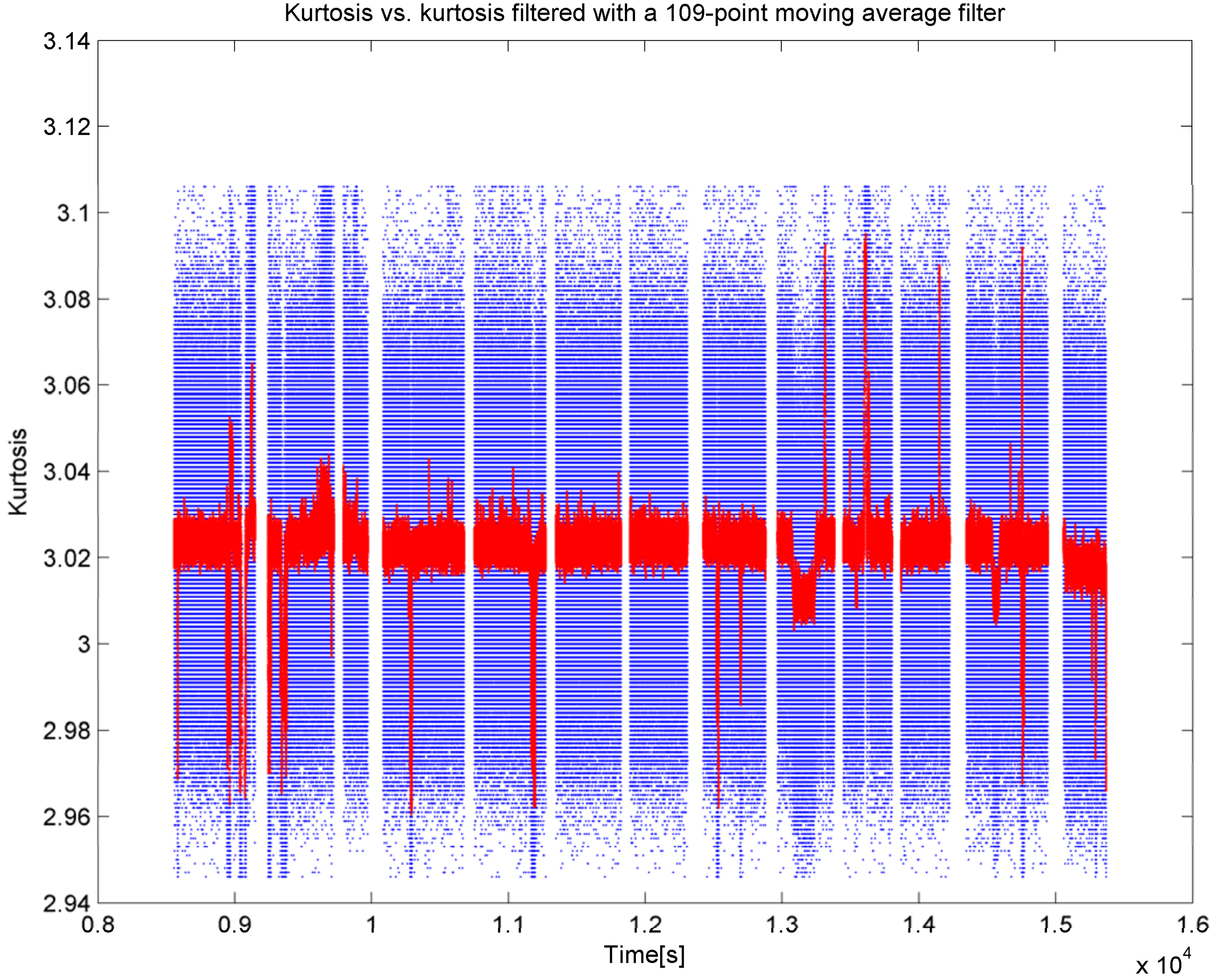

A closer look at kurtosis

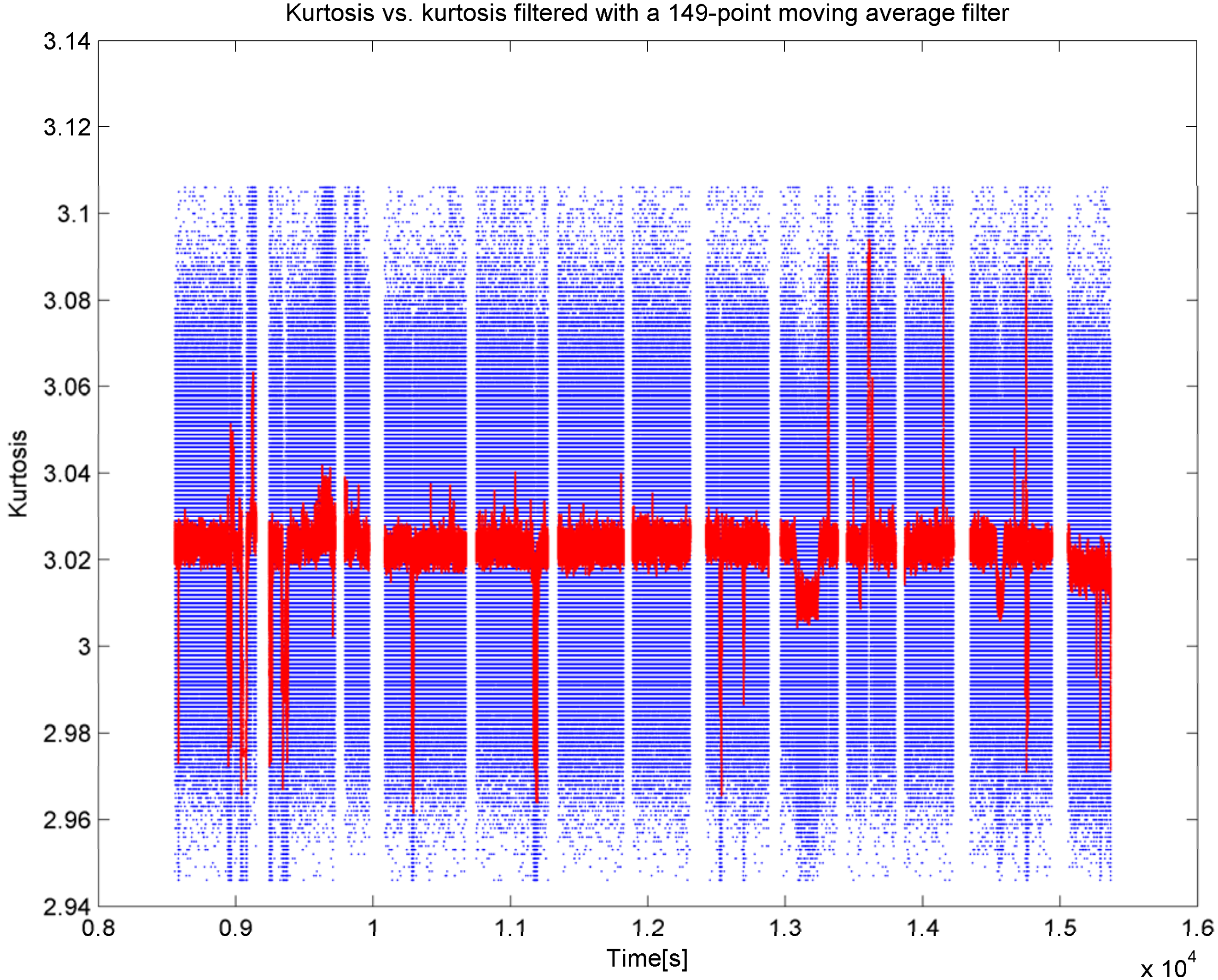

A closer look at kurtosis

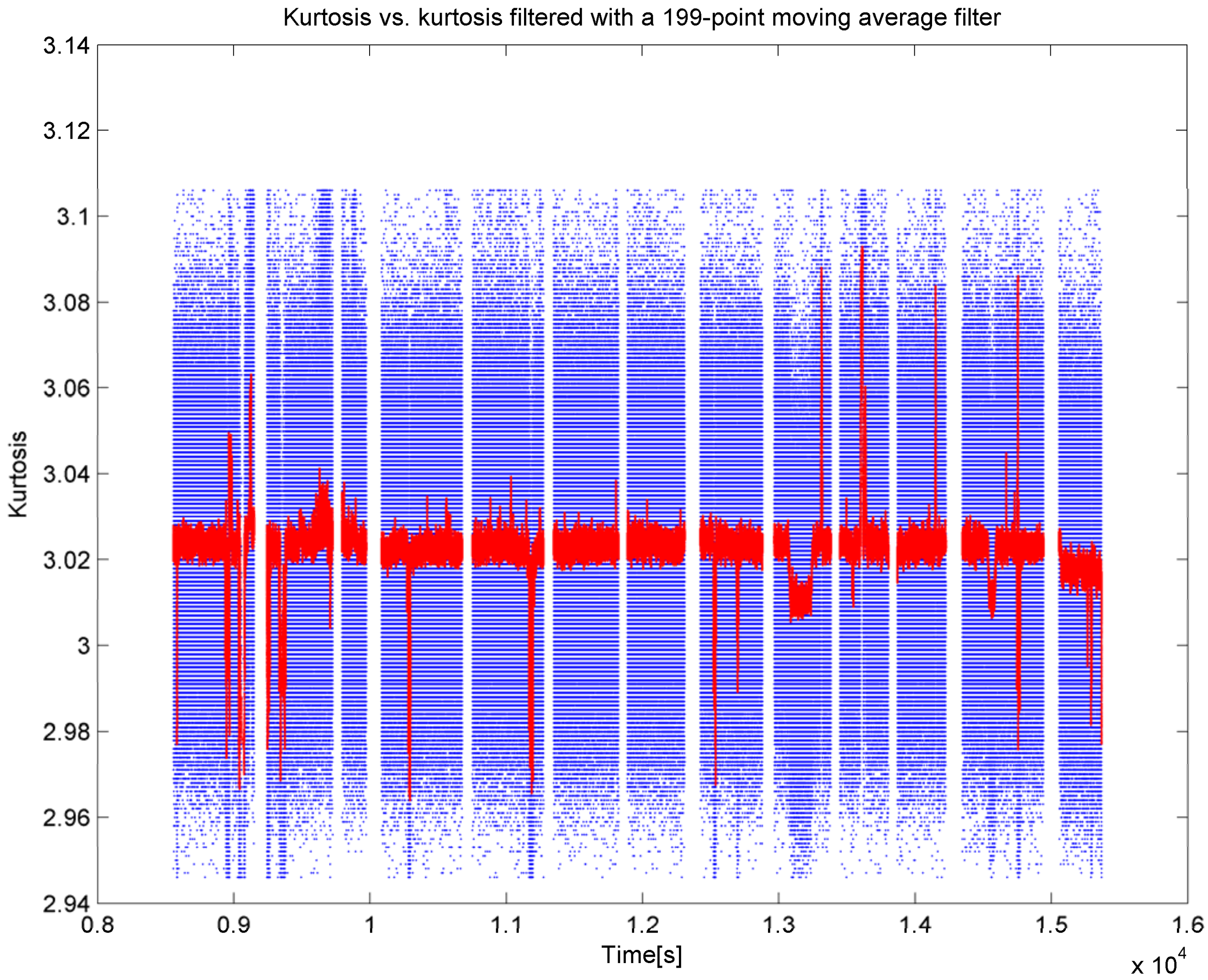

A closer look at kurtosis

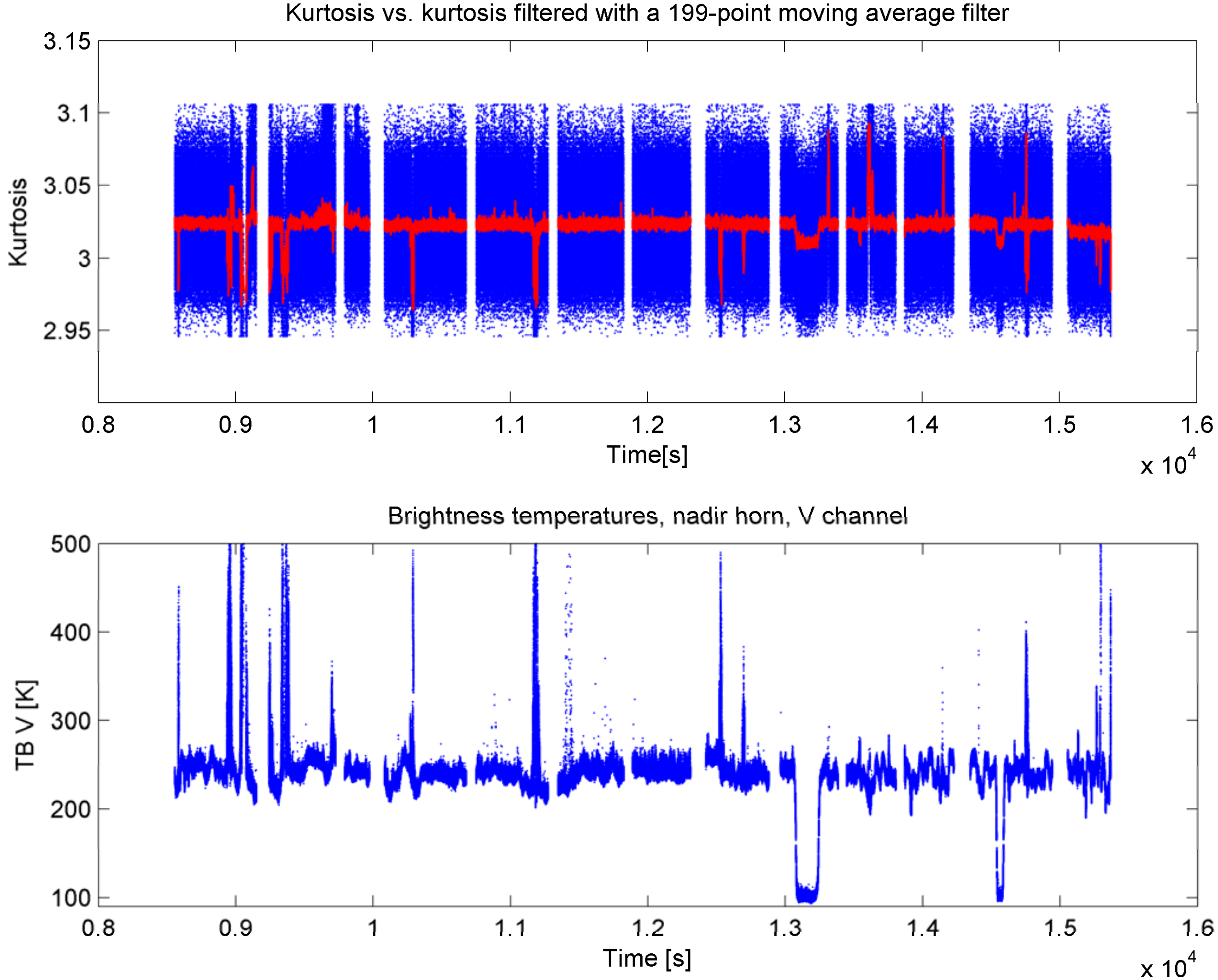

A closer look at kurtosis

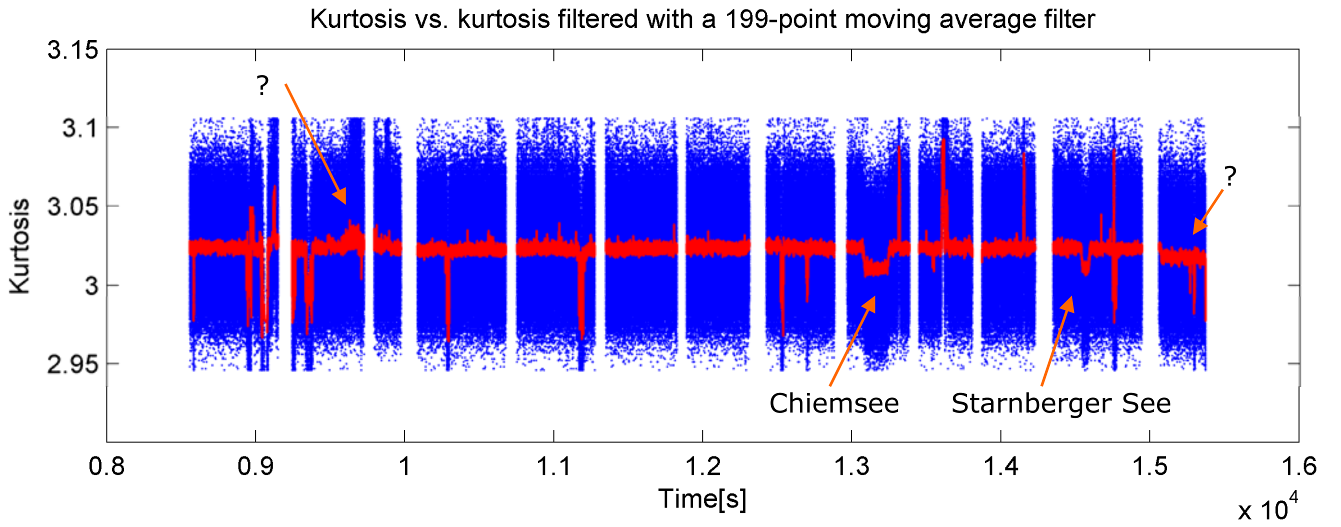

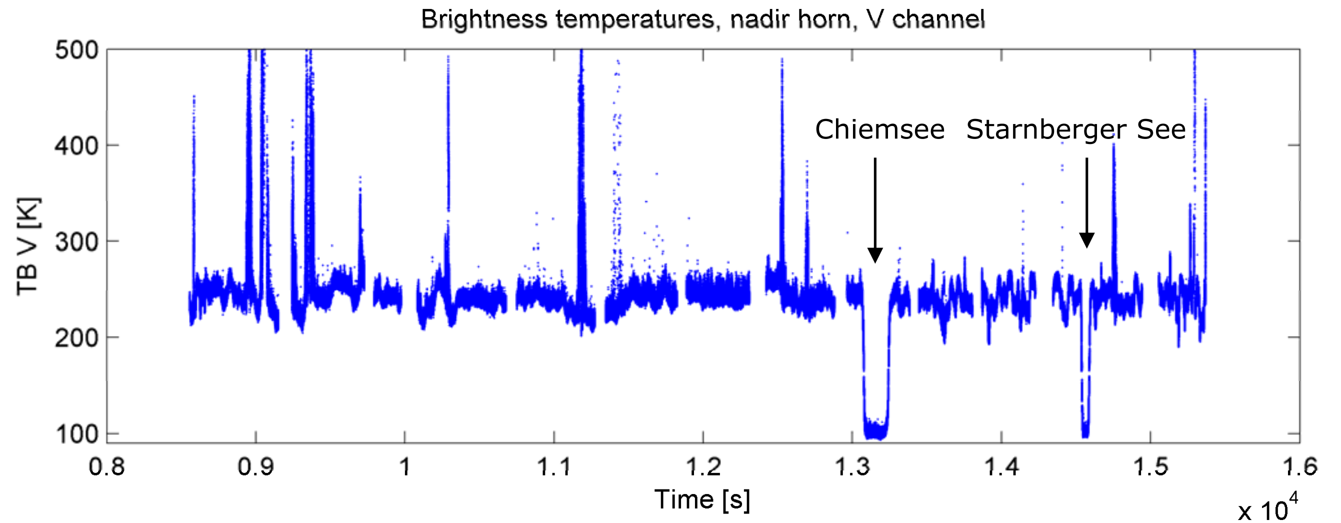

A closer look at kurtosis (lake overpasses removed)

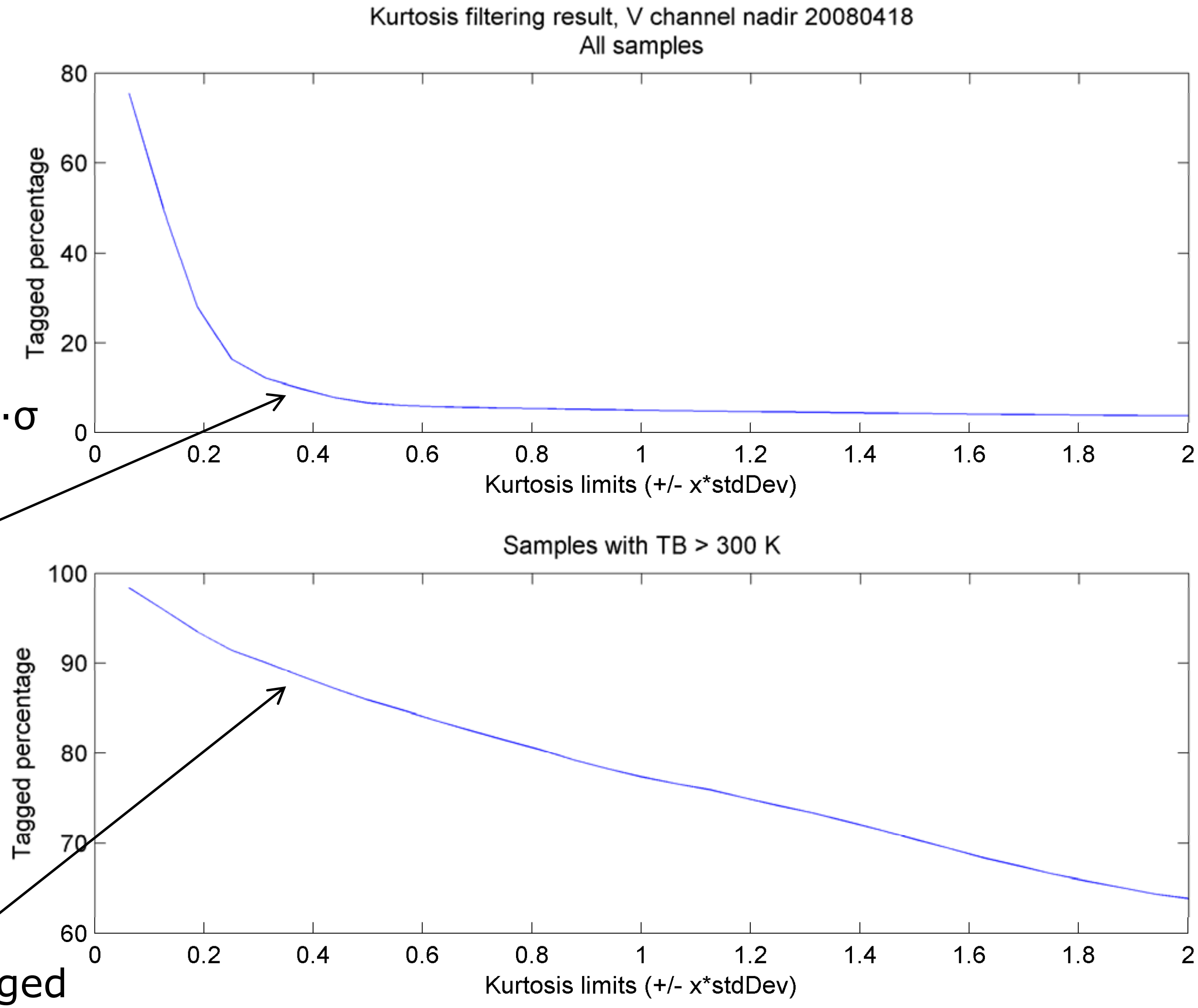

Limit = 0.375·σ

9.9 % tagged

88.62 % tagged

Proposals for improved RFI detection – a closer look at kurtosis

- Filtering kurtosis data with a moving average filter really does bring out more information about the location of RFI contaminated samples
  - If suitable threshold levels can be found, more RFI can be removed

- Kurtosis as calculated by EMIRAD has a dependence on T_B, so finding suitable threshold levels is not a trivial task
  - A priori knowledge about the measurement sites could be used to divide data into e.g. land and water segments
  - An adaptive threshold could be employed

Inspection of moving average-filtered kurtosis data might be useful when manually fine-tuning the data, however, it does not seem suitable as the basis of an automated procedure.

Proposals for improved RFI detection – the kurtosis "blind spot"

In EMIRAD-2, kurtosis is calculated for segments of 1 ms:

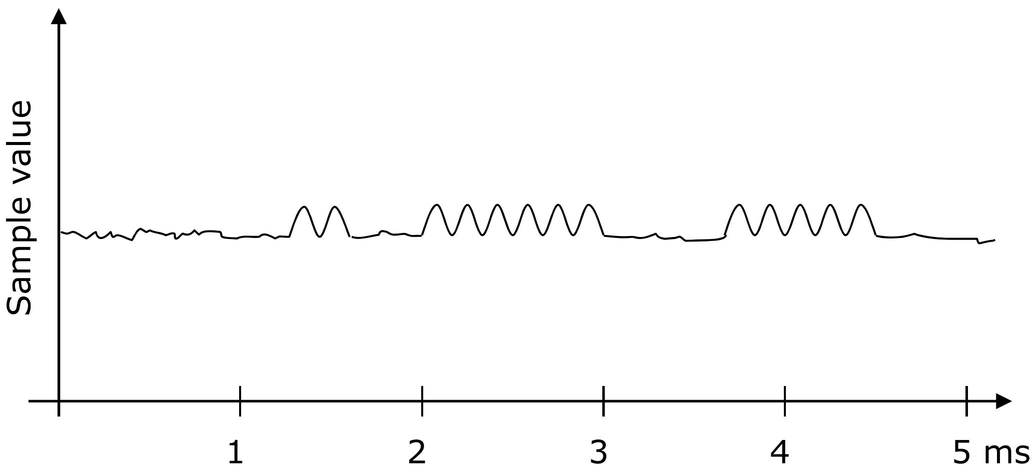

Proposals for improved RFI detection – the kurtosis "blind spot"

In EMIRAD-2, kurtosis is calculated for segments of 1 ms:

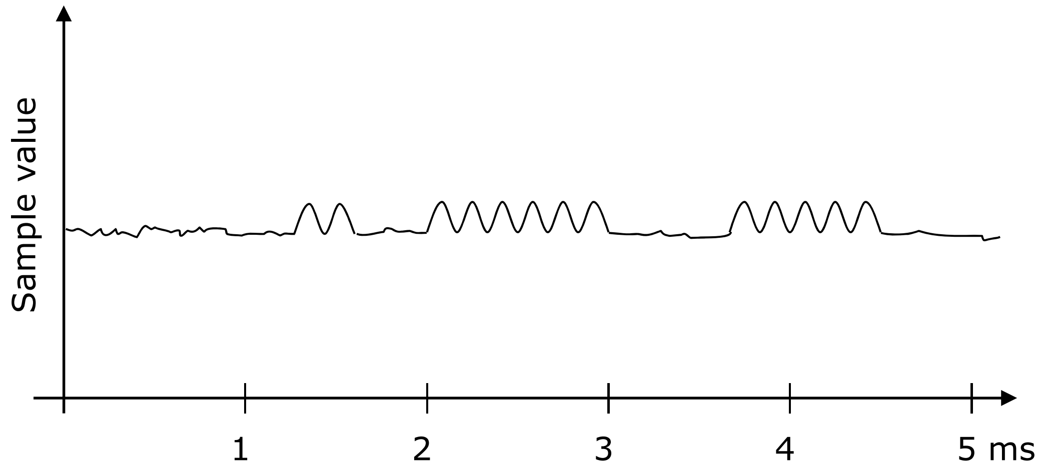

RFI duty cycle	0 %	A few %	100 %	A few %	50 %
Kurtosis result	3	> 3	< 3	> 3	3 !

A pulsed sinusoid with a duty cycle of 50% added to Gaussian noise has a kurtosis of 3 and is therefore invisible when inspecting kurtosis!

Proposals for improved RFI detection – avoiding the kurtosis "blind spot"

- Motivation:
  - If kurtosis is calculated for a range of time spans, apparent RFI duty cycles will change.
- Consequences:
  - Some blind spots will disappear
  - Other blind spots will appear in new places
- Method:
  - Calculate kurtosis for time spans between 1 ms – 1 s
  - Generate RFI tags for each time span in the usual manner
  - Group a number of time spans, creating a new set of RFI tags consisting of the union of the RFI tags belonging to each of the time spans being considered

Avoiding the kurtosis blind spot

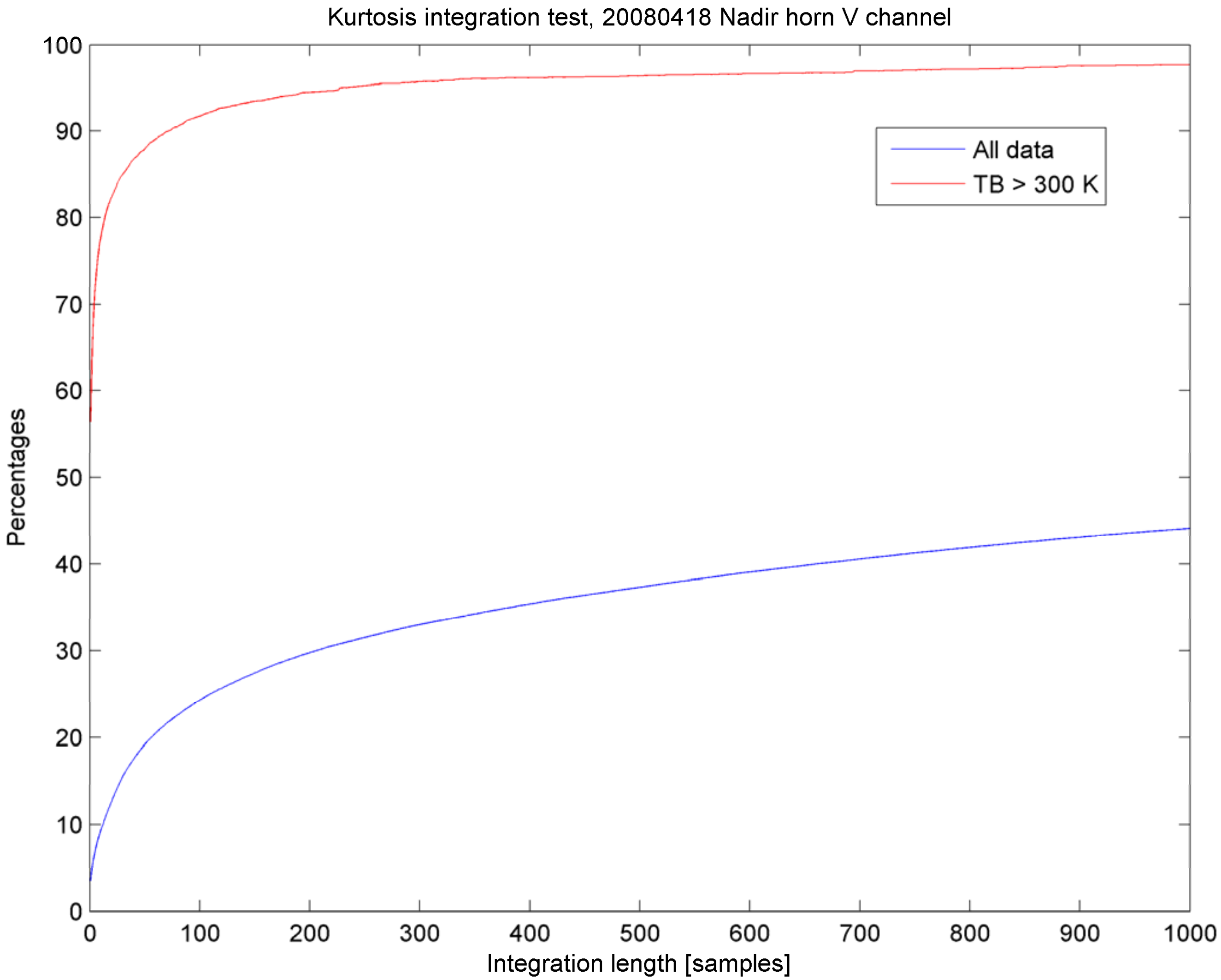

Avoiding the kurtosis blind spot

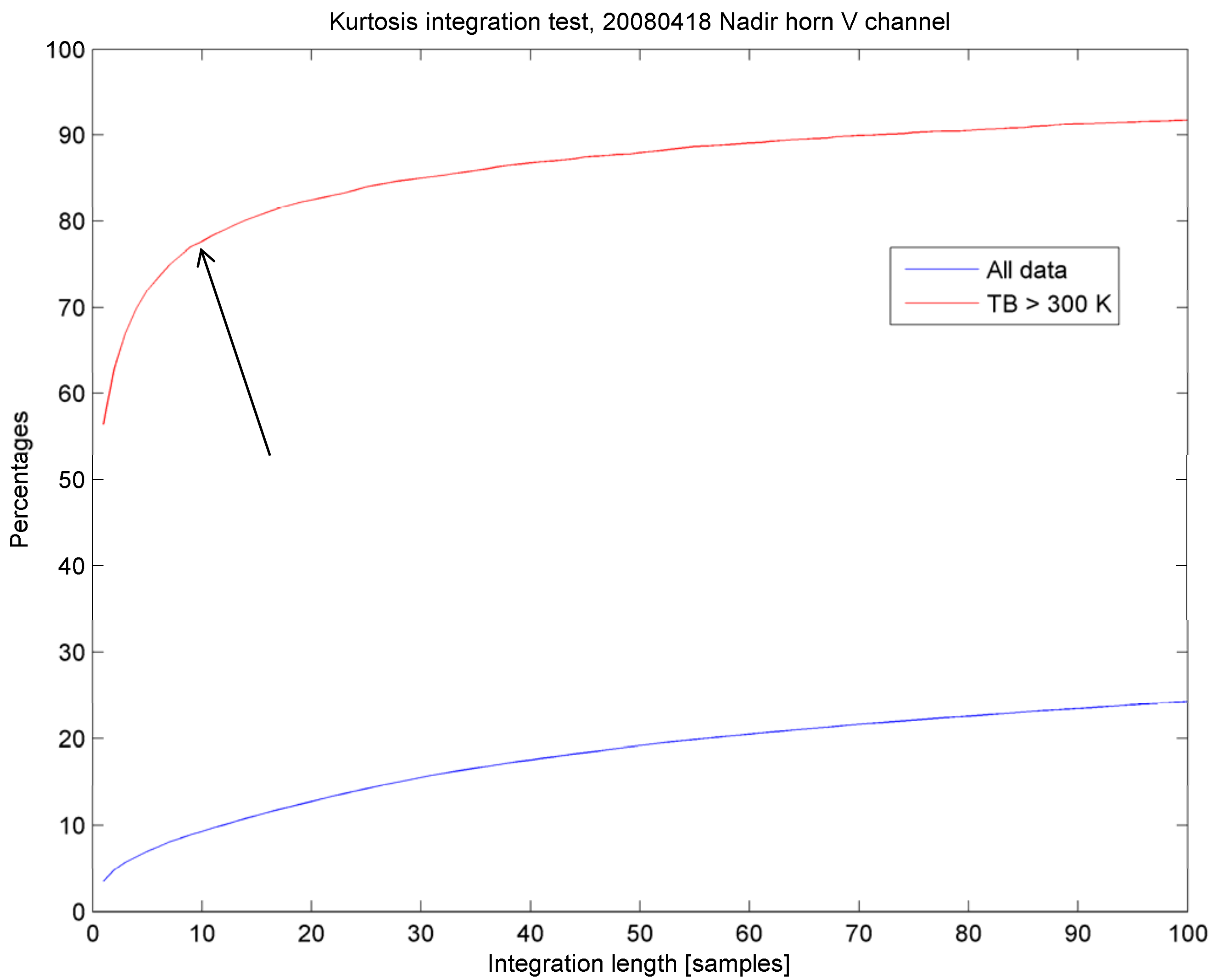

Avoiding the kurtosis blind spot

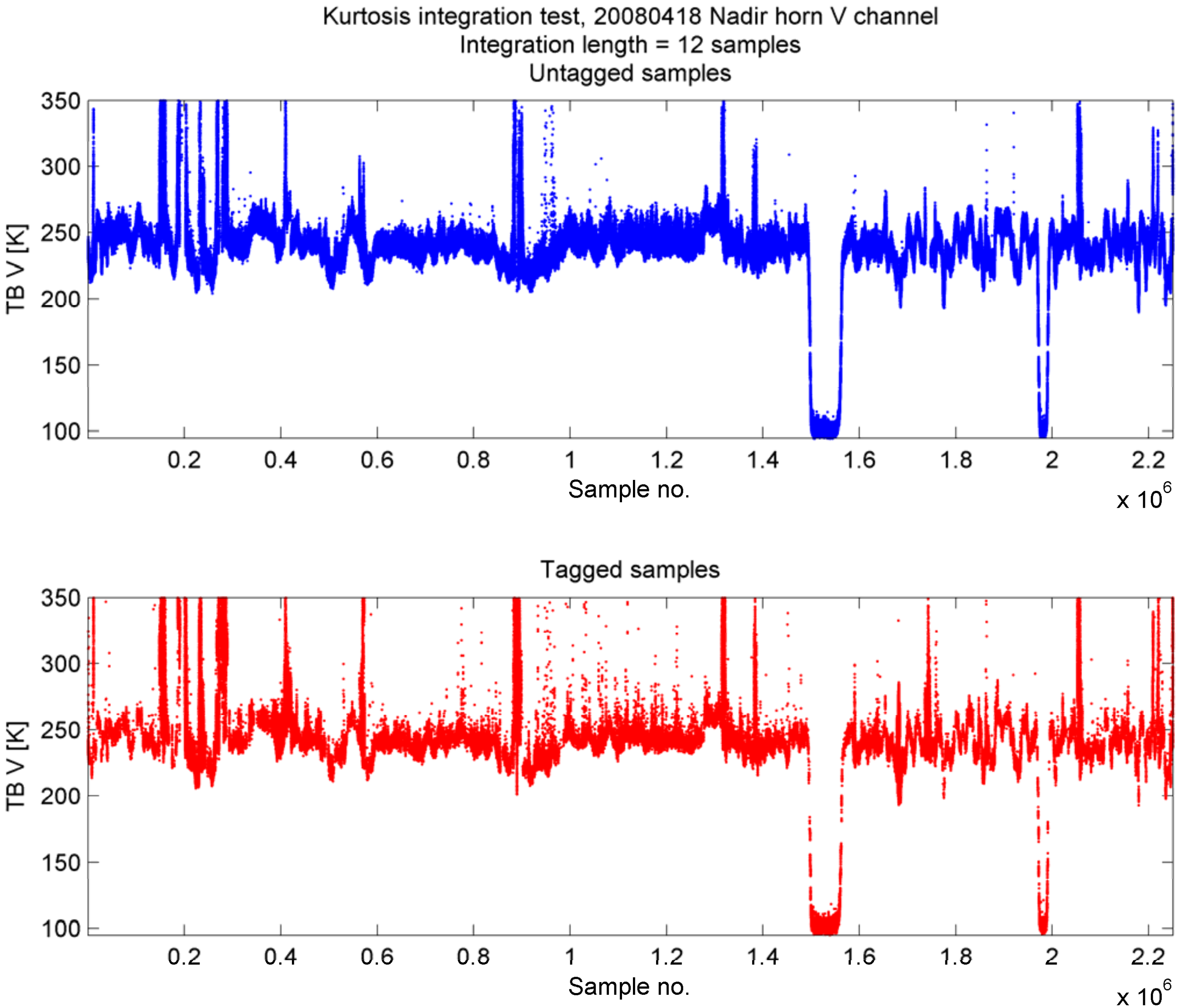

Proposals for improved RFI detection – avoiding the kurtosis "blind spot"

- The detection rate of large values of T_B increases most rapidly when using integration lengths of up to 10 samples, and the percentage of tagged samples still looks reasonable at this point

- When further increasing the integration length, the detection rate increases much more slowly – no significant increase at integration lengths > 300 samples

- The algorithm might remove a number of "blind spots", however the increased sensitivity of kurtosis due to lower (apparent) duty cycles of RFI could also be a factor

- Prominent spikes in TB due to RFI are still present after filtering with RFI tags generated from kurtosis integration

- The true weakness of the kurtosis method is not the "blind spot", but the poor response to high-duty cycle RFI

Polarimetric data inspection

- Natural targets have very small 3rd and 4th Stokes
- Linearly polarized RFI normally not aligned with H and V of our instrument, hence we get 3rd Stokes
- Many surveillance radars use circular polarization, hence we get 4th Stokes
- Experience with EMIRAD shows that often Kurtosis flagged data has significant signals in 3rd and 4th Stokes, but not always. The opposite can also be the case.
- Subject for further investigations
- Anyway, looking for signals in the 3rd and 4th Stokes channels of SMOS can be an important method for RFI detection

Polarimetric inspection – TBV distribution

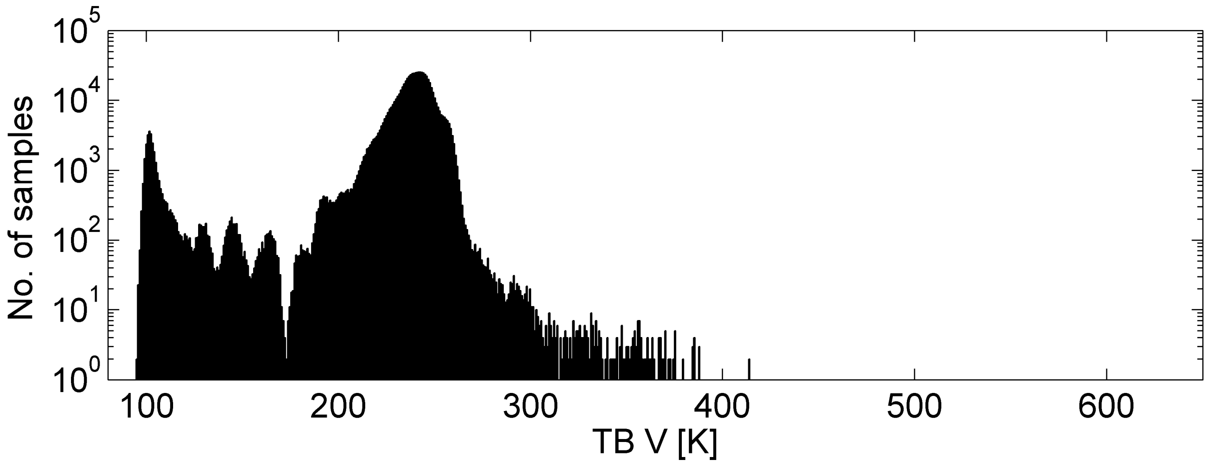

Not flagged

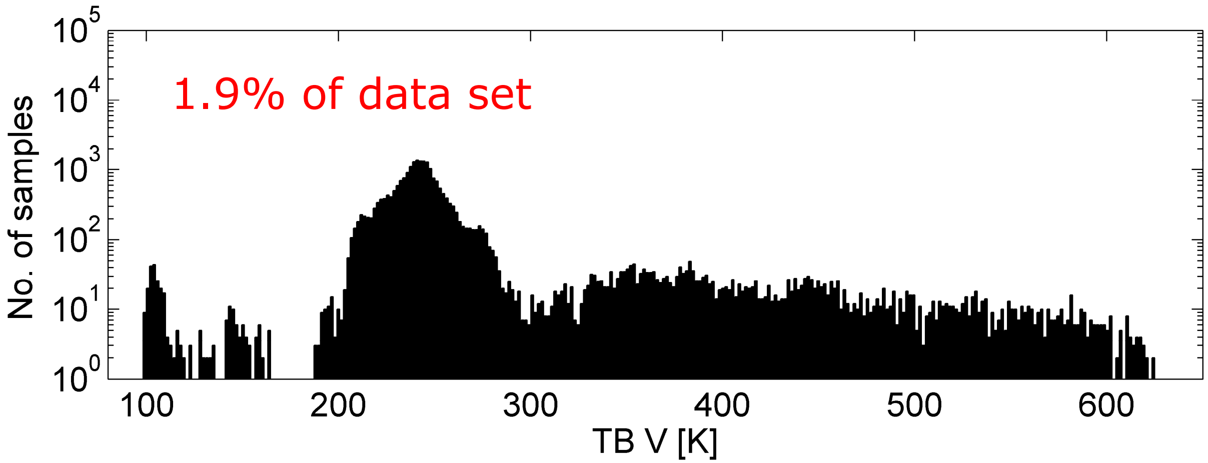

Kurtosis flagged

Data from 2008/04/14 (Emirad, Munich)

Polarimetric inspection – 3rd Stokes distribution

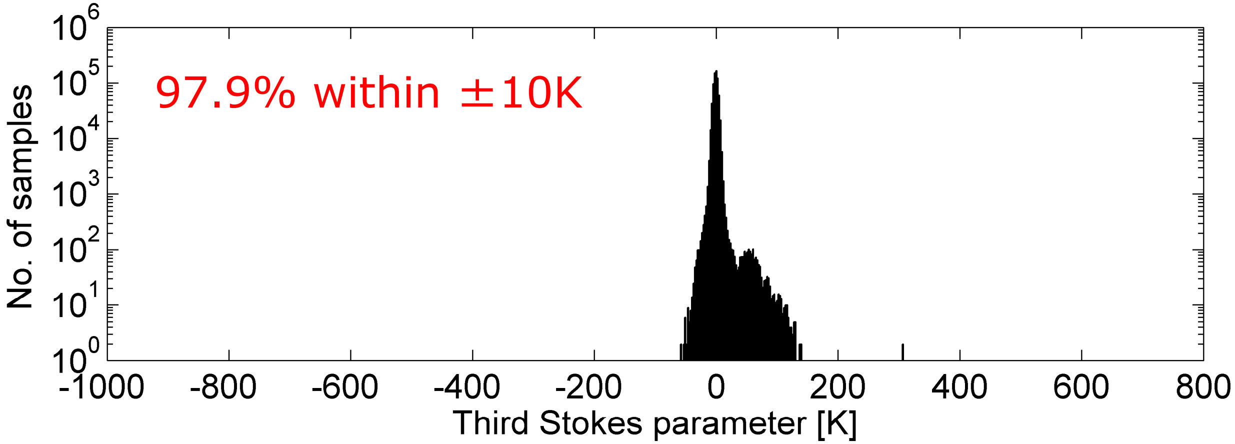

Not flagged

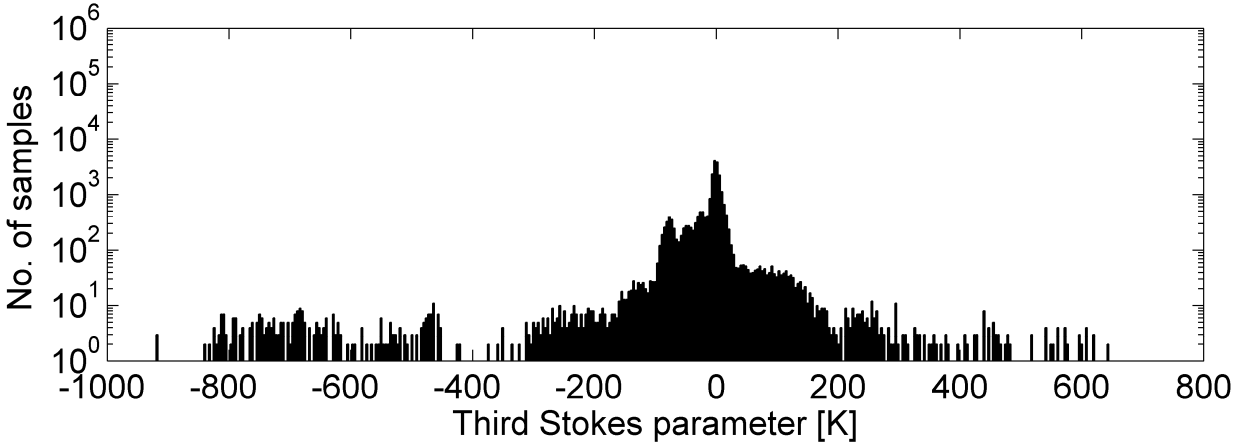

Kurtosis flagged

Data from 2008/04/14 (EMIRAD, Munich), attitude effects removed

Polarimetric inspection – 4th Stokes distribution

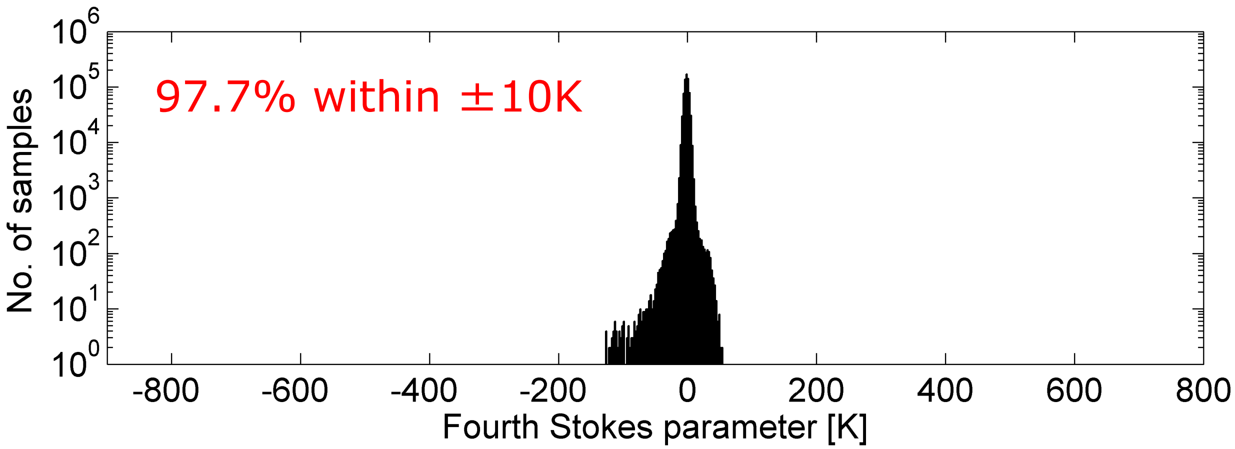

Not flagged

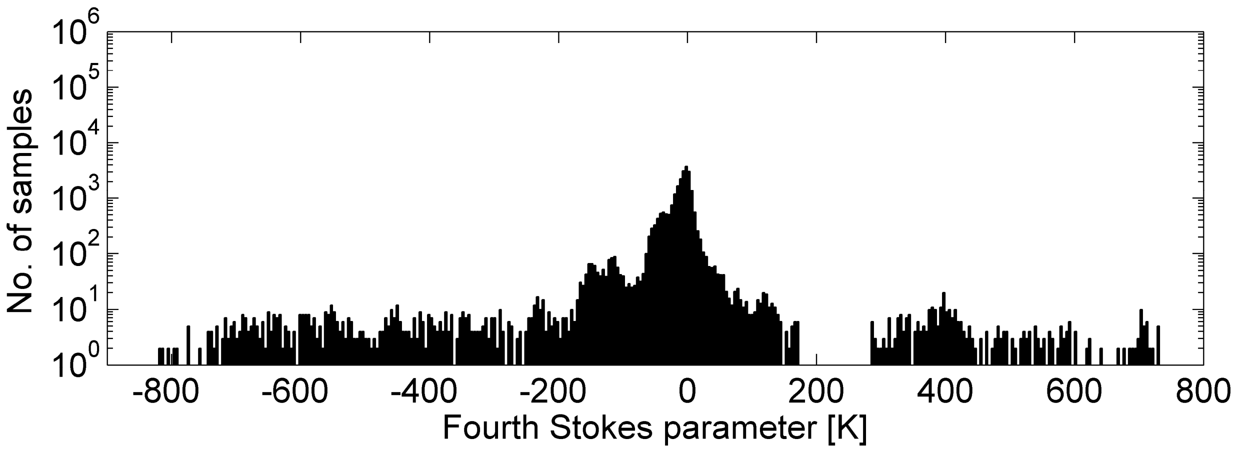

Kurtosis flagged

Data from 2008/04/14 (EMIRAD, Munich), attitude effects removed

Polarimetric inspection – TBV vs. Stokes

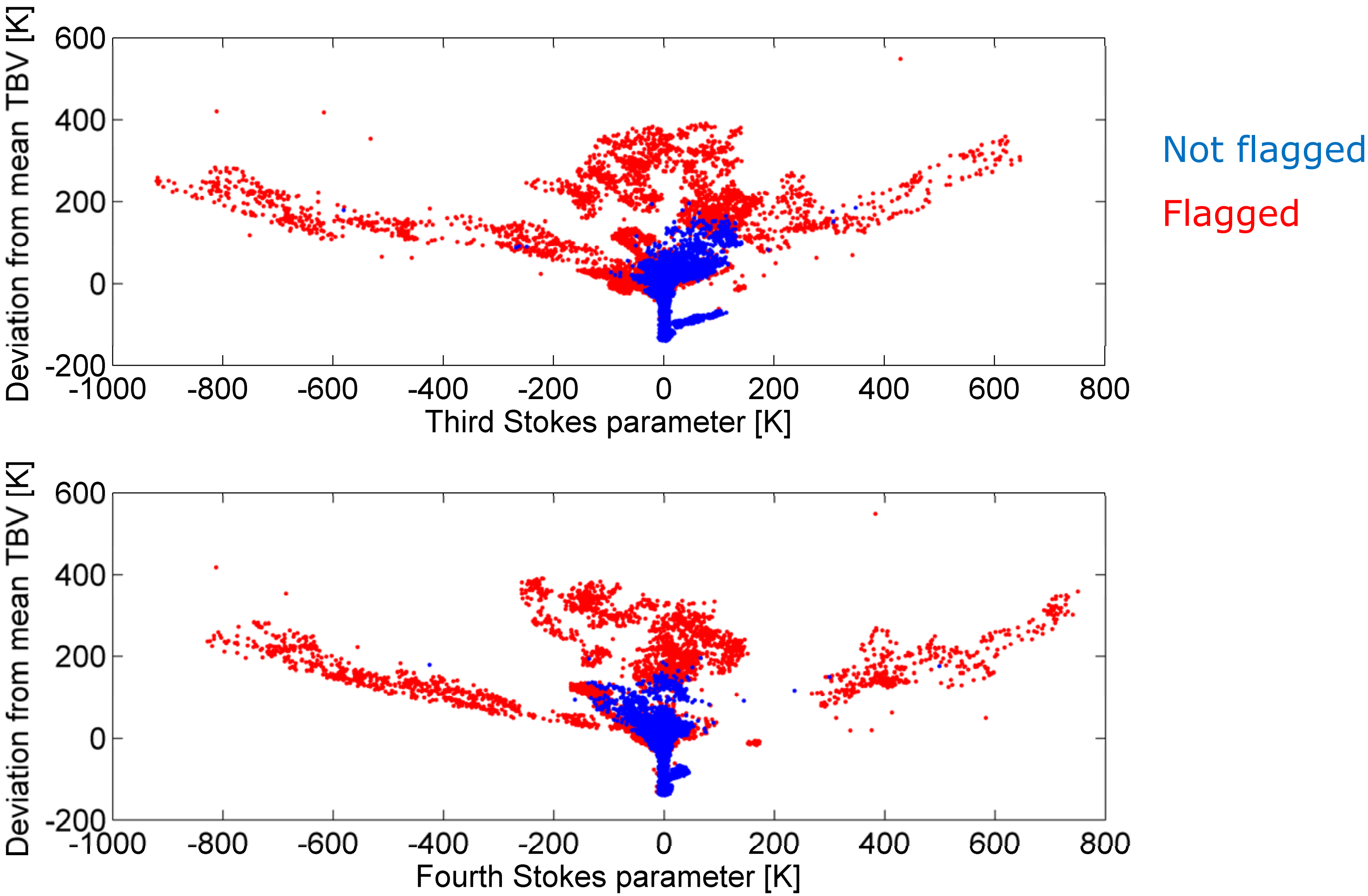

Data from 2008/04/14 (EMIRAD, Munich), attitude effects removed

Inspection of Stokes parameters

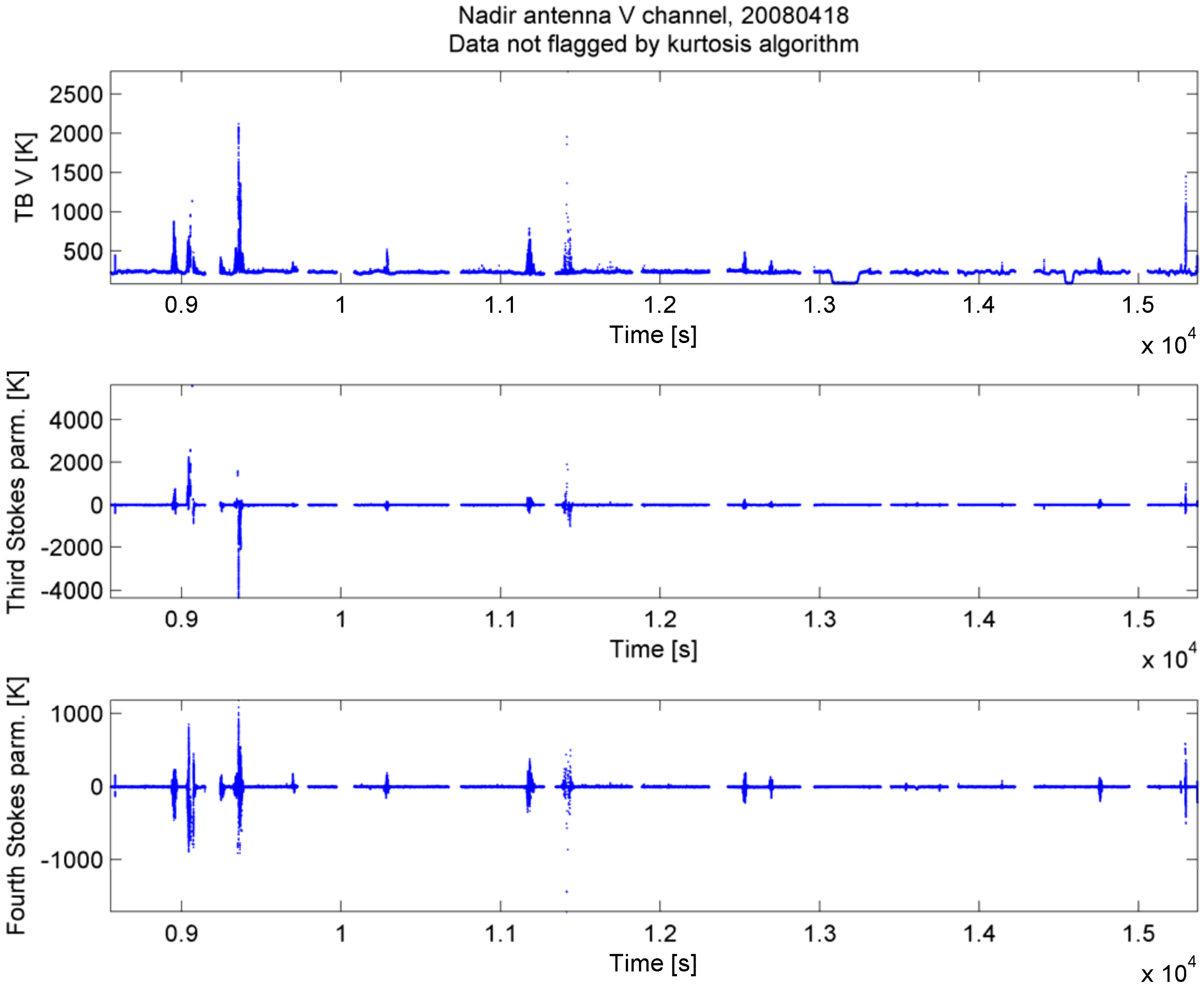

Inspection of Stokes parameters

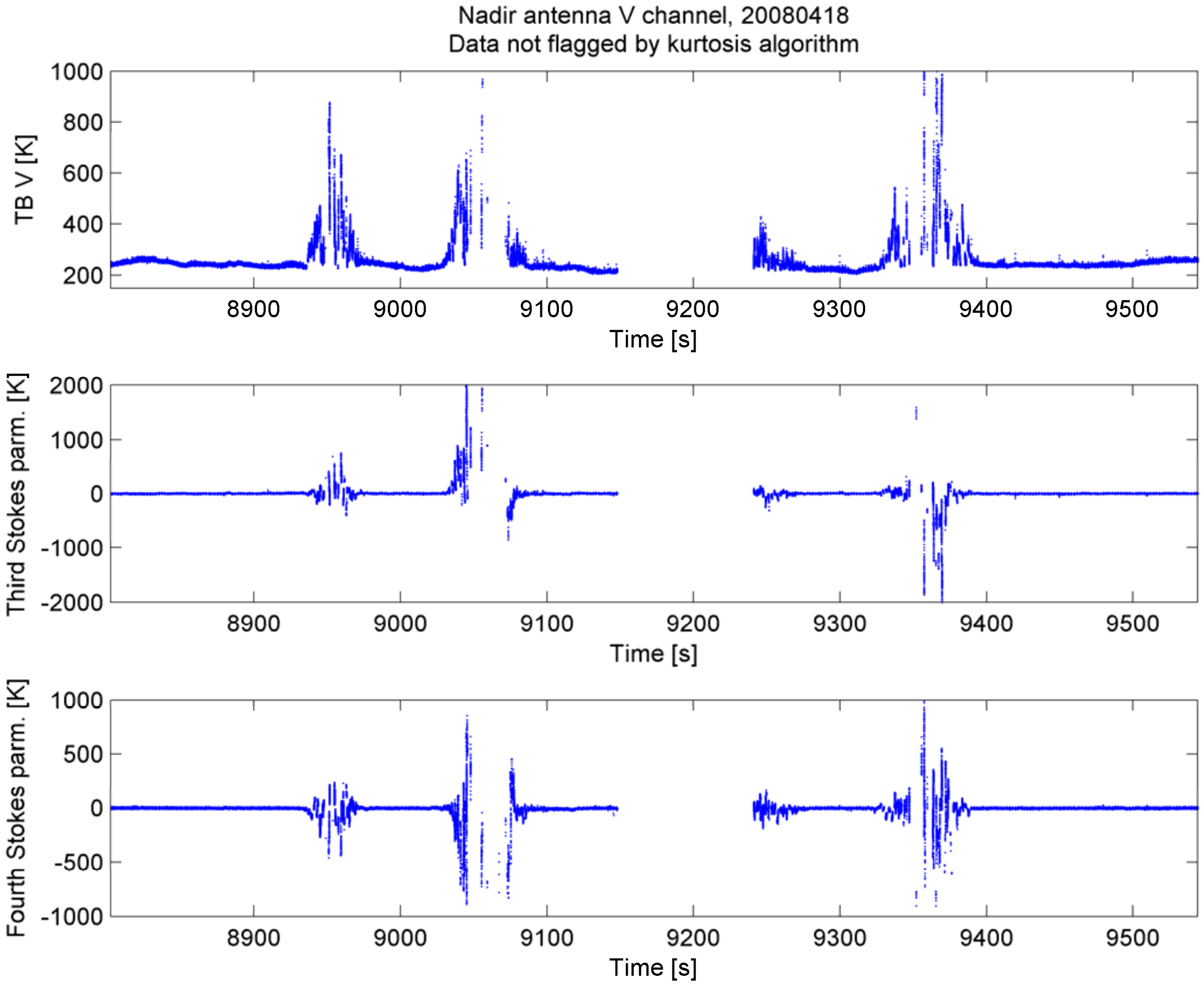

Inspection of Stokes parameters – limits?

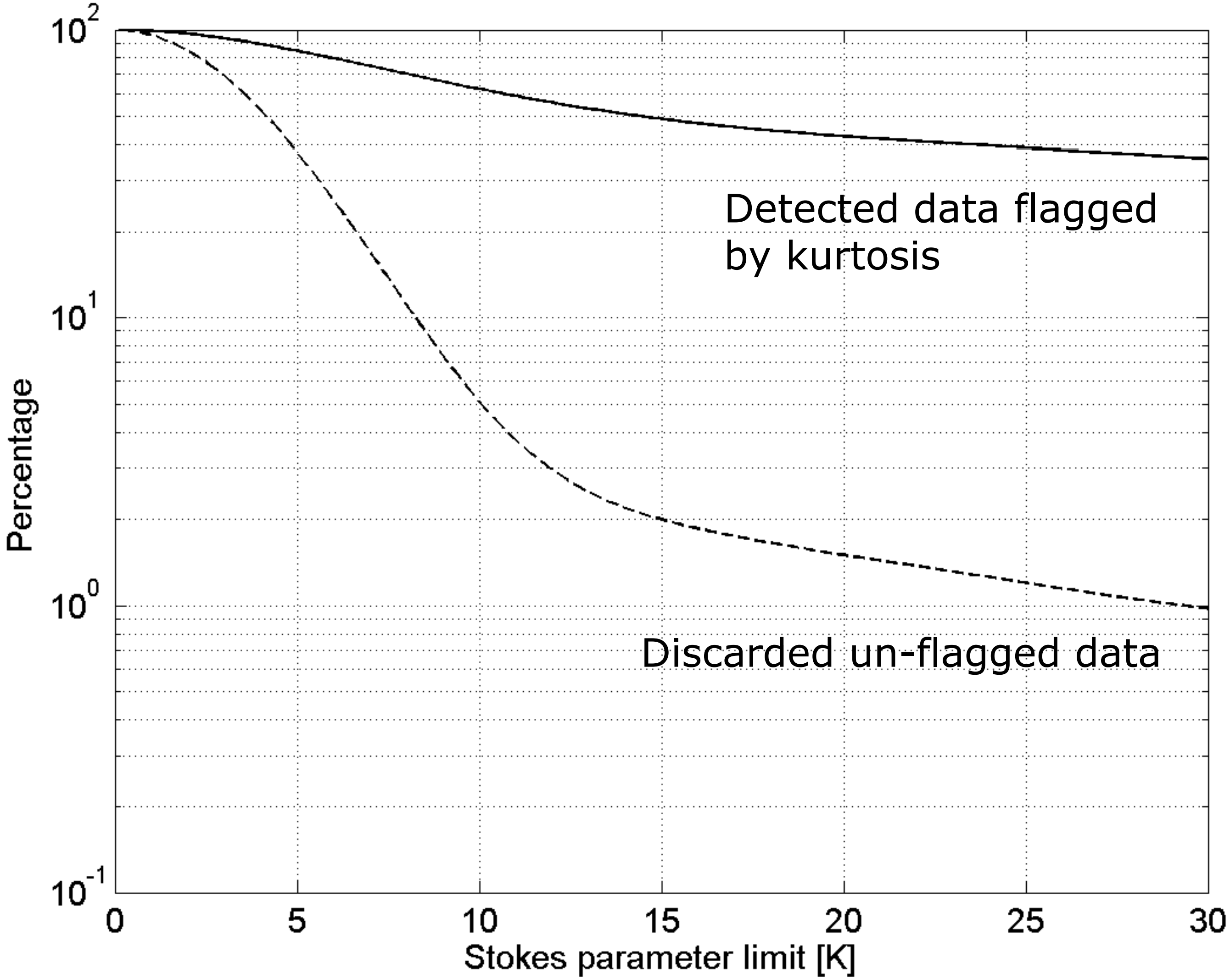

Proposals for improved RFI detection – inspection of Stokes parameters

- T_B peaks due to obvious RFI, which are not detected by kurtosis inspection, stand out clearly by means of elevated levels of particularly the 4th Stokes parameter

- The 4th Stokes parameter shows no large variation otherwise – hence inspection of it is a process well suited for automation

- Low levels of the 3rd and 4th Stokes parameters, however, do not guarantee clean data

- Applying a limit of ±10 K for both 3rd and 4th Stokes parameters looks like a fair choice.

A combination of kurtosis inspection and Stokes parameter inspection is a likely candidate for an improved RFI detection algorithm

Inspection of Stokes parameters – Stokes parameter limits applied

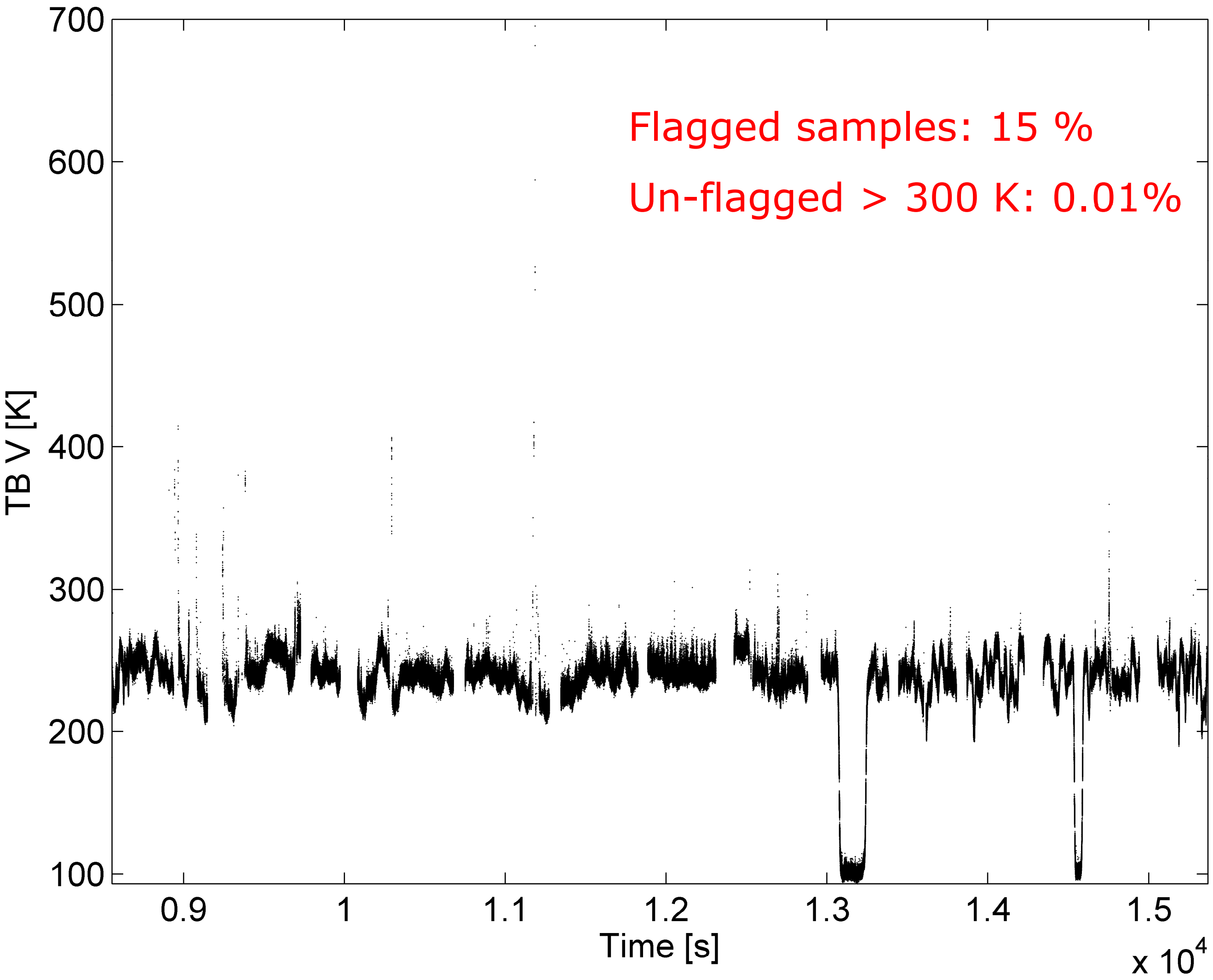

Inspection of Stokes parameters – standard deviations

- Samples affected by RFI affect the 3rd and 4th Stokes parameters in two ways:
  1. Large absolute values
  2. Rapid fluctuations, i.e. large standard deviations

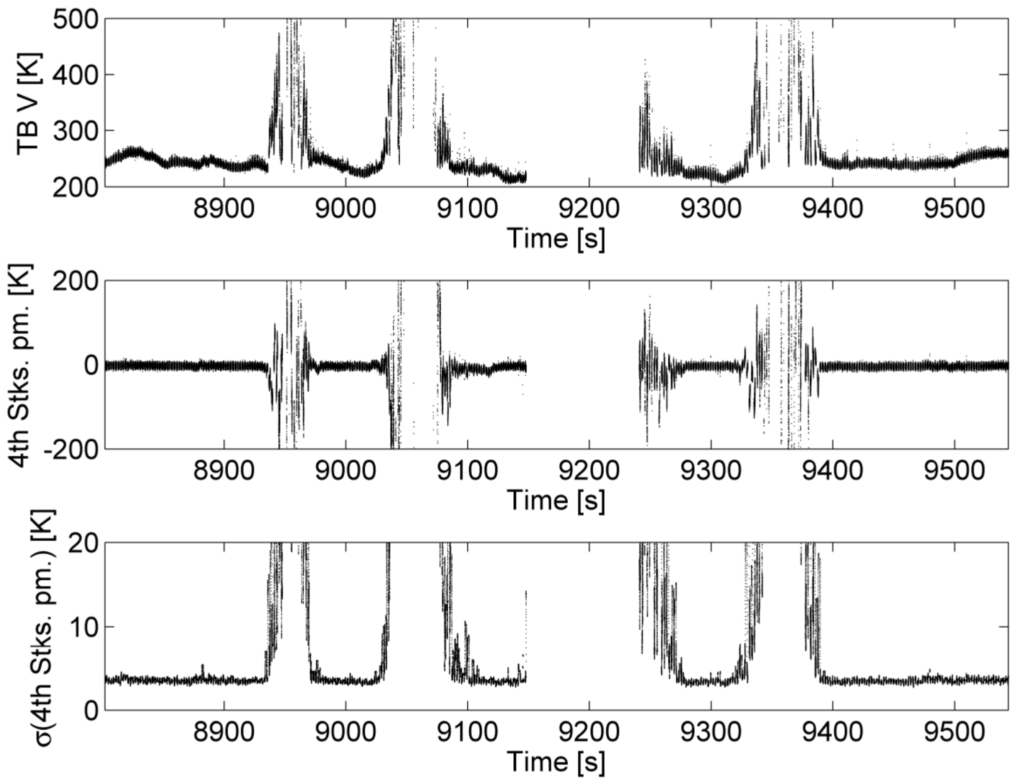

149 samples-wide

sliding window

Stokes parm. standard deviations – finding the limits

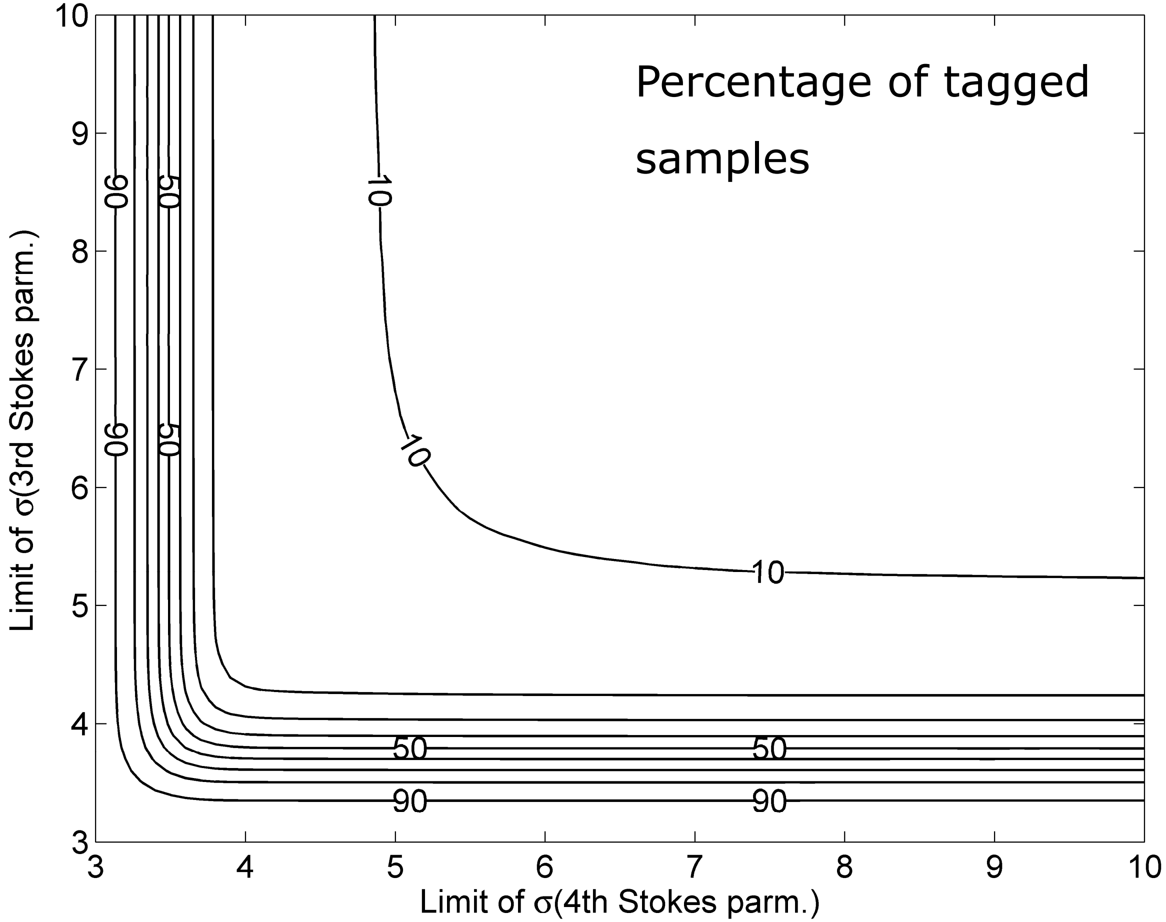

Stokes parm. standard deviations – finding the limits

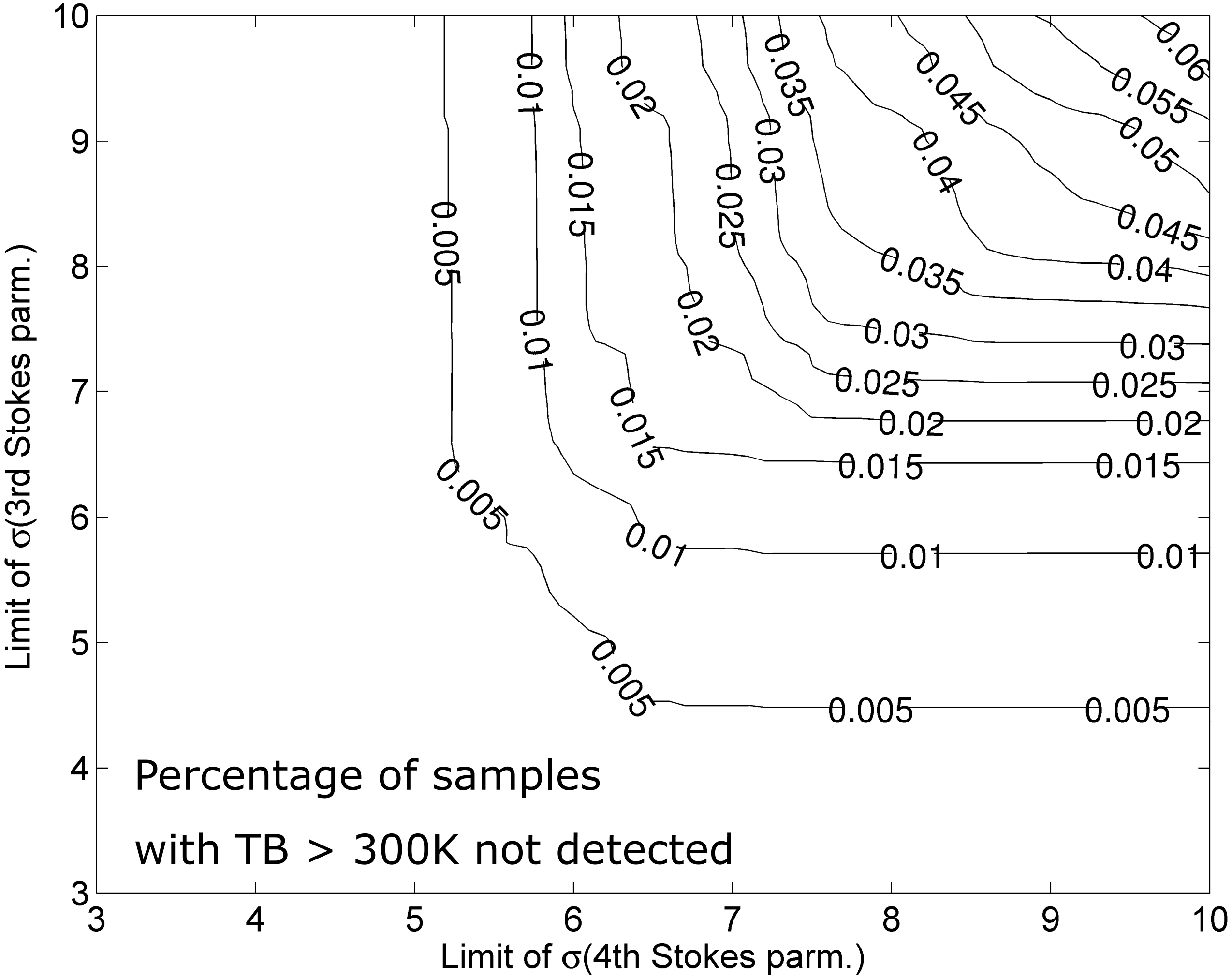

Stokes parm. standard deviations - application

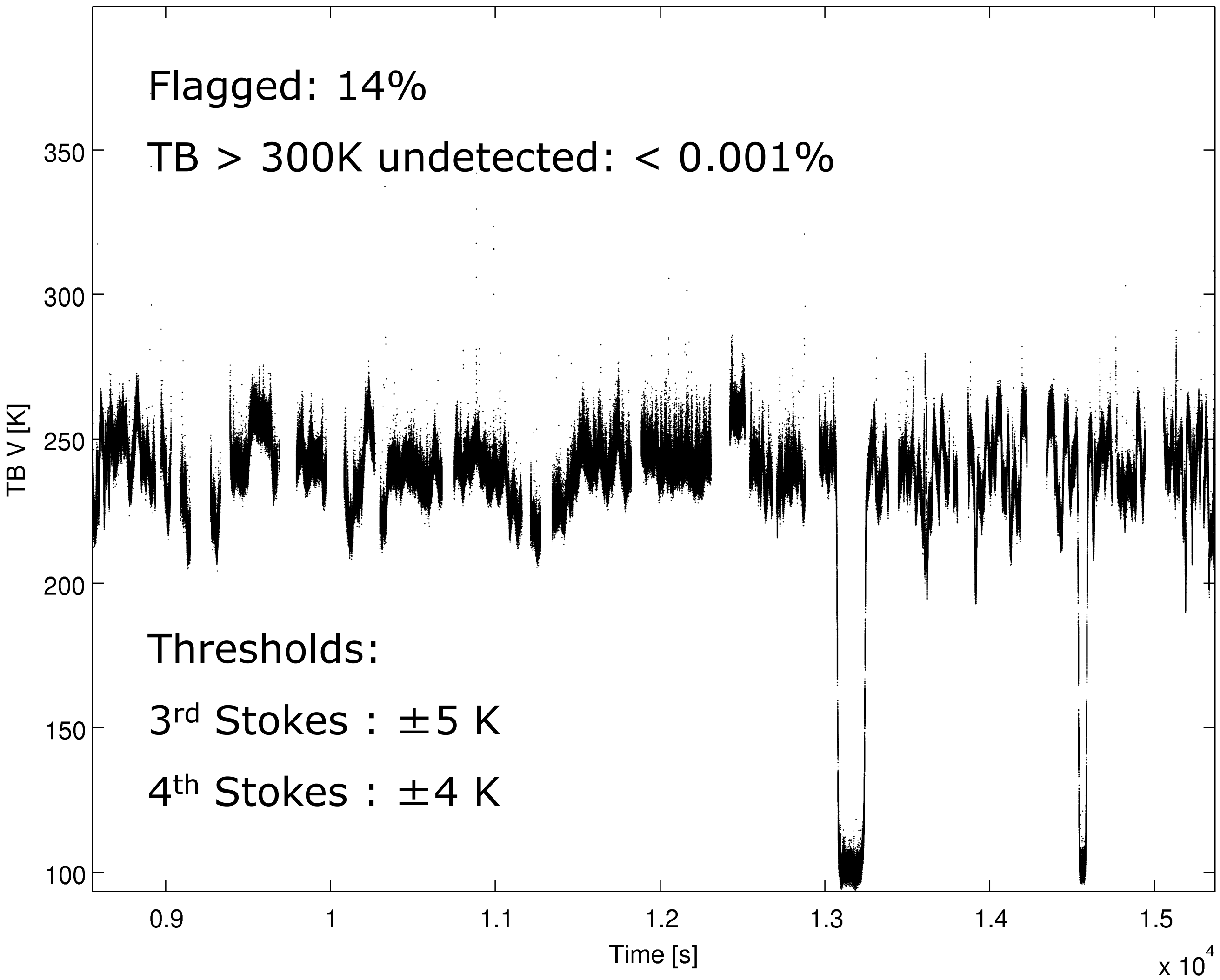

Inspection of Stokes parameters - conclusions

- By setting suitable thresholds for the values and standard deviations of the 3rd and 4th Stokes parameters, it is possible to remove some RFI contamination which has been difficult to remove otherwise.

- The method is suitable for automation, provided that appropriate thresholds for the 3rd and 4th Stokes parameters can be found.

- The previous analyses deal with RFI which result in large spikes which are easily visible. Smaller RFI contributions yielding elevated TB levels of a few K may still be present. These contributions might be detected by kurtosis if their duty cycle is low.

- RFI detection without the use of kurtosis is of interest to SMOS data – especially since SMOS also provides polarimetric data. Work is being carried out in this field.

Glitch detection

- Developed and tested by Chris Ruf et al.
- Each sample is compared with the mean of x neighbouring samples
- x is variable
- If a pre-defined threshold is exceeded, the sample is flagged

Tested in five different cases

1. Before any cleaning
2. After kurtosis application
3. After Stokes parameter threshold application
4. After Stokes parameter threshold **and** kurtosis application
5. After σ(Stokes parameter) threshold **and** kurtosis application

200 samples ≤ x ≤ 2000 samples

Threshold = 10 K (to avoid issues with ΔT)

Glitch detection – an example

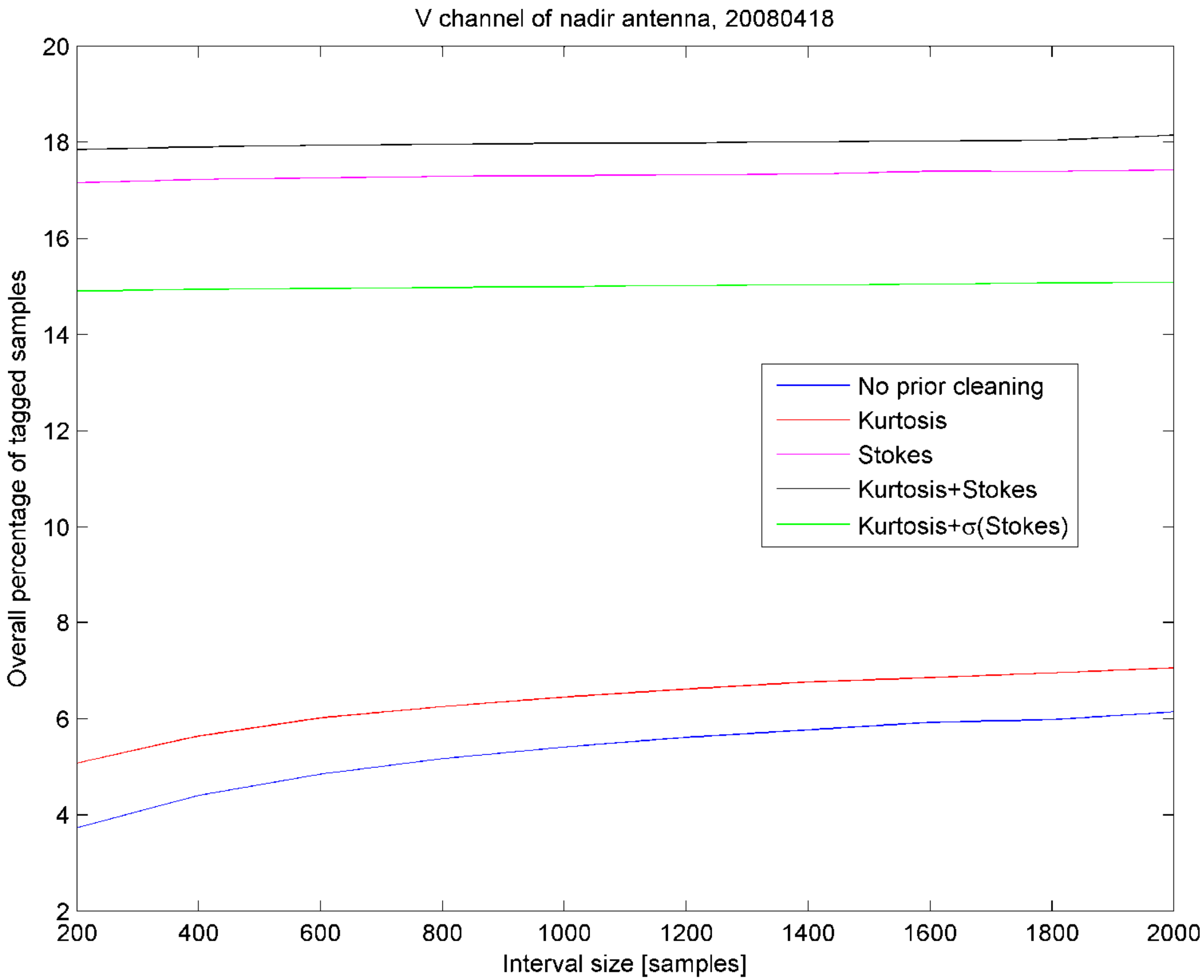

Glitch detection – an example

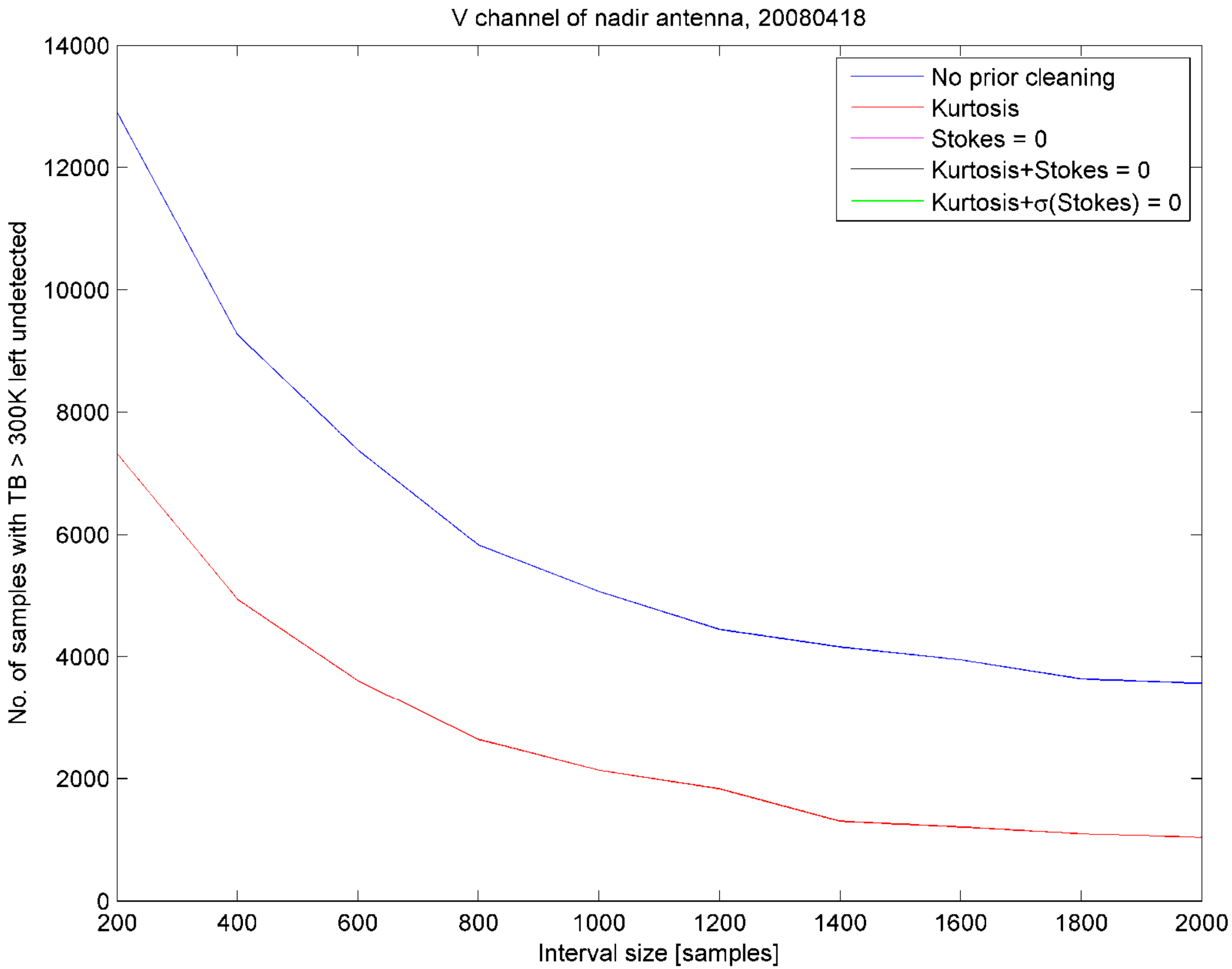

Glitch detection - conclusions

- On its own (case no. 1), glitch detection is capable of significantly reducing the number of data samples with TB > 300K while still maintaining a low overall percentage of tagged samples.
- A longer interval size yields a better detection for cases 1 and 2.
- The graphs representing cases 1 and 2 are shifted versions of each other, suggesting:
  - Most of the samples tagged in the two cases are not only identical; they are also different from the ones tagged by the kurtosis algorithm

- Cases 3, 4, and 5 do not respond differently when the interval size is varied – very few outliers were left upon application of the polarimetric detection methods.
- The remaining outliers have been efficiently removed by the glitch detection algorithm

Glitch detection looks like a valuable complement to the other investigated methods

Improved RFI detection methods – general comments

- Kurtosis inspection on its own is not sufficient as a means of efficient RFI filtering – RFI with high duty cycles is not fficiently detected.

- RFI filtering utilizing polarimetric data shows interesting potential when dealing with higher-duty cycle, large-scale RFI. This filtering should be combined with the kurtosis method.

- Glitch detection complements the other detection methods very well, and is particularly efficient upon application of polarimetric detection methods.

- Priority should be given to detection schemes which
  - Can be automated
  - Do not require a priori knowledge about geographical conditions etc.

Detecting RFI in SMOS data

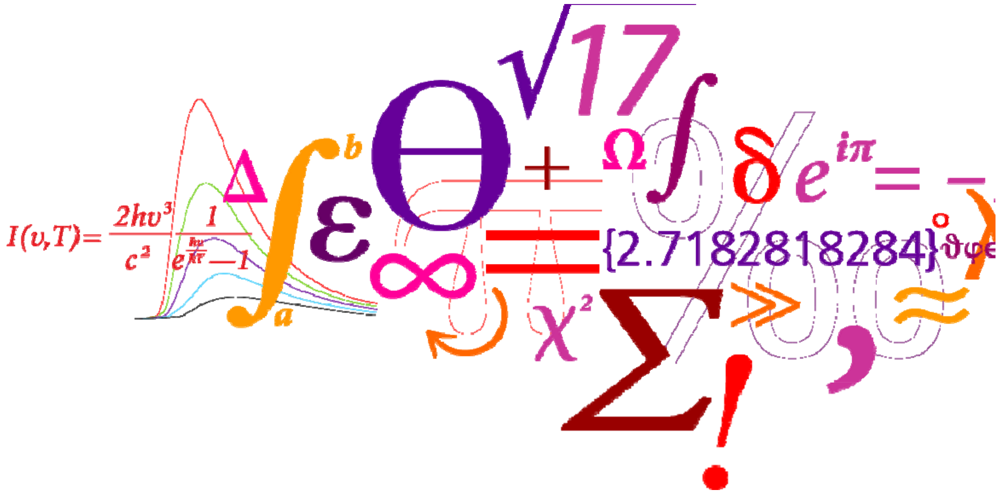

DTU Space
National Space Institute

Europe as seen by MIRAS in April 2010

2010/04/06 – 2010/04/12

TBH [K]

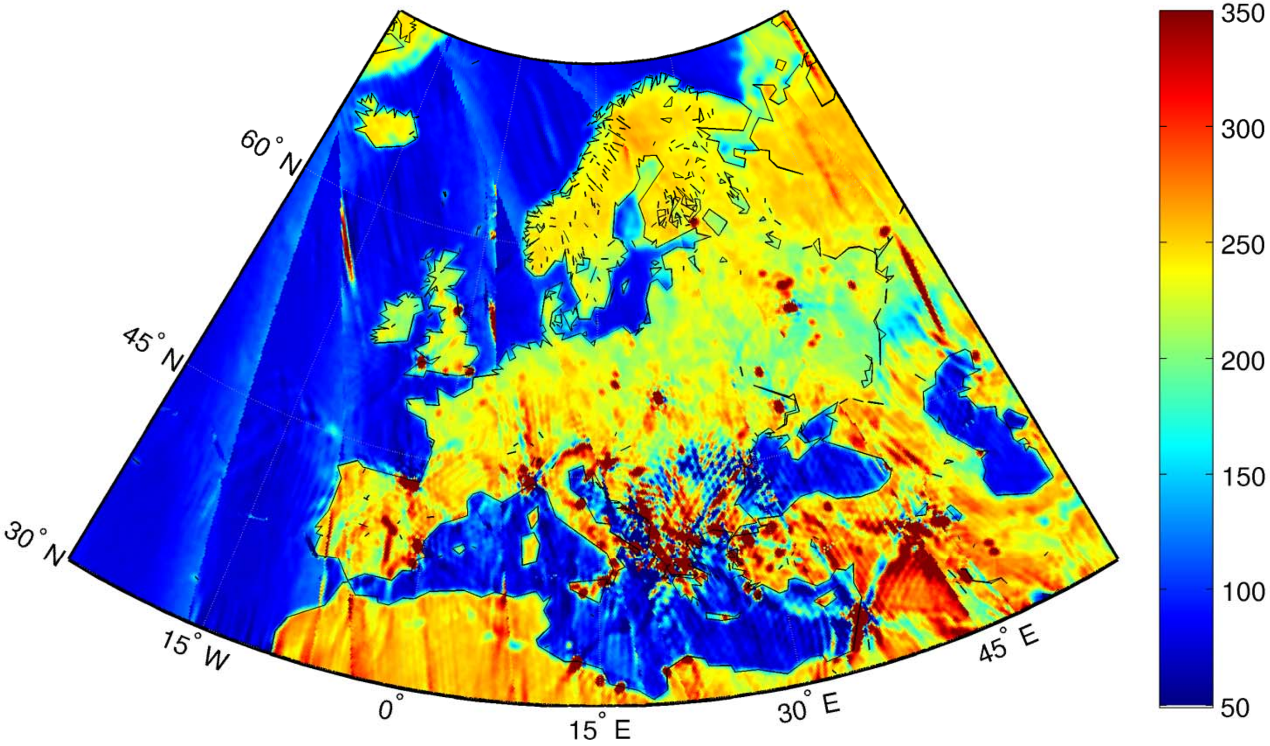

Europe as seen by MIRAS in April 2011

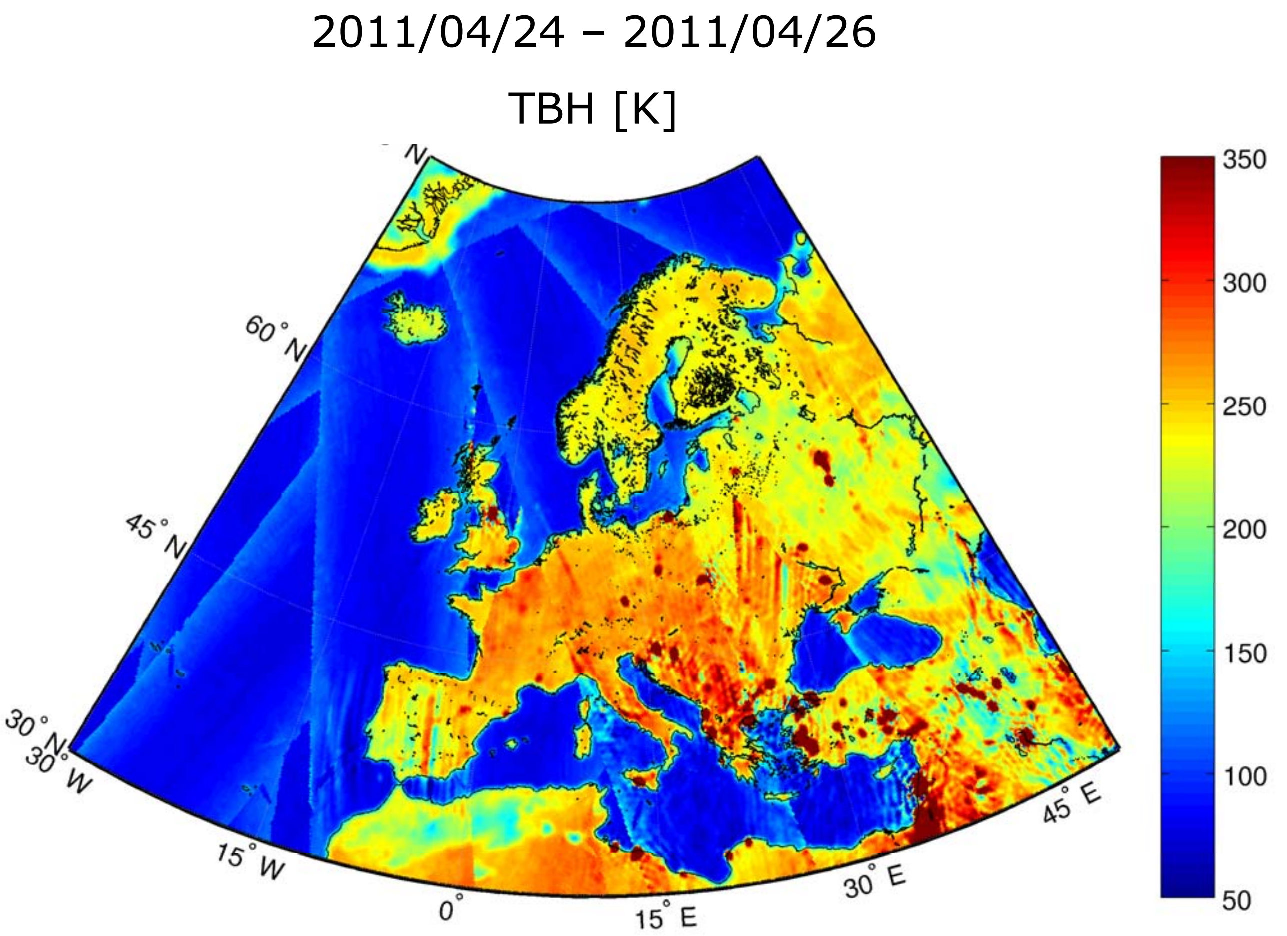

Africa as seen by MIRAS in April 2010

2010/04/06 – 2010/04/12

TBH [K]

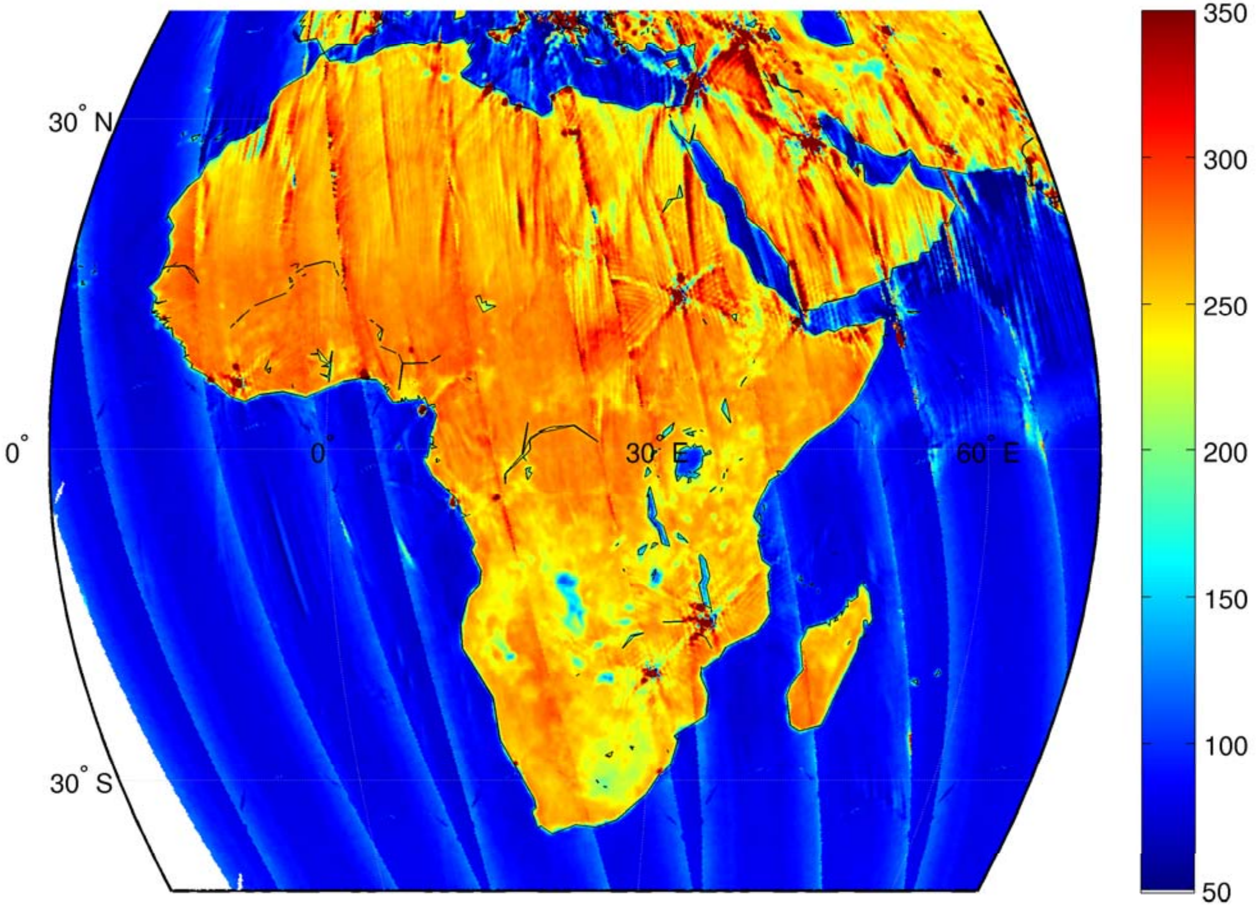

Africa as seen by MIRAS in April 2011

2011/04/24 – 2011/04/26

TBH [K]

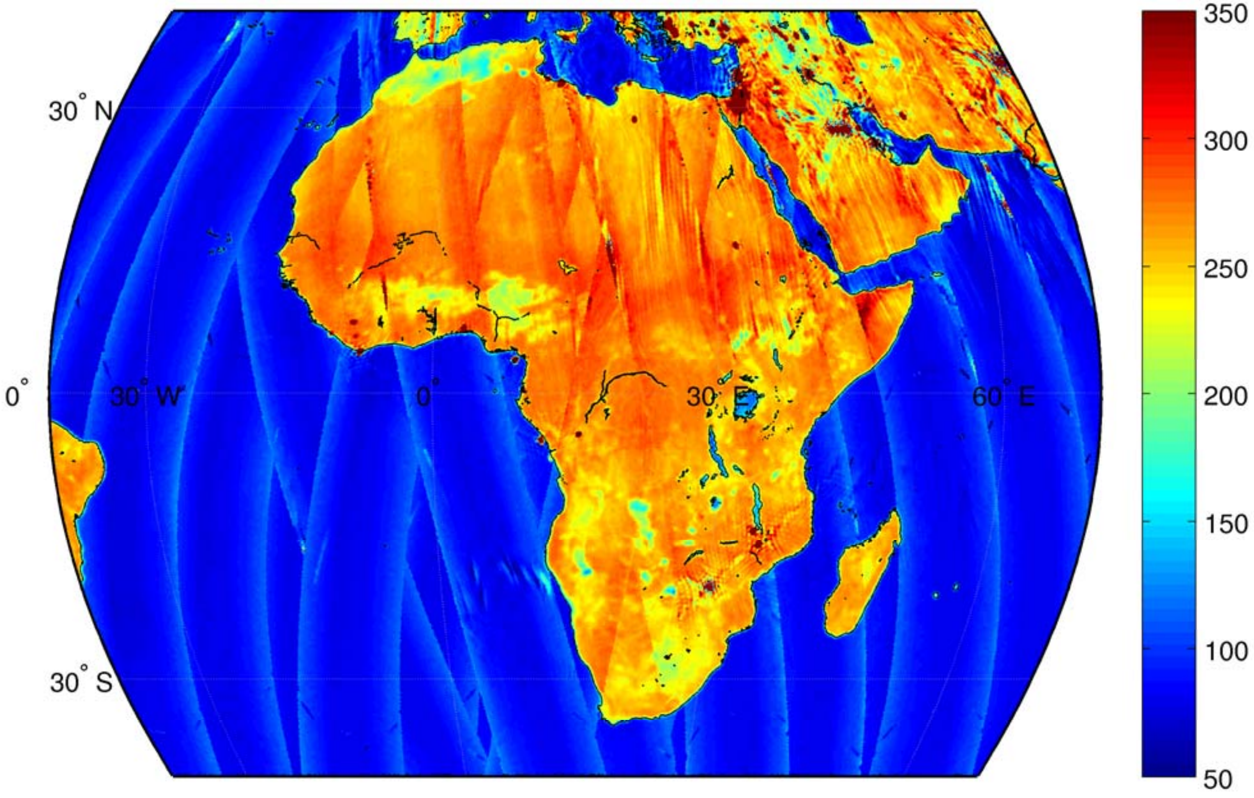

RFI as seen by MIRAS then and now

- The RFI situation has improved considerably, mainly due to
  - Improved algorithms for processing SMOS data
  - Successful identification and elimination of many RFI emitters, particularly in Southern Europe

- Many RFI hot spots have disappeared altogether

- In many cases, remaining RFI hot spots have a more localized appearance without any “red spiders” disturbing adjacent areas

- RFI is still very visible in many places

Eastern Europe as seen by MIRAS on 10 February 2010

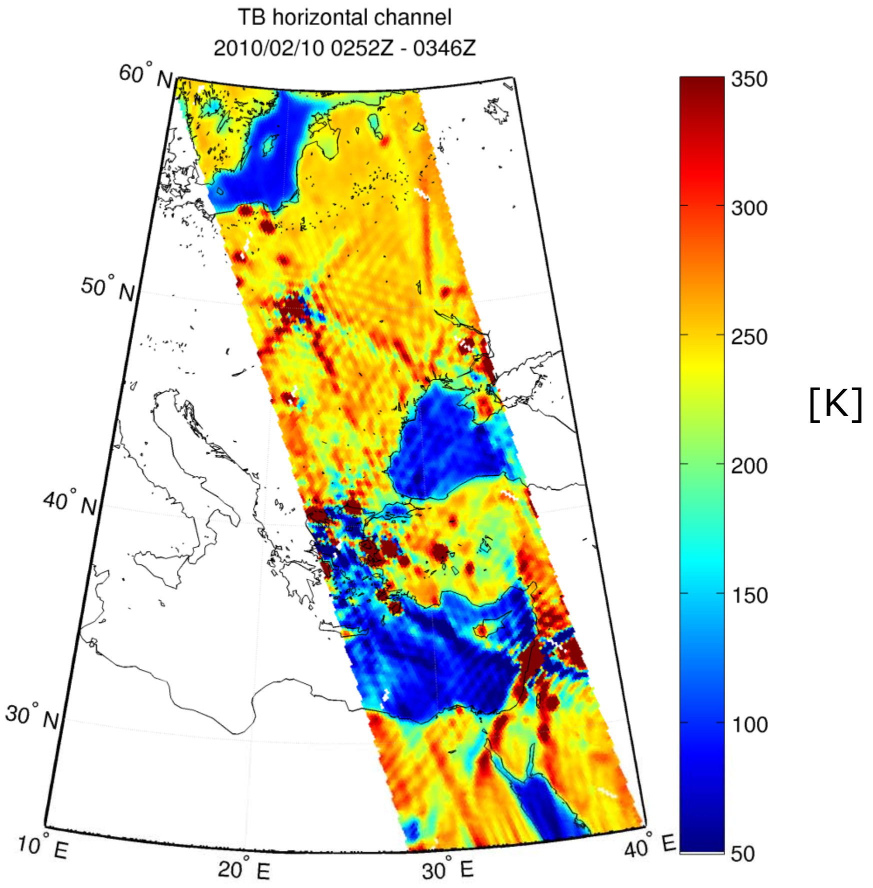

Eastern Europe as seen by MIRAS on 10 February 2010

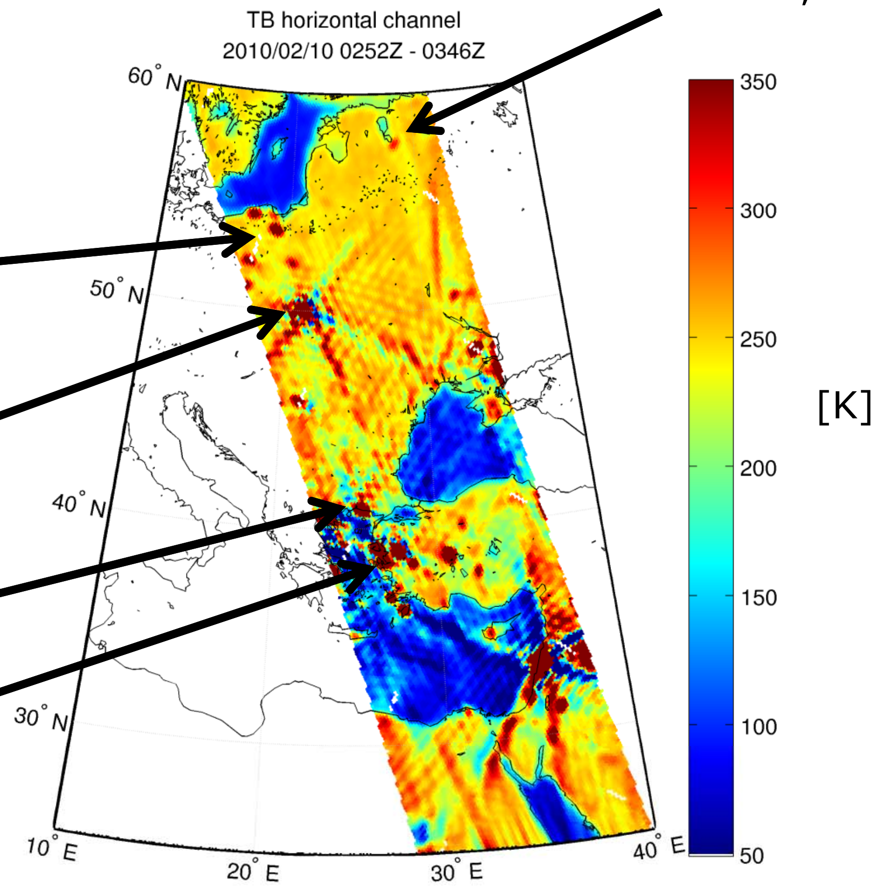

SMOS data – a look at the 3rd Stokes parameter

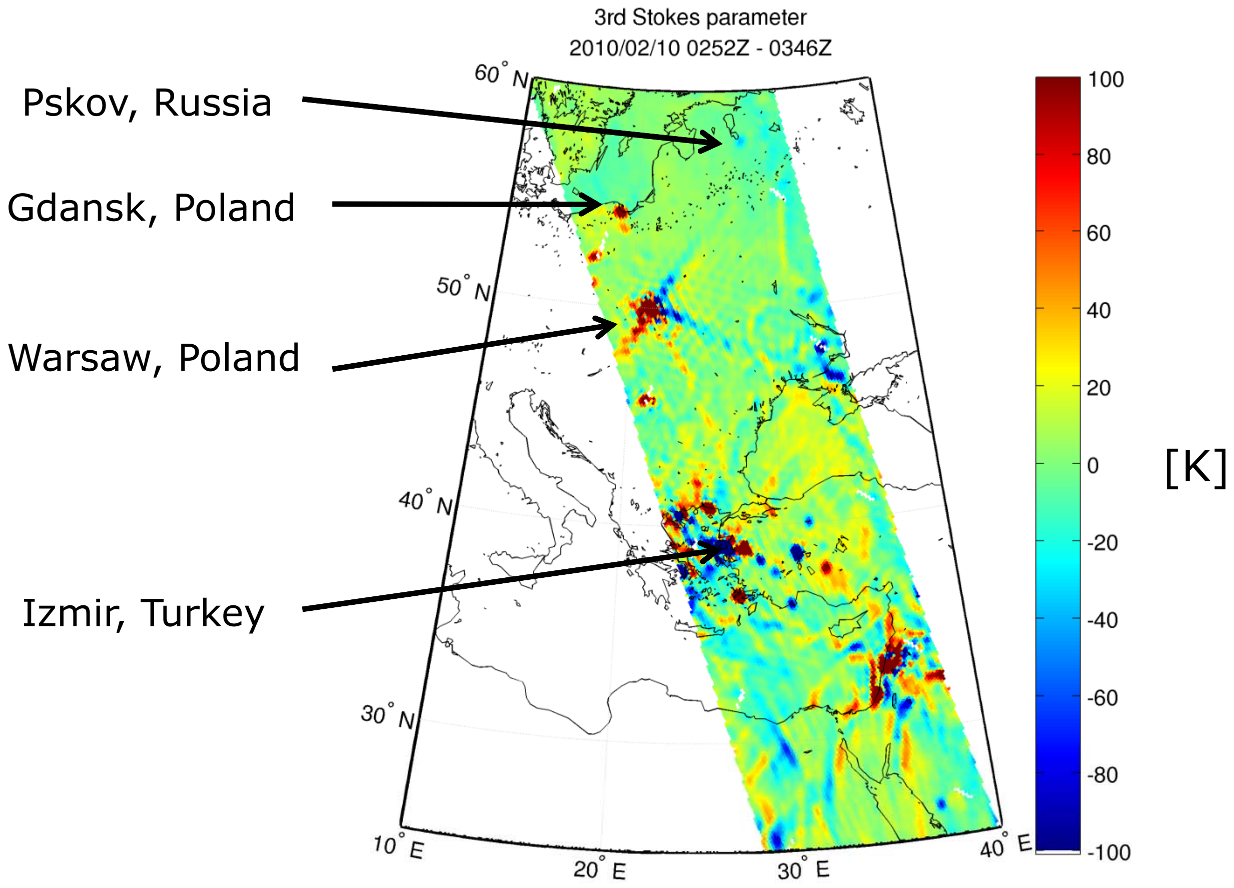

SMOS data – a look at the 4th Stokes parameter

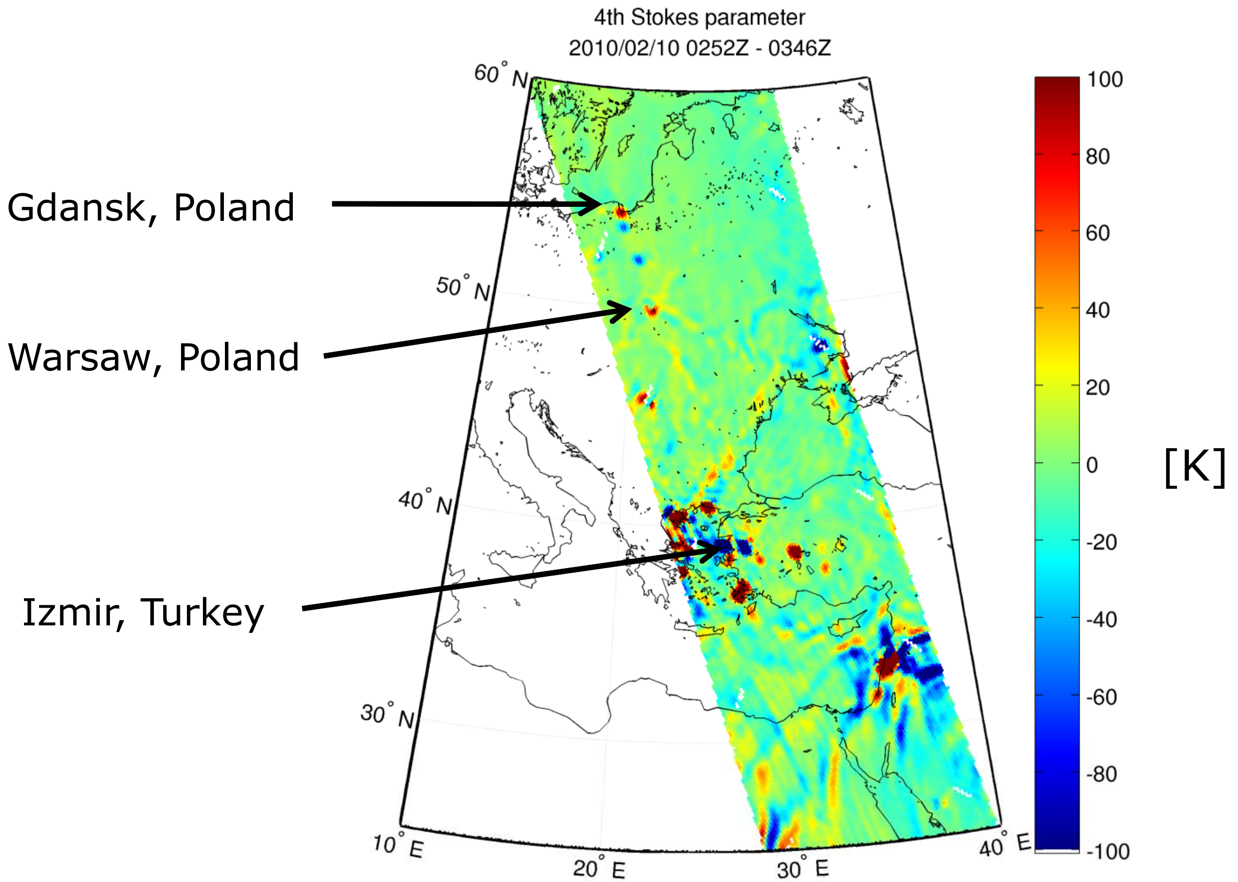

Like EMIRAD data, SMOS data show a correspondence between RFI contamination and elevated values of the 3rd and 4th Stokes parameters

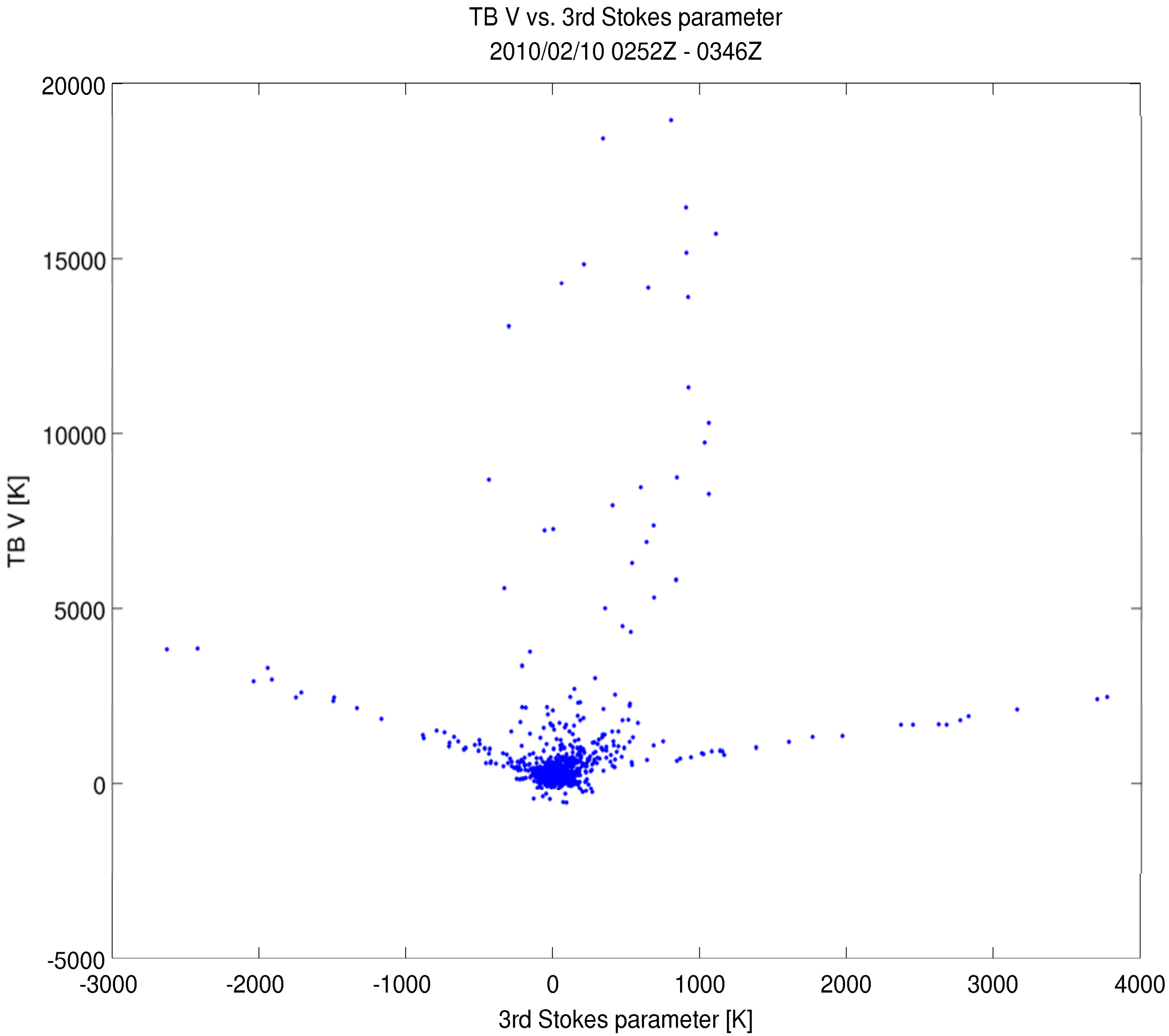

TB V vs. 3rd Stokes parameter
2010/02/10 0252Z - 0346Z
20000
15000
10000
5000
0
-5000
TB V [K]
-3000
-2000
-1000
0
1000
2000
3000
4000
3rd Stokes parameter [K]

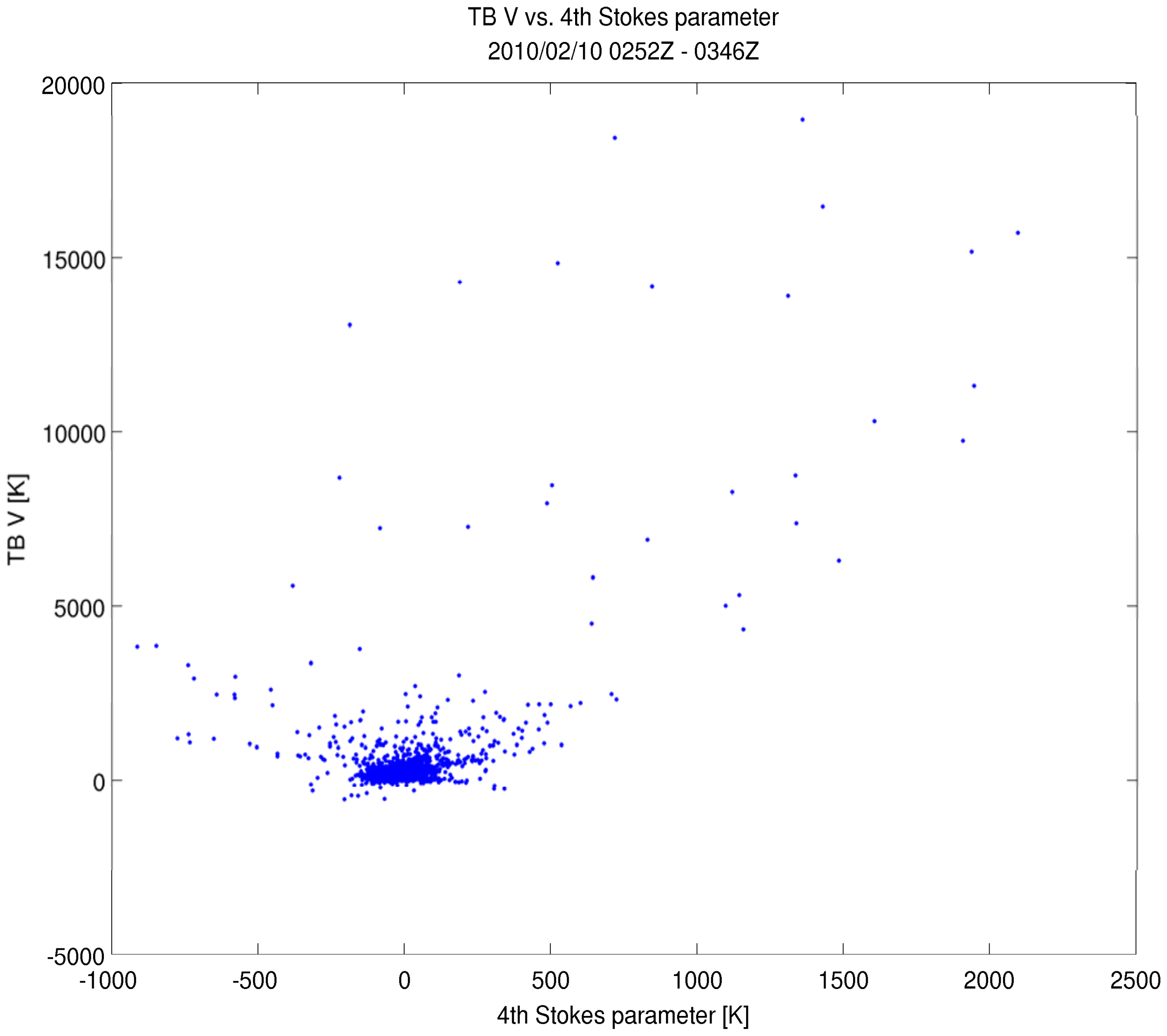
TB V vs. 4th Stokes parameter
2010/02/10 0252Z - 0346Z
20000
15000
10000
5000
0
-5000
TB V [K]
-1000
-500
0
500
1000
1500
2000
2500
4th Stokes parameter [K]

110

SMOS revisited – applying Stokes parameter limits

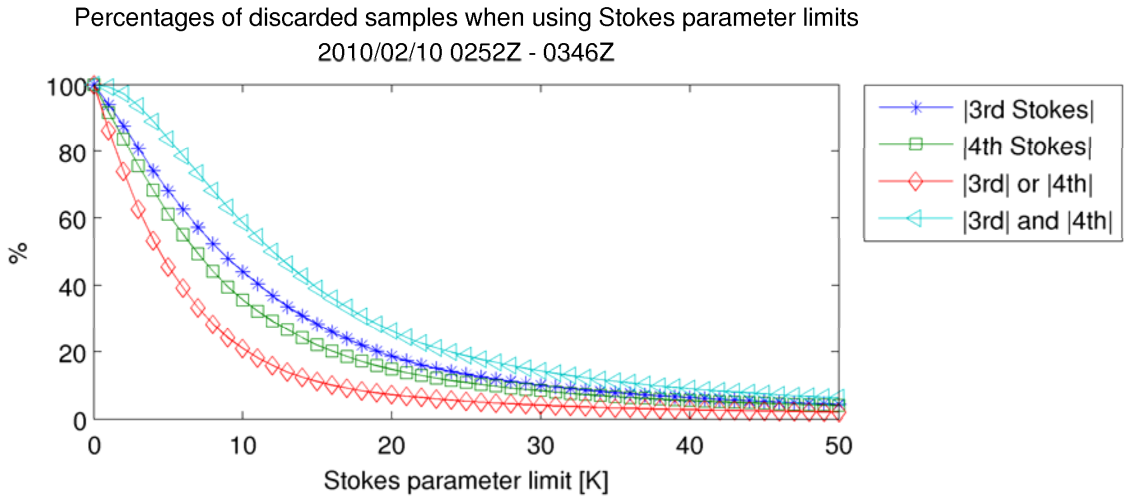

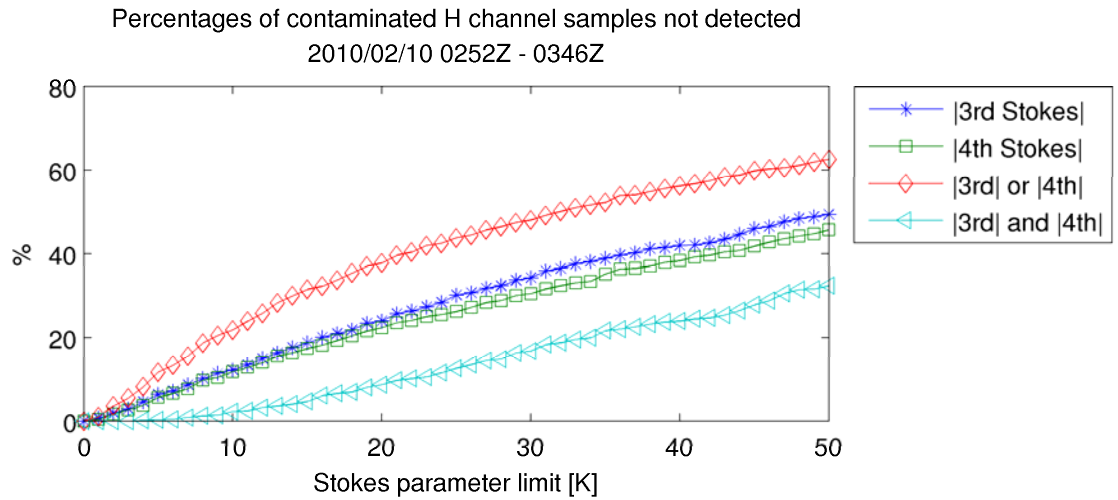

SMOS data – applying Stokes parameter limits

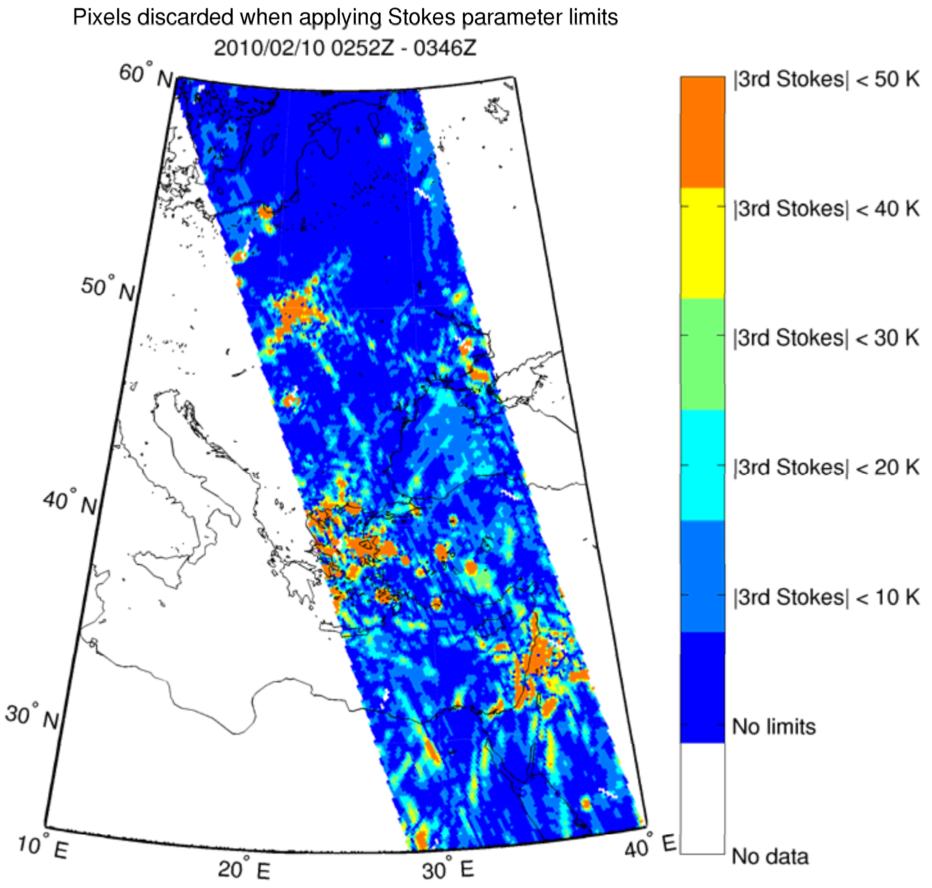

SMOS data – applying Stokes parameter limits

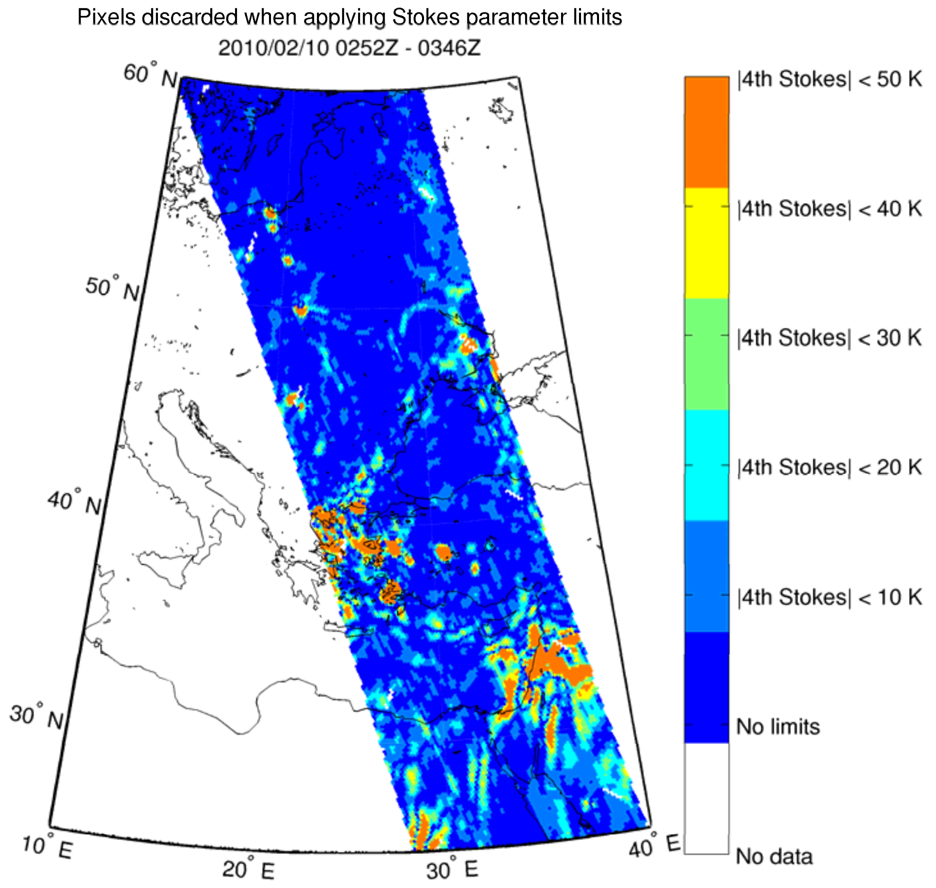

SMOS data – applying Stokes parameter limits

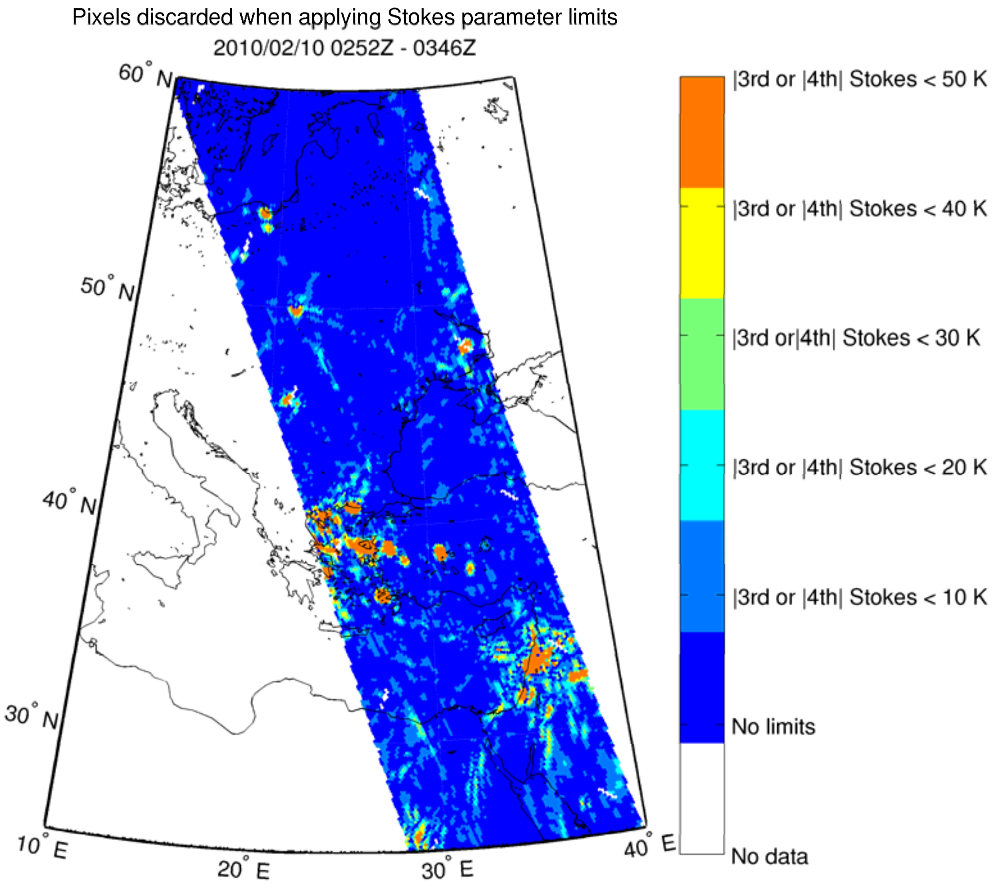

SMOS revisited – applying Stokes parameter limits

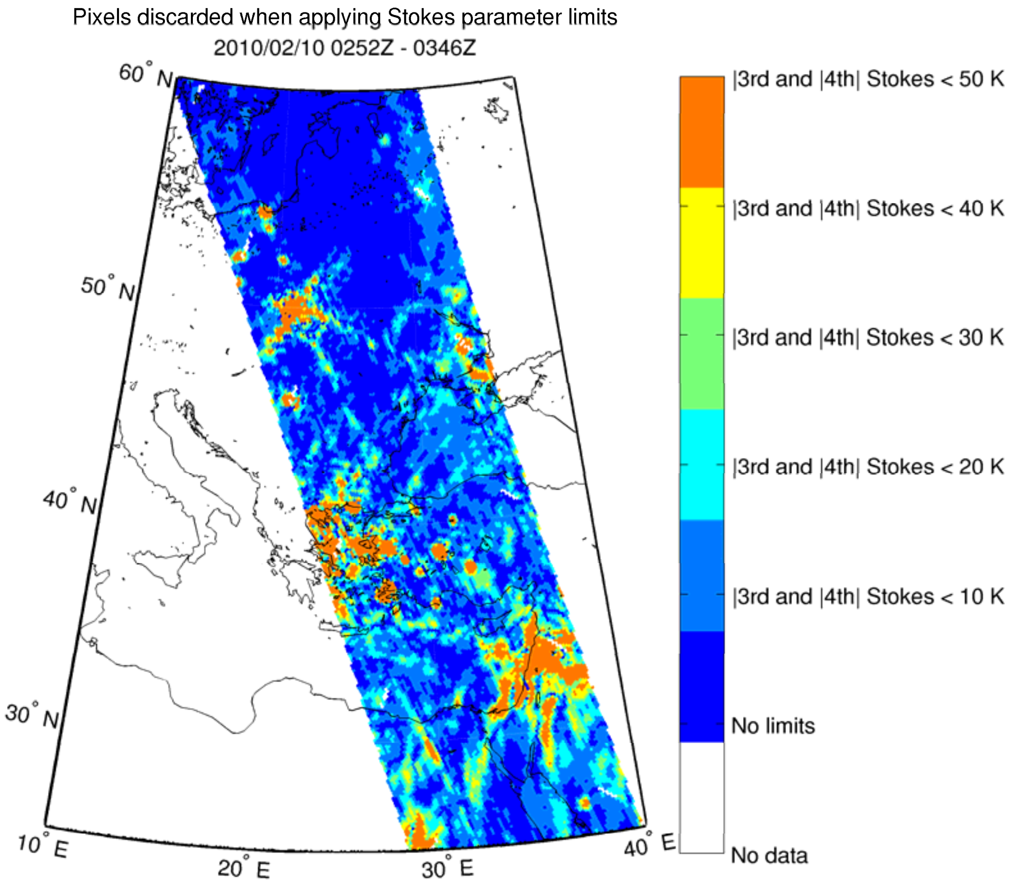

More work is needed in order to find suitable limits of the 3rd and 4th Stokes parameters

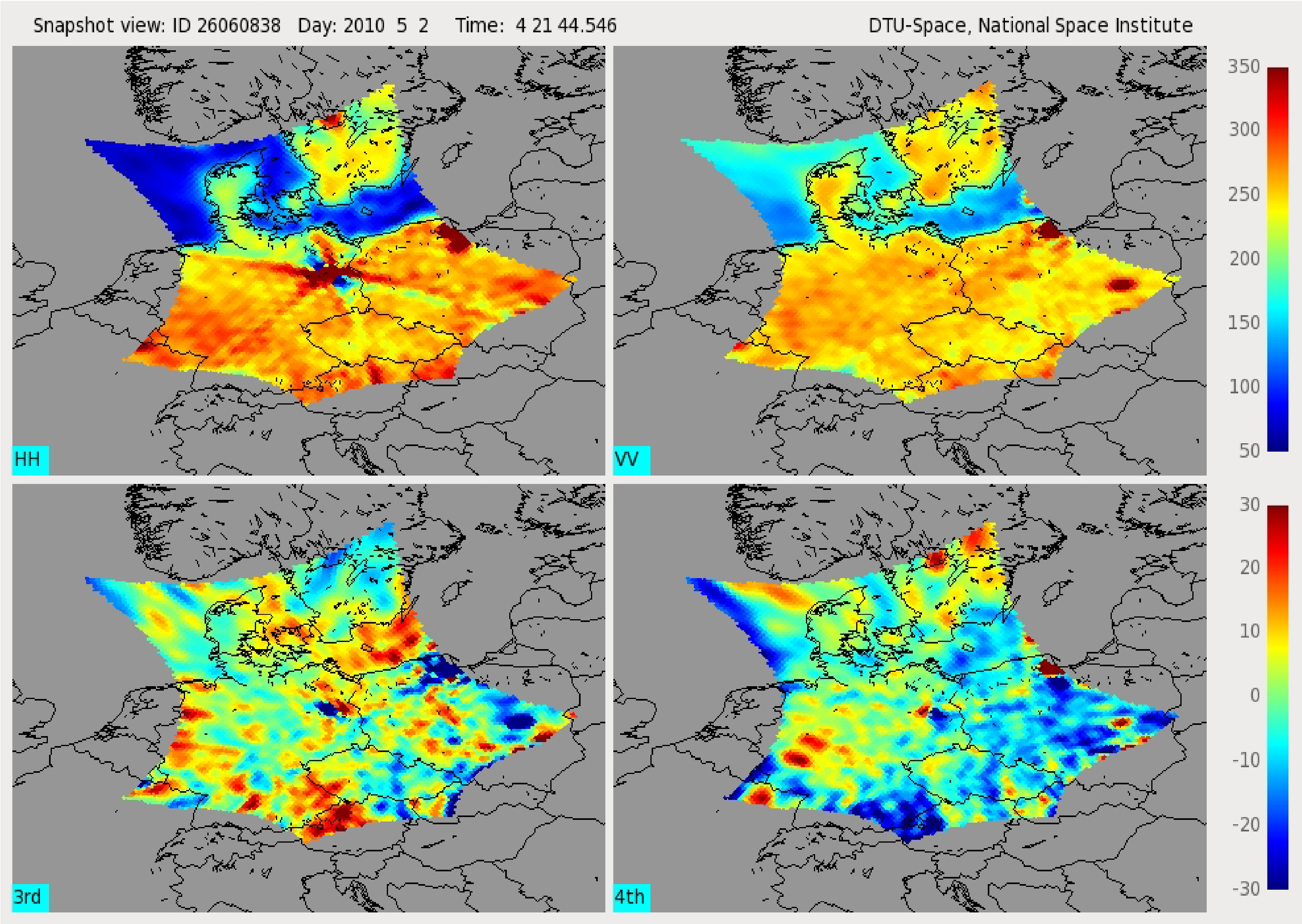
Snapshot view: ID 26060838 Day: 2010 5 2 Time: 4 21 44.546
DTU-Space, National Space Institute
HH
VV
3rd
4th
350
300
250
200
150
100
50
30
20
10
0
-10
-20
-30

SMOS View of Australia

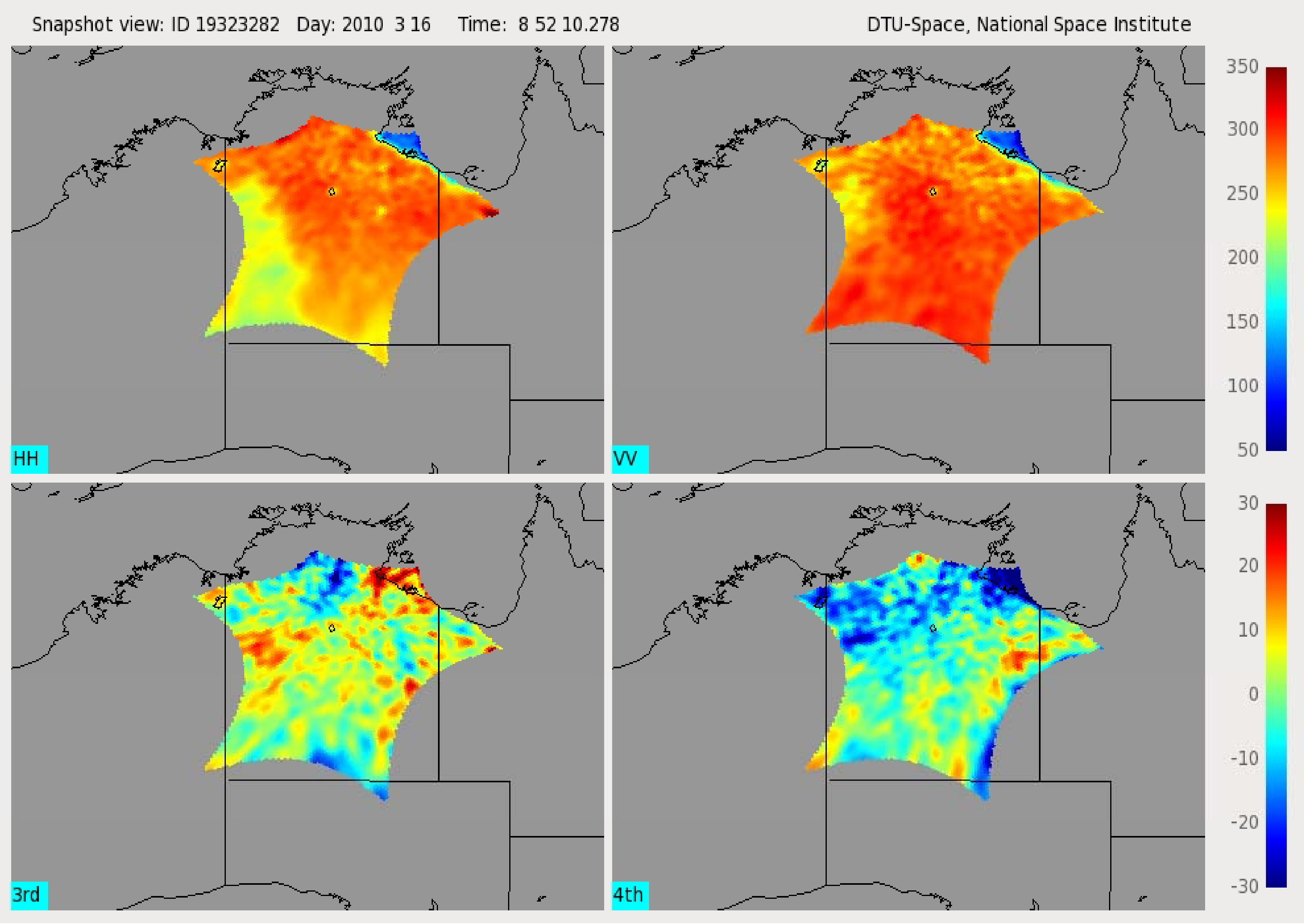

Other ways of detecting RFI in SMOS data

Inspection of the 3rd and 4th Stokes parameters looks like a viable method when it comes to the detection of RFI contamination

It should be noted that:

- EMIRAD measures the full polarimetric information simultaneously
- SMOS does so sequentially

Possible other methods include:

- Glitch detection (as described by C. Ruf and S. Misra, University of Michigan)
- Examination of TB behaviour vs. incidence angle.

Glitch detection – an example

For each pixel under test:

1. Calculate the mean of a number of neighbouring pixels.
2. Subtract this value from the pixel itself
3. Find suitable thresholds for the resulting values (TBD)

Glitch detection yields interesting results with 3rd and 4th Stokes parameters as well

Warsaw (real RFI)

Coastline (false alarm)

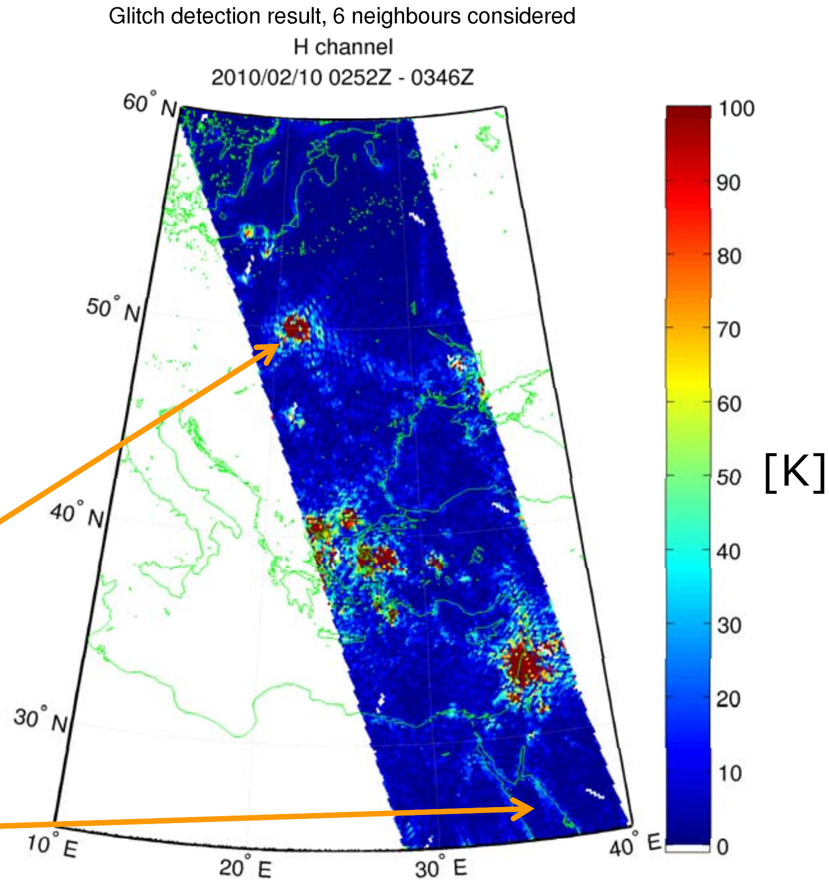

Brightness temperature vs. incidence angle – an example

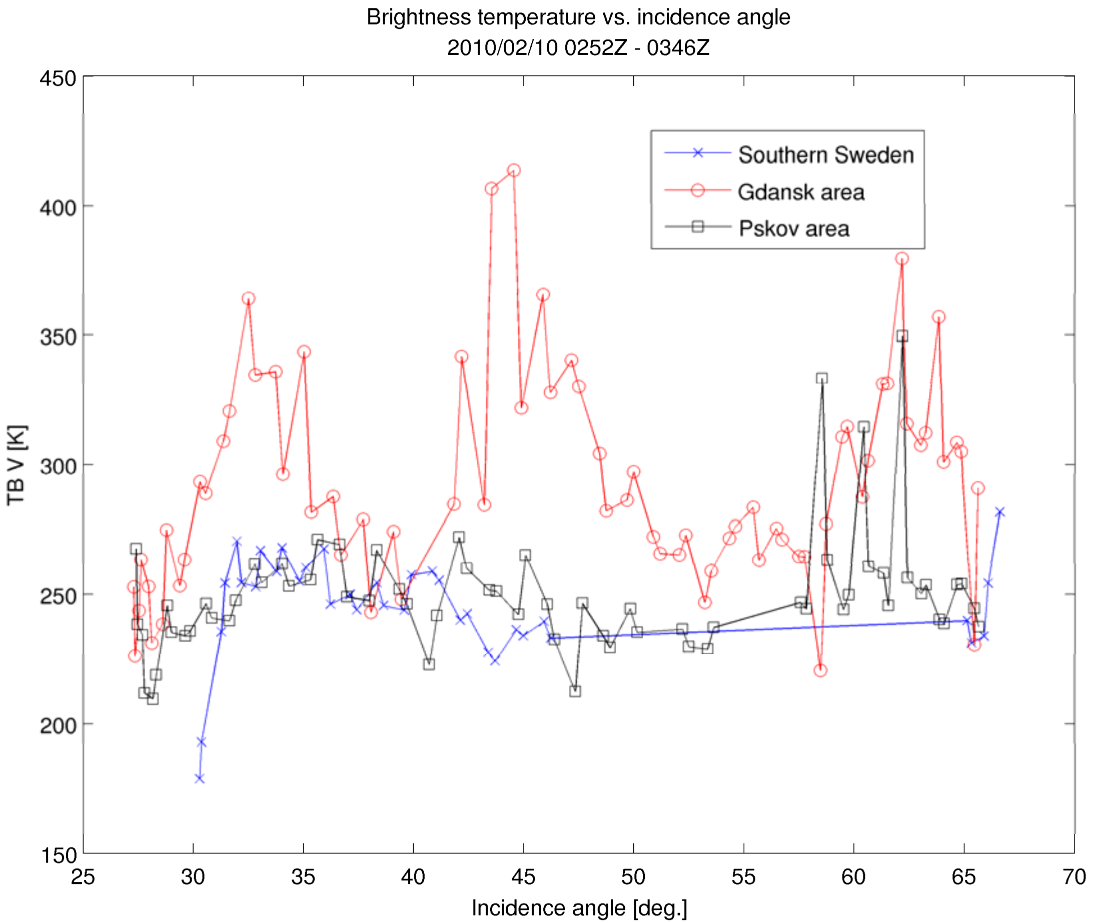

Conclusion

- Observations made with EMIRAD and SMOS show that RFI contamination is a widespread phenomenon.
  - Algorithms for the detection of RFI and mitigation of its impact should be developed
- RFI detection by means of kurtosis inspection does detect a fair amount of contaminated samples, but it should be combined with other methods, since many cases of obvious RFI contamination are left undetected
  - Kurtosis inspection is not directly relevant when dealing with SMOS data
- Inspection of the 3rd and 4th Stokes parameters have a promising potential when it comes to detecting RFI in the EMIRAD and SMOS contexts
- For situations where fully polarimetric measurements are not available, other methods (glitch detection, inspection of TB behaviour vs. incidence angle) carry useful information with respect to RFI contamination